UNIVERSITÄT ZU LÜBECK

From the Institute of Psychology
of the University of Lübeck
Director: Prof. Dr. Nico Bunzeck

The effects of social feedback and underlying neuropsychological mechanisms

Dissertation
for Fulfillment of
Requirements
for the Doctoral Degree
of the University of Lübeck
from the Department of Natural Sciences

Submitted by

Alexandra Sobczak
from Moers (Germany)

Lübeck 2024

First referee: Prof. Dr. rer. nat. Nico Bunzeck

Second referee: Prof. Dr. rer. nat. Ulrike Krämer

Date of oral examination: 10.10.2024

Approved for printing. Lübeck,

Table of contents

Abstract

Social rewards and punishments are potent motivators that shape behavior. The anticipation of both social and non-social incentives engages shared neural substrates, particularly the mesolimbic system. While the involvement of the mesolimbic system in incentive processing is well-established, little is known about how the human substantia nigra (SN) signals positive and negative social information. Furthermore, the basal forebrain (BF) is implicated in learning and motivation. However, it is often neglected in human research and its interaction with the mesolimbic system during the anticipation of social outcomes is unclear. Aging is associated with a neural decline including these brain regions, functional changes in incentive processing, and changes in socio-emotional processing but it is not always clear how this affects learning and motivation, especially in learning from social feedback. Finally, social encounters in the real world are multimodal but the effects of more naturalistic social feedback on motivation, learning, and socio-emotional processing are still poorly understood.

This dissertation consists of three studies investigating the neuropsychological mechanisms underlying social feedback anticipation and its effects on motivation and socioemotional processing in aging. All studies employed the well-established social incentive delay (SID) task with neutral, positive, and negative social feedback. We used intraoperative intracranial electroencephalography (iEEG) in Parkinson's Disease (PD) patients (study I, experiment 1, n = 12, 51-71 years) and high-resolution functional magnetic resonance imaging (fMRI) in healthy young adults (study II, n = 36, 18-33 years) to investigate the coding of social reward and punishment anticipation within the human SN, and to investigate how the interaction between the mesolimbic system and BF contributes to these processes. Effects of social feedback on motivation were assessed via response times (RT) in intraoperative patients OFF medication (study I, experiment 1), non-operated patients ON and OFF medication (study I, experiment 2, n = 24, 53-85 years), and healthy young (18-35 years; study I, experiment 3, n = 52; study II, n = 36; study III, n = 101) and older adults (50+ years; study I, experiment 3, n = 52; study III, n = 107). Furthermore, we tested the effects of social feedback and aging on evaluative learning and socio-emotional processing, and the influence of different feedback modalities on motivation (photo vs video feedback; study III).

On the neural level, the results demonstrate that the human SN signals the anticipation of positive and negative social information via alpha-beta oscillations and consists of functional subregions, including a reward-associated ventral part and a punishment-associated lateral part. Moreover, mesolimbic and BF subregions show valence-unrelated and valence-related functional connectivity patterns during the anticipation of social feedback. Along these lines, we suggest an integrated model of cortical and subcortical social information processing (CASSI) bringing together contributions of the dopaminergic midbrain, striatum, BF, medial temporal lobe, and prefrontal cortex to promote social information processing and motivation. On the behavioral level, anticipating social feedback invigorates motor responses in healthy young and older adults as well as PD patients. We found no motivational benefit of video feedback compared to photos in RT. However, older adults show changes in the evaluation of feedback videos, indicating socio-emotional changes and a positivity effect. Together, this suggests that social feedback is a strong motivator regardless of its modality and age.

This work improves our understanding of motivation, learning, and socioemotional processing in aging and provides novel insights into the neural processing of appetitive and aversive social information within the SN as well as the interplay between the mesolimbic system and the BF. With the proposed CASSI model, we suggest that the contribution of the BF to motivational and social information processing aspects has been neglected in other models and should be given more attention in future research.

Zusammenfassung

Soziale Belohnungen und Bestrafungen sind starke Motivatoren, die sich auf das Verhalten auswirken. Die Antizipation sowohl sozialer als auch nicht-sozialer Anreize aktiviert gemeinsame neuronale Schaltkreise, insbesondere das mesolimbische System. Während die Beteiligung des mesolimbischen Systems an der Anreizverarbeitung etabliert ist, ist wenig darüber bekannt, wie die menschlichen Substantia Nigra (SN) positive und negative soziale Informationen signalisiert. Darüber hinaus ist das basale Vorderhirn (BF) an Lernen und Motivation beteiligt, wird aber dennoch in der Humanforschung oft vernachlässigt und sein Zusammenspiel mit dem mesolimbischen System während der Antizipation sozialer Informationen ist unklar. Das Altern geht mit einer neuronalen Degeneration einher, die diese Hirnregionen betrifft, sowie mit funktionalen Veränderungen in der Anreizverarbeitung und Veränderungen in der sozioemotionalen Verarbeitung. Allerdings ist nicht immer klar, wie sich dies auf Lernen und Motivation, insbesondere beim Lernen aus sozialem Feedback, auswirkt. Schließlich sind soziale Begegnungen in der realen Welt multimodal, aber die Auswirkungen von naturalistischem sozialem Feedback auf Motivation, Lernen und sozioemotionale Verarbeitung sind noch unzureichend verstanden.

Diese Dissertation besteht aus drei Studien, die die neuropsychologischen Mechanismen der Antizipation von sozialem Feedback und dessen Auswirkungen auf Motivation, sozioemotionale Verarbeitung und Lernen im Alter untersuchen. Alle Studien verwendeten die etablierte Social Incentive Delay (SID) Aufgabe mit neutralem, positivem und negativem sozialem Feedback. Wir verwendeten intraoperative Ableitungen mittels intrakranieller Elektroenzephalographie (iEEG) in Patienten mit der Parkinson-Krankheit (PD) (Studie I, Experiment 1, n = 12, 51-71 Jahre) und hochauflösende funktionelle Magnetresonanztomographie (fMRT) bei gesunden jungen Erwachsenen (Studie II, n = 36, 18-33 Jahre), um mögliche unterschiedliche Kodierungen der Antizipation von sozialen Belohnungen und Bestrafungen innerhalb der menschlichen SN zu untersuchen, und um zu untersuchen, wie das Zusammenspiel zwischen dem mesolimbischen System und dem BF zu diesen Prozessen beiträgt. Die Auswirkungen des sozialen Feedbacks auf die Motivation wurden durch Reaktionszeiten (RT) auf einen Zielreiz bei intraoperativen Patienten im OFF-Zustand (Studie I, Experiment 1), nicht operierten Patienten im ON- und OFF-Zustand (Studie I, Experiment 2, n = 24, 53-85 Jahre), und gesunde junge (18-35 Jahre; Studie 1, Experiment 3, n = 52; Studie II, n = 36; Studie III, n = 101) und ältere Kontrollpersonen (50+ Jahre; Studie I, Experiment 3, n = 52; Studie III, n = 107) gemessen. Darüber hinaus testeten wir die Auswirkungen des sozialen Feedbacks und des Alterns auf evaluatives Lernen und sozioemotionale Verarbeitung sowie den Einfluss unterschiedlicher Feedback-Modalitäten auf die Motivation (Foto- vs Video-Feedback; Studie III).

Auf neuronaler Ebene zeigen die Ergebnisse, dass die menschliche SN die Antizipation von positiven und negativen sozialen Informationen über Alpha-Beta-Oszillationen signalisiert und funktionelle Subregionen umfasst, darunter ein belohnungsassoziierter ventraler Teil und ein strafassoziierter lateraler Teil. Darüber hinaus zeigen mesolimbische und BF-Subregionen valenzunabhängige und valenzabhängige funktionelle Konnektivitätsmuster während der Antizipation von sozialem Feedback. In diesem Sinne schlagen wir ein integriertes Modell der kortikalen und subkortikalen sozialen Informationsverarbeitung (CASSI) vor, das Funktionen des dopaminergen Mittelhirns, des Striatums, des BF, des medialen Temporallappens und des präfrontalen Kortex zusammenbringt, um die Verarbeitung sozialer Informationen, Motivation und Verhalten zu fördern. Auf der Verhaltensebene steigert die Antizipation von sozialem Feedback die Geschwindigkeit von motorischen Reaktionen bei gesunden jungen und älteren Erwachsenen sowie bei Patienten mit PD. Wir fanden keinen motivationalen Vorteil von Video-Feedback im Vergleich zu Fotos in RT. Ältere Erwachsene zeigen jedoch Veränderungen bei der Bewertung von Feedback-Videos, was auf sozio-emotionale Veränderungen und einen Positivitätseffekt hinweist. Zusammengenommen deutet dies darauf hin, dass soziales Feedback unabhängig von der Modalität und dem Alter ein starker Motivator ist.

Diese Arbeit verbessert unser Verständnis von Motivation, Lernen und sozioemotionaler Verarbeitung im Alter und liefert neue Erkenntnisse über die neuronale Verarbeitung appetitiver und aversiver sozialer Informationen innerhalb der SN sowie das Zusammenspiel zwischen dem mesolimbischen System und dem BF. Mit dem vorgeschlagenen CASSI-Modell legen wir nahe, dass der Beitrag des BF zu motivationalen und sozialen Informationsverarbeitungsaspekten in anderen Modellen vernachlässigt wurde und in zukünftiger Forschung mehr Beachtung finden sollte.

Abbreviations

ACh	Acetylcholine
AD	Alzheimer's Disease
ASD	Autistic spectrum disorders
BF	Basal forebrain
BOLD	Blood Oxygen Level Dependent
CASSI	Cortical And Subcortical Social Information processing
CS	Conditioned stimulus
Ch1-4	Cholinergic cell groups in the BF
ChI	Cholinergic interneuron
DA	Dopamine
DB	Diagonal band of Broca
DS	Dorsal striatum
(i)EEG	(Intracranial) electroencephalography
ERP	event-related potential
(f)MRI	(Functional) magnetic resonance imaging
GABA	Gamma-aminobutyric acid
GLM	General linear model
lH	Lateral hypothalamus
(l)Hb	(Lateral) habenula
HOA	Healthy older adults
HYA	Healthy young adults
(SC-)IAT	(Single Category) Implicit Association Test
L-DOPA	Levodopa
(ER-)LFP	(Event-related) local field potentials
MID	Monetary incentive delay
MS	Medial septal nucleus
MTL	Medial temporal lobe
MVPA	Multivariate pattern analysis

NAcc	Nucleus Accumbens
NBM	Nucleus Basalis of Meynert
PD	Parkinson's Disease
PE	Prediction error
PET	positron emission tomography
PFC	Prefrontal cortex
ROI	Region of interest
RT	Response time
SD	Standard deviation
SI	Substantia innominata
SID	Social incentive delay
(l/m/v) SN	(Lateral/medial/ventral) substantia nigra
SNc	Substantia nigra pars compacta
SNr	Substantia nigra pars reticulata
SPM	Statistical parametric mapping
SST	Socioemotional selectivity theory
TAN	Tonically active neuron
TE	Echo time
TF	Time-frequency
TR	Repetition time
US	Unconditioned stimulus
VTA	Ventral tegmental area
VP	Ventral pallidum
VS	Ventral striatum

1 Theoretical and empirical foundations

- Psychological concepts of motivation
- Social motivation
- Concepts of learning
- Neural substrates of motivation, learning, and social information processing
- Behavioral invigoration through incentives
- Age-related changes in motivation and learning mechanisms
- Changes of incentive processing in Parkinson’s Disease
- Summary and research objectives

A fundamental part of human behavior is shaped by the desire to achieve social recognition and avoid rejection. The ability to learn and to anticipate positive or negative social responses helps us navigate the social world, but the underlying neurocognitive processes and possible age-related changes remain unclear. This research aims to investigate how the anticipation of positive and negative social feedback is signaled in the human brain and how it drives behavior in young and older adulthood. This chapter introduces the conducted research by explaining the theoretical and empirical foundation of social cognition, motivation, and learning, including their neural mechanisms, and their development in healthy aging and Parkinson's disease (PD). The chapter culminates by presenting the research gap, aims, questions, and objectives. Chapter two outlines the methodological framework employed in this thesis. Chapters three to five cover the studies, including the respective background, research questions and hypotheses, methods, results, and a discussion of the findings and their implications. An integrated summary and discussion of the work are provided in chapter six.

1.1 Psychological concepts of motivation

In psychology and behavioral neuroscience, a pivotal concept to explain behavior is motivation, which is defined as the energizing force that initiates and sustains goal-directed activities (Simpson and Balsam, 2015). It can be distinguished into three categories: biological, social, and growth motivation. Biological motivation describes factors directly related to survival, self-maintenance, and reproduction, for example eating and drinking. Social motivation refers to efforts to establish social interactions and bonds. Growth motivation relates to the accumulation of knowledge, the development of skills, and seeking novel experiences (Freed, 2022). Each form of motivation can lead to goal-directed behavior to satisfy a particular need.

Motivational theories view motivation as a process that includes an interplay between behavior and consequences (Cook and Artino, 2016). Incentive motivation theories suggest that when behavior is rewarded, the individual may develop a desire for that pleasant outcome, resulting in a willingness to engage in goal-directed behaviors to obtain it. Conversely, when encountering negative consequences, individuals will try to avoid such outcomes in the future. Along these lines, cues that signal the potential availability of the desired reward trigger wanting and elicit goal-directed behavior, while cues signaling aversive outcomes elicit avoidance behavior (Berridge, 2018). The cue phase and the outcome phase are of particular interest in neuroimaging research and are key features of established paradigms. In this context, they are also often referred to as anticipation and outcome (Knutson and Greer, 2008).

Motivational processes are closely linked to affective responses and emotions. Outcomes that have the potential to induce pleasant emotions and elicit an approach response have a positive value and are referred to as *rewards*. On the contrary, outcomes that induce unpleasant emotions and elicit avoidance have a negative value and are referred to as *punishers* (Schultz, 2015). For instance, simple responses such as smiling or angry faces can act as rewards or punishments, respectively (Spreckelmeyer et al., 2009). Moreover, not only outcomes but also cues are linked to an affective state (anticipatory affect) and can change affective arousal (i.e. high or low) and *valence* (i.e. positive or negative), influencing our behavior and decisions (Knutson and Greer, 2008).

Two components that play a role in motivational processes are value and salience. The *value* of an outcome describes the subjective assessment of the outcome’s utility. As such, it depends on subjective preferences and mediates behavioral and emotional effects of outcomes (Schultz, 2015). In other words, the value of an outcome that follows successful behavior is an important component in determining whether goal-directed behavior will be performed (Berridge, 2018). Stimulus *salience* is determined by specific properties such as physical intensity, novelty, surprise, and motivational impact (Schultz, 2015). Both value and salience of a potential outcome can be influenced by internal states. For example, hunger or loneliness would increase the attractiveness of and the pleasure derived from food or meeting a close friend (Berridge, 2018).

Together, motivation is a dynamic process of behavioral adaptation driven by the pursuit of positive and the avoidance of negative outcomes. Different characteristics of cues and outcomes influence goal-directed behavior, including value, salience, and emotional valence.

1.2 Social motivation

The notion that social connectedness is one of the basic human needs is incorporated in several theories, for example in Murray’s system of needs (‘need for affiliation’; Murray and Harvard University, 1938), Maslow’s hierarchy of needs ('belongingness and love needs'; Maslow, 1943; Maslow and Frager, 1987), Alderfer’s Existence, Relatedness, and Growth theory (Alderfer, 1969), and the self-determination theory (‘need for relatedness’; Ryan and Deci, 2000). The common idea behind these theories is that the desire for affectionate social relationships shapes a fundamental part of human behavior, cognition, and emotion.

Social motivation is reflected in several behaviors characterized by social orienting, seeking and liking, and social maintaining (Chevallier et al., 2012). This includes attentional preferences for social stimuli, exerting efforts to gain social rewards, building affectionate relationships with family members, forming friendships and communities, cooperation, conversation, and taking pleasure from engaging in social activities (e.g. going to local bars), and prosocial behaviors such as charity work or volunteering. Similarly, people will try to avoid loneliness and preserve existing relationships (Murray and Harvard University, 1938; Maslow and Frager, 1987; Baumeister and Leary, 1995; Chevallier et al., 2012; Freed, 2022).

But why is social connectedness relevant to humans? From an evolutionary perspective, belonging to a social group ensures survival (e.g. food sharing, protection, and care (Baumeister and Leary, 1995). Similarly, being receptive to feedback from others, such as praise or criticism, supports learning and adequate social behavior that benefits the individual and community (Freed, 2022). Therefore, mechanisms increasing the tendency to form social bonds have likely created a selective advantage and may be part of the biological heritage (Baumeister and Leary, 1995).

Social interactions influence immediate emotions: positive social interactions elicit positive emotions while deprivation (rejection, exclusion, isolation, loneliness, separation) leads to negative emotions (Baumeister and Leary, 1995). In addition, positive social relationships can promote stress reduction (Gunnar, 2017) and health (Vila, 2021) while weak social bonds are associated with increased risk for mortality (Holt-Lunstad and Smith, 2012). Adverse circumstances, such as social isolation, can harm mental health in children and adolescents (Almeida et al., 2022) and cognitive function in older adults (Evans et al., 2019; Shen et al., 2022). Together, social relationships have an impact on emotions, cognition, health, and well-being. Therefore, being able to successfully engage in behaviors that ensure social connection and effective processing of social information are essential.

1.3 Concepts of learning

The expectation of positive or negative outcomes can contribute to motivation. Therefore, the important question is how these expectations are formed. How does an individual know that a reward can be obtained or that a certain behavior will probably lead to the desired outcome? Making such predictions requires learning.

The traditional paradigm to study predictive learning is classical conditioning (Balleine and Dickinson, 1998) which was first used by Ivan Pavlov in 1927 (Houwer and Hughes, 2020). In this paradigm, an initially neutral stimulus is paired with another stimulus (unconditioned stimulus; US; e.g. food) that naturally evokes a certain response (unconditioned response; UR; e.g. salivation). Through the repetition of this contingency, the previously neutral stimulus becomes a conditioned stimulus (CS) and elicits the response that was originally stimulated by the US. The pairing of the two stimuli leads to learning this association (Houwer and Hughes, 2020).

In contrast to classical conditioning, instrumental (operant) conditioning describes the learning of regularities between behavior and stimuli. When a behavior is followed by pleasant consequences, its frequency can be increased while unpleasant consequences decrease the frequency of a behavior (Houwer and Hughes, 2020). Consequences are categorized into reinforcement and punishment and can be implemented by adding or removing stimuli. Adding an appetitive stimulus is referred to as positive reinforcement while negative reinforcement means the removal of an aversive stimulus. On the contrary, adding a negative stimulus is labeled as positive punishment while removing an appetitive stimulus is denoted as negative punishment (Hersen and Sledge, 2002). Overall, stimuli that elicit or strengthen desired and reduce undesired behavior are referred to as incentives (Schultz, 2015). When a behavior is reinforced in the presence of a stimulus, this stimulus gains the capacity to control behavior and becomes a so-called discriminative stimulus. Through the regularity among the (discriminative) stimulus, behavior, and reinforcement, the discriminative stimulus signals that a specific behavior will most likely be followed by a particular consequence, whereas the same behavior in a different situation may not lead to the same consequence (Hersen and Sledge, 2002).

Classical and instrumental conditioning involve the acquisition of predictive value that creates the expectation to gain a reward, referred to as contingency learning (Balleine and Dickinson, 1998) or expectancy learning (Hermans et al., 2002). In addition to learning the predictive value of a stimulus for a positive or negative outcome, the stimulus itself can be perceived as positive or negative depending on the valence of the associated outcome (Hermans et al., 2002). Processes that lead to the acquisition and change of evaluative representations, i.e. the valence of stimuli and objects, are referred to as evaluative learning (De Houwer, 2007). For instance, mental representations can be changed through the mere frequency of exposure to a stimulus ('mere exposure effect' (Zajonc, 1968), contingent pairing of initially neutral stimuli and valent stimuli (De Houwer, 2007) exposure to evaluative information about a stimulus (Petty and Briñol, 2012), or by instruction (De Houwer, 2006). The result of evaluative learning should be changes in perception, thought, and behavior (Hütter and Rothermund, 2020) which are typically assessed using direct or indirect measures, for example questionnaires, ratings, or tasks that evaluate biases such as the Implicit Association Test (IAT) (Greenwald et al., 1998).

Current human neuroimaging research often uses so-called incentive delay tasks that are based on instrumental conditioning paradigms to investigate the neural mechanisms underlying the anticipation and outcome phases of incentive processing as well as its impact on behavior. The monetary incentive delay (MID) task was developed and first used by Knutson et al. (2000), and later adapted by Spreckelmeyer et al. (2009) using social stimuli, constituting the social incentive delay (SID) task. Both tasks are widely used and recognized in incentive processing research and are well suited for human neuroimaging as they allow the separate analysis of anticipation and outcome. Consequently, the research presented in this thesis employed the SID task.

1.4 Neural substrates of motivation, learning, and social information processing

Motivation and learning rely on a complex brain network that includes the mesolimbic system and basal forebrain (BF), among others (Robbins and Everitt, 1996; Haber and Knutson, 2010). The mesolimbic system, particularly the striatum and the substantia nigra/ventral tegmental area (SN/VTA), is fundamentally involved in the anticipation and outcome phases of motivation and processes of learning associated with them (Bromberg-Martin et al., 2010; Haber and Knutson, 2010; Haber, 2016). The BF is also implicated in learning and memory (Everitt and Robbins, 1997), for example conditioning (Guo et al., 2019), and reward and punishment processing (Wilson and Rolls, 1990; Hangya et al., 2015; Monosov et al., 2015). However, it has received less attention compared to the striatum and SN/VTA. In addition, both the mesolimbic system and, more recently, the BF have been implicated in motivational aspects of social cognition but their interaction remains unclear. Consequently, the present thesis focuses on the investigation of these subcortical brain regions in the context of motivational processing, particularly regarding social motivation.

The following sections first illustrate key structural characteristics of these subcortical brain regions. Then, a broad overview of their implication in social cognition is given, and the neural mechanisms underlying the anticipation and outcome phases of motivational processes are specifically addressed. As the understanding of these mechanisms is largely based on research in animals and humans utilizing different types of reinforcers, such as liquids, electric shocks, money, or social feedback, this section considers findings from these diverse areas of study. Finally, possible differential mechanisms of value processing are elaborated. These mechanisms are currently discussed in the scientific community and are addressed by the work in this thesis.

1.4.1 Relevant neuroanatomical concepts

The striatum comprises a dorsal (DS) and ventral (VS) portion (Haber, 2016). The Nucleus Accumbens (NAcc) is a major component of the VS and is connected with a wide range of brain structures, such as the amygdala, prefrontal cortex (PFC), and SN/VTA (Haber and Knutson, 2010).

The SN/VTA resides in the midbrain and comprises neurons that synthesize and release dopamine (DA) (Nair-Roberts et al., 2008; Barker et al., 2016), which, along with acetylcholine (ACh), is one of the two primary neuromodulators in learning from reward and punishment (Aosaki et al., 1994; Schultz et al., 1997; Atri et al., 2004; Hasselmo, 2006; Bromberg-Martin et al., 2010; Berke, 2018). The majority of DA neurons are located in the SN pars compacta (SNc) (Nair-Roberts et al., 2008). In addition to DA neurons, the SN/VTA also contains gamma-aminobutyric acid-containing (GABAergic) neurons, which are mainly found in the SN pars reticulata (SNr), and glutamatergic neurons (Nair-Roberts et al., 2008; Barker et al., 2016). VTA DA neurons are distributed across the VTA, with major populations in two lateral nuclei (Barker et al., 2016). Furthermore, the SN/VTA provides dopaminergic and GABAergic input to the NAcc (Creed et al., 2014; Salgado and Kaplitt, 2015) with modulating GABAergic projections within the NAcc that influence dopaminergic signaling (Creed et al., 2014).

The SN/VTA DA neurons project to the striatum, cortical regions, the amygdala, and the hippocampus, among others (Haber, 2014). A common categorization of DA neurons in the midbrain distinguishes three subpopulations that are organized along different pathways and serve different functions (Björklund and Dunnett, 2007): The nigrostriatal pathway (i), serving motor functions, and projecting from the SNc to the dorsal striatum (DS; i.e. caudate and putamen); the mesolimbic pathway (ii), being involved in incentive learning and motivation, and projecting to limbic regions such as the VS, NAcc and amygdala; the mesocortical pathway (iii), being involved in cognition, and projecting to cortical regions (e.g. the PFC) (Fallon and Moore, 1978; Volkow et al., 1996b; Tritsch and Sabatini, 2012; Luo and Huang, 2016). However, this categorization is now recognized as oversimplified. There is no clear spatial separation between the VTA and SNc and both share connections with limbic and cortical regions (Björklund and Dunnett, 2007). Distinguishing between the SNc and the VTA is particularly difficult in humans and primates (Düzel et al., 2009). More specifically, the VTA and dorsal cell portion of the SNc form a continuum of DA cells (Fallon and Moore, 1978; Haber, 2014), also called the dorsal tier, projecting to the VS (Björklund and Dunnett, 2007; Haber and Knutson, 2010). The ventral and densocellular cell groups of the SNc are referred to as the ventral tier (Haber, 2014). Therefore, the origin of these projections should be considered to be the SN/VTA as whole, forming a meso-cortico-limbic system.

The BF is the major source of cortical, hippocampal, and amygdalar cholinergic innervation (Mesulam et al., 1983) and can be divided into four subdivisions referred to as Ch1-4 (Mesulam et al., 1983; Zaborszky et al., 2008). The subdivisions Ch1-3 comprise the medial septal nucleus (MS), and the vertical and horizontal limb nuclei of the diagonal band (DB). Ch4 largely corresponds to the Nucleus basalis of Meynert (NBM) (Zaborszky et al., 2008), which is a major element of the substantia innominata (SI; Ezrin-Waters and Resch, 1986). This parcellation was initially based on histological research in rodents and non-human primates (Mesulam et al., 1983) but could also be identified in humans (Zaborszky et al., 2008). In addition to cholinergic neurons, the BF also contains GABAergic and glutamatergic neurons (Gritti et al., 1993, 2006). The BF is anatomically linked with the mesolimbic system. For instance, neurons from the VS project to the NBM, which in turn provides cholinergic projections to the amygdala (Haber and Knutson, 2010; Avena and Rada, 2012). Moreover, studies in rats have shown that the BF is innervated by the SN/VTA in a topographical manner. Precisely, the DB is targeted by afferents from the medial VTA, and the SI receives input from the lateral VTA and medial SNc (Gaykema and Zaborszky, 1996).

1.4.2 The role of the subcortical brain in social information processing

Among several cortical and subcortical brain regions, the striatum, SN/VTA, and BF play a role in processing social information and shaping behavior related to social motivation. The striatum and SN/VTA respond to a broad spectrum of relevant social stimuli. For instance, studies have shown SN/VTA activation in response to fearful faces (Toller et al., 2015), social cues associated with social craving after social isolation (Tomova et al., 2020), images of the beloved person in individuals who are in love (Fisher et al., 2010), and a significant correlation between SN/VTA activity to spouse images and marital satisfaction (Acevedo et al., 2012). Similarly, the striatum shows increased activity to images of attractive persons (Aharon et al., 2001) and beloved individuals (Fisher et al., 2010).

Social norms and hierarchies influence and guide social behavior and are therefore another piece of relevant social information (Cummins, 2000; Chung and Rimal, 2016). The NAcc and SN/VTA process information on social rank (Ghosal et al., 2019), for example viewing people with high social rank and losing against a superior individual activates the VS (Zink et al., 2008). Social norms generate expectations for behavior, e.g. fair sharing, and it can be advantageous to know the trustworthiness or fairness of others for possible future cooperation. Learning whether an individual can be trusted or not and adapting behavior accordingly involves the striatum, SN/VTA, and septum in the BF (Smith-Collins et al., 2013; Diaconescu et al., 2017). The SN/VTA is involved in updating contextual social norms and detecting deviant actions (Hétu et al., 2017). Punishing individuals for violating social norms elicits responses in the DS (de Quervain et al., 2004) and watching unfair players receiving pain compared to observing fair players in pain increased NAcc activity (in men) (Singer et al., 2006) which is similar to the striatal responses to positive social interactions (Wake and Izuma, 2017) and the receipt of reward in general (Zhang et al., 2017). For a review on social information processing in the human striatum see also Bhanji and Delgado (2014).

Along the same lines, social recognition memory (i.e., the ability to remember individuals e.g., group members or rivals) is essential and is associated with the NBM and MS (Okada et al., 2021; Griguoli and Pimpinella, 2022) as research in rodents has shown. Moreover, learning to behave in a prosocial manner (i.e. actions with the intention of benefiting others) involves both the striatum and the BF, and empathy as a personality trait affects prosocial learning speed and BF activity during prosocial learning (Lockwood et al., 2016). The role of the BF in social behavior is further demonstrated in autistic spectrum disorders (ASD) where individuals experience problems with social relations, communication, and adaptive behavior, and show specific reductions in gray matter volume of the BF (Riva et al., 2011). Furthermore, ASD is associated with reduced striatal responses to social but not monetary reward (Delmonte et al., 2012). Preference for social stimuli also relates to the BF as indicated by diminished social preference after MS/DB damage (Okada et al., 2021) and inhibition of inhibitory BF projections to the VTA (Wang et al., 2021) in mice.

Together, these findings demonstrate the role of the striatum, SN/VTA, and BF in a variety of social attributes and functions including social valuation, prosocial behavior, empathy, social recognition memory and thereby helping individuals understand, evaluate, and interact with the social world around them.

1.4.3 The neural mechanisms of reward and punishment processing

The most studied response to rewarding outcomes and reward predicting stimuli is elicited in midbrain DA neurons. Single-unit recordings in animals revealed that rewarding events that occur unexpectedly excite DA neurons and lead to increased firing, often also referred to as phasic activity (Schultz et al., 1993; Schultz, 2007). When stimuli become reward predictors, e.g., through classical conditioning, the response shifts from the reward delivery to the presentation of the predictive stimulus, signaling reward anticipation. When rewards are anticipated, the actual delivery of a reward no longer elicits the phasic DA response and omission of an expected reward leads to response inhibition (Schultz et al., 1997). Discrepancies between the expectation and the outcome, are commonly referred to as prediction errors (PE) (Schultz, 2007).

Measuring the activity of small brain regions such as the SN/VTA can be challenging in human neuroimaging, but functional magnetic resonance imaging (fMRI) and electrophysiological recordings in humans have shown SN/VTA activation during reward anticipation and delivery. For instance, direct intracranial recordings from the SN in patients with Parkinson's Disease (PD) showed increased spiking activity in the human SN in response to unexpected monetary rewards (Zaghloul et al., 2009). In fMRI, the delivery of unexpected liquid and monetary rewards was associated with increased VTA activity (D'Ardenne et al., 2008). Along the same lines, the anticipation of rewards showed responses in the human midbrain for different kinds of rewards, e.g. social reward (Goerlich et al., 2017; Gu et al., 2019; Martins et al., 2021), monetary gains (Wittmann et al., 2005; Adcock et al., 2006; Krebs et al., 2011; Oldham et al., 2018), and pleasant taste (O'Doherty et al., 2002; Pauli et al., 2015) using fMRI. This thesis aims to expand our understanding of SN/VTA signaling of social incentive anticipation.

Responses to reward anticipation and delivery are also found in the terminal structures of the midbrain DA neurons, such as the NAcc, which has received more attention than the SN/VTA in the field of human neuroimaging reward research. The implication of the VS, including the NAcc, in the anticipation and delivery of monetary rewards is consistent across a wide range of studies (Knutson et al., 2001a; Adcock et al., 2006; Carter, 2009; Spreckelmeyer et al., 2009; Samanez-Larkin et al., 2010; Zhang et al., 2017) including meta-analyses (Oldham et al., 2018; Gu et al., 2019). Similarly, studies provide evidence for anticipatory responses to cues signaling prospective social rewards in the VS/NAcc (Spreckelmeyer et al., 2009; Rademacher et al., 2010, 2014; Kohls et al., 2013; Barman et al., 2015) which was further supported in recent meta-analyses (Gu et al., 2019; Martins et al., 2021). Analogous to the response of midbrain DA neurons, some studies report no NAcc activation when expected rewards are consumed (Rademacher et al., 2010; Kohls et al., 2013; Martins et al., 2021). However, there are also studies that show NAcc involvement in the delivery of anticipated rewards (Oldham et al., 2018). The interaction between the NAcc and SN/VTA and the role of DA are further emphasized by a study showing a correlation between NAcc DA release and NAcc and SN/VTA fMRI activity during (monetary) reward anticipation (Schott et al., 2008). Together, evidence from the SN/VTA, VS, and NAcc indicates shared functional characteristics in processing appetitive stimuli in the mesolimbic system.

However, as mentioned earlier, not only DA but also ACh is involved in reward processing. For example, tonically active neurons (TANs) in the striatum are thought to be cholinergic interneurons (ChIs) (Apicella, 2007) and respond to unexpected rewards (Apicella et al., 1997; Morris et al., 2004; Joshua et al., 2008) as well as to reward predicting cues (Aosaki et al., 1994; Joshua et al., 2008). Furthermore, ChIs' activity is influenced by DA neurons (Graybiel et al., 1994; Cai and Ford, 2018) and GABA neurons (Creed et al., 2014) in the SN/VTA. In turn, striatal ChIs activity can trigger striatal DA release (Threlfell et al., 2012). Together, this demonstrates the close interaction between the striatum and SN/VTA as well as between DA and ACh.

Reward-related responses are also observed in the BF. For instance, BF cholinergic neurons in the NBM and DB respond with a firing increase to reward delivery in mice (Hangya et al., 2015) and electrophysiological recordings in primates revealed that neurons in the SI and MS/DB respond to reward predicting stimuli (Wilson and Rolls, 1990; Monosov et al., 2015). Moreover, similar to DA neurons, cholinergic reward delivery signals shift to reward predicting cues during contingency learning (Crouse et al., 2020). While the roles of the mesolimbic system and BF in motivation and learning are well-documented, less is known about their interaction in these processes.

Finally, signatures of reward processing can be found in non-invasive measures of the electrical activity of large neuronal populations. Studies in humans show that positive outcome processing (monetary gains) involves beta-gamma (20 - 35 Hz) oscillations in electroencephalography (EEG) (Cohen et al., 2007; Marco-Pallares et al., 2008; Mas-Herrero et al., 2015; Andreou et al., 2017) as well as theta (4-8 Hz), alpha (8-13 Hz), and beta-gamma oscillations in magnetoencephalography (MEG) (Doñamayor et al., 2011). The anticipation of monetary reward is associated with theta and beta oscillations as shown in EEG and MEG (Bunzeck et al., 2011; Steiger and Bunzeck, 2017). Together, theta and beta oscillations have a prominent role in reward processing but direct measurements of neural oscillations from the human SN are scarce.

Not only rewards, but also punishments are a powerful way to influence behavior. However, the investigation of the neural mechanisms underlying punishment processing has received less attention, especially in humans (Dugré et al., 2018). Similar to rewards, animal studies have identified neural signatures of punishment processing in midbrain DA neurons, but the exact functional dynamics are still debated since the results are partly inconsistent. The most prominent response to the anticipation of aversive events and to unexpected aversive outcomes is firing depression (Mirenowicz and Schultz, 1996; Ungless, 2004; Matsumoto and Hikosaka, 2009; Wang and Tsien, 2011). In some of these studies a group of DA neurons also responded with excitation (Mirenowicz and Schultz, 1996; Matsumoto and Hikosaka, 2009; Wang and Tsien, 2011) while one suggested the origin of the excitation response in non-dopaminergic neurons (Ungless, 2004). According to the current understanding, the majority responds with firing depression while the portion responding with excitation is smaller (Mirenowicz and Schultz, 1996; Matsumoto and Hikosaka, 2009; Wang and Tsien, 2011). DA neurons within the interconnected VS also show DA release depression to aversive events followed by short excitation during a subsequent safety period and to predictors of unavoidable aversive events as well (Stelly et al., 2019).

Evidence from fMRI research in humans on punishment processing revealed increased midbrain activation during the anticipation of pain (Fairhurst et al., 2007; Bauch et al., 2014; Hennigan et al., 2015), unpleasant liquids (Pauli et al., 2015), monetary losses (Carter, 2009; Bjork et al., 2010; Oldham et al., 2018), and social punishment (Martins et al., 2021). In one study, the anticipation of monetary loss elicited both, activation increase and decrease, in different parts of the SN/VTA (Guitart-Masip et al., 2011) which possibly relates to the different types of neurons observed in animal research described earlier. The processing of aversive outcomes, such as monetary losses in a gambling task, also recruits the SN (Zhang et al., 2017).

The human VS responds to the anticipation of aversive stimuli such as unpleasant electrical stimulation (Jensen et al., 2003), monetary loss (Wrase et al., 2007; Carter, 2009; Guitart-Masip et al., 2011; Yan et al., 2016; Oldham et al., 2018), and social punishments (Kohls et al., 2013) as well as to the delivery of pain stimuli (Becerra et al., 2001) and monetary losses (Delgado et al., 2000; Zhang et al., 2017). Furthermore, striatal responses to aversive outcomes also frequently involve the dorsal striatum (Delgado et al., 2000, 2003; Filbey et al., 2013; Dugré et al., 2018; Martins et al., 2021). Together, research in animals and humans suggests that the mesolimbic system, including the SN/VTA and VS, is not only concerned with the processing of appetitive but also aversive stimuli.

The processing of aversive stimuli further involves the BF. Lesion studies in rabbits and mice show impaired aversive learning after lesions to the MS (Berry and Thompson, 1979) and NBM (González et al., 2000). Recordings in monkeys revealed that neurons in the SI and MS/DB respond to the anticipation of punishment (Wilson and Rolls, 1990; Monosov et al., 2015) as well as to expected and unexpected punishment outcomes (Monosov et al., 2015; Robert et al., 2021). Especially cholinergic neurons in the NBM and DB were found to respond with increased firing to the delivery of punishment in mice (Hangya et al., 2015). Moreover, in monkeys, cholinergic striatal TANs signal the delivery and anticipation of aversive stimuli (Ravel et al., 2003; Joshua et al., 2008). In terms of neural oscillations, theta oscillations in EEG relate to monetary losses (Cohen et al., 2007; Marco-Pallares et al., 2008; Mas-Herrero et al., 2015; Andreou et al., 2017). Together, animal studies underline the role of the BF and acetylcholine in punishment processing but less is known about the processes in the human BF and oscillatory signatures during (social) punishment processing.

In summary, reward and punishment processing involves the SN/VTA, the VS/NAcc, and the BF and largely relates to dopaminergic and cholinergic signaling. Neuroimaging studies show that these processes are associated with neural excitation or depression, fMRI signal increases or decreases, and oscillatory differences. However, it remains unclear whether social reward and punishment anticipation are processed via the same or different mechanisms within the human SN/VTA. Furthermore, the contribution of interactions between the mesolimbic system and BF to social incentive anticipation is still poorly understood. These research gaps are addressed in study I and II of this thesis.

1.4.4 Processing of valence or salience?

In the previous section, the role of the mesolimbic system and the BF in predicting and processing positive and negative events has been described. However, it is still under debate whether these structures, or subregions of them, signal valence (i.e. positive vs. negative) or salience (i.e. potentially relevant vs. irrelevant) of future events, or both. Rewards and punishments are salient events but also differ in their valence. Other kinds of salience can be for example novelty, surprise, or contextual deviance.

The dopaminergic midbrain is a heterogeneous structure that potentially signals valence, salience, or both (Bromberg-Martin et al., 2010). Research in monkeys suggests that dorsolaterally located SN neurons respond to predictors of positive and negative events alike and therefore process these events in terms of salience while neurons in the ventromedial SN process valence since they show differential responses to these stimuli (Matsumoto and Hikosaka, 2009). Evidence from human fMRI has been inconsistent. While one study suggests differential coding of positive and negative events in the medial SN (mSN) (Zhang et al., 2017), other studies indicate the engagement of the ventromedial SN (Pauli et al., 2015) and VTA (Richter et al., 2020) in reward processing while learning about aversive stimuli was associated with the dorsolateral SN (Pauli et al., 2015). Salience processing has been found in the SNc (Richter et al., 2020), specifically in the ventral and lateral SN (vSN and lSN) (Zhang et al., 2017). Together, an increasing number of studies suggest a functional topography of the SN/VTA, but the exact delineations are unclear.

The human VS signals the valence of received positive and negative outcomes by differential responses, i.e. activation for monetary gains and inhibition for losses (Delgado et al., 2000; Zhang et al., 2017). However, during anticipation, the VS codes both positive and negative vs. neutral predictors with increased activation which argues against valence coding in the VS (Jensen et al., 2003; Kohls et al., 2013; Yan et al., 2016).

The BF responds to various salient events and their anticipation, including rewards, punishments, novel, and surprising stimuli (Zhang et al., 2019; Monosov, 2020). Regarding rewards and punishments, some studies show increased firing to both, rewards and punishments (Hangya et al., 2015) while others report firing increases to positive predictors and decreases to negative predictors (Wilson and Rolls, 1990). Recent advances suggest a functional topography of the cholinergic BF, which could account for the diversity of findings (Robert et al., 2021).

Together, parts of the mesolimbic system (SN/VTA, VS) and the BF are prominently engaged in reward and punishment processing, but it is still unclear whether, where, and how valence- and salience-related features of these stimuli are processed. These open questions are addressed in studies I and II of this thesis.

1.5 Behavioral invigoration through incentives

Rewards and punishments promote learning the (predictive) values of stimuli but also act as incentives that stimulate changes in motivation and behavior. The anticipation of incentives can lead to increasing efforts to obtain pleasant and avoid unpleasant outcomes, for example increased invigoration of movement. For instance, response times (RT) to a target stimulus are faster when money can be gained or will be lost compared to neutral outcome (Knutson et al., 2001b; Carter, 2009; Spaniol et al., 2015;

Steiger and Bunzeck, 2017; Bowen et al., 2019). Similar RT effects have been found for social reward and punishment using photo (Spreckelmeyer et al., 2009; Rademacher et al., 2010, 2014) and video feedback (Kohls et al., 2013) in the SID task. Moreover, when different amounts of reward are at stake, high rewards lead to faster RT than low rewards in the monetary (e.g. increasing amount of money) as well as in the social (photos of persons with increasingly positive mimics) domain (Rademacher et al., 2010, 2014). Similarly, another study showed increased hand-grip force for higher (one pound) compared to lower (one penny) monetary rewards (Pessiglione et al., 2007). Together, the anticipation of reward and punishment invigorates behavior, and the degree of effort is adapted to the expected amount of reward.

1.6 Age-related changes in motivation and learning mechanisms

Healthy aging is accompanied by changes in neural, cognitive, and emotional processing. After the age of 50, several abilities show a strong decline, such as perceptual speed, inductive reasoning, numeric and verbal abilities, and verbal memory while emotional functioning, semantic knowledge, and autobiographical memory remain relatively stable (Hedden and Gabrieli, 2004). Furthermore, neural systems involved in motivation and learning undergo age-related structural and systemic degeneration and show functional differences associated with aging. In the following, these changes and their impact on motivation, learning, and emotion will be explained.

1.6.1 The mesolimbic system and basal forebrain

In the mesolimbic system, age-related changes include a decrease of dopaminergic neurons in the SN by approximately 2-7% per decade between the ages of 20 and 90 (Fearnley and Lees, 1991; Vaillancourt et al., 2012), overall decreased SN volume (Bunzeck et al., 2007), reductions of gray matter volume in the DS, and increased levels of iron in the DS and VS (Steiger et al., 2016). Iron correlates negatively with myelination, indicating reduced structural integrity of the striatum (Steiger et al., 2016). Several aspects of dopaminergic neuromodulation are affected: striatal DA availability (Snow et al., 1993; Ota et al., 2006) and DA transporter density are reduced (Volkow et al., 1996a; Erixon-Lindroth et al., 2005), and DA receptor density, specifically D1 (Suhara et al., 1991; Wang et al., 1998) and D2 (Rinne et al., 1993), is reduced in the striatum as well as in extrastriatal regions such as the frontal cortex, amygdala, and hippocampus (Kaasinen et al., 2000).

The BF is also affected by age-related changes resulting in cholinergic hypofunction. For instance, normal aging is associated with moderate cell loss (Schliebs and Arendt, 2011), a decrease in grey matter (Grothe et al., 2012), and an accumulation of neurofibrillary tangles (Mesulam et al., 2004) in the BF. These changes are, however, moderate and must be distinguished from aggravated pathological changes in, for example, early and late stages of Alzheimer's Disease (AD) (Grothe et al., 2012). According to current findings, normal aging processes seem to impair the function of the BF via mechanisms other than cell loss, such as dendritic, synaptic, and axonal degeneration (Schliebs and Arendt, 2011).

1.6.2 Social motivation and emotion

Humans have an innate interest in social interaction and attachment. Even though individuals may have multiple social aspirations simultaneously, for example meeting new people at a party or spending quality time with one close friend, their priorities may differ, and some goals might be selectively preferred over others. As people age, there is a shift in the importance placed on different social and emotional goals with emotional goals taking precedence for older adults. According to the socioemotional selectivity theory (SST), the driving force behind this change is that older adults perceive the remaining lifetime as limited (Carstensen et al., 1999). Therefore, they engage more in behaviors motivated by emotional goals. For instance, in later life, humans tend to focus on close social relationships and to be more selective in social interactions (Fredrickson and Carstensen, 1990) which is one reason why the size of the social network often shows a noticeable reduction in older age (Antonucci et al., 2010) along with other factors such as the of death of a close person (Antonucci et al., 2010) and decreased mobility (van den Berg et al., 2016). Moreover, neural evidence suggests that older adults value positive social interaction over other rewarding events. In fact, cues predicting social rewards elicit stronger NAcc responses in older adults than monetary reward cues, whereas the response pattern is reversed in younger adults (Rademacher et al., 2014).

The emotional development in older age is characterized by an overall increase of positive emotions and greater emotional stability (Carstensen et al., 2011). This is potentially achieved by avoiding negativity. Indeed, older adults prefer negativity avoidance strategies for emotion regulation over positivity seeking ones (Wolfe et al., 2022) and show perceptual biases towards positive information, also known as the positivity effect. For instance, older adults have better memory for positive than negative faces and respond slower to stimuli when these are presented next to a negative face compared to a neutral face (Mather and Carstensen, 2003). Moreover, negative and neutral faces are judged less negative (Czerwon et al., 2011) and amygdalar responses to negative faces are reduced with increasing age (Iidaka et al., 2002; Mather et al., 2004).

Similarly, responsiveness to regret is reduced in healthy older adults and missed opportunities cause less activation of the VS compared to young adults (Brassen et al., 2012). Together, older adults prioritize emotional well-being and this manifests itself in cognitive and perceptual biases as well as in motivation, behavior, and neural measures.

1.6.3 Memory, learning, and incentive processing

Age-related cognitive and neuronal decline are interlinked. The relationship between dopaminergic neuromodulation and cognitive performance across the lifespan is often described as an inverted U-function with optimal DA functioning in early adulthood but insufficient signaling in childhood and old age (Li et al., 2010). For example, striatal D2 receptor binding decreases with age and is related to deterioration in recognition memory (Bäckman et al., 2000). Furthermore, the structural integrity of the BF is associated with cognitive functioning in healthy older adults, e.g. verbal learning, memory (Mesulam et al., 2004; Düzel et al., 2010) and general intelligence (Wolf et al., 2014).

In the older population, difficulties in explicit learning and memory are frequently noticed (Hedden and Gabrieli, 2004; Verneau et al., 2014). That is, consciously and intentionally acquiring and recalling information declines with age. On the contrary, implicit learning and memory occurs incidentally and without intentional effort and conscious awareness of between-stimuli relations (Rieckmann and Bäckman, 2009), such as associative learning in conditioning. It is often presumed to be well preserved in older age, but this assumption is not without controversy (Ward et al., 2020). For instance, age-related deficits have been observed in at least one form of implicit learning known as probabilistic sequence learning (Howard and Howard, 2013).

As explained in 1.3 Concepts of learning, the pairing of two stimuli can lead to associative learning, and stimuli can gain predictive value by the experience of contingencies. On the neural level, learning the predictive value of a stimulus leads to a shift in the dopaminergic reward response to the predictive stimulus, whereas the response to reward delivery is absent (see 1.4.3 The neural mechanisms of reward and punishment processing). Neuroimaging studies suggest that this process is impaired in aging and learning issues may result from compromised updating of predictions while reward value processing at outcome seems to be intact (Samanez-Larkin et al., 2014). These issues with information updating and integration seem to be associated with reduced dopaminergic functioning in the midbrain, VS, and PFC (Hämmerer and Eppinger, 2012). More specifically, reward anticipation signals are absent in the VS and midbrain (Schott et al., 2007; Dreher et al., 2008) and anticipatory value signals in the PFC are reduced (de Boer et al., 2017). Furthermore, healthy older adults show reduced PE signals in the PFC and NAcc during probabilistic learning (Samanez-Larkin et al., 2014). Using other complex learning tasks, older adults also show poorer performance and differential striatal and PFC activation compared to younger adults (Eppinger et al., 2015). These functional deviations may be linked with changes in dopaminergic neuromodulation as indicated by correlations of reward anticipation signals in the PFC with DA D1 receptor binding in the NAcc (de Boer et al., 2017) and DA availability in the midbrain (Dreher et al., 2008). Furthermore, direct evidence was provided by a study using the DA precursor levodopa (L-DOPA) vs. a placebo and showing better performance as well as restored reward PEs after L-DOPA administration in older adults while learning and PE signaling in the NAcc were impaired under placebo (due to abnormal reward anticipation) (Chowdhury et al., 2013a).

With respect to possible differences in reward and punishment processing, some studies report selective learning impairments. Some findings indicate preserved gain but reduced loss anticipation in the striatum (Samanez-Larkin et al., 2007) while others point in the other direction and show reduced PE signaling in the PFC and NAcc in reward but not loss learning (Eppinger et al., 2013) using monetary incentives. On the contrary, using social stimuli, the NAcc showed enhanced responses to reward predictors, which could relate to increased value of social rewards in aging (Rademacher et al., 2014).

On the behavioral level, a reduced ability to anticipate rewards should be associated with a decreased motivation to respond to stimuli in older adults, reflected in reduced response vigor (Hird et al., 2022). Some studies show that the anticipation of reward and punishment invigorates behavior, i.e. faster RT to gain rewards or avoid punishments, in young (see 1.5 Behavioral invigoration through incentives) but not older adults (Spaniol et al., 2015; Steiger and Bunzeck, 2017; Bowen et al., 2019). This is in line with the age-related decline of the DA system and decreased neural anticipation signals. In others, the RT effect seems to be intact in older age, suggesting intact predictive reward learning (Rademacher et al., 2014). This is surprising given the neurodegenerative processes associated with aging. However, these inconsistencies may be due to differences in the complexity of the learning task or the reward domain (social vs. monetary).

To summarize, age-related neurodegeneration and impaired learning also affect functional processes of motivation and goal-directed behavior. However, the directions of effects in the behavioral and functional neural data are mixed, and the influence of age-related changes on reward and punishment processing as well as related behavioral effects is still unclear. To address these open questions, studies I (experiment 3) and III of this thesis examine the effects of aging on social motivation, learning, and socio-emotional processing.

1.8 Changes of incentive processing in Parkinson's Disease

PD is a neurodegenerative disorder affecting the mesolimbic system, offering insights into its role in motivation and learning. The crucial pathological characteristic of PD is a loss of dopaminergic neurons in the SN that exceeds the typical age-related neuronal loss. Specifically, PD is associated with an exponential decline in the beginning of the disease, with approximately 45% in the first decade (Fearnley and Lees, 1991; Kalia and Lang, 2015). Concurrent with neuronal degeneration, PD is characterized by motor and non-motor symptoms including muscle stiffness, tremor, and bradykinesia (i.e. slow voluntary movements), cognitive impairment, executive dysfunction, depression (prevalence of 20%), learning impairments, and deficits in processing reward stimuli (Kalia and Lang, 2015; Gasiorowska et al., 2021). Clinical treatment for PD is focused on drugs enhancing DA concentration or stimulating DA receptors but can also include deep brain stimulation (Kalia and Lang, 2015).

Regarding incentive processing, fMRI measurements suggest that unmedicated PD patients do not show signals of (monetary) reward anticipation in the midbrain and VS, but instead show responses to the outcome of the reward (Schott et al., 2007) which is similar to the changes observed in healthy aging that were explained in the previous section. Abnormal anticipatory processing of monetary rewards was also found in scalp EEG recordings of unmedicated PD patients (Mattox et al., 2006). Using intraoperative electrophysiological recordings from the human SN in PD patients revealed responses to unpredicted but not predicted monetary rewards indicating the preserved function of remaining DA neurons (Zaghloul et al., 2009). However, there is no direct evidence from the human SN during the anticipatory phase and it remains unclear whether previous findings generalize to the social domain.

On the behavioral level, PD patients display problems with associative learning, as indicated by failing to learn from trial and error in a probabilistic classification task (Knowlton et al., 1996). Despite these issues and deficient predictive signaling in the midbrain and VS, some studies indicate that motivational effects of (monetary) reward anticipation, i.e. the RT effect (see 1.5 Behavioral invigoration through incentives), are preserved in unmedicated PD patients (Schott et al., 2007). Conversely, one study found that patients exhibit better learning of negative outcome avoidance after medication is withdrawn (OFF medication) whereas they show better learning from positive outcomes while medicated (ON) (Frank, 2004). Together, PD influences the neurobehavioral processes of learning and motivation, and this may be modulated by dopaminergic medication, but the differential effects are not well understood. To elucidate these issues, experiments 1 and 2 of study I investigated the effects of social feedback anticipation on motivation in PD, as well as potential modulatory effects of dopaminergic medication.

1.9 Summary and research objectives

Previous research has shown that the SN is involved in reward and punishment processing, but there is an ongoing debate about whether and how the human SN signals the valence (positive or negative) or the salience (relevant or irrelevant) of future events, or both. Furthermore, although the BF is known to play a role in learning and motivation, it is often neglected in human research and its interaction with the mesolimbic system is unclear. Aging is associated with a structural decline of these brain regions, functional changes in incentive processing, and changes in socio-emotional processing but it is not always clear how this affects learning and motivation, especially in learning from social feedback.

In general, the aim of this thesis is to investigate the subcortical neural mechanisms of anticipation of positive and negative social feedback and its effects on behavior in young and older adulthood. More specifically, the ensuing empirical studies aim to investigate a) whether the human SN processes the valence (positive or negative) of social stimuli during anticipation, b) the contribution of interactions between subcortical structures, specifically the mesolimbic system and BF, to the process of social feedback anticipation, c) the impact of aging and d) different social feedback modalities (i.e. static vs. dynamic) on behavioral outcomes related to motivation and learning processes in response to social feedback anticipation. These questions will be addressed in chapter 6.

Study I used intraoperative intracranial EEG (iEEG) recordings from the SN of PD patients to investigate whether the human SN differentiates between social reward and punishment during anticipation and outcome. On the behavioral level, motivational changes were investigated via the acceleration of motor responses to a target in the SID task, i.e. the RT effect, in intraoperative patients OFF medication, non-operated patients ON and OFF medication, and healthy young and older controls. We expected that anticipation is related to changes in oscillatory power between 4 – 30 Hz and that the RT effect is reduced in healthy older adults (HOA) and PD patients, and altered by DA medication in PD.

Study II used high-resolution fMRI in healthy young adults (HYA) to investigate how the mesolimbic system and BF interact and contribute to processing social reward and punishment anticipation. Multiple analysis tools, including mass-univariate analysis, multivariate pattern analysis, and functional connectivity analysis, were utilized. It was hypothesized that social feedback anticipation is associated with salience-related responses in all subregions of interest in the mesolimbic system and BF, valence-related responses in the mSN, and differential representations of salience and valence processing in interregional functional connectivity.

Study III aimed to investigate whether motivation in HYA and HOA is modulated by static vs dynamic social feedback, considering the ecological validity of these stimuli, and the influence of aging on evaluative learning and socio-emotional processing. We hypothesized that dynamic social feedback holds greater motivational value due to its more engaging nature, resulting in a more pronounced RT effect. Based on the results of study I, we did not expect a modulation of the RT effect by age. Further, we expected more positive evaluations of social feedback stimuli in HOA, and evaluative learning for cues predicting social feedback.

2 General methods

- Study overview
- Social incentive delay task
- Intracranial electroencephalography
- Functional magnetic resonance imaging

2.1 Study overview

This dissertation consists of three studies investigating the effects of social feedback and the underlying neuropsychological mechanisms. Study I comprises three experiments involving different cohorts. Experiment 1 includes PD patients OFF medication with intraoperative iEEG recording. Experiment 2 includes a group of non-operated patients tested ON and OFF medication in a repeated measures design, and experiment 3 includes healthy young and older adult controls. Experiments 2 and 3 used behavioral readouts only. Study II used high-resolution fMRI in healthy young adults, and study III included healthy young and older adults. All studies employed the SID task with neutral, positive, and negative social feedback. Study I and II employed photos of volunteers as feedback while study III employed photos and prerecorded videos with audio. Table 1 provides a brief overview of the studies and methods, including participant samples, feedback modality, and neuroimaging technique.

Table 1.

Method summary for study I, II, and III.

	Study I	Study II	Study III*
Participants	Experiment 1 Intraoperative PD patients n = 12; 51-71 years Experiment 2 Non-operated PD patients n = 24; 53-85 years Experiment 3 Healthy young adults n = 52; 18-32 years Healthy older adults n = 52; 51-75 years	Healthy young adults n = 36; 18-33 years	Healthy young adults n = 101; 18-35 years Healthy older adults n = 107; 50-84 years
Feedback modality	Photos	Photos	Photos Videos
Neuroimaging technique	Experiment 1 iEEG Experiment 2 - Experiment 3 -	High-resolution fMRI	-

* Please note that in study III, we combined new and previously recorded and published behavioral data (from experiment 3 in study I) to compare the SID task using photo vs video stimuli in young and older adults. PD,Parkinson’s Disease; RT, response time; SID, social incentive delay task; iEEG, intracranial electroencephalography; fMRI, functional magnetic resonance imaging.

2.2 Social incentive delay task

The SID task is the main experimental task of the research conducted in this dissertation (Fig. 1). It was designed to study the anticipatory and outcome phases of motivational processes and their neural correlates. Typically, each trial consists of three events: a cue (e.g. a rhombus), a target, and an outcome (e.g. a smiling face). The participants had to respond to the target as quickly as possible. In the reinforcement context, faster RTs are used as an indicator of increased motivation (Mir et al., 2011). Here, we used the SID task with three conditions: neutral, positive, and negative social feedback. The outcomes were tied to the cue and depended on the RT to the target. In total, there were five trial types: positive cue – hit – positive feedback, positive cue – miss – neutral feedback, negative cue – hit – neutral feedback, negative cue – miss – negative feedback, and neutral cue – neutral feedback (Fig. 1a). The neutral condition served as a control condition with respect to aspects of visual, motor, and valence processing. The RT required to achieve a hit was matched to the participants' individual RT and adapted on a trial-to-trial basis using a staircase scenario such that an average hit rate of ~83% was achieved. Specifically, the threshold for obtaining a hit is lowered after several hits in a row, increasing the difficulty of the task, while it is raised after misses such that task difficulty is decreased (Fig. 1b). All studies employed the SID task in a block design.

Depending on the research question, the task may involve different valence (e.g. neutral, reward, or punishment), quantities (e.g. low reward, medium reward, high reward) or probabilities (e.g. 25%, 50%, 75%) of outcomes as experimental conditions. Moreover, feedback stimuli can vary, and conditions may change on a trial-by-trial basis or may be presented in a blocked fashion. Furthermore, trial timings can vary as EEG and fMRI require specific adaptations. The timings used for purely behavioral, EEG, and fMRI paradigms in this dissertation are described in the methods sections of the manuscripts.

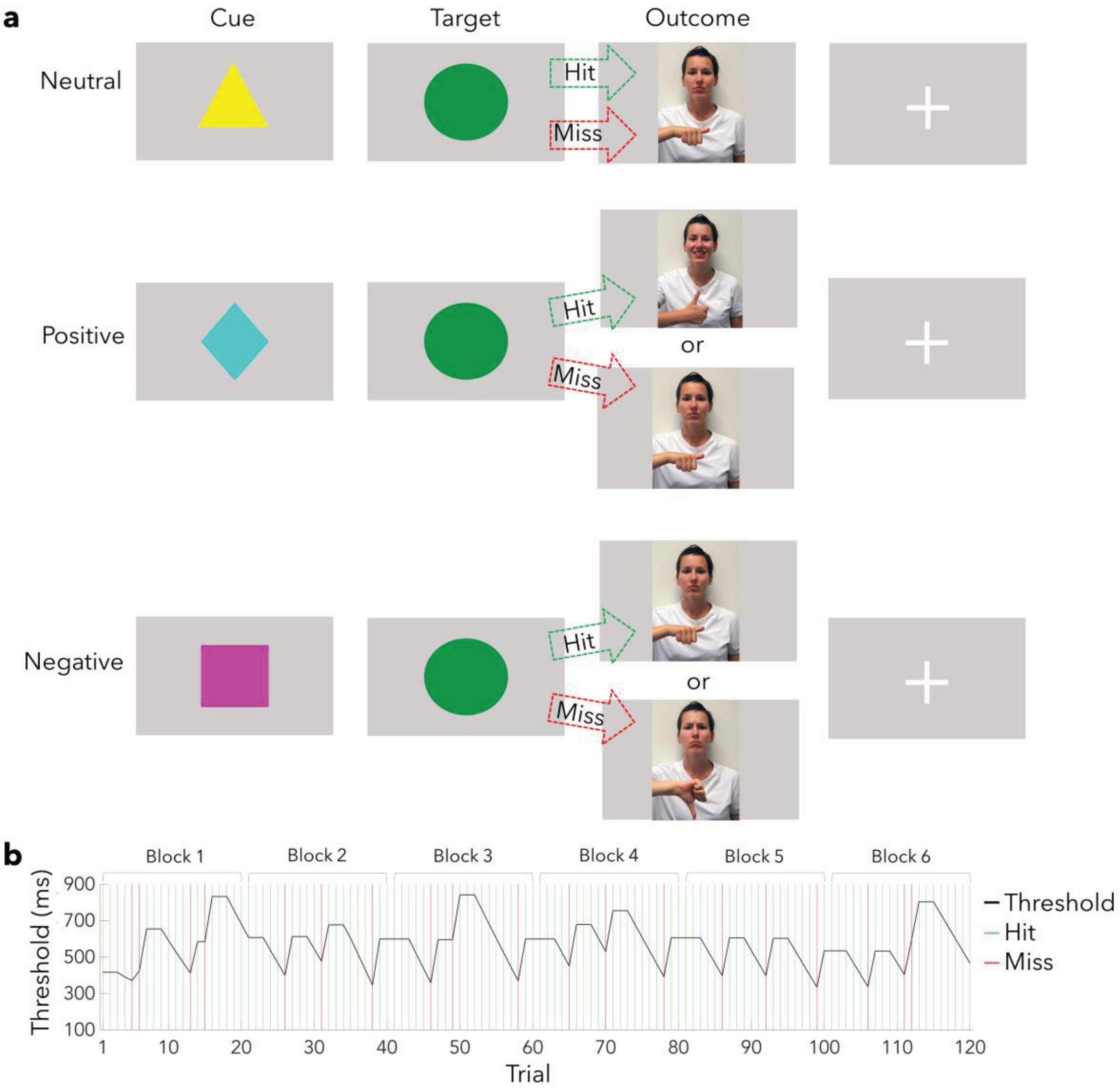

Figure 1. Design of the main experimental task. **a** The typical trial structure of the social incentive delay task. **b** Trial-wise adaptive adjustment of the response time threshold (black line) throughout the task using the staircase scenario. Hits are depicted by green vertical lines and misses are depicted by red vertical lines. Response times (RTs) below the threshold are defined as hits while RTs above the threshold are defined as misses.

2.3 Intracranial electroencephalography

2.3.1 Basic functionality of iEEG

The iEEG is an invasive electrophysiological recording technique that uses electrodes implanted inside the brain to measure neural activity. These recordings can only be obtained under specific circumstances and stem from a unique group of patients who undergo brain surgery, such as patients with epilepsy, PD, or brain tumors. For neurocognitive research, iEEG offers a unique window to the human brain as it combines the spatial resolution of fMRI and positron emission tomography (PET) with the temporal resolution of EEG/MEG (Lachaux et al., 2003). The iEEG signal is a complex combination created by different types of brain activity, including for example brief brain responses and ongoing rhythmic brain activity, referred to as neural oscillations. Two common iEEG measures are local field potentials (LFPs) or spikes (Lachaux et al., 2003). Spikes are related to fast action potentials while LFPs are mostly generated by activity from vast neuron populations, including action potentials and postsynaptic potentials (Lachaux et al., 2003; Buzsáki et al., 2012). In this work, study I analyzed iEEG LFPs that were directly recorded from the SN in PD patients.

2.3.2 Analysis methods

One approach to examining LFPs is through event-related potentials (ERPs) which is a measure of the average electrical signal associated with the sensory and/or cognitive processing of an event (Lachaux et al., 2003). The underlying rationale of ERP analysis is that the neural responses to repeated presentations of a given event enfold systematically, i.e., over the same period, with the same neural activation, and involving the same brain regions. Meanwhile, brain activity that occurs at the same time but is unrelated to the event (i.e. noise) should not be systematic over these repeated presentations and therefore be reduced by averaging (Lachaux et al., 2003). A major advantage of this approach is that it provides a high temporal resolution and a direct measure of electrical brain activity that is closely related to neurotransmission (Luck, 2014).

However, one disadvantage of ERP analysis is that oscillations that are not phase-locked to the stimulus event are canceled out by the averaging procedure (Luck, 2014). Since neural communication is not necessarily phase-locked, ERPs can only provide partial insights into the underlying neural processes (Maguire and Abel, 2013). A complementing approach that allows to analyze non-phase-locked oscillations is the so-called time-frequency (TF) analysis. It decomposes the iEEG signal into underlying frequencies by using variants of Fourier analysis or wavelet analysis (Luck, 2014) and measures their spectral power (Maguire and Abel, 2013). Frequencies are classified into bands which are typically defined as delta (< 4Hz), theta (4-8 Hz), alpha (8-13 Hz), beta (13-30 Hz), and gamma (> 30 Hz) (Luck, 2014). It is assumed that neural oscillations provide a crucial link between distributed neural populations supporting dynamic connections to integrate information between brain regions and produce behavior (Lachaux et al., 2003; Buzsaki and Draguhn, 2004).

The statistical analysis of both ERP- and TF-data can be performed via nonparametric cluster-based permutation tests which make few a priori assumptions about the data structure. In EEG, data points can be multi-dimensional encompassing temporal, spatial, and spectral information, collectively referred to as a sample. The general idea behind this test is to identify when (in terms of time) and where (in terms of sensor location and/or frequency bands) the effect of interest arises. This is achieved by comparing samples by means of a test statistic, such as an F- or t-value and then clustering all test statistics above a specified threshold corresponding to their temporo-spatio-spectral adjacency. The sum of all test statistics within the largest cluster provides the maximum cluster-level statistic and is used to evaluate the effect of interest. This procedure dramatically reduces the number of tests needed to draw statistical inferences on multidimensional data and thereby controls for multiple comparisons. The significance test is performed using the Monte Carlo significance probability (Maris and Oostenveld, 2007).

2.4 Functional magnetic resonance imaging

2.4.1 Basic functionality of fMRI

FMRI is a popular, non-invasive neuroimaging technique. The underlying rationale of this method is the hemodynamic response which describes the increased cerebral blood flow to supply active brain regions with highly oxygenated blood. The primary measure in fMRI is the Blood Oxygen Level Dependent (BOLD) signal which is caused by the local change in levels of oxygenated or deoxygenated blood and can be detected with MRI due to their different magnetic properties (Deichmann et al., 2022). As such, fMRI is a secondary measure of neural activity with a relatively low temporal resolution due to its reliance on slow metabolic changes. The major strengths of this technique are its availability, non-invasive nature, and high spatial resolution (Glover, 2011; Luck, 2014).

The measurement of magnetic properties with MRI involves three key components: the static magnetic field of the scanner (*B0*), the net magnetization (*M*), and the radiofrequency field (*B1*). When a subject is placed in the MR scanner, the body tissue's molecules align along the field lines of *B0*. Since each of the molecules has its own small magnetic moment, this alignment leads to a summation of these moments resulting in the creation of *M* which is parallel to *B0*. The measurement of *M* is achieved by the application of a radiofrequency field, i.e. *B1*, which is basically an electromagnetic wave with a specific frequency, called the Larmor Frequency. *B1* application leads to a tilt in *M* which gradually realigns with *B0*, also called relaxation, after the radiofrequency field is turned off. Specific components of relaxation can be captured by different types of scan sequences which are used to measure different characteristics of the brain. For instance, so-called T1-weighted scan sequences are mostly applied to assess brain morphology, for example to discriminate white and gray matter (Deichmann et al., 2022). T2*-weighted sequences are most used to measure brain activity, as oxygenated compared to deoxygenated blood prolongs T2* relaxation, which leads to a signal increase in T2*-weighted images. To achieve the optimal image weighting, other MR parameters such as the time interval between the application of two radiofrequency fields (repetition time; TR), time between the application of *B1* and the measurement of the MR signal (echo time; TE), and the flip angle of *B1*, can be adjusted (Weishaupt et al., 2009).

2.4.2 Analysis methods

FMRI data can be analyzed using various approaches. In this work, study II used the standard mass univariate analysis, multivariate pattern analysis, and functional connectivity analysis.

The *mass-univariate analysis* provides information about brain activation signatures (Shahhosseini and Miranda, 2022) by identifying brain regions showing greater or reduced activation in the experimental condition compared to the control condition. The analysis is based on statistical inferences on functional images and typically consists of two levels. The first level analysis is performed for each subject individually. First, regression coefficients (also called beta weights or betas) are estimated by fitting a general linear model (GLM) to the data using the hemodynamic response function. Then, statistical parametric maps are created by conducting a statistical test at each voxel, e.g. a one-sample *t*-test. These maps, also known as contrast images, are subsequently entered into a second level model. The second level analysis compares conditions on the group level using classical methods such as *F*- or *t*-tests (Friston, 2007) and can be performed on the whole brain or on a priori defined regions of interest (ROIs) (Poldrack, 2007).

Functional connectivity analysis examines the statistical dependency among brain responses by exploring the correlation of the activity in different brain regions. As such, it is an undirected, symmetrical measure of inter-regional interaction (Göttlich et al., 2015). This method is based on the idea that different brain areas are functionally linked and constantly exchange information (Shahhosseini and Miranda, 2022). Moreover, baseline correlations should change during task execution (Rogers et al., 2007). As such, this approach extends the mass-univariate analysis by providing insight into the organization of functional communication in the brain (Shahhosseini and Miranda, 2022). The betas of the first level GLM are used for inter-regional correlation. In the seed-based connectivity analysis, the mean betas of a specified region (i.e. the seed) are correlated with all voxels inside of a ROI or the whole brain. Then, all correlations are z-scored creating the connectivity maps used for second level analysis on the group level. This usually involves classical methods such as *F*- or *t*-tests (Göttlich et al., 2015).

Multivariate pattern analysis yet uses a different approach to identify patterns of brain activity associated with cognitive processes. Here, we used multivariate decoding which analyzes the mapping of multiple dependent variables, i.e. the voxels, onto one or more independent variables simultaneously. By combining information across multiple voxels, this approach can achieve greater sensitivity than the classical mass-univariate analysis. In decoding, a GLM is fitted to the non-normalized, unsmoothed data in the native space. Then, a machine learning algorithm is trained to classify conditions based on a partition of the multivariate brain data, i.e. the betas of the GLM. The data is processed in small spherical ROIs, called searchlights, typically with the size of only a few voxels (e.g. 4). The data within this searchlight is split into a training and test data set. The training set is used to train the classifier while the test set is used to assess its performance accuracy. This procedure is repeated until all voxels have been processed, resulting in an accuracy map. For group analyses on the second level, these maps are spatially normalized and smoothed. Effects of interest can then be assessed via classical parametric tests such as the *t*-test (Hebart et al., 2015). A detailed explanation of the analyses is given in the respective sections (3.3 Materials and methods, 4.3 Materials and methods, and 5.3 Materials and methods).

Manuscripts

- Study I: Anticipating social incentives recruits alpha-beta oscillations in the human substantia nigra and invigorates behavior across the life span
- Study II: Anticipating social feedback involves basal forebrain and mesolimbic functional connectivity
- Study III: Effects of positive and negative social feedback on motivation, evaluative learning, and socio-emotional processing

3 Anticipating social incentives recruits alpha-beta oscillations in the human substantia nigra and invigorates behavior across the life span

This chapter deals with the research questions a) and c) stated in the introduction (1.9 Summary and research objectives). The content of this chapter has been adapted for this dissertation for consistency and has been published in *NeuroImage*:

Sobczak A, Repplinger S, Bauch EM, Brueggemann N, Lohse C, Hinrichs H, Buentjen L, Voges J, Zaehle T, Bunzeck N. 2021. Anticipating social incentives recruits alpha-beta oscillations in the human substantia nigra and invigorates behavior across the life span. NeuroImage 118696. doi:10.1016/j.neuroimage.2021.118696

3.1 Abstract

Anticipating social and non-social incentives recruits shared brain structures and promotes behavior. However, little is known about possible age-related behavioral changes, and how the human SN signals positive and negative social information. Therefore, we recorded iEEG from the SN of PD patients (n = 12, intraoperative, OFF medication) in combination with a social incentive delay task including photos of neutral, positive or negative human gestures and mimics as feedback. We also tested a group of non-operated PD patients (n = 24, ON and OFF medication), and a sample of healthy young (n = 52) and older (n = 52) adults with behavioral readouts only. Behaviorally, the anticipation of both positive and negative social feedback equally accelerated response times in contrast to neutral social feedback in healthy young and older adults. Although this effect was not significant in the group of operated PD patients – most likely due to the small sample size – iEEG recordings in their SN showed a significant increase in alpha-beta power (9–20 Hz) from 300 to 600 ms after cue onset again for both positive and negative cues. Finally, in non-operated PD patients, the behavioral effect was not modulated by medication status (ON vs OFF medication) suggesting that other processes than dopaminergic neuromodulation play a role in driving invigoration by social incentives. Together, our findings provide novel and direct evidence for a role of the SN in processing positive and negative social information via specific oscillatory mechanisms in the alpha-beta range, and they suggest that anticipating social value in simple cue-outcome associations is intact in healthy aging and PD.

3.2 Introduction

The ability to process social information is a hallmark of human behavior, but the underlying neural mechanisms remain unclear. The SN/VTA is involved in reward anticipation and outcome processing (Haber and Knutson, 2010), but also in signaling aversive information including air-puffs to the eye (Matsumoto and Hikosaka, 2009) and electrical shocks to the hand (Bauch et al., 2014). While anticipating social (i.e. images of faces with different emotional expression) and non-social (i.e. money or pain stimuli) incentives recruits overlapping parts of the ventromedial prefrontal cortex, left inferior frontal gyrus (Park et al., 2018), and the mesolimbic system, including the NAcc, caudate nucleus and putamen (Rademacher et al., 2010), the role of the interconnected SN/VTA remains unclear. Therefore, we used iEEG recordings from the human SN/VTA in patients with PD to investigate the neurodynamics underlying positive and negative social information processing.

In non-human primates, the SN/VTA comprises two types of DA neurons: the first is distinctly activated by reward cues and rewarding events (e.g. receipt of apple juice), and depressed by aversive cues and aversive events (e.g. air-puffs to the eye); the second type is activated by both, rewarding and aversive, cues and events (Matsumoto and Hikosaka, 2009). In humans, fMRI revealed SN/VTA activation during the anticipation of rewarding (i.e., monetary gains; Krebs et al., 2011) and aversive stimuli (i.e., pain stimuli; Fairhurst et al., 2007; Bauch et al., 2014; Hennigan et al., 2015), and a direct comparison between appetitive and aversive stimuli (sweet juice vs salty tea) suggests that SN/VTA activity reflects expected value (Pauli et al., 2015). In one single study, direct microelectrode recordings from the SN in PD patients revealed the typical excitation after unexpected monetary rewards (Zaghloul et al., 2009). Together, the SN/VTA responds to both appetitive and aversive non-social information through prediction and prediction error signals.

Communication between the SN/VTA and other interconnected brain regions mentioned above (Haber and Knutson, 2010) may rely on neural oscillations, which bind the distributed neural assemblies that jointly signal information (Buzsaki and Draguhn, 2004). Indeed, a combined EEG-fMRI study in humans using monetary incentives showed that a network for feedback processing, largely overlapping with the reward circuit, communicates via theta and beta oscillations with theta being specific to losses and beta to rewards (Andreou et al., 2017). Other studies have shown that cue and outcome processing of monetary gains and losses are associated with scalp recorded theta (4–8 Hz), alpha (8– 13 Hz), and beta-gamma (20–35 Hz) band activity in healthy humans (Marco-Pallares et al., 2008; Bunzeck et al., 2011). In PD patients (ON medication), cues signaling monetary rewards have also been associated with beta oscillations in LFPs recorded from the subthalamic nucleus (STN; Duprez et al., 2019). Together, this suggests that theta, alpha, and beta band oscillations may signal non-social motivationally relevant information in the human SN/VTA.

In tasks with potential rewards, HYA show increased approach behaviors, such as speed or vigor of movements (Pessiglione et al., 2007). This is often studied using the MID task and a socially modified version, called the SID task. Studies using these tasks demonstrate faster RT following the anticipation of positive non-social and social feedback in younger and older adults (Knutson et al., 2001b; Rademacher et al., 2014), monetary gains and losses in young adults (Spaniol et al., 2015; Bowen et al., 2019), and negative social feedback in young adults (Kohls et al., 2013). In line with an age-related decline of the DA system, some studies demonstrated faster RTs following monetary gain (Steiger and Bunzeck, 2017) and loss (Spaniol et al., 2015; Bowen et al., 2019) predicting cues in HYA but not HOA. On the contrary, other studies, also using monetary gains and losses, suggest that age-related maladaptation is specific to tasks requiring more complex stimulus-outcome learning (Samanez-Larkin et al., 2014). PD is characterized by a loss of midbrain DA neurons that goes beyond typical age-related neurodegeneration and is, as one of the core symptoms, associated with slow movements (bradykinesia; Kalia and Lang, 2015). Similar to HOA, PD patients show impaired learning from feedback in probabilistic learning tasks (Knowlton et al., 1996; Frank, 2004) or reward / loss learning tasks (using monetary gains and losses; Schott et al., 2007) but it remains unclear how this translates to the social domain. While this is a specific research question, PD patients that undergo brain surgery offer a unique research method to directly record EEG data from the SN.

Using the SID paradigm in older participants and PD patients poses certain challenges since not only learning but also socioemotional processing is subject to change in healthy aging and PD. A prominent observation in healthy older adults is the positivity effect. It describes a bias towards positive emotional information resulting in increased attention and better memory for positive faces (Mather and Carstensen, 2003), as well as less negative ratings of negative and neutral faces (Czerwon et al., 2011). In PD, facial hypomimia (i.e. a loss or reduction of facial expressions) is commonly observed (Jankovic, 2008) but it remains unclear if this relates to problems in emotion recognition (Prenger et al., 2020). Furthermore, there is only limited knowledge about how dopaminergic treatments may affect emotion recognition (Prenger et al., 2020). While one study finds that emotion recognition is generally reduced in PD patients ON medication compared to healthy controls and further decreased OFF medication (Sprengelmeyer et al., 2003), another study suggests that dopaminergic treatment can have beneficial and detrimental effects depending on disease progression as well as comorbid dementia and depression (Delaveau et al., 2009). A possible underlying process may be the alteration of amygdala function by levodopa administration (Delaveau et al., 2005, 2009). Together, it remains unclear how age-related changes of socioemotional processing and possible impairments in disease-related emotion recognition in PD relate to behavior in the SID task.

To address these open questions, we used iEEG recordings in PD patients OFF medication (iEEG-PD-OFF) to directly measure SN activity during a SID task with cues predicting positive, negative, and neutral social feedback. We expected power changes between 4 and 30 Hz in response to positive and negative cues. Moreover, HYA, HOA, and non-operated PD patients (ON and OFF medication) performed the SID task in a behavioral study. We expected faster RTs following positive and negative cues and hypothesized that this effect would be reduced with age (HYA vs HOA) and PD (HOA vs PD), and modulated by DA (PD-OFF vs PD-ON).

3.3 Materials and methods

3.3.1 Participants

Experiment 1

In a first experiment, sixteen PD patients (referred to as iEEG-PD-OFF) participated in a study using the SID task (see 3.3.2 Paradigm) and iEEG of the SN (see 3.3.3 iEEG data recording and preprocessing). These were recruited from the Departments of Neurology and Stereotactic Neurosurgery at the University of Magdeburg, Germany. Experiments with the iEEG-PD-OFF patients were conducted during awake surgery for the implantation of a subthalamic nucleus deep brain stimulator (STN-DBS). Recordings from two patients were missing iEEG and behavioral data of one entire experimental condition due to technical issues and thus were excluded. Two patients ended the experiment before completion. For one, a sufficient amount of data remained while the other was not included in the analyses. Another patient was unable to perform the task, leaving twelve patients for the analysis (female = 4, male = 8, age range 51–71 years, *M* ± SD = 61.7 ± 7.2 years). Prior to surgery, all patients received neuropsychological assessment including the assessment of motor symptom severity, attentional performance, visuomotor processing speed and flexibility, executive functions, long-term memory, working memory, frontal-executive functions, Dementia, and Depression using the Unified Parkinson Rating Scale (UPDRS; Goetz et al., 2008) – part III, Test of Attentional Performance (TAP; Zimmermann and Fimm, 2002), Trail Making Test (TMT; Reitan and Wolfson, 1985), Regensburger Word Fluency Test (RWT; Aschenbrenner et al., 2000), Verbal Learning and Memory Test (VLMT; Helmstaedter et al., 2001), Wechsler Memory Scale (WMS-R; Härting and Wechsler, 2000), Frontal Assessment Battery in German (FAB-D; Benke et al., 2013), Mattis Dementia Rating Scale (MDRS; Mattis, 1988), and Beck Depressions-Inventar (BDI-II; Hautzinger et al., 2009), respectively. All tests were performed in German. In preparation for the surgery, patients withdrew from anti-parkinsonian medication in the afternoon on the day before (> 12 h before surgery), which will be referred to as the OFF-state. In the ON-state, patients had a mean UPDRS III score of 15.1 (SD = 5.58) and a mean score of 29.7 (SD = 9.95) in the OFF-state. All other neuropsychological measures were obtained during the ON-state. Individual demographic data, recording site, levodopa equivalent daily dose (LEDD), UPDRS III scores ON and OFF medication, and FAB scores are summarized in Table 2. The detailed individual test results of the neuropsychological assessment (TAP, TMT, RWT, VLMT, WMS-R, and BDI-II) are summarized in supplementary table A S1.

Table 2.

Individual demographic data, recording site, levodopa equivalent daily dose (LEDD), UPDRS III scores ON and OFF medication, and FAB scores for iEEG-PD-OFF patients.

Patient No.	1	2	4	6	7	8	9	10	11	12	13	15
Sex	M	M	F	F	M	M	M	M	F	F	M	M
Age	63	55	67	52	70	55	68	50	71	61	68	59
Recording Site	LH	LH	RH	RH	RH	RH	LH	LH	RH	RH	LH	LH
LEDD	925	1815	1037	603	1579	465	1057	193	0	731	1263	780
UPDRS III OFF	58	21	34	26	31	21	26	30	23	24	33	29
UPDRS III ON	10	8	25	13	11	12	12	15	15	14	24	22
FAB (total)	16	16	16	16	15	17	17	18	15	16	16	18

Note: LH, left hemisphere; RH, right hemisphere; UPDRS, Unified Parkinson Rating Scale; FAB, Frontal Assessment Battery.

Experiment 2

In a second experiment, another independent sample of 29 PD patients performed the SID task on two days (time between measurements: *M* = 3.5 days, SD = 2.2 days) without iEEG (or any other imaging method). These patients will be referred to as PD2 – or PD2-ON and PD2-OFF, depending on the medication status. For two patients, the second measurement could not be obtained, and three patients were excluded due to depression, resulting in a final sample size of 24 patients (female = 8, male = 16, age range = 53–85 years, *M* = 70.4 years, SD = 9.0 years). These were recruited during a two- to three-weeks hospital stay at the Department of Neurology. Patients were tested once during the ON-state (time between measurement and last Levodopa (L-Dopa) intake: *M* = 129.5 min, SD = 161.6 min) and once during the OFF-state (time between measurement and last L-Dopa intake: *M* = 786.3 min, SD = 163.2 min). Twelve patients performed the first test in the ON-state and the second in the OFF-state; for the remaining twelve patients it was the other way around to avoid a confound between medication status and possible training effects. All patients received assessment of motor symptom severity using the UPDRS III (ON: *M* = 31.4, SD = 11.1; OFF: *M* = 40.5, SD = 12.7), frontal-executive functions using the FAB-D (ON: *M* = 14.0, SD = 2.4; OFF: *M* = 14.9, SD = 2.2), and global cognitive function. 22 participants were assessed using the Montreal Cognitive Assessment (MoCA; *M* = 24.2, SD = 3.8; Nasreddine et al., 2005). Seven patients showed signs of cognitive dysfunction (< 22 points; Freitas et al., 2013) although clinically relevant dementia was not present. One participant was assessed using the Parkinson Neuropsychometric Dementia Assessment (PANDA; Kalbe et al., 2005) and showed slight cognitive impairment. For one of the patients, psychological assessment data was not available. Note that the UPDRS III in this sample was assessed by a different person than in the iEEG-PD-OFF group.

Experiment 3

In a third experiment, 52 HYA (female = 29, male = 23, age range = 18–32 years, *M* = 22.8 years, SD = 3.1 years) and 52 HOA (female = 29, male = 23, age range = 51–75 years, *M* = 64.0 years, SD = 6.4 years) were tested using the SID task in a behavioral version without any imaging methods. None of the HOA showed signs of fundamental cognitive decline, as verified by the MoCA (< 22 points; Freitas et al., 2013).

All participants gave written informed consent before taking part in the study. The iEEG study was approved by the local ethics committee of the University of Magdeburg, Germany, the other studies were approved by the local ethics committee of the University of Lübeck, Germany, and they were in accordance with the Declaration of Helsinki.

3.3.2 Paradigm

We used a modified version of the MID task (Knutson et al., 2000) allowing a distinction between anticipation and outcome processing (Lutz and Widmer, 2014). Here, we employed social incentives using photographs of five male and seven female volunteers (i.e. people who did not take part in this study and were unfamiliar to the participants) showing neutral, positive or negative mimics (i.e. neutral, smiling, angry) and gestures (i.e. right thumb horizontally, right thumb up, right thumb down). Photos of two female volunteers were used in a training, the remaining ones were used in the main task. This experiment was performed using Cogent Graphics developed by John Romaya at the Laboratory of Neurobiology at the Wellcome Department of Imaging Neuroscience.

First, the participants performed a simple RT task consisting of 50 trials. The RTs from this task were subsequently used in a staircase scenario of the SID task, which will be described below. After the RT task, participants performed the SID task and a short training (Fig. 2). The SID task comprised three conditions (neutral, positive, and negative) in a block design (six blocks, 120 trials in total, two blocks per condition and 20 trials per block). The training consisted of one block per condition (20 trials each). The order of blocks was randomized to prevent ordering effects. Each trial consisted of a cue (1200 ± 500 ms), a target and a feedback (750 ms) which depended on the RT to the target. Trials were separated by a fixation cross (1050 ± 500 ms) and the cues were randomly assigned to the conditions. At the beginning of each block, participants were informed about the condition of the upcoming block. In the neutral condition, participants received neutral social feedback regardless of their performance. In the positive condition, participants received positive feedback for hits and neutral feedback for misses. In the negative condition, participants received neutral feedback for hits and negative feedback for misses.

The average hit rate was 83%. To ensure similar hit rates across participants, we applied a staircase method including a threshold calculation on the basis of hits and misses. Hits were defined as RTs below a threshold, while misses were defined as RTs above a threshold. The threshold was adjusted to the current individual performance on a trial-by-trial basis. More specifically, the threshold for the first trial of the SID was defined as the 80th percentile of all RTs in the RT task. Depending on the outcome (hit or miss) the threshold for the next trial was calculated. In the first and second trial of a block, the current threshold was either kept, following a hit, or set to the 100th percentile of all RTs in the RT task, following a miss. For all remaining trials, we applied a so-called three-down one-up rule (Leek, 2001): after three hits in a row, difficulty was increased by subtracting one standard deviation of all previous trials' RTs from the current threshold. After one or two hits, the threshold was kept the same as in the trial before. After one miss, difficulty was decreased by adding three standard deviations of all previous trials' RTs to the current threshold.

Finally, participants rated their subjective emotional valence to the photos of the SID task on a mannequin scale (Bradley and Lang, 1994) from one (negative) to nine (positive). All photos were presented twice in randomized order. HYA and HOA had to respond within four seconds. Since PD leads to bradykinesia, the PD2 group faced no time constraint. Note that we did not collect rating data on the photos from iEEG-PD-OFF patients. iEEG-PD-OFF patients performed the RT task and the SID training on the day before the surgery while withdrawing from medication. The SID task with simultaneous iEEG recording was conducted on the following day during surgery. HYA, HOA, and the PD2 group performed all tasks in one session.

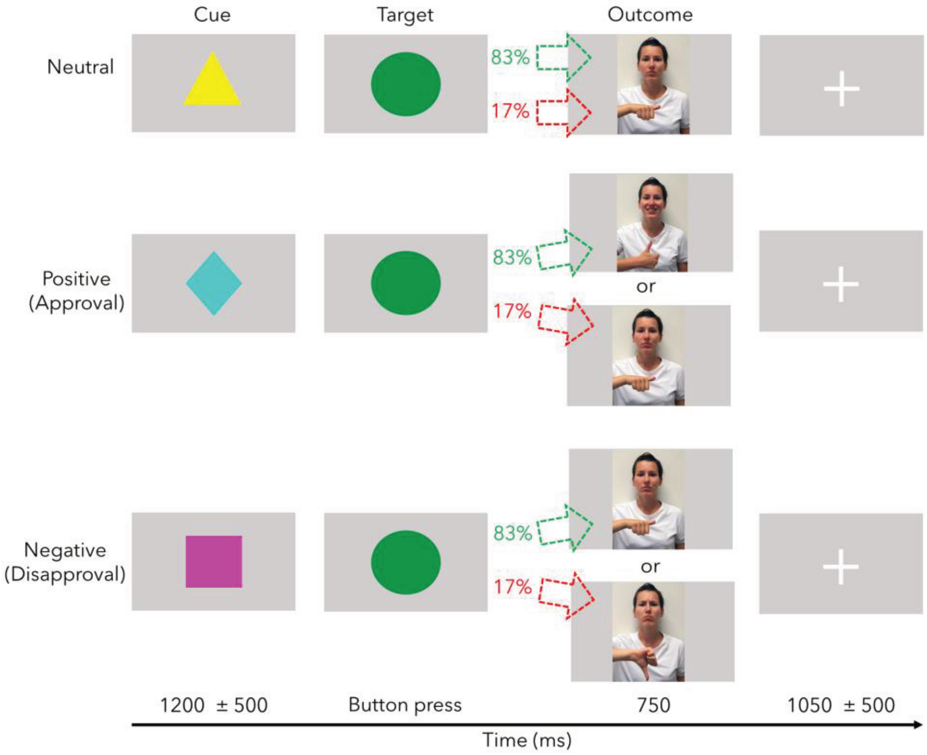

Figure 2. Trial structure and timing of the social incentive delay task. Depending on individual RTs to the target, three different types of social feedback were provided in six different blocks of 20 trials each (see 3.3.2 Paradigm).

The three conditions (neutral, positive, negative) did not change on a trial-by-trial basis but between blocks, to keep the task as simple as possible for our iEEG-PD patients. In fact, while undergoing (awake) surgery, working memory capacity and attentional resources may be reduced (see 3.5 Discussion) and an event-related structure could have been too challenging. In order to be able to compare the different groups, we did not change the block design in the course of our study.

3.3.3 iEEG data recording and preprocessing

We simultaneously recorded scalp-EEG from three electrodes (Fz, Cz, Pz) and unilateral iEEG from the SN (left hemisphere = 6, right hemisphere = 6) during DBS surgery. Placement of the intracranial electrodes was performed stereotactically via microelectrode recording (MER). During MER, the neurosurgeon introduces five microelectrodes into the subcortical target region. First, monitoring the recorded electrophysiological signal, the upper and lower margins of the STN were determined. Second, as the SN is located directly underneath the STN, the microelectrodes were placed slightly below the STN (1,2 mm in 0.5 mm steps) until the electrophysiological activity of the SN could be recorded. During this critical procedure, we had a time window of 15 min to conduct our measurement. Data were acquired using the ipsilateral mastoid as online reference and an electrode over the ipsilateral parietal cortex as ground. Digitization was at 2.5 kHz with an online low-pass filter at 1 kHz and a vertical resolution of 0.1 μV using a BrainAmp System (Brain Products GmbH, Gilching, Germany).

We analyzed event-related local field potentials (ER-LFP) and time frequency (TF) representation of the cue phase data using MATLAB 2016b and the FieldTrip toolbox (Oostenveld et al., 2011). For both types of analyses, electrodes were initially re-referenced to the guide tube. Signals from electrodes located in the SN were included in the analyses while the other electrodes were discarded. Information about electrode location (within vs outside the SN) was provided by the surgeon on the basis of a pre-operative MRI and CT as well as the neuronal discharge pattern as recorded during electrode implantation (MNI coordinates for electrode positions cannot be provided since the MR/CT images were not normalized to MNI space). For the ER-LFP analysis, data were high-pass filtered at 0.5 Hz and low-pass filtered at 20 Hz using two-pass finite impulse response (FIR) filters. Filtered data were epoched from −2000 s to 2000 ms around the event onsets, resampled to 250 Hz and epoch durations were redefined as −100 ms to 700 ms. Subsequently, data were visually inspected for artifacts and manually rejected if necessary. On average, 25.67% (SD = 13.33%) of cue trials were removed. Then, individual condition means were computed by averaging over all epochs per condition for each participant. The individual condition means were baseline-normalized using the interval from −100 ms to 0 ms relative to event onset and a decibel baseline type. When more than one electrode per participant was identified within the SN, the signals from these electrodes were averaged. Finally, condition grand means were computed by averaging across all participants.

For the TF analysis, data were high-pass filtered at 0.5 Hz and low-pass filtered at 40 Hz using two-pass FIR filters, epoched from −1500 ms to 200 ms, resampled to 250 Hz, and subsequently visually inspected for artifacts and manually rejected if necessary. On average, 11.1% (SD = 15.43%) of cue trials were removed. Eventually, condition-specific spectrograms were calculated in a frequency range from 4 Hz – 30 Hz (0.2857 Hz steps), thus including theta (4–8 Hz), alpha (8–13 Hz) and beta (13–30 Hz) frequency bands, for each participant. Spectrograms were calculated by a time-frequency transformation using a single Hanning taper with a frequency-dependent window length and 4 cycles per time window. Then, data were baseline-normalized using the interval from −100 ms to 0 ms and a decibel baseline type. In the case of multiple electrodes being located in the SN in one participant, signals from these electrodes were averaged before finally calculating condition grand averages across all participants.

For the sake of completeness, ER-LFPs of the outcome phase were analyzed in a similar way as for the cue phase data, but epochs were defined from −100 ms to 750 ms. On average, 25.82% (SD = 12.74%) of trials were removed. Note that the outcome analysis included all trials of the neutral condition because the feedback was always neutral. For the other two conditions, only the hit trials were included because the emotional valence of the feedback photos differed for hits vs misses and could therefore not be analyzed together. Since outcome processing was not the focus of the study and, hence, trial structure and timing were not designed accordingly, we did not perform TF analysis on the outcome data.

To summarize, iEEG data quality was ensured by careful stereotactic placements of the electrodes by the surgeon, visual inspection of the raw EEG signal and preprocessing (including removal of trials containing artifacts). Since time was limited by the surgery, the experiment had to be rather short but still contained 40 trials per cue condition. Finally, it should be noted that iEEG signals are not attenuated by the scalp, which is also beneficial.

3.3.4 Statistical analysis

Response time

We measured RT to the target as an indicator of motivation depending on the possibility to gain positive feedback or to avoid negative feedback. All trials (hits and misses, see 3.3.2 Paradigm) were included in the analysis. In order to control for trials in which participants initiated the motor response before target presentation and trials contaminated by attentional lapses, individual data was filtered for improbably short (< 200 ms and < 25th percentile – 1.5 * inter quartile range) and improbably long RTs (> 75th percentile + 1.5 * inter quartile range). Based on the filtered RTs, condition-specific average RTs were calculated for each participant.

Participants were defined as outliers and excluded from the analysis when their average RT exceeded the 75th percentile by more than three times the interquartile range. All 52 HOA were included in the analysis while in the HYA group one outlier was excluded, resulting in 51 subjects. In the iEEG-PD-OFF group, one outlier was excluded from the behavioral analysis, resulting in eleven subjects. Two outliers were identified and excluded in the PD2 patient sample. One patient was unable to perform the task due to dyskinesias in the ON-state and was excluded from this analysis, leaving 21 subjects for the analysis.

RTs of HYA and HOA were compared using a permutation *F* -test with a 2 × 3 mixed (between-subject factor group; within-subject factor condition) design in MATLAB. Pair-wise comparisons of the condition factor levels were calculated using permutation paired *t* -tests with an adjusted alpha-level of 0.016 (0.05 / 3) using Bonferroni correction. RTs of the iEEG-PD-OFF patients were analyzed in a permutation *F* -test with a 1 × 3 repeated measures design. The PD2 sample was analyzed using a permutation *F* -test with a 2 × 3 repeated measures (within-subject factor medication status ON/OFF; within-subject factor condition) design. Permutation paired *t* -tests were used for pair-wise comparisons of condition factor levels with an adjusted alpha-level of 0.016 (0.05 / 3) using Bonferroni correction.

The permutation tests were computed as followed: first, empirical test statistics of interest (*F*-values or *t*-values) were obtained for the original sample. Second, to create the null condition, factor labels were permuted. Between-factor labels were permuted between subjects, while within-factor labels were permuted within subjects, keeping measurements together that belonged to the same subject. Third, the test statistics were computed for the permutation samples. In each analysis, 5000 permutation samples and corresponding test statistics were obtained to generate the permutation distribution. Fourth, it was assessed whether the observed empirical test statistic was unusually large for the distribution of permutation test statistics using a Monte Carlo p-value.

Furthermore, we compared RTs of HOA and iEEG-PD-OFF patients using a permutation F-test in a 2 × 3 mixed (between-subject factor group; within-subject factor condition) design with subsampling in MATLAB. Since the groups had unequal sample sizes and unequal variances with larger variance in the smaller sample, a standard permutation test would result in inflated Type I error rates (Mewhort et al., 2009). Therefore, we employed a bootstrap-like permutation test adapted from (Mewhort et al., 2009). Specifically, we took 100 subsamples ($n = 11$) without replacement from the HOA data to match the sample size of the iEEG-PD-OFF patients group. For each of the subsamples, a permutation test was calculated applying the standard procedure as described above. Finally, we calculated the proportion of subsample permutation tests (out of 100) rejecting the H0 as an estimate of the overall probability of the H0 being rejected.

Additionally, we used Bayesian repeated measures ANOVAs to further analyze the non-significant effect of condition from the permutation F-test with the 1 × 3 repeated measures (within-subject factor condition) design in the iEEG-PD-OFF sample and the non-significant interaction in the permutation F-test with the 2 × 3 repeated measures (within-subject factor medication status ON/OFF; within-subject factor condition) design in the PD2 sample. The analyses were conducted in jamovi (Version 1.1.9; The jamovi project, 2020) using the default settings. For the iEEG-PD-OFF sample, we report the evidence against the effect of condition. For the PD2 sample, we report the evidence against the interaction which is calculated by dividing the evidence for the main effects model by the evidence for the main effects plus interaction model. See supplement A S2 - S4 for additional analyses.

Emotional valence

We measured subjective emotional valence of the feedback stimuli to investigate the congruence between intended and subjectively perceived valence. Each photo of the five male and five female volunteers which were used in the SID task was rated twice. We averaged the emotional valence ratings per photo and then per condition (neutral, positive, negative) for each subject to obtain the average subjective emotional valence of each condition.

Participants were excluded from the analysis when missing 20% or more data from the rating task. This led to one exclusion in the HYA group and one in the PD2 sample. Participants were defined as outliers and excluded from the analysis when their average rating exceeded the 75th percentile by more than the three times the interquartile range. Accordingly, one outlier was excluded in each of the following groups: HYA, HOA, and PD2 sample. Thus, 50 HYA, 51 HOA, and 22 PD patients were analyzed.

We compared ratings of HYA and HOA using a permutation *F*-test with a 2 × 3 mixed (between-subject factor group; within-subject factor condition) design and ratings of the PD2 sample using a 2 × 3 repeated measures (within-subject factor medication status ON/OFF; within-subject factor condition) design following the same steps as in the analysis of RT. Permutation paired *t* -tests were conducted as pair-wise comparisons of condition factor levels with an adjusted alpha level of 0.016 (0.05 / 3).

Intracranial EEG data

Statistical analyses were conducted using FieldTrip (Oostenveld et al., 2011) and custom MATLAB scripts. First, ER-LFP analysis was run for cue and outcome phase separately. Here, corresponding time windows were defined as 0 to 700 ms (cue) and 0 to 750 ms (outcome) relative to event onset, respectively. Second, TF analysis was run for the cue phase from 0 to 600 ms relative to event onset but not for the outcome since trial structure and timing did not allow for this kind of analysis. Specifically, a cue was presented for a minimum of 700 ms and directly followed by the target, which was associated with a motor response, followed by the outcome. Since ER-LFP analysis is temporally more precise, the properties of our TF analysis would have led to temporal smearing between motor response and outcome associated activity.

Differences between conditions were assessed using the nonparametric permutation test based on dependent samples F-statistics with 1000 random partitions implemented in FieldTrip (see Maris and Oostenveld, 2007 for a detailed description of this method). To be exact, the sample significance threshold was defined as a two-sided nonparametric common threshold of 0.05 and the cluster minimum size was set to 0, which is the default. The analysis was corrected for multiple comparisons using the maximum cluster-level test statistic and effects were evaluated by means of Monte Carlo *p* -values. Note that a cluster-based permutation test does not provide a statistical test of the exact times and frequency ranges of effects. Therefore, cluster extensions should be interpreted with care, time-wise and frequency-wise. However, including only very few a priori assumptions, it provides a fairly objective and data-driven alternative compared to a visually based preselection of a time and frequency range.

Since the initial analysis did not reveal any significant effects for the ER-LFP data, no pair-wise comparisons were performed. However, to clarify the direction of the significant effects in the TF data, condition-specific cluster power averages were computed by averaging the power values of all samples within the significant cluster derived from the *F*-test. Differences between cluster power averages were assessed by means of permutation paired *t* -tests, following the same logic as described for behavioral data analysis of HYA vs HOA. Results of permutation paired *t*-tests are reported at an adjusted alpha-level of 0.016 (0.05 / 3). Since the pair-wise comparison of the averaged cluster power between the positive and negative condition indicated no significant difference, the TF data was averaged across the positive and negative condition and compared to the neutral condition using a dependent samples cluster-based permutation *t*-test.

Correlations of response time and UPDRS III OFF with intracranial EEG data

To establish a link between behavior and electrophysiological measures, we conducted two analyses using the cluster which was identified by the *F*-test. In the first analysis, we correlated the average RT with the averaged power of the cluster for each condition. Here, one behavioral outlier was excluded, leaving eleven participants for the analysis. In the second analysis, we correlated RT with the average cluster power on the single-subject level using RT and average cluster power of corresponding trials. The resulting correlation coefficients were transformed into Fisher's z. The z-values of each condition were tested against zero using one-sample *t*-tests. Finally, we correlated the averaged power of the cluster across all conditions with the UPDRS III OFF medication to establish a link between motor impairment and electrophysiological measures. Here, one outlier in the UPDRS III was excluded, leaving eleven subjects for the analysis. Spearman correlations were used for all analyses.

3.4 Results

3.4.1 Behavioral data

Response time

On a descriptive level (Fig. 3a), HYA displayed the fastest RTs, followed by HOA, and PD patients. The PD2-OFF sample showed RTs similar to iEEG-PD-OFF patients. In the PD2 sample, RT was slower OFF medication than ON medication. We used permutation *F*-tests in mixed and repeated measures designs as well as pair-wise permutation t-tests to analyze the RT data. We report the corresponding empirical test statistics, Monte Carlo p-values, confidence intervals and standardized effect sizes (see Ruxton and Neuhäuser, 2013).

First, we compared RT of HYA and HOA in a 2 × 3 permutation F-test with the factors group (HYA, HOA) and condition (neutral, positive, negative). This analysis revealed significant main effects of group and condition (Group: $F(1, 101) = 30.83$, $p = 0.0001$, CI95% = [−0.0001 , 0.0005], $\eta^2_p = 0.233$; Condition: $F(2, 202) = 11.44$, $p = 0.0001$, CI95% = [−0.0001 , 0.0005], $\eta^2_p = 0.101$) but no significant interaction ($F(2, 202) = 0.35$, $p = 0.7022$, CI95% = [0.6895, 0.7149], $\eta^2_p = 0.003$). Pair-wise permutation t-tests showed significant differences between neutral and positive ($t(102) = 4.17$, $p = 0.0001$, CI95% = [−0.0001 0.0005], Cohen's $d = 0.411$) as well as neutral and negative ($t(102) = 3.97$, $p = 0.0003$, CI95% = [−0.0003 0.0009], Cohen's $d = 0.391$), but not between positive and negative ($t(102) = −0.34$, $p = 0.6427$, CI95% = [0.6293 0.6559], Cohen's $d = −0.033$) – see Fig. 3b.

Second, we analyzed RT of the iEEG-PD-OFF group in a 1 × 3 repeated measures permutation F-test. There was no significant difference between conditions ($F(2, 20) = 0.81$, $p = 0.4765$, CI 95% = [0.4626 0.4903], $\eta^2_p = 0.4483$ – see Fig. 3d), which might be due to the small sample size. This issue was addressed using a Bayesian 1 × 3 repeated measures ANOVA and a 2 × 3 mixed design permutation F-test with subsampling for HOA and iEEG-PD-OFF patients (see 3.3.4 Statistical analysis). The Bayesian 1 × 3 repeated measures ANOVA indicated weak evidence against the effect of condition ($BF_{10} = 0.333$). The 2 × 3 mixed subsampling permutation F-test revealed a significance ratio of 1 for the main effect of group, meaning that 100% of the permutation tests showed significant results. The significance ratios for the main effect of condition and the interaction were 0, meaning that 0% of the permutation tests showed a significant result. Fig. 3a indicates that iEEG-PD-OFF patients responded slower as compared to HOA. Together, there was a statistically significant difference in RTs for HOA vs iEEG-PD-OFF patients across all conditions but there were no significant differences in RT between conditions, and, importantly, no significant interaction between group and condition, when limiting the analysis to $n = 11$ HOA and $n = 11$ iEEG-PD-OFF patients. For an overview of the mean F-values, p-values and partial eta squared of the permutation results see Table 3.

Finally, we compared RT between PD2-ON and PD2-OFF in a 2 × 3 repeated measures design permutation F-test. The analysis revealed significant main effects of medication status and condition (Medication status: $F(1, 20) = 4.55$, $p = 0.0454$, CI95% = [0.0396, 0.0511], $\eta^2_p = 0.1854$; Condition: $F(2, 40) = 4.47$, $p = 0.0188$, CI95% = [0.0150, 0.0225], η^2_p

= 0.1830) but no significant interaction (F (2, 40) = 0.24, p = 0.7898, CI95% = [0.7785, 0.8011], η^2_p = 0.0122) – see Fig. 3c. Pair-wise permutation t-tests showed significant differences between neutral and positive (t (20) = 2.92, p = 0.0036, CI95% = [0.0019, 0.0052], Cohen's d = 0.637) as well as neutral and negative (t (20) = 2.21, p = 0.0166, CI95% = [0.0130, 0.0201], Cohen's d = 0.482), but not between positive and negative (t (20) = −0.42, p = 0.6757, CI95% = [0.6626, 0.6886], Cohen's d = −0.092). To inspect the non-significant interaction, we conducted a subsequent Bayesian repeated measures ANOVA which indicated moderate evidence against the interaction (Medication Status + Condition BF_{10} = 24.42; Medication Status + Condition + Medication Status * Condition BF_{10} = 3.52; Medication Status + Condition / Medication Status + Condition + Medication Status * Condition = 6.93). This means that the data is 6.93 times more likely under the two main effects model than under the model that adds the interaction. Together, medication accelerated overall RT in PD patients, but it had no impact on the RT effect by positive and negative social feedback.

Table 3.

Result summary of the permutation mixed F-test with subsampling comparing HOA and iEEG-PD-OFF.

Effect	Mean F (± SD)	Mean p (± SD)	Mean η^2_p (± SD)
Main Effect Group	16.33 (± 2.53)	0.00074 (± 0.00072)	0.446 (± 0.039)
Main Effect Condition	1.19 (± 0.31)	0.34549 (± 0.10038)	0.056 (± 0.013)
Interaction	0.53 (± 0.2)	0.63692 (± 0.10929)	0.025 (± 0.009)

Note: Means and standard deviations of F-values, p-values, and partial eta squared.

Emotional valence

The ratings by HYA, HOA, PD2-ON, and PD2-OFF of the images were in accordance with their intended emotion valence: positive mimics and gestures were rated as more positive than the neutral images, followed by negative images (Fig. 4). As in the analysis of RT, we applied permutation F-tests and pair-wise permutation t-tests and report empirical test statistics, Monte Carlo p-value, confidence intervals and standardized effect sizes (see Ruxton and Neuhäuser, 2013).

We compared ratings of HYA and HOA in a 2 × 3 mixed design permutation F-test. The analysis revealed a significant main effect of condition (F (2, 198) = 1080.11, p = 0.0001, CI95% = [−0.0001 0.0005], η^2_p = 0.916) but no effect of group (F (1,99) = 1.29, p = 0.2621, CI95% = [0.2499 0.2743], η^2_p = 0.01), and no interaction (F(2, 198) = 1.11, p = 0.3271, CI95% = [0.3141 0.3401], η^2_p = 0.01). Pair-wise permutation t-tests showed that ratings of

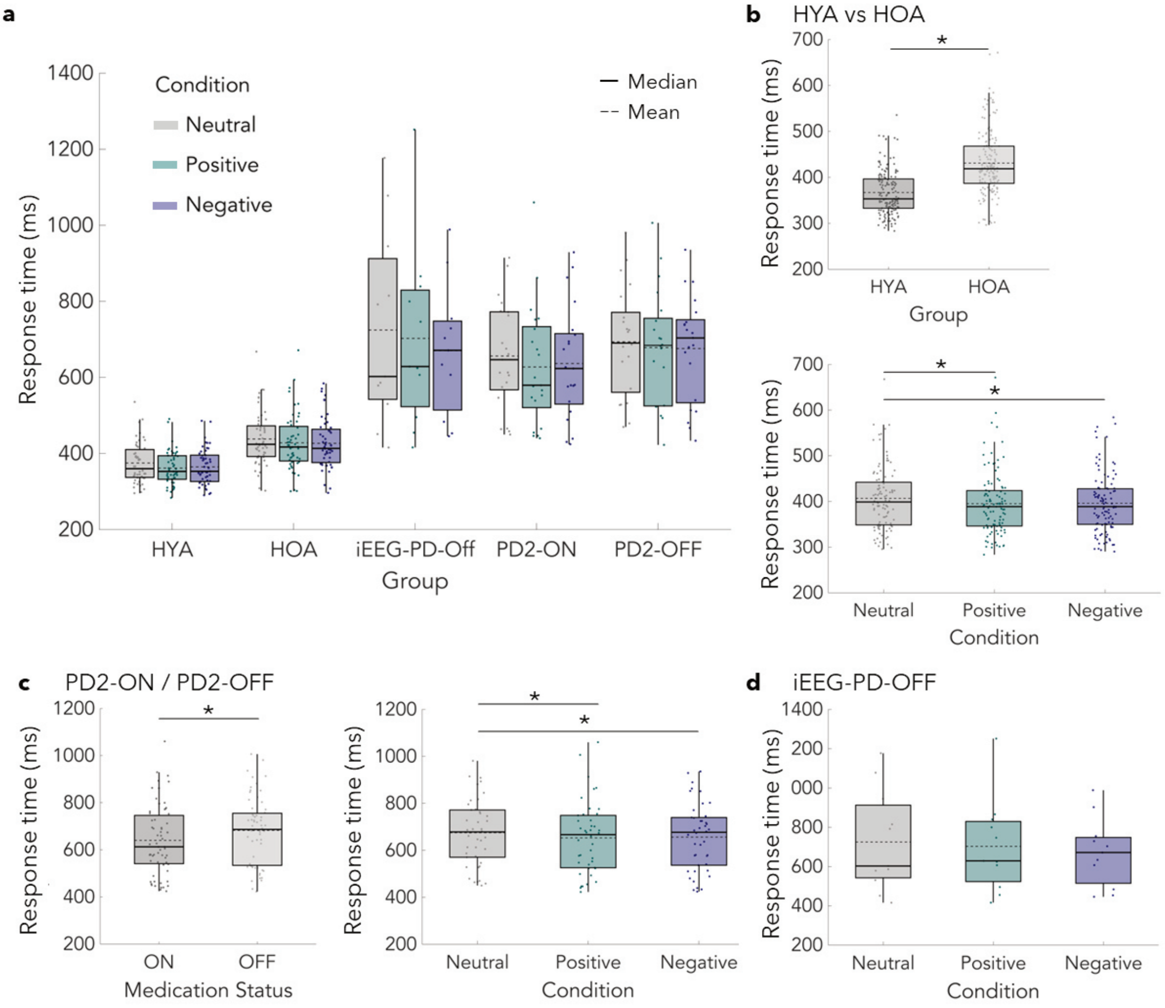

Figure 3. Mean RTs to the target in the SID task. **a-d** Boxplots showing average RTs in the SID task across groups and conditions. Bold solid horizontal lines mark the median and light dashed horizontal lines mark the mean. **a** RTs of all groups per condition. **b** Significant main effect of group (data aggregated across conditions) and condition (data aggregated across groups) for HYA and HOA. Pair-wise comparisons revealed significant differences between neutral vs positive and neutral vs negative. **c** RTs of PD2-ON and PD2-OFF medication. Significant main effect of group (i.e. medication status; data aggregated across conditions) and significant main effect of condition (data aggregated across groups). Pair-wise comparisons revealed significant differences between neutral vs positive and neutral vs negative. **d** RTs of iEEG-PD-OFF patients in all conditions. Whiskers depict data points that are the furthest form the center while still being inside the range of 1.5 times the interquartile range from the lower or upper quartile. Data points outside this range are also displayed. · indicates $p < \alpha$ (see 3.3.4 Statistical analysis).

the three feedback conditions were significantly different from one another (neutral vs positive: $t\ (99) = -40.26$, $p = 0.0001$, CI95% = [−0.0001 0.0005], Cohen's $d = -4.006$; neutral vs negative: $t(99) = 21.003$, $p = 0.0001$, CI95% = [−0.0001 0.0005], Cohen's d = 2–08; positive vs negative: $t(99) = 35.14$, $p = 0.0001$, CI95% = [−0.0001 0.0005], Cohen's d = 3.49).

The comparison of ratings between the PD2-ON and PD2-OFF in a 2 × 3 repeated measures design permutation F-test indicated a significant main effect of condition ($F(1, 21) = 57.26$, $p = 0.0001$ CI95% = [−0.0001 0.0005], $\eta^2_{\text{p}} = 0.731$) but no main effect of medication status ($F(2, 42) = 0.49$, $p = 0.5045$, CI95% = [0.4906 0.5184], $\eta^2_{\text{p}} = 0.023$) and no interaction ($F(2, 42) = 0.58$, $p = 0.6049$, CI95% = [0.5913 0.6184], $\eta^2_{\text{p}} = 0.026$). Pair-wise permutation t-tests showed that ratings of the three feedback conditions were significantly different from one another (neutral vs positive: $t(21) = -7.67$, $p = 0.0001$, CI95% = [−0.0001 0.0005], Cohen's $d = -1.63$; neutral vs negative: $t(21) = 6.7$, $p = 0.0001$, CI95% = [−0.0001 0.0005], Cohen's $d = 1.42$; positive vs negative: $t(21) = 7.7$, $p = 0.0001$, CI95% = [−0.0001 0.0005], Cohen's $d = 1.64$).

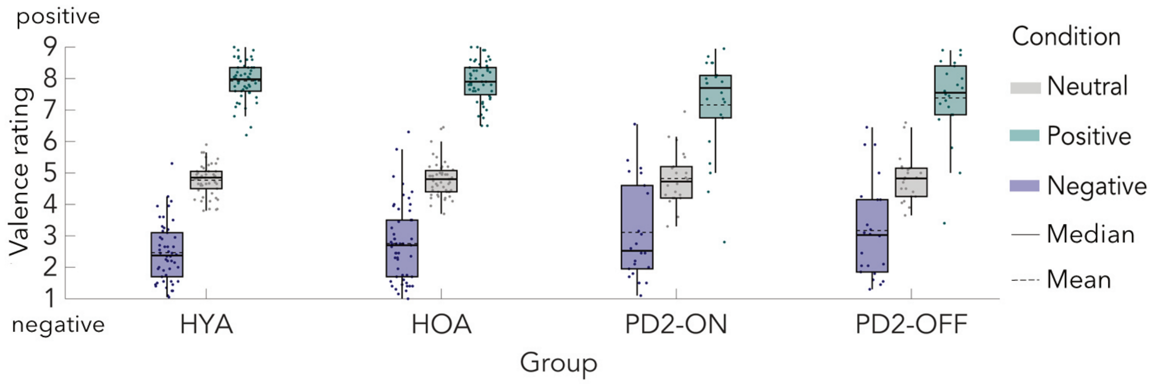

Figure 4. Rating of emotional valence for social feedback stimuli. Boxplots showing the average valence ratings of social feedback stimuli for groups and conditions. Bold solid horizontal lines mark the median and light dashed horizontal lines mark the mean. HYA and HOA showed a significant main effect of condition. Pair-wise comparisons revealed significant differences between neutral vs positive, neutral vs negative, and positive vs negative. PD2-ON and PD2-OFF showed a significant main effect of condition. Pair-wise comparisons revealed significant differences between neutral vs positive, neutral vs negative, and positive vs negative. Whiskers depict data points that are the furthest form the center while still being inside the range of 1.5 times the interquartile range from the lower or upper quartile. Data points outside this range are also displayed.

3.4.2 Intracranial EEG data

We analyzed ER-LFP and TF representation of the iEEG data. The ER-LFP analysis did not show any significant effects of condition, neither in the cue phase, nor in the outcome phase (Fig. 5). In contrast, the TF cluster-based permutation *F*-test revealed a significant effect of condition in the cue phase ($F_{cluster}$ = 15,812, *P* = 0.038, CI95% = [0.0262 0.0498]). The formed cluster was located in the alpha-beta frequency range, precisely 9 Hz to 20 Hz, extending from 260 ms to 600 ms (Fig. 6a–c). Subsequently, we compared the average cluster power between conditions using pair-wise permutation *t*-tests. We report the corresponding empirical test statistics, Monte Carlo *p*-values, confidence intervals, and standardized effect sizes. Pair-wise comparisons showed significantly higher average cluster power in the positive vs neutral (*t* (10) = −3.159, *p* = 0.0047, CI95% = [0.0028 0.0067], Cohen's *d* = −0.911), and the negative vs neutral (*t* (10) = −3.998 , *p* = 0.0013, CI95% = [0.0037 0.0024], Cohen's *d* = −1.154) condition. There was no significant difference between positive and negative condition (*t* (10) = −0.603, *p* = 0.2887, CI95% = [0.2761 0.301], Cohen's *d* = −0.174).

Finally, the TF cluster-based permutation *t* -test jointly comparing positive and negative cues vs neutral cues exposed a significant effect (F_{cluster} = 6,746, *p* = 0.004, CI95% = [0.0020 0.0039]). The cluster closely resembled the cluster from the *F*-test while starting approximately 40 ms earlier. Precisely, the cluster extended from 9 Hz to 23 Hz and 216 ms to 600 ms (Fig. 7).

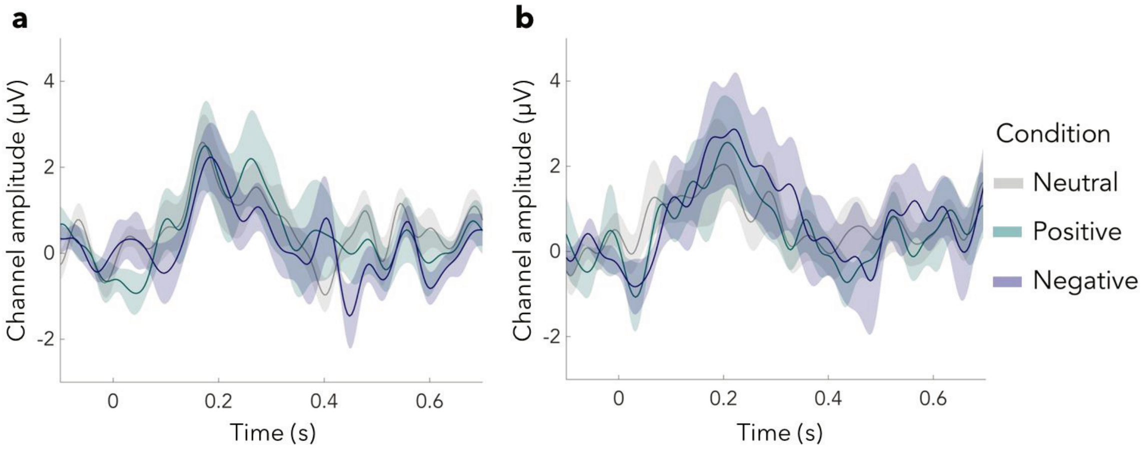

Figure 5. Event-related potentials (ER-LFPs) during the cue phase and the outcome phase for all conditions. Shaded error bars indicate standard error of the mean. The cluster-based permutation test did not reveal significant effects or formed clusters. **a** ER-LFPs during the cue phase. **b** ER-LFPs during the outcome phase (feedback presentation).

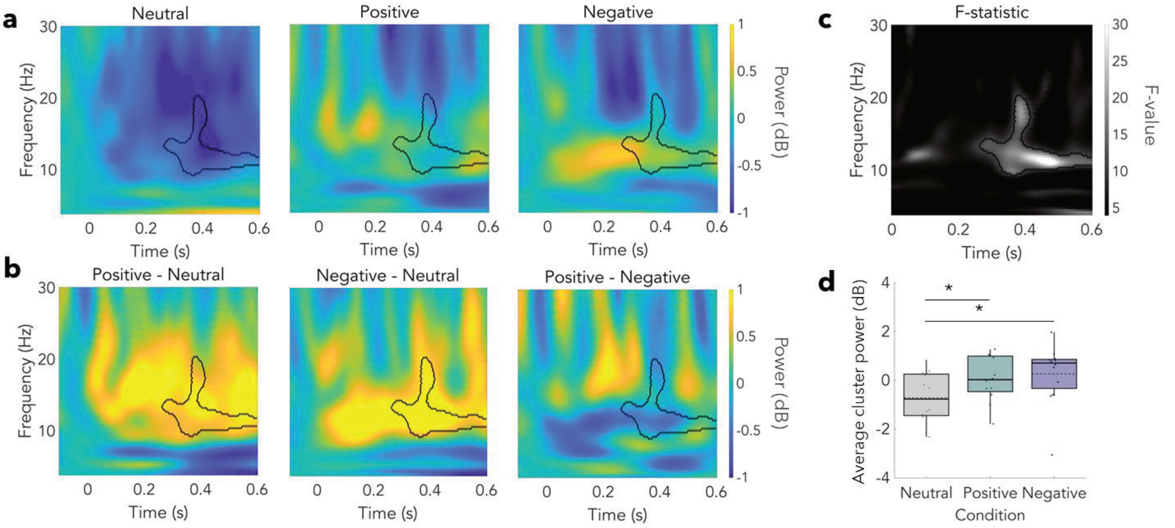

Figure 6. Oscillatory power during the cue phase. **a** Power spectra for the cue phase in each condition. **b** Power spectra contrasts for the cue phase in the SID task. Marked area indicates significant cluster identified in a cluster-based permutation *F*-test. **c** *F*-values with cluster overlay. **d** Average cluster power for each condition. Bold solid horizontal lines mark the median and light dashed horizontal lines mark the mean. Average cluster power is significantly higher in positive vs neutral and negative vs neutral condition. Whiskers depict data points that are the furthest form the center while still being inside the range of 1.5 times the interquartile range from the lower or upper quartile. Data points outside this range are also displayed. $*$ indicates $p < \alpha$ (see 3.3.4 Statistical analysis).

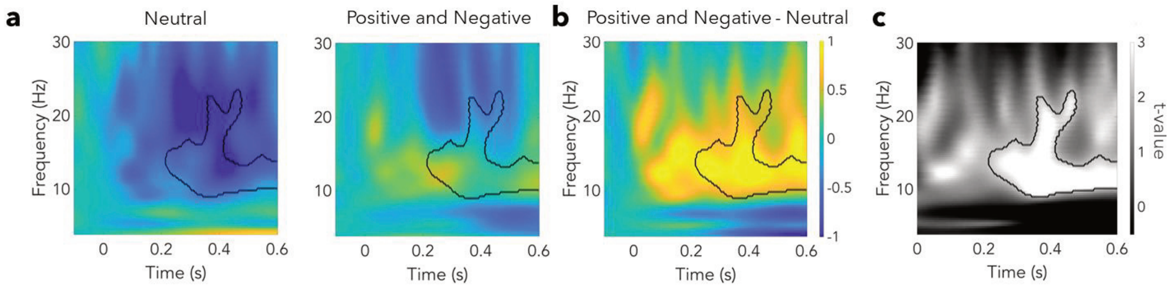

Figure 7. Oscillatory power during the cue phase in the SID task for the joint analysis of positive and negative vs neutral cues. **a** Power spectrum for the neutral condition and power spectrum averaged across the positive and negative condition. **b** Power spectrum contrast for the average of positive and negative vs neutral trials. Marked area indicates significant cluster identified in a cluster-based permutation t test. **c** F -values with cluster overlay.

3.4.3 UPDRS III OFF, response time and intracranial EEG data

Across iEEG-PD-OFF patients, individual RTs and individual power of the cluster were not significantly correlated in any of the conditions ($p > 0.2$; Fig. 8a). The second analysis, using correlations of RT and cluster power on the trial level, also did not reveal significant effects; that means, the averaged *z* -values for each condition across participants were not significantly different from zero (neutral $t(10) = 0.311$, $p = 0.761$; positive $t(10) = 0.861$, $p = 0.407$; negative $t(10) = 0.594$, $p = 0.564$; Fig. 8b). The correlation between the averaged power of the cluster across all conditions and the UPDRS III OFF medication was not significant ($p > 0.2$; Fig. 8c).

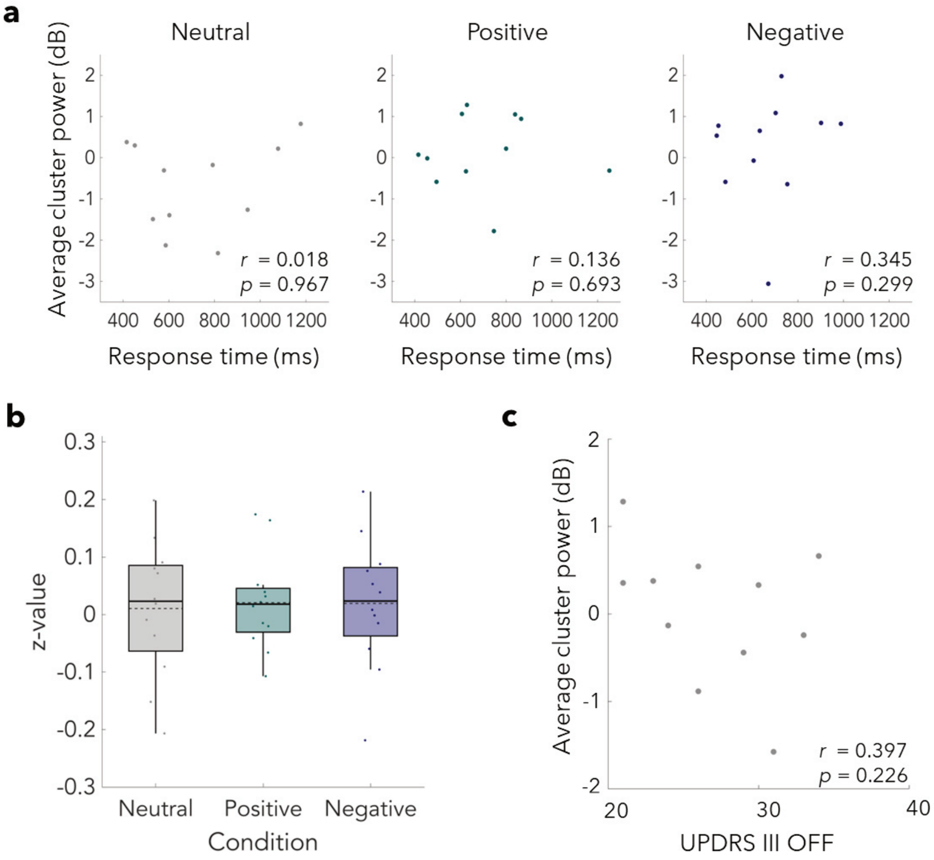

Figure 8. Relationship between neural responses and behavior in iEEG-PD-OFF patients. **a** Correlation plots showing averaged response time and cluster power. **b** Correlation coefficients from the single-subject level (RT*average cluster power) were transformed into Fisher's z. Bold solid horizontal lines mark the median and light dashed horizontal lines mark the mean. Whiskers depict data points that are the furthest form the center while still being inside the range of 1.5 times the interquartile range from the lower or upper quartile. Data points outside this range are also displayed. **c** Correlation plot showing UPDRS III scores OFF medication and cluster power averaged across all conditions.

3.5 Discussion

We investigated the underlying processes of anticipating social feedback using iEEG in PD patients and behavioral experiments in a group of HYO, HOA, and PD patients ON/OFF medication. As expected, anticipating positive and negative social feedback accelerated RTs, underlining the importance of social information in invigorating behavior. Importantly, for the first time, our findings show that the human SN signals the anticipation of positive and negative social feedback by increased oscillatory power in the alpha-beta (9–20 Hz) frequency range. Our findings provide novel insights into the physiological properties of the human SN by suggesting that alpha-beta oscillations play a role in signaling social information within the dopaminergic mesolimbic system.

Initial fMRI studies in humans showed that terminal regions of the dopaminergic midbrain, such as the striatum and NAcc, signal the anticipation and processing of reward and punishment (Knutson et al., 2000; Samanez-Larkin et al., 2007; Haber and Knutson, 2010). Subsequently, similar fMRI response patterns were reported in the human SN/VTA. For instance, anticipating monetary rewards activates not only the ventral striatum (VS) but also the SN/VTA (Wittmann et al., 2005; Adcock et al., 2006), and anticipating aversive electric shocks also recruits the SN/VTA (Bauch et al., 2014). Finally, in a study with human iEEG recordings, SN/VTA neurons signaled unexpected monetary gains, further underlining their importance in reinforcement learning (Zaghloul et al., 2009). Together, these results are compatible with our iEEG findings showing that the human SN/VTA responds to cues predicting both positive and negative social incentives. Within the context of social information processing, our data also fit the recent observation that midbrain DA neurons in mice play a role in prosocial behavior possibly via projections from the BF to the VTA (Wang et al., 2021).

How can midbrain neurons signal reward and aversive information? The long-held view that DA neurons inhibit firing to aversive cues (Schultz et al., 1997) has been challenged by electrophysiological studies in monkeys (Matsumoto and Hikosaka, 2009) and mice (Cohen et al., 2012) showing that different types of midbrain neurons have unique functional properties. Accordingly, one type of DA neurons in non-human primates is excited by both appetitive and aversive cues (Matsumoto and Hikosaka, 2009). More recently, high resolution fMRI in humans demonstrated increased activation in the SN to positive and negative cues, reflecting magnitude but not valence (Pauli et al., 2015). Therefore, our observation of enhanced alpha-beta power to both positive and negative cues might reflect, at least partly, the activity of one underlying type of neuron population. However, the SN/VTA is characterized by regional specificity and functional topography (Matsumoto and Hikosaka, 2009; Hennigan et al., 2015; Pauli et al., 2015), which cannot further be addressed in our work. In fact, LFPs mirror pre- and postsynaptic synchronous activity of neuronal populations from the entire targeted region (Jaeger and Jung, 2015). While this means limited spatial resolution, it offers a different level perspective, which has not been studied intensively with regard to reward processing.

Although it is difficult to infer single-neuron activity from LFP power, in primates DA neuron firing contributed to low frequency (<32 Hz) LFP oscillations in the SN (Pasquereau et al., 2019). Furthermore, increases in low frequency LFP power was associated with reward anticipation, which corresponds to our finding of increased alpha-beta power to positive and negative cues. Similarly, scalp recorded beta oscillations were linked to monetary reward anticipation (Bunzeck et al., 2011), monetary outcome processing (Cohen et al., 2007; Marco-Pallares et al., 2008; Marco-Pallarés et al., 2015), and fMRI activity in the VS (Mas-Herrero et al., 2015) further supporting the relationship between beta oscillations and reward processing. Indeed, communication between brain regions can be achieved by oscillations at the same frequency with a stable phase (Fries, 2005). Therefore, beta oscillations may provide a mechanism to allow communication between the SN/VTA and terminal regions including the VS and possibly prefrontal cortex.

Apart from alpha/beta oscillations, other frequency bands may play a role in social processing within the mesocorticolimbic system. For instance, on the basis of combined intracranial and MEG recordings in human patients, a recent study could show that during the processing of negative emotional stimuli theta/alpha synchrony between the habenula and PFC increases, pointing towards a functional network (Huang et al., 2021). Since the habenula constitutes a critical node for limbic and basal ganglia circuits to control motivated behaviors (Hikosaka et al., 2008), such a link might also exist in our task. However, since our data do not allow direct conclusions with regard to functional connectivity between the SN and other brain regions, future studies need to address this open question.

PD is characterized by an excessive degeneration of DA cells within the SN (Kalia and Lang, 2015), which potentially affects intracranial recordings from that region. Specifically, the recordings may involve a much smaller population as compared to a healthy system, possibly leading to attenuated signals (Fried et al., 2014). Indeed, using fMRI Schott et al. (2007) found reduced reward prediction signals in the VS of PD patients OFF medication, which is compatible with a reduced stimulus-preceding negativity – a cortical EEG response reflecting the anticipation of motivationally significant events – also in PD patients after medication withdrawal (Mattox et al., 2006). Similarly, positron emission tomography demonstrated reduced neural monetary reward processing in PD on medication (Künig et al., 2000 p.20900). However, the remaining DA neurons in PD patients responded to unexpected monetary rewards during intracranial recordings (Zaghloul et al., 2009), resembling the commonly observed pattern. Therefore, despite progressive degeneration, our intracranial recordings most likely captured signals of intact dopaminergic neurons. Whether the observed LFPs are merely attenuated or functionally altered could, theoretically, be assessed by comparing recordings from HOA and PD patients, which is practically unfeasible.

Our behavioral results of age-related slowing in HOA is in line with others showing decreased RT in healthy aging (Panek et al., 1978; Gottsdanker, 1982). In simple RT-tasks this may be caused by perceptuomotor slowing and attentional decline with age (Godefroy et al., 2010). Importantly, HOA and HYA were (contrary to our hypothesis) invigorated alike by the expectation of positive and negative social feedback, which is reflected in faster RTs following their corresponding cues. Therefore, the proposed age-related decline of the DA system may not affect performance in the SID. This may have at least two possible explanations: first, seeking social information and affiliation is an essential human motive across the life-span (Carstensen, 1998), and possible age-related changes may require a more sensitive task. Second, age-related changes in reward-learning tasks (independent of social information) may be more pronounced when cue-outcome contingencies are unknown or change probabilistically over time (Chowdhury et al., 2013a, 2013b; Samanez-Larkin et al., 2014). In our task, however, stimulus-outcome associations were explicitly stated in the instructions and fix throughout the experiment. Although this may be a limitation, it kept the experiment simple, short and therefore applicable for PD patients during the operation. Finally, our results of a preserved RT advantage for both positive and negative social feedback in HOA might be contrary to implications from neuroimaging studies, suggesting preserved gain anticipation but not loss anticipation in HOA (Samanez-Larkin et al., 2007). This might be explained by the incentive type (social vs monetary) since age-related changes have been revealed for monetary vs social reward anticipation on the neural level but not behaviorally (Rademacher et al., 2014).

In our iEEG-PD-OFF sample, there was no RT advantage by social feedback, and no direct relationship with neural activity, which might be due to the small sample size, pathological processes or a combination of both. The first aspect (i.e. sample size) is supported by our permutation *F*-test comparing subsamples of HOA ($n = 11$) with the iEEG-PD-OFF patients ($n = 11$) showing an effect of group (HOA were faster than PD patients) but no effect of condition, and no interaction between group and condition. Together with only weak evidence against the effect of condition in our Bayesian ANOVA, this indicates that the iEEG-PD-OFF group was simply too small in order to detect an equally sized effect if it were present. Indeed, a RT advantage by both positive and negative social feedback could be replicated in a larger sample of non-operated PD patients ($n = 21$) without iEEG. Despite reduced DA functioning OFF medication due to disease characteristics, these PD patients benefited from anticipating positive and negative feedback ON and OFF medication, which is contrary to our interaction hypothesis. However and as alluded to above, it is compatible with the notion that basal ganglia degeneration during healthy and pathological aging more likely impairs probabilistic stimulus-response learning rather than fixed cue-outcome association (Knowlton et al., 1996; Frank, 2004; Mattox et al., 2006; Shohamy et al., 2008; Samanez-Larkin et al., 2012, 2014). Importantly, this interpretation converges with our preserved anticipatory signal in the SN further suggesting that value anticipation in simple cue-outcome associations is intact in healthy aging and PD. Finally, the absence of an RT advantage by social feedback in iEEG-PD-OFF patients may, at least partly, also be due to the fact that these patients underwent surgery and, hence, were under anesthetic monitoring while being kept awake. Therefore, behavior in our iEEG-PD-OFF patients during the task could have been affected by impaired emotional judgement or cognitive abilities.

The absence of a direct relationship between neural activity and behavior in our iEEG-PD-OFF sample may have similar explanations: the sample may have been too small or it was modulated by anesthetics. Alternatively but not mutually exclusive, motor output is not only generated by the SN but also involves other parts of the motor system including the motor cortex, cerebellum and basal ganglia (Gazzaniga et al., 2002), which suffer from structural and functional pathological changes during PD (Blandini et al., 2000; Wu and Hallett, 2013; Burciu and Vaillancourt, 2018). Moreover, other measures of neuronal synchronization between these brain areas, such as phase-amplitude coupling, may display a direct relationship with motor output rather than power itself (de Hemptinne et al., 2013; Hirschmann et al., 2013).

As expected, healthy young and older adults rated the social feedback according to their intended valence (Fig. 4). However, there was no significant difference between age groups indicating similar emotional evaluation of social information and, therefore, no evidence in favor of a positivity effect in our healthy older adults. The absence could be due to the fact that the positivity effect depends on attentional resources and cognitive control strategies (Ziaei and Fischer, 2016). Specifically, a change in emotional assessment with age appears to relate to shifts in socioemotional goals and the desire to optimize emotional welfare (Carstensen et al., 1999), e.g., through emotion regulation. Emotion regulation, in turn, is linked with cognitive control (Mather and Knight, 2005), which may help to explain why the positivity effect may only be observed when full attentional and cognitive resources are available and can be used for active emotion regulation (Knight et al., 2007; Ziaei and Fischer, 2016). Indeed and in contrast to other studies (Czerwon et al., 2011), our valence rating included a time constraint, possibly limiting attentional resources for emotional processing. Along the same lines, attentional resources and cognitive control to emotional information may have also been limited during the actual SID task through the focus on the target rather than the social feedback, which was only presented for 750 ms.

PD patients often suffer from facial hypomimia (Jankovic, 2008) but the relationship to emotion recognition and dopaminergic medication remains largely unexplored (Prenger et al., 2020). Our data give novel insights by showing, first, no impairments in distinguishing socioemotional valence in PD patients, and, second, that dopaminergic medication does not modulate this ability. This is in line with a recent fMRI study showing no difference in valence ratings for emotional stimuli between PD patients ON medication and healthy controls. Since PD patients displayed additional prefrontal activation, this may indicate a compensatory neural mechanism to achieve comparable behavior (Moonen et al., 2017). However, in our study images were presented and labeled as neutral, positive, or negative in the SID task prior to the valance rating. Therefore, we cannot fully rule out a social desirability bias although we instructed the participants to subjectively rate all images.

With regard to our SID task, the following caveats need to be pointed out. First, positive (83%) and negative (17%) feedback was unbalanced, which was intended to not frustrate our participants through permanent negative feedback in the negative condition. This, however, implies differences in perceived saliency and possibly emotional intensity (Thayer, 1980), which could affect SN signals (Redgrave et al., 1999; Horvitz, 2000; Richter et al., 2020) and behavior (Hoofs et al., 2020). Second, the neutral condition differs from the positive and negative condition in both valence and the number of possible outcomes.

Therefore, differences in cue-related activity could reflect the possibility of one vs two different feedbacks. Although we cannot fully rule out this alternative view, our findings are in line with previous research indicating that the SN signals reward anticipation (Krebs et al., 2011) and expected value (Pauli et al., 2015). Third, the neutral feedback condition is uninformative with regard to behavioral performance, which might affect motivation and neural response patterns (Daniel and Pollmann, 2010). Fourth, since we did not include a non-social feedback condition, it remains unclear whether the observed neural effects in the SN are domain specific or independent of the type of reward and punishment. This open question could be addressed in a study using both monetary and social rewards. Finally, it remains unclear if an event-related design leads to different results, possibly due to higher predictive specificity of the cues. As mentioned in the methods, a block design was preferred here to keep the task as simple as possible for our iEEG PD patients, and it was not changed throughout the study to be able to compare the different groups.

To conclude, the anticipation of positive and negative social feedback invigorated behavior in human subjects across the life span including patients with PD. During the prediction of social feedback, the SN signaled positive and negative valence through changes in alpha-beta power as revealed by iEEG recordings. As such, alpha-beta oscillations in the SN may provide a mechanism to signal information about the possible consequences of successful and unsuccessful behavior, including social feedback, throughout the dopaminergic mesolimbic system.

4 Anticipating social feedback involves basal forebrain and mesolimbic functional connectivity

This chapter addresses the research questions a) and b) stated in the introduction (1.9 Summary and research objectives). The content of this chapter has been adapted for this dissertation for consistency and has been published in *NeuroImage*:

Sobczak A, Yousuf M, Bunzeck N. 2023. Anticipating social feedback involves basal forebrain and mesolimbic functional connectivity. NeuroImage ***274****:120131. doi:10.1016/j.neuroimage.2023.120131*

4.1 Abstract

The mesolimbic system and BF are implicated in processing rewards and punishment, but their interplay and functional properties of subregions with respect to future social outcomes remain unclear. Therefore, this study investigated regional responses and interregional functional connectivity of the lateral (l), medial (m), and ventral (v) SN, NAcc, NBM, and MS/DB during reward and punishment anticipation in a social incentive delay task with neutral, positive, and negative feedback using high-resolution fMRI (1.5mm3). Neuroimaging data (n = 36 healthy humans) of the anticipation phase was analyzed using mass-univariate, functional connectivity, and multivariate-pattern analysis. As expected, participants responded faster when anticipating positive and negative compared to neutral social feedback. At the neural level, anticipating social information engaged valence-related and valence-unrelated functional connectivity patterns involving the BF and mesolimbic areas. Precisely, valence-related connectivity between the lSN and NBM was associated with anticipating neutral social feedback, while connectivity between the vSN and NBM was associated with anticipating positive social feedback. A more complex pattern was observed for anticipating negative social feedback, including connectivity between the lSN and MS/DB, lSN and NAcc, as well as mSN and NAcc. To conclude, functional connectivity patterns of the BF and mesolimbic areas signal the anticipation of social feedback depending on their emotional valence. As such, our findings give novel insights into the underlying neural processes of social information processing.

4.2 Introduction

One of the most powerful ways to change human behavior is by feedback from others. While recent work has identified an extensive set of brain regions in anticipating and processing a diverse set of reinforcers, their precise functional properties and possible interactions remain unclear. Specifically, it is still under debate whether parts of the mesolimbic system, namely the SN/VTA and NAcc, as well as the BF distinguish between appetitive and aversive future social events. Such a functional dissociation could be based on connectivity patterns or activity of subregions. We addressed these issues, using high-resolution fMRI in combination with an established behavioral paradigm, to gain further insights into the underlying neural mechanism of motivated human behavior.

Social connectedness is a valuable resource for humans and positive outcomes of social interaction can serve as rewards while negative outcomes can serve as punishment. The SN/VTA and interconnected striatum, especially the NAcc in the ventral portion (Heimer et al., 1999), are core regions involved in anticipating appetitive and aversive events across social and non-social domains. This includes, for example, positive social feedback (Kirsch et al., 2003; Spreckelmeyer et al., 2009; Rademacher et al., 2010; Kohls et al., 2013; Barman et al., 2015; Cremers et al., 2015; Goerlich et al., 2017; Sobczak et al., 2021), monetary gains (Knutson et al., 2001b; Kirsch et al., 2003; Wittmann et al., 2005; Adcock et al., 2006; Carter, 2009; Rademacher et al., 2010; Krebs et al., 2011), pleasant tastes (O'Doherty et al., 2002; Matsumoto and Hikosaka, 2009), negative social feedback (Kohls et al., 2013; Cremers et al., 2015; Sobczak et al., 2021), monetary losses (Carter, 2009), air-puffs to the eye (Matsumoto and Hikosaka, 2009), and painful stimuli (Jensen et al., 2003; Fairhurst et al., 2007; Bauch et al., 2014). Moreover, responses of the VS to predictors of social but not monetary rewards are modulated in social anxiety disorder and autism spectrum disorder (Richey et al., 2014, 2017). These psychiatric conditions are characterized by social deficits and decreased reward value of social stimuli (Delmonte et al., 2012; Williams and Cross, 2018), which further underlines the implication of the VS in social reward anticipation. In addition to single studies arguing in favor of a role of the SN/VTA and striatum in social reward anticipation, this function is further supported by evidence from a recent meta-analysis (Gu et al., 2019). Beyond the striatum and the midbrain, social reward and punishment anticipation also engages a wide network of brain regions with partially overlapping neural substrates including the frontal cortex, pallidum, insula, and amygdala (see Martins et al., 2021 for recent meta-analysis on the neural correlates of anticipation and outcome processing of social reward and punishment in the SID task).

The BF has also long been implicated in learning and memory (Everitt and Robbins, 1997) and closely interacts with the mesolimbic system (Graybiel et al., 1994). Anatomically, the human BF is comprised of subdivisions, organized into the MS/DB and NBM (Fritz et al., 2019). Work in rats indicates that distinct areas of the BF receive specific inputs from different parts of the SN/VTA (Gaykema and Zaborszky, 1996) suggesting well defined anatomical connections between both brain regions. Functionally, electrophysiological recordings in primates have shown that neurons within the BF respond to reward and punishment (Hangya et al., 2015) and to predictors of positive and negative reinforcement (Wilson and Rolls, 1990). Corresponding to the anatomical segregation, recent work in mice indicates distinct functions of BF subdivisions in reinforcement learning (Robert et al., 2021). In humans, the septal part of the BF was found to code prediction errors about the certainty of estimated cue-outcome contingencies used for belief-updating during associative (Iglesias et al., 2013) and social learning (Diaconescu et al., 2017). Furthermore, the meta-analysis by Martins et al. (2021) showed increased activation of the septal nuclei during social punishment (avoidance) anticipation, but so far there are only first advances providing evidence for a role of the BF in social incentive anticipation in humans.

Together, parts of the mesolimbic system (SN/VTA, NAcc) and BF share anatomical connections and are involved in anticipating social incentives. In addition, studies have shown increased functional connectivity between the VS and SN/VTA during resting state (Cauda et al., 2011), the receipt of unexpected monetary gains and losses (Camara, 2008), during social and monetary reward anticipation (Gu et al., 2019), and increased functional coupling between portions of the NAcc and SN/VTA associated with salience and reward processing (Richter et al., 2020). These findings further underline that the VS and SN/VTA work together in salience processing, anticipation of social and monetary reward, and receipt of monetary reward and punishment, but associations during social punishment anticipation and the functional relationship with the BF complex remains unclear.

Currently, it is still under debate whether the SN/VTA distinguishes between appetitive and aversive predictors, reflecting valence coding, or whether it merely codes the salience of potentially relevant events. Some studies indicate no differences between anticipating positive and negative stimuli in the human SN/VTA while other studies draw a different picture, which is in line with the anatomical organization of the SN/VTA. In our own previous study we investigated predictive coding of social incentives in local field potentials of intracranial recordings from the human SN in patients with Parkinson's disease using the SID task and found significant differences in alpha-beta oscillations for positive and negative versus neutral predictors but no differential activation for positive versus negative predictors (Sobczak et al., 2021). On the contrary, electrophysiological recordings in monkeys indicate that ventromedial but not dorsolateral SN neurons discriminate between appetitive and aversive predictors (Matsumoto and Hikosaka, 2009). The results of fMRI recordings of the human SN/VTA are mixed. While one study reported a strikingly similar finding to Matsumoto and Hikosaka (2009) in humans showing valence processing of predictive stimuli in the medial but not lateral SN using monetary incentives (Guitart-Masip et al., 2011), others indicate no differences between anticipating monetary gains and losses (Carter, 2009). Another study demonstrated a slightly different functional topography where the ventromedial SN was engaged in learning about rewards and the dorsolateral SN in learning about aversive stimuli using high-resolution fMRI in humans (Pauli et al., 2015). Finally, Zhang et al. (2017) suggested a tripartite anatomical parcellation into medial, ventral, and lateral portions of the SN (mSN, vSN, lSN) with specific functional properties. Precisely, all portions of the SN responded with increased activity to monetary gains and losses in a gambling task; but only the mSN revealed greater activations to gains vs. losses and a greater response to gains compared to the lSN and vSN, indicating coding of valence in the mSN and salience in the vSN and lSN at outcome. Therefore, the SN/VTA potentially encodes both, salience and valence, and appears to be organized into distinct anatomical and functional subdivisions when using non-social information such as monetary gains and losses in humans (Zhang et al., 2017) or water drops and air puffs to the eye in animals (Matsumoto and Hikosaka, 2009). It remains unclear, however, whether a similar distinction also translates to social information in humans. Regarding the VS, valence coding has been reported in gambling tasks at outcome (Zhang et al., 2017) but not during anticipation in incentive delay tasks (Oldham et al., 2018; Martins et al., 2021).

Together, parts of the mesolimbic system (SN/VTA, NAcc) and BF are prominently engaged in reinforcement learning but little is known about the functional properties of their anatomical subdivisions and their interplay during the anticipation of social information. Therefore, this study used high-resolution fMRI of the SN (mSN, vSN, lSN), BF (MS/DB, NBM), and NAcc in combination with an SID task in humans with three conditions: neutral, positive, and negative social feedback. Behaviorally, we expected faster responses following positive and negative cues compared to neutral cues since this effect has been shown in previous work, including our own (Sobczak et al., 2021), with different types of feedback, such as written text (Williams et al., 2020), social photos (Rademacher et al., 2014; Sobczak et al., 2021), social videos (Kohls et al., 2013), and monetary incentives (Knutson et al., 2001b; Spaniol et al., 2015; Bowen et al., 2019). At the neural level, we hypothesized that social feedback anticipation involves salience-related (neutral vs. positive and neutral vs. negative) responses in all regions of interest (ROIs), and a valence-related (neutral vs. positive vs. negative, positive vs. negative cues) response in the mSN. To test this, we analyzed the cue phase using mass-univariate and more sensitive MVPA. Moreover, we investigated the functional interactions of the NAcc with SN and BF subregions, and the SN subregions with BF subregions during the cue phase using functional connectivity analysis. We expected that social feedback anticipation is associated with general, but also salience- and valence-related functional links.

4.3 Materials and methods

4.3.1 Participants

A group of 38 healthy young adults participated in this study (21 female, mean age = 23.23 years, SD = 4.03 years, age range = 18 – 33 years). All were right-handed, had normal or corrected-to-normal vision, and reported no history of neurologic or psychiatric disorders, or current medical problems. All anatomical MRI scans were reviewed by a radiologist and yielded medical findings for two subjects, which were therefore excluded from the fMRI analysis (final $n = 36$). These MRI findings were of no concern for the behavioral analyses, which therefore included all $n = 38$ subjects. This study was approved by the local ethics committee of the University of Lübeck, Germany. All participants gave written informed consent, in accordance with the Declaration of Helsinki, before taking part in the study.

4.3.2 Paradigm

The experiment was based on Sobczak et al. (2021) and included (1) a simple RT task, followed by (2) a training of the SID task (Fig. 9), (3) the main SID task, and (4) a rating of the emotional valence of the feedback stimuli from the main SID task. The first three parts were performed inside the MRI scanner, while the last part was performed outside.

The simple RT task aimed to determine the individual response speed for a personalized threshold calculation using 50 trials in total. Each trial consisted of a white circle (500 ms), a fixation cross (3000 ± 1000 ms), a green circle (target stimulus), and another fixation cross

(3000 ± 1000 ms). Participants had to respond as fast as possible to the target via button press with the right index finger.

The SID task was presented in a block design (six blocks, 20 trials per block, 120 trials in total) with three conditions (neutral, positive, and negative social feedback; two blocks per condition). The blocks were presented in a randomized fashion to prevent ordering effects. We used photographs of five male and five female volunteers showing neutral, positive, and negative mimics (neutral, smiling, angry) and gestures (right thumb horizontally, right thumb up, right thumb down) as social feedback. The short training comprised three blocks with one block per condition. Photographs of another two female volunteers were used in the training.

Each trial consisted of a cue (500 ms), a fixation cross (3000 ± 1000 ms), a green circle (target stimulus), a fixation cross (3000 ± 1000 ms), the feedback image (750 ms), and another fixation cross (3000 ± 1000 ms) at the end of the trial. Again, the participants had to respond as fast as possible to the target via button press with the right index finger. The cues (a yellow triangle, a magenta square, and a turquoise rhombus) were randomly assigned to the conditions at the beginning of the experiment. At the beginning of each block, the participants were informed about the condition of the upcoming block, i.e. they were aware of the pairing of cue and condition. Further, it was explained to them that the feedback depended on RT and which feedback they would receive for fast and slow responses in the respective condition, i.e. in the positive condition, positive feedback for fast responses (hits) and neutral feedback for slow responses (misses); in the negative condition, neutral feedback for hits and negative feedback for misses; in the neutral condition, the feedback was always neutral (Fig. 9). The difficulty was adapted throughout the task to achieve an average hit rate of 83% using a staircase method where hits were defined as RTs below a threshold and misses as RTs above a threshold (figure B S1). For details on the staircase method and the calculation of the threshold see Sobczak et al. (2021). The adaptive design and predefined feedback probabilities were not communicated to the participants.

In the final task, ratings were given on a mannequin scale (Bradley and Lang, 1994) ranging from one (negative) to nine (positive). Each photograph was rated twice for four seconds each and the order of the photographs was randomized.

All tasks were coded in MATLAB using the Psychophysics Toolbox extensions (Brainard, 1997; Pelli, 1997).

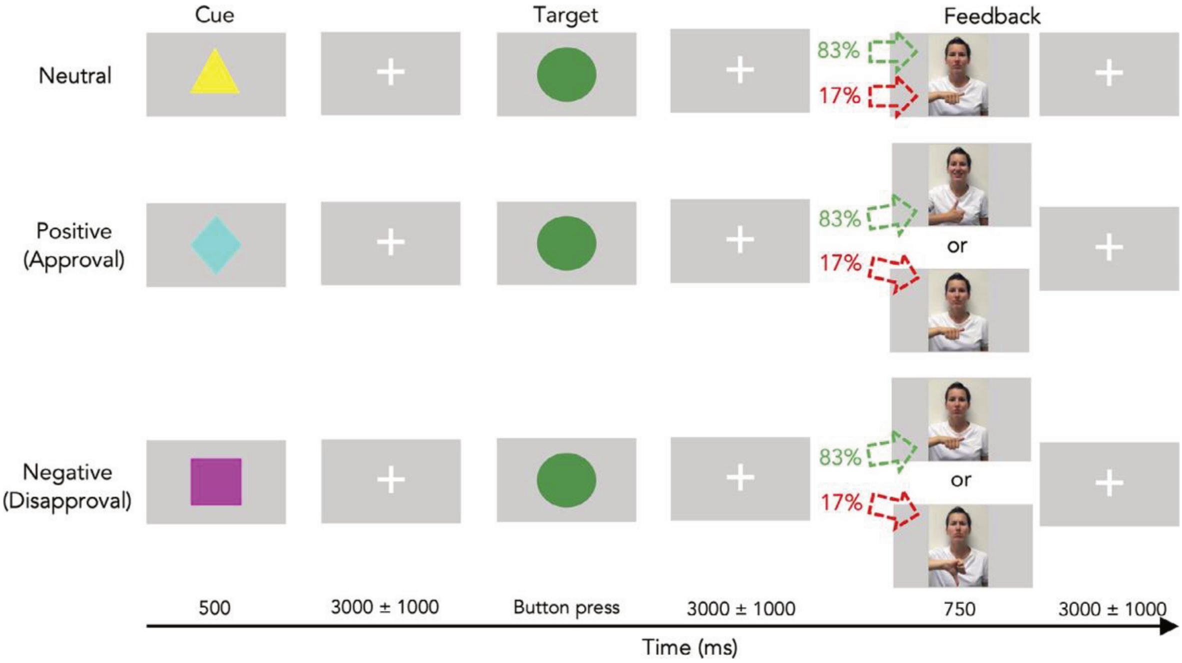

Figure 9. Experimental paradigm. The difficulty was adapted throughout the task to achieve an average hit rate of ~83% using a staircase method. In the positive and negative condition, the given feedback depended on hits (green arrows) vs. misses (red arrows) while in the neutral condition, the feedback was always neutral.

4.3.3 MRI data acquisition

We performed functional imaging on a 3-T Siemens MAGNETOM Skyra whole-body scanner (Siemens Healthcare, Erlangen, Germany) using a 64-channel head coil at the Center for Brain, Behavior and Metabolism (CBBM), University of Lübeck. For the functional images, we applied a simultaneous multi-slice acquisition with a gradient-echo EPI sequence (voxel dimensions 1.5 × 1.5 × 1.5 mm, 28 slices, 144 × 144 matrix size, TE = 26 ms, TR = 1.1 s, 60° flip angle, 1.5 mm slice thickness). To account for equilibrium effects, five additional dummy volumes were acquired at the beginning of each block, which were subsequently discarded. In the current study, we were interested in high resolution imaging in a priori defined regions of interest, including the basal ganglia (covering NAcc and SN/VTA) and the BF (covering the MS/DB, and NBM). To keep the voxel size proportional to the signal to noise ratio (SNR) of fMRI blood oxygenation level-dependent signals, smaller voxel size could be combined with either longer scan time (i.e., TR) or higher SNR (Edelstein et al., 1986; Murphy et al., 2007). Here, we acquired a partial volume (covering our region of interest) which provides two major advantages: first, it allows to maintain the balance between smaller TR and higher spatial resolution and second, it might also increase the SNR within the regions of interest (Amaro and Barker, 2006).

To improve EPI data quality, field map imaging (FMI) was performed before the start of the first and fourth experimental block using a double-echo spoiled gradient-echo sequence (104 × 104 matrix size TR = 0.61 s, TE_1 = 4.92 ms, TE_2 = 7.38 ms, voxel dimensions = 2 × 2 × 2 mm, 60° flip angle, 2 mm slice thickness), which generated a magnitude image and two-phase images. The field map image, which was used during preprocessing (see below), was computed from the two-phase images.

4.3.4 Anatomical masks of the regions of interest

The anatomical masks of the SN and its subfields (ventral, medial, and lateral SN; Fig. 10) were taken from Zhang et al. (2017) and retrieved from https://identifiers.org/neurovault.collection:2860 . We retrieved the anatomical masks of the NAcc from the Harvard-Oxford Subcortical Structural Atlas using FSL (50% probability; Jenkinson et al., 2012) and the anatomical masks of the BF (MS/DB and NBM) from the anatomy toolbox (50% probability; Eickhoff et al., 2005) in SPM (Wellcome Trust Center for Neuroimaging, London). The resolution of all masks was 1 × 1 × 1 mm. We used MarsBar region-of-interest toolbox (Brett et al., 2002) to extract parameter estimates for conducting the ROI analyses. For the ROI MVPA, all masks were transformed to native space using the individual inverse deformation fields saved from segmentation and resliced to match the dimensions of the beta images (Figure B S3).

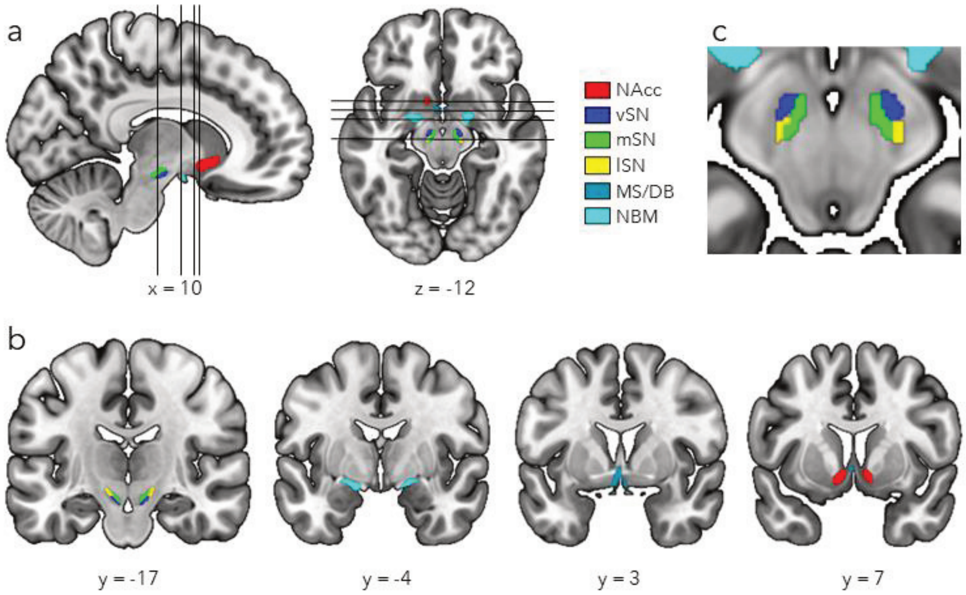

Figure 10. Regions of Interest of the ventral substantia nigra (vSN), medial substantia nigra (mSN), lateral substantia nigra (lSN), nucleus accumbens (NAcc), medial septum/diagonal band (MS/DB) and Nucleus basalis of Meynert (NBM) overlayed on an MNI T1 template. **a** Saggital and axial views indicating locations of coronal slices depicted in **b**. Gray boxes in A and B indicate the field of view of the partial volume. **c** Axial closeup of the ROIs.

4.3.5 Analysis of behavioral data

RTs

For RT analysis in the SID task, we first eliminated trials with improbably short (< 200 ms and < 1st quartile – 1.5 * inter quartile range) and improbably long RTs (> 3rd quartile + 1.5 * inter quartile range) for each participant. Next, condition-specific average RTs were calculated for each participant. The RT data did not contain any extreme outliers according to the Tukey method (Tukey, 1977). All 38 subjects were included in the analysis. We analyzed RT in a 1 × 3 repeated measures design (within-subject factor condition with three levels: neutral, positive, negative; $\alpha = 0.05$) using a permutation *F* -test. Pair-wise comparisons between condition levels were calculated using permutation paired *t*-tests with an adjusted alpha-level controlling for multiple comparisons using Bonferroni correction ($\alpha = 0.05/3 = 0.0167$).

Emotional valence

For each subject, we averaged the two ratings of each photo and then calculated the mean rating across all photos in one condition. There were no extreme outliers in the data as assessed by Tukeys method (Tukey, 1977) and all 38 subjects were included in the analysis. As in the RT analysis, we conducted a permutation *F*-test with a 1 × 3 design (within-subject factor condition with three levels: neutral, positive, negative; $\alpha = 0.05$) and pair-wise permutation *t*-tests and adjusted the alpha-level accordingly (see above).

Analysis of fMRI data

Preprocessing

Data was processed using MATLAB 2018b (The MathWorks, Inc., 2018) and SPM12 (https://www.fil.ion.ucl.ac.uk/spm/software/spm12/). For the mass-univariate, multivariate pattern, and functional connectivity analysis, DICOM images were converted to nifti format, and slice time corrected for each block using the middle slice as a reference. Next, a voxel displacement map (VDM) was calculated using the field map acquired before the first run and subsequently applied in the unwarping of the functional images to correct for distortions due to field inhomogeneities. The functional images were spatially realigned to the first functional image of the first block using rigid body transformation. Then, T1 images were co-registered to the mean functional image. For the mass-univariate and functional connectivity analysis, data was normalized using diffeomorphic anatomical registration through exponentiated lie algebra (DARTEL; Ashburner, 2007) and smoothed with a 3 mm full width at half maximum (FWHM) kernel. The decoding in the MVPA required non-normalized and unsmoothed data.

Mass-univariate analysis

For the first level analysis, we specified a concatenated generalized linear model to assess the average effects of the experimental conditions. We used a high-pass filter with a cutoff at 128 s to reduce low frequency noise and applied SPM's pre-whitening method for more accurate temporal autocorrelation modeling with short TRs (in our case 1.1 s; FAST; Corbin et al., 2018). The design matrix contained the cue phase, target, feedback phase, and movement parameters estimated from realignment. In the positive and negative condition, feedback for hits and misses was modeled separately. In the neutral condition, feedback for hits and misses was not modeled separately because the feedback was always neutral. First level contrast images were generated using one-sample *t*-tests for neutral, positive, and negative cues.

In the second level analysis, we performed a region of interest (ROI) analysis by extracting the cue phase parameter estimates from the vSN, mSN, lSN, NAcc, MS/DB, and NBM. The extracted values did not contain any extreme outliers according to the Tukey method (Tukey, 1977). The condition parameter estimates were analyzed using permutation *F*-tests with a 1 × 3 repeated measures design (within-factor condition with the levels neutral, positive, and negative; $\alpha = 0.05$). All tests were two-tailed and performed in MATLAB.

Multivariate pattern analysis

The first level analysis was conducted in the native space with a multi-session full model using SPM. The design matrix contained the same regressors as the mass-univariate analysis (see above). Data was high-pass filtered (cutoff at 128 s) and pre-whitened (FAST). Next, we used The Decoding Toolbox (Hebart et al., 2015) to run a searchlight analysis (spherical searchlight radius = 4 voxels) on the beta maps using a support-vector machine as a classifier. We computed the following four decoding models for the cue phase: 1) neutral vs. positive vs. negative, 2) positive vs. neutral, 3) negative vs. neutral, 4) positive vs. negative. Due to the block design, we applied a split-half cross-validation instead of the default leave-one-run-out cross-validation. Precisely, the design for one decoding step was created by assigning one block of each condition to the training set while the remaining blocks were assigned to the test set. The assignment of blocks to the training and test set was repeated for all valid permutations. For each permuted design, the classifier was trained on the training set and its performance was assessed on the test set. The average classification accuracy across all permuted designs, i.e. decoding steps, is then used to evaluate the classifier. Out of various information maps that can be chosen as output, reflecting different aspects of the classifier's performance, we selected the *accuracy minus chance* . Note that the chance level depends on the number of categories to be classified in the decoding. Hence, the first model had a chance level of 0.333 while the other models had a chance level of 0.5.

For the second level analysis in SPM, the accuracy minus chance maps were normalized using the DARTEL group template and smoothed with a 3 mm FWHM kernel. We conducted a ROI analysis by extracting the accuracy minus chance values from the normalized and smoothed maps of each decoding model from the vSN, mSN, lSN, NAcc, MS/DB, and NBM. The extracted values did not contain any extreme outliers according to the Tukey method (Tukey, 1977). The values were analyzed using one-tailed bootstrap one-sample *t* -tests in MATLAB with alpha levels adjusted for the number of comparisons in each ROI using Bonferroni-correction ($\alpha = 0.05/4 = 0.0125$).

Functional connectivity analysis

To explore the interaction between brain regions involved in anticipating social feedback, we conducted a seed-based functional connectivity analysis on the cue phase using the BetA Series COrrelation (BASCO) toolbox (Göttlich et al., 2015). Based on our hypotheses, we used the NAcc, vSN, mSN, and lSN as anatomical seed regions. The first level analysis was performed by fitting a general linear model with a separate covariate modeling the evoked brain activity in each trial to the data. The design matrix contained the same regressors as for the mass-univariate analysis and MVPA (see above). Then, we computed Fisher's z-transformed brain maps for the cue phase of each experimental condition by correlating the mean beta-series estimated for the seed region to the beta-series of each individual voxel within the brain (Göttlich et al., 2015). For the second level analysis, we extracted the Fisher's z-values reflecting the correlation of the NAcc with the vSN, mSN, lSN, MS/DB, and NBM as well as the correlation of the vSN, mSN, and lSN with MS/DB and NBM. We did not compute the correlations of SN subfields or correlations of the MS/DB and NBM since this was not the focus of our study (see 3.2 Introduction).

We analyzed the extracted Fisher's z-values using permutation *F*-tests with a 1 × 3 repeated measures design (within-subject factor condition with three levels: neutral, positive, negative; $\alpha = 0.05$), pair-wise permutation paired *t* -tests (positive vs. neutral, negative vs. neutral, and positive vs. negative) when applicable (i.e. when the *F*-test was significant), and bootstrap one-sample *t*-tests. All tests were two-tailed and performed in MATLAB. For the permutation paired *t*-tests, the alpha levels were adjusted for the number of pair-wise comparisons between conditions (positive vs. neutral, negative vs. neutral, and positive vs. negative) within each pair of correlated ROIs (e.g. NAcc with vSN) using Bonferroni-correction ($\alpha = 0.05/3 = 0.0167$). For the bootstrap one-sample *t*-tests, the alpha levels were adjusted for the number of tested correlations (neutral, positive, and negative) within each pair of correlated ROIs using Bonferroni-correction ($\alpha = 0.05/3 = 0.0167$). Outliers were defined using the Tukey method (Tukey, 1977). In each ROI, a maximum of one extreme outlier was identified. The outliers were included in the analysis since semiparametric methods (i.e. permutation tests and bootstrap tests) were used.

Correlational analyses of fMRI data and RTs

To investigate the link between neural activity measures and behavior, we performed correlational analyses between fMRI data and RT using Spearman correlation coefficients. Correlational analyses were limited to ROIs and conditions which yielded significant effects in the respective analysis. Accordingly, for the MVPA, we correlated the accuracy minus chance values extracted from the vSN and mSN in the second model (positive vs. neutral) with RT in the neutral condition, RT in the positive condition, and the difference in RT between the positive and neutral condition. The alpha-level was adjusted for the number of correlations using Bonferroni-correction ($\alpha = 0.05/6 = 0.0083$).

For the functional connectivity analysis, we correlated the z-values indicating the functional connectivity between two ROIs (denoted as ROI1 * ROI2) with RT. We correlated NAcc * MS/DB, NAcc * NBM, and mSN * NBM with RT in all three conditions. In the neutral condition, we correlated lSN * NBM with RT and in the positive condition vSN * NBM with RT. In the negative condition, we correlated NAcc * mSN, NAcc * lSN, and lSN * MS/DB with RT. The alpha-level was adjusted for the number of correlations using Bonferroni-correction ($\alpha = 0.05/14 = 0.0035$).

Sample size

We analyzed neuroimaging data from $n = 36$ healthy young subjects in a within-subject design and a priori defined (unbiased) ROIs. A power analysis revealed that a sample size of $n = 34$ in a within-subject design is sufficient to achieve a power of 80% for medium effects ($d = 0.5$) (in a paired *t*-test). In the literature, similar studies have reported medium to large effects in the SN/VTA, NAcc, and BF. For instance, using the MID task (Adcock et al., 2006), reward anticipation elicited effects in the bilateral VTA (R $z = 7.66$, $d = 2.21$; L $z = 6.89$, $d =$

1.98), NAcc (R$z = 6.50$, $d = 1.87$; L$z = 7.76$, $d = 2.24$), and BF (R$z = 7.24$, $d = 2.09$; L$z = 7.32$, $d = 0.11$). Furthermore, Wittmann et al. (2005) reported reward anticipation effects in the right SN ($z = 3.54$, $d = 0.88$) and Fairhurst et al. (2007) showed effects in the bilateral VTA (R $z = 2.32$, $d = 0.66$; L $z = 2$, $d = 0.57$) during the anticipation of pain. We calculated Cohen's *d* effect sizes based on the *z*-scores provided in the publications.

4.4 Results

4.4.1 Behavior

RTs

Responses following the positive and negative cue were faster than responses following the neutral cue (Fig. 11a). On average, RT was 402 ms (SD = 49 ms) in the neutral condition, 392 ms (SD = 45 ms) in the positive condition, and 395 ms (SD = 49 ms) in the negative condition. The 1 × 3 permutation *F*-test showed a significant main effect of the within-factor condition ($F_{(2,74)} = 9.283$, $pp = 0.0001$, $\eta^2_p = 0.20$). Pair-wise permutation *t*-tests showed significant differences between neutral and positive condition ($t_{(37)} = 4.392$, $p = 0.0001$, $d = 0.712$) and neutral and negative condition ($t_{(37)} = 2.730$, $p = 0.0050$, $d = 0.443$), but no significant difference between positive and negative condition ($t_{(37)} = -1.298$, $p = 0.2126$, $d = -0.210$).

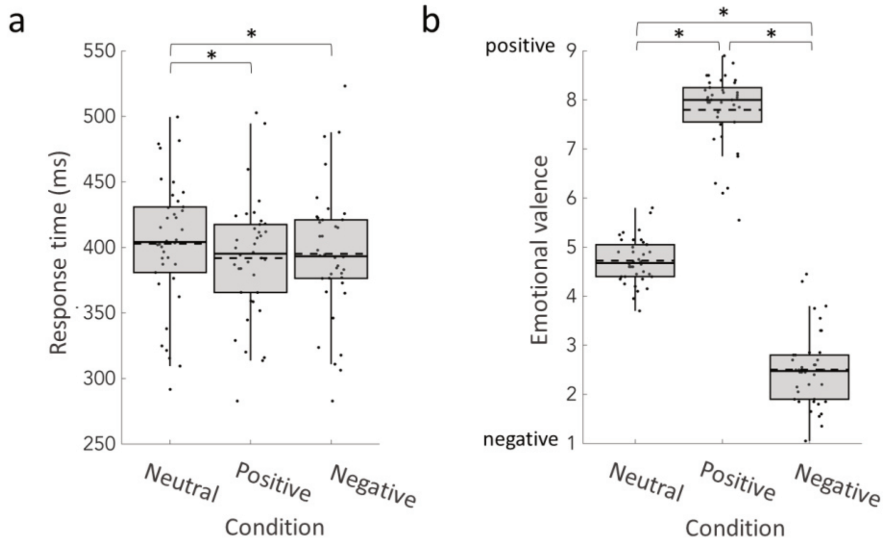

Figure 11. Behavioral results. **a** Mean RTs to the target in the social incentive delay (SID) task across all conditions. **b** Emotional valence ratings across all conditions. Photos were rated on a scale from 1 (negative) to 9 (positive). Data is presented in boxplots overlayed with data points. Whiskers of the boxplots depict data points that are the furthest from the center while still being inside the range of 1.5 times the interquartile range from the lower or upper quartile. Solid lines indicate the median, dashed lines indicate the mean. Asterisks indicate significant results of the permutation paired t-tests ($\alpha = 0.05/3 = 0.0167$).

Emotional valence

The subjective ratings of the social feedback images were in accordance with their intended emotional valence: neutral, positive, and negative (Fig. 11b). On average, neutral images were rated 4.72 (SD = 0.46), positive images 7.79 (SD = 0.76), and negative images 2.50 (SD = 0.77) on a scale from one (negative) to nine (positive). The 1 × 3 permutation F-test revealed a significant main effect of the within-factor condition ($F_{(2,74)} = 490.096$, $p = 0.0001$, $\eta^2_p = 0.92$). Emotional valence ratings were significantly different from one another for the three conditions, as revealed by pair-wise permutation t-tests (neutral vs. positive: $t_{(37)} = -22.457$, $p = 0.0001$, $d = -3.643$; neutral vs. negative: $t_{(37)} = 16.072$, $p = 0.0001$, $d = 2.607$; positive vs. negative: $t_{(37)} = 23.988$, $p = 0.0001$, $d = 3.891$).

fMRI results

Mass-univariate analysis

In the mass-univariate ROI analysis, the main effect of condition in the 1 × 3 permutation F-tests was not significant in any of the ROIs (NAcc: $F_{(2,70)} = 0.74$, $p = 0.4789$, $\eta^2_p = 0.02$; vSN: $F_{(2,70)} = 0.71$, $p = 0.5006$, $\eta^2_p = 0.02$; mSN: $F_{(2,70)} = 0.02$, $p = 0.9792$, $\eta^2_p = 0.00$; lSN: $F_{(2,70)} = 1.13$, $p = 0.3307$, $\eta^2_p = 0.03$; MS/DB: $F_{(2,70)} = 0.08$, $p = 0.9138$, $\eta^2_p = 0.00$; NBM: $F_{(2,70)} = 0.66$, $p = 0.5178$, $\eta^2_p = 0.01$; Fig. 12).

Multivariate pattern analysis

In the ROI MVPA, the one-tailed bootstrap one-sample t-tests revealed that the model decoding positive vs. neutral performed significantly above chance in the vSN (accuracy minus chance = 2.34, $t_{(35)} = 2.66$, $p = 0.0042$, $d = 0.45$) and mSN (accuracy minus chance = 2.66, $t_{(35)} = 2.95$, $p = 0.0014$, $d = 0.53$) but not in any other ROI (Fig. 13). The remaining models showed no significant effects in any of the ROIs. The average accuracy minus chance, t-values, p-values, and effect sizes are summarized in the appendix (Table B S4).

Functional connectivity analysis

In the functional connectivity analysis, the main effect of condition in the 1 × 3 permutation F-tests revealed a significant main effect of condition in the correlation between lSN and MS/DB ($F_{(2,70)} = 4.28$, $p = 0.0173$, $\eta^2_p = 0.10$). The post-hoc permutation paired t-tests showed a significant difference between negative vs. positive ($t_{(35)} = -2.94$, $p = 0.0075$, $d = -0.49$; Fig. 14) but not between positive vs. neutral ($t_{(35)} = -0.64$, $p = 0.5146$, $d = -0.10$) and negative vs. neutral ($t_{(35)} = 2.34$, $p = 0.0231$, $d = 0.39$) condition when controlling for multiple comparisons ($\alpha = 0.05/3 = 0.0167$). The 1 × 3 permutation F-tests on the remaining correlations were not significant (NAcc * vSN: $F_{(2,70)} = 0.85$, $p = 0.4277$, $\eta^2_p = 0.02$; NAcc * mSN: $F_{(2,70)} = 1.79$, $p = 0.1745$, $\eta^2_p = 0.04$; NAcc * lSN: $F_{(2,70)} = 1.81$, $p = 0.1691$, $\eta^2_p = 0.04$; NAcc * MS/DB: $F_{(2,70)} = 0.75$, $p = 0.4739$, $\eta^2_p = 0.02$; NAcc * NBM: $F_{(2,70)} = 0.17$, $p = 0.8418$, $\eta^2_p = 0.00$; vSN * MS/DB: $F_{(2,70)} = 0.46$, $p = 0.6198$, $\eta^2_p = 0.01$; vSN * NBM: $F_{(2,70)} = 0.56$, $p = 0.5800$, $\eta^2_p = 0.01$; mSN * MS/DB: $F_{(2,70)} = 0.15$, $p = 0.8564$, $\eta^2_p = 0.00$; mSN * NBM: $F_{(2,70)} = 0.72$, $p = 0.4963$, $\eta^2_p = 0.02$; lSN * NBM: $F_{(2,70)} = 0.07$, $p = 0.9256$, $\eta^2_p = 0.00$).

The bootstrap one-sample *t*-tests (Fig. 14) revealed a significant correlation of the NAcc with the mSN and lSN in the negative condition (NAcc * mSN: $z = 0.10$, $t_{(35)} = 3.26$, $p = 0.0021$, $d = 0.57$; NAcc * lSN: $z = 0.11$, $t_{(35)} = 3.22$, $p = 0.0009$, $d = 0.55$). Additionally, activity in the NAcc significantly correlated and with the MS/DB and NBM across all conditions (NAcc * MS/DB: Neutral: $z = 0.11$, $t_{(35)} = 3.28$, $p = 0.0025$, $d = 0.56$; Positive: $z = 0.12$, $t_{(35)} = 3.66$, $p = 0.0003$, $d = 0.62$; Negative: $z = 0.17$, $t_{(35)} = 3.93$, $p = 0.0001$, $d = 0.67$; NAcc * NBM: Neutral: $z = 0.14$, $t_{(35)} = 3.97$, $p = 0.0001$, $d = 0.67$; Positive: $z = 0.15$, $t_{(35)} = 4.05$, $p = 0.0001$, $d = 0.69$; Negative: $z = 0.16$, $t_{(35)} = 4.30$, $p = 0.0001$, $d = 0.73$). The vSN showed a significant correlation

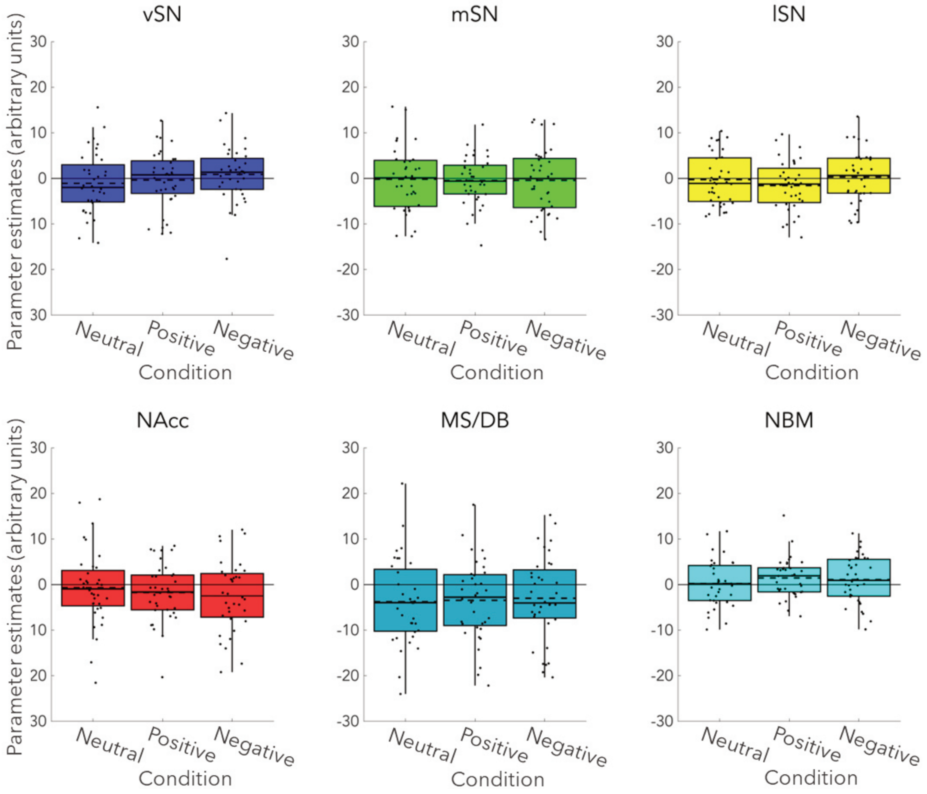

Figure 12. Parameter estimates (arbitrary units) extracted from the regions of interest. Dashed lines indicate the mean, solid lines indicate the median. NAcc: Nucleus accumbens; vSN: ventral substantia nigra; mSN: medial substandia nigra; lSN: lateral substantia nigra; MS/DB: medial septum/ diagonal band; NBM: Nucleus basalis of Meynert.

with the NBM in the positive condition ($z = 0.09$, $t_{(35)} = 3.01$, $p = 0.0033$, $d = 0.50$). The mSN showed a significant correlation with the NBM across all conditions (Neutral: $z = 0.08$, $t_{(35)} = 2.97$, $p = 0.0023$, $d = 0.50$; Positive: $z = 0.13$, $t_{(35)} = 3.88$, $p = 0.0003$, $d = 0.66$; Negative: $z = 0.10$, $t_{(35)} = 3.58$, $p = 0.0011$, $d = 0.61$). The lSN demonstrated a significant correlation with the NBM in the neutral condition ($z = 0.06$, $t_{(35)} = 2.36$, $p = 0.0157$, $d = 0.40$) but also significant correlations with the NAcc and MS/DB in the negative condition (lSN * NAcc: $z = 0.11$, $t_{(35)} = 3.22$, $p = 0.0009$, $d = 0.55$; lSN * MS/DB: $z = 0.11$, $t_{(35)} = 3.39$, $p = 0.0017$, $d = 0.58$). All z-values, t-values, p-values, and effect sizes are summarized in the supplement (Table B S5).

Correlational analyses of fMRI data and RTs

There were no significant correlations between accuracy minus chance values and RT (supplementary figure B S6) and between z-values and RT (supplementary figure B S7).

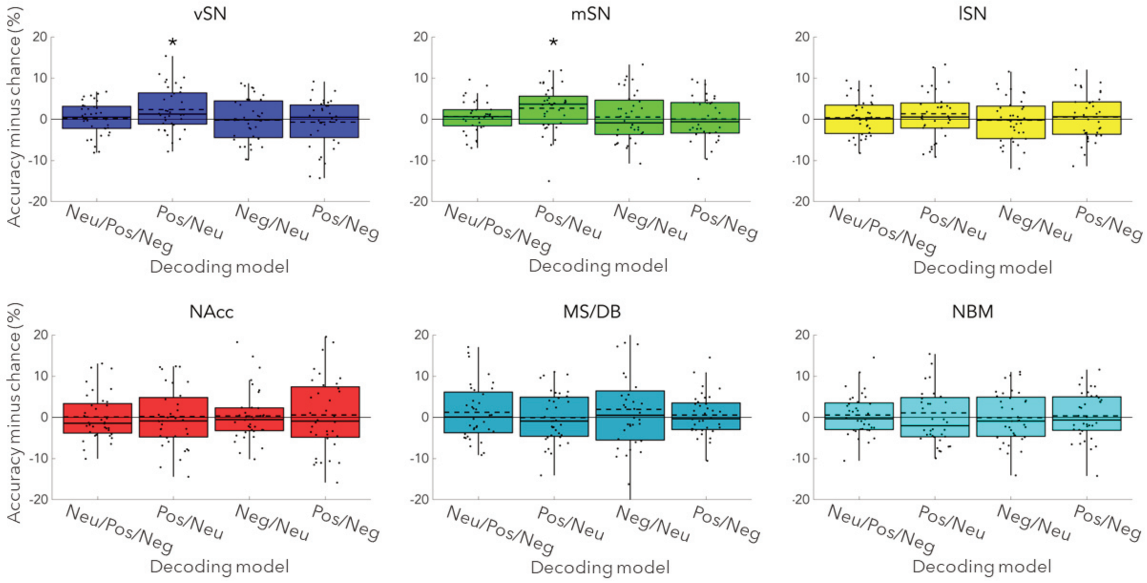

Figure 13. Results of the multivariate pattern analysis. Boxplots show accuracy minus chance values extracted from the regions of interest. The model decoding the positive vs. the neutral condition (Pos/Neu) performed significantly above chance in the vSN and mSN. Asterisks indicate $p < 0.0125$ (Bonferroni-corrected alpha-levels). Dashed lines indicate the mean, solid lines indicate the median. vSN: ventral substantia nigra; mSN: medial substantia nigra; lSN: lateral substantia nigra; NAcc: nucleus accumbens. MS/DB: medial septum/ diagonal band; NBM: Nucleus basalis of Meynert.

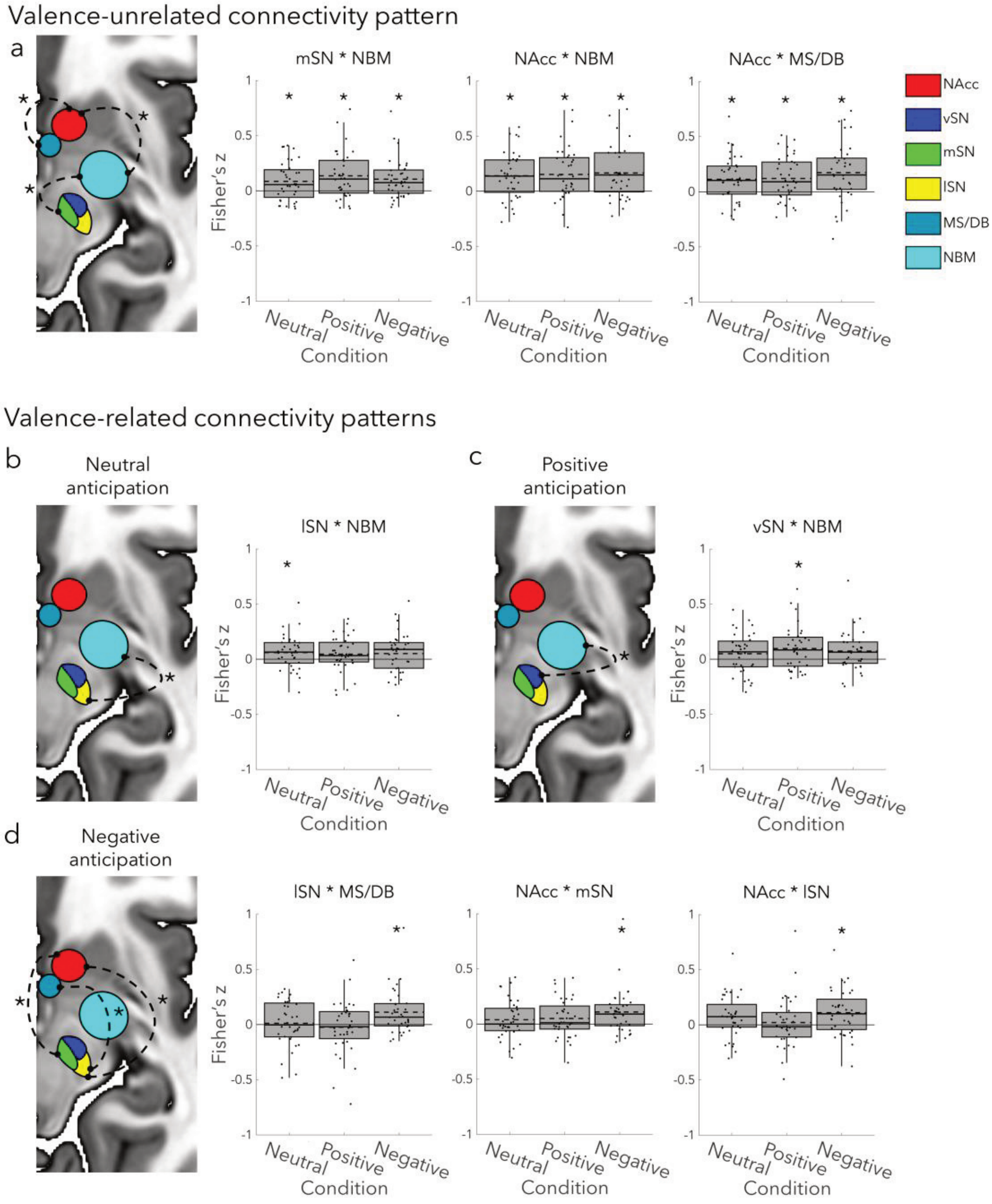

Figure 14. Results of the functional connectivity analysis. Schematic illustrations of functional connectivity patterns between the regions of interest (ROIs) and boxplots showing the Fisher's z-values extracted from the ROIs. Dashed lines indicate the mean, solid lines indicate the median. The ROIs named first in the figure title indicate the defined seed region. Asterisks indicate significant results of the bootstrap one-sample t-tests (α= 0.05/3 = 0.0167). **a** Correlations that were significant for all conditions, i.e. independent of the emotional valence of the social feedback (i.e. valence-unrelated). **b-d** Correlations that were significant in one of the three conditions (i.e. valence-related). vSN: ventral substantia nigra; mSN: medial substantia nigra; lSN: lateral substantia nigra; NAcc: nucleus accumbens; MS/DB: medial septum / diagonal band; NBM: Nucleus basalis of Meynert.

4.5 Discussion

We investigated the neural mechanisms of anticipating social information with a focus on the interaction between mesolimbic and BF subregions. As a main finding, we can show functional connectivity patterns between parts of the SN, BF and NAcc that are independent from emotional valence and could, therefore, be observed in all conditions (neutral, positive, and negative). Importantly, we also observed connectivity patterns that relate to the emotional valence of the social feedback: anticipating neutral social feedback involved the lSN–NBM; anticipating positive social feedback involved the vSN–NBM; and anticipating negative social feedback involved the lSN-MS/DB, NAcc-mSN and NAcc-lSN. These results give novel insights into how the mesolimbic system and BF communicate to promote social information processing.

Research on reward and punishment processing has previously identified a large set of brain regions including the striatum, NAcc, SN/VTA, and BF (e.g., Knutson et al., 2001b; Kirsch et al., 2003; Wittmann et al., 2005; Adcock et al., 2006; Carter, 2009; Matsumoto and Hikosaka, 2009; Rademacher et al., 2010; Kohls et al., 2013; Richey et al., 2014; Hangya et al., 2015; Pauli et al., 2015; Goerlich et al., 2017; Sobczak et al., 2021; see Oldham et al., 2018; Gu et al., 2019; Martins et al., 2021 for recent meta-analyses). While previous research has shown functional coupling of the VS and NAcc with the SN/VTA during rest (Cauda et al., 2011), salience processing (Richter et al., 2020), social and non-social reward anticipation (Gu et al., 2019), and receipt of unexpected monetary gains and losses (Camara, 2008), their functional connectivity during social punishment anticipation and the functional relationship with the BF complex remained unknown. Based on the increasing evidence for functional segregation of SN subregions in the processing of appetitive and aversive events, we hypothesized that the anticipation of social reward and punishment might involve differential functional coupling of mesolimbic and BF subregions. Indeed, our findings extend the previous literature by demonstrating valence-related and valence-unrelated interactions of mesolimbic and BF regions (Fig. 14), which may relate to dopaminergic and cholinergic neuromodulation. For instance, the excitation of midbrain DA neurons by reward predicting stimuli (Ljungberg et al., 1992) has differential effects on cholinergic interneurons within the striatum depending on their location with dorsomedial cholinergic interneurons showing the so-called pause response (Aosaki et al., 1994; Cai and Ford, 2018), and dorsolateral cholinergic interneurons responding with short bursts (Cai and Ford, 2018). Moreover, the pause response vanishes after the destruction of SN DA neurons (Graybiel et al., 1994), and synchronized activity of striatal cholinergic interneurons triggers axonal DA release within the striatum while circumventing the need for action potentials arising from DA neurons in the midbrain (Threlfell et al., 2012). In humans, the SN/VTA can dynamically shift their hemodynamic responses depending on the balance of cholinergic and dopaminergic neurotransmission, which can influence subsequent memory retention (Bunzeck et al., 2014). Finally, a dopamine-acetylcholine interaction in striatal subregions may have further implications for behavior (Cai and Ford, 2018), which is in line with our patterns of functional connectivity associated with emotional valence. Along these lines, it is important to note that fMRI activity, as used here, only allows conclusions regarding the involved brain regions. Further and more direct insights into neurotransmission could be gained with psychopharmacological fMRI or other measures such as PET.

Within the SN, our MVPA revealed a significant discrimination between positive and neutral social feedback anticipation in the mSN and vSN but not lSN (Fig. 13), which emphasizes and further delineates their role in social reward processing. This finding is in line with previous work showing that the ventromedial SN is involved in reward anticipation in monkeys (Matsumoto and Hikosaka, 2009) and humans (Pauli et al., 2015). However, the models decoding valence discrimination (neutral vs. positive vs. negative and positive vs. negative) did not perform significantly above chance in any of the ROIs, therefore this analysis does not provide direct evidence of valence coding. These findings differ from the suggested functional topography in humans with valence coding in the mSN (Zhang et al., 2017) and may be explained by methodological differences, such as the experimental task (SID task vs. a gambling task; Barch et al., 2013), the type of reward (social vs. monetary), and the two different stages of reward processing (anticipation vs. outcome). It may be possible that the SN expresses distinct functional topographies for anticipation and outcome processing since the delivery of social and monetary rewards is more modality-specific than reward anticipation (Rademacher et al., 2010). Moreover, a concurrent signaling of positive and aversive predictors in the monkey ventromedial SN (Matsumoto and Hikosaka, 2009) could not be confirmed by our MVPA, which could be due to differences in the nature of neurophysiological recordings of neurons and fMRI BOLD signals (Logothetis, 2003). Despite these discrepancies between the literature and our findings, our data provide novel empirical evidence for a role of the medial and ventral SN in anticipating positive social information.

While the role of the vSN in reward anticipation is further supported by our functional connectivity analysis – demonstrating a relationship of vSN–NBM during the anticipation of positive social feedback (Fig. 14c) – the function of the mSN appears more ambiguous. In fact, the MVPA implicated the mSN in social reward anticipation (Fig. 13), but the functional connectivity analysis indicated a valence-unrelated effect (mSN –NBM correlation for all conditions, Fig. 14a) and a punishment-related effect with the NAcc (i.e. NAcc-mSN, Fig. 14d). Therefore, the mSN appears to be involved in anticipating neutral, positive, and negative social feedback, possibly through different mechanisms depending on the communication with other mesolimbic or BF regions. Finally, the lSN showed relationships with the NAcc and MS/DB during the anticipation of negative social feedback (Fig. 14d), and a relationship with the NBM during the anticipation of neutral social feedback (Fig. 14b). This is partly in line with the finding that the dorsolateral SN is particularly important for aversive learning in humans (Pauli et al., 2015), and excitement of dorsolateral SN DA neurons by aversive predictors in monkeys (Matsumoto and Hikosaka, 2009). Together, while the role of the mSN seems to be more complex and requires further investigation, our results implicate the vSN in positive social feedback anticipation.

Regarding the NAcc, the MVPA did not provide evidence for valence coding (Fig. 13) as suggested by Zhang et al. (2017) and the functional connectivity showed valence-unrelated significant correlations with the MS/DB and NBM but also significant correlations with the mSN and lSN during negative anticipation (Fig. 14). However, we would like to point out that we only focused on the entire NAcc instead of other meaningful subregions such as the core and shell (Haber and Knutson, 2010). Precisely, it has been hypothesized that the core is concerned with salience and the shell with valence signaling (Bromberg-Martin et al., 2010). Therefore, neglecting possible functional topography of the NAcc can lead to controversial outcomes and future research could follow up on a possible distinction of the NAcc core and salience vs. NAcc shell and valence signaling signaling (Bromberg-Martin et al., 2010), as well as their interactions with the SN/VTA and BF.

With regard to salience coding, we did not find similar responses for positive vs. neutral and negative vs. neutral anticipation within the SN, which is in line with the study by Pauli et al. (2015) , or any other ROI. Instead, our data provide evidence in favor of valence-unrelated functional connectivity between mesolimbic and BF regions (Fig. 14), which may reflect rather general anticipatory processes, since it was observed in all three conditions. The identified valence-related functional interactions between different mesolimbic and BF subregions reflect correlations that were significant in one condition but not always significantly different from the other conditions. Therefore, a simple categorization into salience or valence coding is not suitable. Yet, it may indicate different patterns of functional connectivity between mesolimbic and BF subregions implicated in signaling the anticipation of social feedback.

The prospect to obtain social rewards or avoid social punishments accelerated RTs compared to neutral social feedback in the SID task (Fig. 11a). This was expected and corresponds with previous studies using monetary (Knutson et al., 2001b; Rademacher et al., 2014; Spaniol et al., 2015) and social (Kohls et al., 2013; Rademacher et al., 2014; Sobczak et al., 2021) incentives. However, unlike previous studies that have shown an association between RT and NAcc activity (Schott et al., 2007; Delmonte et al., 2012; Kohls et al., 2013), we found no such relationship (figure B S6 and B S7), which might be due to different outcome measures. In fact, here we focused on functional connectivity (i.e. beta-series correlation) and decoding model performance in conjunction with RT, while others used BOLD responses within the NAcc.

Finally, we would like to point out some limitations. First, our study focused on social information processing and therefore did not involve any other reinforcers such as money or food. While several studies (Rademacher et al., 2010) support the idea of a common currency of reward value across social and non-social reinforcers on a larger scale, e.g. in the striatum, this does not necessarily exclude the possibility that different subregions of larger structures or different types of neurons selectively respond to different types of reinforcers (Behrens et al., 2008; Ruff and Fehr, 2014). Thus, the observed effects may be unique for the anticipation of social reinforcers, and it remains unclear whether they can be generalized to other domains.

Second, our task design is limited by the fact that feedback uncertainty differed between the experimental conditions. In other words, the amount of neutral, positive, and negative feedback received within condition blocks was imbalanced (100%, 83%, 17% respectively). This could potentially affect salience or perceived emotional intensity (Thayer, 1980) as well as neural responses since the midbrain (Aron et al., 2004), DA neurons (Fiorillo et al., 2003) and acetylcholine (Yu and Dayan, 2005) are involved in coding probability and uncertainty. However, a lower proportion of negative feedback (in the negative condition) was introduced to avoid high levels of frustration or demotivation. Interestingly, our results are partly in line with the work by Pauli et al. (2015) with equal levels of uncertainty for the appetitive and aversive conditions, which also suggests regional specialization pending on the valence of incentives. Along these lines, hit rates in the MID task, or variations of it, differ between studies (see for instance Knutson et al., 2000; Wittmann et al., 2005; Schott et al., 2007; Spreckelmeyer et al., 2009; Guitart-Masip et al., 2010). Although this could influence comparability, it not only has the advantage to fully understand how the brain processes rewards and punishments, but also related aspects such as salience, probability and uncertainty.

Together, the possibility to obtain positive and avoid negative social feedback modulates behavioral responses, and anticipating social information is based on valence-unrelated and valence-related connectivity patterns involving mesolimbic and BF subregions. Valence-related functional connectivity was observed in the lSN –NBM for neutral feedback anticipation, vSN –NBM for positive feedback anticipation, and lSN-MS/DB, NAcc-mSN and NAcc-lSN for negative feedback anticipation. As such, these findings provide novel insights into how mesolimbic and BF subregions interact to promote social information processing.

5 Effects of positive and negative social feedback on motivation, evaluative learning, and socio-emotional processing

This chapter deals with the research questions c) and d) stated in the introduction (1.9 Summary and research objectives). The content of this chapter has been adapted for this dissertation for consistency and has been published in *NPJ Science of Learning*:

Sobczak A, Bunzeck N. 2023. Effects of positive and negative social feedback on motivation, evaluative learning, and socio-emotional processing. npj Sci Learn ***8****:28. doi:10.1038/s41539-023-00178-7*

5.1 Abstract

Social rewards and punishments are strong motivators. Since experimental work has focused on young adults using simplistic feedback, the effects of more naturalistic stimuli on motivation, evaluative learning, and socio-emotional processing with advanced age remain unclear. Therefore, we compared the effects of static (photos) vs dynamic (videos) social feedback in an SID task in young (18-35 years) and older adults (50-84 years) with neutral, positive, and negative feedback, on RTs, and assessed the emotional valence of feedback cues and feedback videos. We found that anticipating positive and negative social feedback accelerated RTs regardless of age and without additional effects of video feedback. Furthermore, the results suggest a valence transfer from positive feedback videos to predictive cues in both groups (i.e. evaluative learning). Finally, older adults reported less pronounced negative affect for negative feedback videos, indicating age differences in socio-emotional processing. As such, our findings foster our understanding of the underlying cognitive and emotional aspects involved in the processing of social rewards and punishments.

5.2 Introduction

Social encounters in the real world are multimodal but our scientific understanding of social information processing is often based on abstract paradigms and simplistic stimuli in highly controlled experiments. While this approach provides high internal validity, it comes at the cost of external validity and generalizability with respect to real world social interactions. In fact, real-life social information is much richer due to visual, semantic, and prosodic aspects, as well as dynamic properties, i.e., it involves serial and simultaneous information (Zaki and Ochsner, 2009). Although recent advances in social psychology and cognitive neuroscience try to bridge this gap by using more sophisticated experimental designs (De Jaegher et al., 2010; Schilbach et al., 2013), the effects of more naturalistic social feedback on motivation, learning, and socio-emotional processing and possible age-related changes are still poorly understood. For example, age-related changes in emotional memory (Charles et al., 2003) and valence judgement of emotional faces (Czerwon et al., 2011) have been shown with static stimuli, but the effect of more realistic social information remains unclear. To address these open questions, we compared the effects of static (photos) vs dynamic (pre-recorded videos) social feedback on RTs as well as the subjective emotional valence of feedback predicting cues and feedback stimuli in young (18–35 years) and older (50–84 years) adults using the SID task. In this variation of the widely used MID task (Knutson et al., 2000), faster RTs are used as an indicator of increased motivation in a reinforcement learning context.

The prospect of reward and punishment leads to changes in motivation and behavior. This effect has been reported in studies using different types of feedback, including written texts (Williams et al., 2020), social photos (Rademacher et al., 2014; Sobczak et al., 2021), social videos of faces and gestures (Kohls et al., 2013), social videos of body movements (Williams et al., 2020), as well as monetary incentives (Knutson et al., 2001b; Spaniol et al., 2015; Bowen et al., 2019). Generally, RTs are faster when anticipating high vs low monetary and social rewards (Rademacher et al., 2010, 2014) as well as positive and negative vs neutral social feedback (Kohls et al., 2013; Sobczak et al., 2021). While videos possess more engaging properties (Sato and Yoshikawa, 2007; Rymarczyk et al., 2016), and natural human body movement (also called biological motion) is also valued more than rigid machine-like motion (Williams and Cross, 2018), viewing body movement video feedback without faces does not lead to faster RT compared to text feedback in the SID task (Williams et al., 2020). Thus, biological motion alone appears not to be a stronger motivator, but a feeling of social presence may be critical. For instance, video feedback in online teaching creates a greater social presence of the teacher than written text and it helps to perceive the teacher as a real person (Borup et al., 2012; Thomas et al., 2017). However, it is unknown whether videos including biological motion in mimics and gestures plus verbal feedback leads to faster RTs vs photos showing static mimics and gestures since the two variants of social feedback have not been compared directly.

Rewards and punishments are associated with pleasant and unpleasant affect, respectively. Stimuli that predict rewards and punishments have been argued to acquire predictive value (expectancy learning) and emotional valence (evaluative learning) (Hermans et al., 2002 p.20). Evaluative learning refers to the transfer of emotional valence from the valent to the initially neutral stimulus and occurs when a neutral and a valent stimulus are repeatedly paired (De Houwer, 2007). Accordingly, the mental representation of the stimulus is changed, which can lead to biases in perception, thoughts, or actions (Hütter and Rothermund, 2020). Indeed, verbal ratings of human faces changed from neutral to negative after contingent pairing with unpleasant but tolerable electrical stimulation in an aversive conditioning paradigm (Hermans et al., 2002). While the SID and MID task have been used to study motivational changes and neural correlates associated with anticipating rewards and punishments, behavioral measures of the emotional valence of the predictive cues are scarce and evidence in favor of evaluative learning in the context of social reward and punishment predicting cues as well as possible age effects remains elusive.

Learning from reward and punishment seems to be impaired with age to some degree, and neuroimaging studies suggest a link to compromised updating of predictive value (Hämmerer and Eppinger, 2012; Samanez-Larkin et al., 2014). In fact, aging is associated with the neural degeneration of the dopaminergic mesolimbic system (Bäckman et al., 2006; Howard and Howard, 2013), which provides the key brain structures implicated in learning (Haber and Knutson, 2010). In terms of motivation, a reduced anticipation of positive or negative events would also impair goal-directed behavior. For instance, older adults (66–86 years) showed worse performance than younger adults (19–33 years) in decision tasks that require probabilistic learning to optimize reward outcome (Samanez-Larkin et al., 2014; de Boer et al., 2017). Importantly, in less demanding settings, such as the SID task, the motivational effect of anticipating rewards and punishments, reflected in faster RTs, is preserved in older adults (51–78 years) (Rademacher et al., 2014; Sobczak et al., 2021) in spite of typical age-related motor slowing (Panek et al., 1978; Sobczak et al., 2021).

Being judged by others is associated with emotional responses and emotional processing of social stimuli changes with age. For instance, empirical studies reported the so-called positivity effect, which was expressed in lower scores of negative affect (59–69 < 29–57 < 19–28 years) and less negative ratings of negative and neutral faces (19–69 years) (Czerwon et al., 2011), increased attention and better memory for positive faces

(60–94 > 18–35 years) (Mather and Carstensen, 2003), reduced amygdala activation to negative emotional facial expression (62–72 < 19–39 years) (Iidaka et al., 2002), and reduced neural responses to regret in a gambling paradigm (mean age 65 years < 25 years) (Brassen et al., 2012). Stronger neural responses to cues predicting social than monetary reward in older (60–78 years) compared to young (20–28 years) adults (Rademacher et al., 2014) suggest that age-related changes in socio-emotional processing play a role in the SID task. A theoretical framework to explain these effects is the SST, which suggests that old age is associated with a stronger realization that the remaining lifetime is limited, leading to motivational changes such as a stronger focus on emotional goals (Carstensen, 1998). Moreover, substantial age effects in recognizing the emotional valence of facial expressions also depend on the dynamic properties of the employed stimuli, as shown in a large cross-sectional study. Here, older adults performed significantly worse in the recognition of emotions in static images while recognition of dynamic facial expressions was relatively stable (over a period of 30 years from 61–90) (Richoz et al., 2018). Together, aging is associated with changes in socio-emotional processing but the interaction with dynamic social feedback and a possible relationship in motivational settings remains unclear.

Addressing the effects of dynamic social feedback on basic processes of motivation, learning, and emotion may lead to insights that could have direct consequences in educational contexts. For instance, digital learning tools are increasingly used and implementing dynamic social feedback could potentially increase the motivation to perform well on a task, e.g., studying vocabularies with an app. Moreover, the expectation of a pleasurable learning experience via dynamic social feedback could increase learning effort such as frequency or duration of interaction with the learning material. As a result, learning success could be enhanced. Further, concerning adult education, it would be beneficial to understand possible age-related changes.

To investigate the effects of dynamic social feedback on motivation, evaluative learning, and socio-emotional processing in aging, we collected a new set of data from 49 young and 55 older adults using the SID task with dynamic video feedback (prerecorded; with audio). We compared these to the 52 young and 52 older healthy controls from experiment 3 in study I which used static photos as social feedback. In this article, these experiments will be referred to as the SID-Video study and the SID-Photo study, respectively. The SID comprises three phases: cue, response to the target, and feedback (Fig. 15a). The cues signaled the condition and the potential feedback to be received.

Obtaining rewards and avoiding punishment depended on RT to the target. We assessed baseline RT for each participant in a separate simple RT task prior to conducting the SID. In experiment 2, we also examined the emotional valence of the predictive cues by a direct and an indirect measure to assess evaluative learning. The direct measure was an explicit rating task (Fig. 15b) and implemented at the end of the SID task by adding

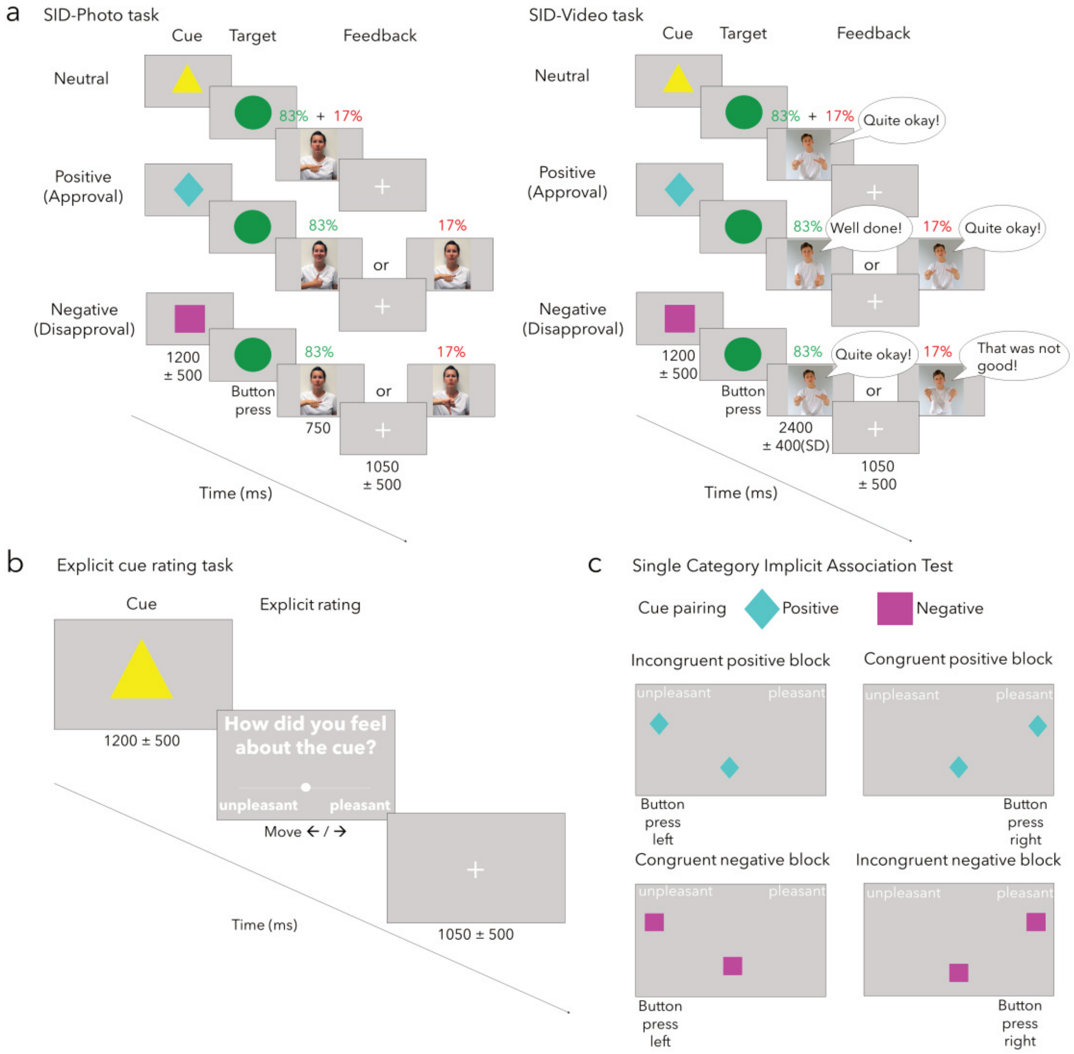

Figure 15. Schematic illustrations of experimental tasks. **a** Social incentive delay (SID) task. Feedback on task performance (i.e., RT) was given via photos or videos also including verbal feedback. Task difficulty was adapted from trial to trial achieving an average hit rate of 83% using a staircase method. In the positive and negative condition, the given feedback depended on hits (green) vs misses (red) while feedback in the neutral condition was always neutral. **b** Trial design in the explicit cue rating task. **c** Example trials for each block in the Single Category Implicit Association Test (SC-IAT). The bottom texts indicate the correct response to the target presented in the center of the screen (left indicates pressing the x-key and right indicates pressing the m-key).

extra trials. Here, the cue was followed by a screen instead of the target, asking the participants to rate their emotion on the previously presented cue. The indirect measure was an adapted version of the Implicit Association Test (IAT) (Greenwald et al., 1998) for single categories (SC-IAT; Fig. 15c) (Karpinski and Steinman, 2006). In the last part of experiment 2, we evaluated the emotional processing of the social video feedback stimuli by presenting them to the participants and asking them to rate the emotional valence (from negative to positive). Further, credibility (in the sense of authenticity and naturality) of the feedback stimuli was assessed in the last part. See the methods section for more details on the tasks.

Based on our previous findings (Sobczak et al., 2021), we expected faster RTs for young and older adults following positive and negative cues (as compared to neutral cues), which was hypothesized to be more pronounced for videos vs photos as social feedback. We further expected emotional cue valence to correspond with the valence of the associated feedback (i.e., more positive evaluations for cues associated with positive feedback in contrast to cues associated with neutral and negative feedback). Finally, we predicted a positivity effect (i.e., more positive evaluations in older adults) and a positive correlation between cue valence and video feedback valence independent of age.

5.3 Materials and methods

5.3.1 Inclusion criteria

All participants were screened for pre-established inclusion and exclusion criteria prior to the experiment. Participants were required to be currently healthy, of adult age (18–35 years, or >50 years), contractually capable, right-handed, fluent in German, not consume any illegal drugs, consume less than 15 glasses of alcohol per week, and less than 15 cigarettes per day. Exclusion criteria were defined as previous or current medical conditions including psychiatric illnesses, mild cognitive impairment (MCI), dementia, heart conditions, cardiovascular diseases, or other severe illnesses (in particular those that affect the central nervous system), current medical treatment up to 2 weeks before the study excluding prescription-free medications and oral contraceptives.

5.3.2 Participants

In this study, we combined new and previously recorded and published behavioral data (Sobczak et al., 2021) to compare the SID task using photo vs video stimuli in young and older adults. All older adults were screened for MCI and dementia using the Montreal

Cognitive Assessment (MoCA; scores <22 indicate MCI or dementia; Nasreddine et al., 2005; Freitas et al., 2013). One young and three older participants of the SID-Video study were excluded due to fulfilling pre-established exclusion criteria (the young participant reported depression in clinical history, one older participant reported a stroke in clinical history and two older participants scored below 22 in the MoCA). We included 52 young (age range = 18–32; M ± SD = 22.8 ± 3.1 years; n female = 29) and 52 older adults from experiment 3 in study I which used the SID-Photo task (age range = 51–75; M ± SD = 64.0 ± 6.4 years; n female = 29) and another 49 young (age range = 18–35; M ± SD = 23.9 ± 3.7 years ; n female = 36) and 55 older adults using the SID-Video task (age range = 50–84; M ± SD = 64.2 ± 8.2 years; n female = 31; MoCA mean score = 27.9; SD = 1.5; all MoCA scores ≥22). Final sample sizes for each task (see statistical analyses) can vary due to technical problems in data acquisition and will therefore be reported separately for each task. This study was approved by the local ethics committee of the University of Lübeck, Germany. All participants gave written informed consent, in accordance with the Declaration of Helsinki, before taking part in the study.

5.3.3 Recruitment and testing procedure

We recruited our participants for both studies via student mailing lists, newspapers, public spaces, and the department's database (Greiner, 2015). The younger group mainly includes students from the University of Lübeck and Technische Hochschule Lübeck, while the older group mainly consists of volunteers from Lübeck and its greater catchment area. For the SID-Photo study, data for the young sample was collected from March 2016 until May 2016 and data for the older was collected from February 2019 until April 2019. The data collection for the SID-Video study (young and older sample) was initially planned to start in April 2020 but it was postponed due to the COVID-19 pandemic. Data for the SID-Video study was collected from October 2020 until June 2021—a time of social distancing and contact restriction measures. Specifically, the data collection period for the SID-Video study included partial and full lockdowns from November 2020 until March 2021.

Data collection in the SID-Photo study was carried out by two female experimenters. One collected data for the young participants and the other for the older participants. Data collection for the SID-Video study was carried out by four other female experimenters who collected data for both young and older participants. Importantly, all experimenters followed a standardized instruction protocol to avoid potential biases. The experiments were performed in a lab environment and the participant performed the tasks in a separate test room while the experimenter was in a control room.

Both studies used similar laptops to perform the tasks. The SID-Photo study was programmed using Cogent Graphics developed by John Romaya at the Laboratory of Neurobiology at the Wellcome Department of Imaging Neuroscience. The SID-Video study was programmed in MATLAB 2018b, using the Psychophysics Toolbox extensions (Version 3; Brainard, 1997; Pelli, 1997) since video playback was not possible using Cogent.

The SID-Photo study included three parts: (1) a simple RT task, (2) the SID-Photo task (preceded by a short training), and (3) a rating task assessing emotional valence of the feedback videos. We reused and reanalyzed the behavioral data from the young and older healthy controls from the simple RT task and the SID-Photo task. The SID-Video study included five parts: (1) a simple RT task, (2) the SID-Video task (preceded by a short training), (3) an explicit rating task assessing explicit cue valence, (4) a version of the Single Category Implicit Association Test (Karpinski and Steinman, 2006) assessing implicit cue associations, and (5) a rating task assessing emotional valence and credibility of the feedback videos. Please note that the design of the emotional valence rating differed between the SID-Photo and the SID-Video study (Bradley and Lang, 1994; Sobczak et al., 2021). Therefore, the data from this task in study I was neither reused nor reanalyzed as part of study III.

5.3.4 Paradigm

The simple RT task comprised 50 trials and was subsequently used in a staircase scenario of the SID task as described in our previous publication (Sobczak et al., 2021). The SID task used the same trial structure and timings as in our previous publication (Sobczak et al., 2021) and only differed with regard to the feedback stimuli and their timing (Fig. 15a). Photos were presented for 750 ms and videos had an average duration of 2400 ms (SD = 400 ms). In brief, we presented a cue, followed by a target (green circle), followed by the feedback. Participants had to respond to the target as fast as possible via button press (keyboard or mouse were used). The cues signaled condition (neutral, positive, negative) and potential feedback to be received. In the positive condition, positive feedback was received for fast responses and in the negative condition, negative feedback was received for slow responses, in the neutral condition the feedback was always neutral. Here, we used videos of one female and one male volunteer with acting experience showing neutral, positive, and negative mimics (e.g., neutral, smiling, angry), gestures (e.g., thumbs horizontal, thumbs up, thumbs down, but also other hand movements), and verbal feedback (e.g., "Quite okay.", "Well done!", "That was not good."). We varied hand movements, verbal feedback, and mimic details to make the feedback more realistic. Each condition comprised 16 different videos (8 female, 8 male) as feedback. A pool of 12 videos (4 per condition) were used in the short training. The SID comprised six blocks (2 per condition) in a randomized order. Note that social feedback in the SID Photo task was provided by 10 different volunteers (5 female, 5 male). Each condition comprised 10 photographs as feedback, one of each volunteer. On these photographs, the volunteers showed neutral, positive, or negative mimics (i.e., neutral, smiling, angry) and gestures (i.e., right thumb horizontally, right thumb up, right thumb down).

The explicit rating task, assessing explicit cue valence, was implemented by appending the SID task by one extra block per condition including four extra trials each. In these trials, the cue was followed by a screen instead of the target, asking the participants to rate their emotion about the previously presented cue ranging from unpleasant to pleasant. The rating was made on a line with two end points (coded as −10 and 10, respectively) and a dot in the middle that could be moved by pressing the arrow keys on the keyboard (Fig. 15b).

The SC-IAT was used to assess implicit cue valence. It is a modification of the implicit association test (Greenwald et al., 1998) and was adapted according to Karpinski and Steinman (2006). Here, we presented four experimental blocks (60 trials each; positive congruent, positive incongruent, negative congruent, and negative incongruent) each preceded by a short training block (20 trials). In each trial, a target stimulus appeared in the middle of the screen and the participants had to respond by pressing either "x" or "m" on a keyboard. Depending on the block, the target stimuli were words with positive and negative valence and the respective positive or negative cue from the previous SID task (Fig. 15c). In the positive congruent block, we presented 17 pleasant words, 26 unpleasant words, and 17 cues as targets; the positive incongruent block comprised 26 pleasant words, 17 unpleasant words, and 17 cues as targets; the negative congruent block comprised 26 pleasant words, 17 unpleasant words, and 17 cues as targets; the negative incongruent block comprised 17 pleasant words, 26 unpleasant words, and 17 cues as targets. The pleasant and unpleasant words were selected from the Berlin Affective Word List Reloaded (BAWL-R; Võ et al., 2009). Each block was preceded by a detailed instruction regarding the categorization and corresponding key responses. The participants always had to press the x-key for unpleasant words and the m-key for pleasant words. Additionally, in the positive congruent block the m-key had to be pressed for the previously positive cue while in the positive incongruent block the x-key was pressed for the previously positive cue. In the negative congruent block, the x-key had to be pressed for the previously negative cue and in the negative incongruent block the m-key had to be pressed for the previously negative cue. Generally speaking, congruency means that the valence that was signaled by the cue in the SID task (positive or negative cue) matches the valence of the assigned response key (i.e., press x-key for unpleasant words and negative cue) which was achieved by always pressing “x” for unpleasant words and “m” for pleasant words. Blocks in which the valence of the cue did not match the valence of the response key (i.e., press x-key for unpleasant words and positive cue) are labeled as incongruent trials. After a key press, participants received a green O as feedback for correct responses or a red X for incorrect responses. We prepared four versions of the SC-IAT with varying block order to prevent ordering effects and randomly select one of these versions for each participant.

A general idea of the IAT is that processing highly associated categories (i.e., congruent information) is associated with faster RTs (Greenwald et al., 1998). Hence, if participants developed an association between a cue and emotional valence of the subsequent feedback, RTs in congruent blocks should be faster than in incongruent blocks.

The last part of the experiment aimed to evaluate the video feedback stimuli by presenting them to the participants, who were asked to rate the emotional valence and credibility (in the sense of authenticity and naturality). The order was randomized and each video was presented twice. The emotional valence was rated from negative to positive on a line with two end points (coded as −10 and 10, respectively) and a dot in the middle that could be moved by pressing the arrow keys on the keyboard. Credibility was rated from unbelievable to believable using the same scale design as for the valence rating.

5.3.5 Creation and selection of video feedback stimuli material

We recorded a new set of social video feedback stimuli with one female (27 years old) and one male volunteer (24 years old) with acting experience. In total, we generated a set of 120 videos, 60 per volunteer matched for mimics, gesture, and verbal feedback (called matched video pairs in the following).

The videos were created to match the photos to a certain degree. For example, the gestures in the photos showed one thumb up, horizontal, or down. Therefore, we recorded the videos to show one thumb up, horizontal, or down, but additionally both thumbs up, horizontal, or down, as well as other gestures, e.g., a fist pump as a celebratory gesture in the positive feedback condition, to make the feedback appear more realistic, varied, and less like a playback. Moreover, all volunteers were Caucasian and wore white t-shirts in front of a gray background.

All videos were evaluated in an online study with n = 76 participants reporting fluent German reading and speaking skills (age range = 16–65 years, M ± SD = 27.3 ± 10.3, n female = 42, n male = 32, n diverse = 2) using lab.js (Henninger et al., 2019) and JATOS (Lange et al., 2015) for rating their emotional valence and credibility. Further, we assessed the sympathy of the two volunteers, which was rated 2.6 for the female and 4.6 for the male actor (on a scale ranging from −10 to 10). The final selection process for the SID-Video task was based on a series of criteria: We selected videos pairs with a difference smaller than 1.5 in the average valence and credibility ratings. We then selected videos with an average credibility above 0 on a scale from −10 to 10. The remaining videos were selected based on matching gestures (showing two thumbs vs one thumb vs other gesture) across conditions. Finally, five matched video pairs (10 videos in total) per condition were selected for the SID-Video study. One showed one thumb up, horizontal, or down, and four showed both thumbs up, horizontal, or down. See Table 4 for an overview of the average valence and credibility ratings.

Table 4.

Average ratings of emotional valence and credibility for the selected videos.

	Emotional Valence			Credibility		
	Neutral	Positive	Negative	Neutral	Positive	Negative
Female volunteer	-0.2	5.9	-6.2	1.0	2.1	1.3
Male volunteer	0.0	5.2	-5.1	1.4	2.1	2.0
Average	-0.1	5.5	-5.7	1.2	2.1	1.7

5.3.6 Statistical analyses

All permutation tests described in this study were computed in MATLAB 2018b (The MathWorks, Inc., 2018) using built-in functions, custom scripts, and MATLAB code retrieved from File Exchange (Caplette, 2017). The permutation tests were computed as followed: first, empirical test statistics of interest (*F*-values or *t*-values) were obtained for the original sample. Second, to create the null condition, factor labels were permuted. Between-factor labels were permuted between subjects, while within-factor labels were permuted within subjects, keeping measurements together that belonged to the same subject. Third, the test statistics were computed for the permutation samples. In each analysis, 5000 permutation samples and corresponding test statistics were obtained to generate the permutation distribution. Fourth, it was assessed whether the observed empirical test statistic was unusually large for the distribution of permutation test statistics using a Monte Carlo *p*-value. Cohen's *d* was calculated using MATLAB code retrieved from File Exchange (Bettinardi, 2017).

Simple RT task

We compared RT from the simple RT task between the SID-Photo and SID-Video study. First, for each individual data set, we eliminated trials with improbably short (<150 ms and <1st quartile – 1.5 * inter quartile range) and improbably long RTs (>3rd quartile + 1.5 * inter quartile range). We calculated the condition averages for each participant and conducted an outlier analysis using the Tukey method (Tukey, 1977). We removed one outlier in the group of older adults from the SID-Photo study and one from the SID-Video study resulting in n = 52 young and n = 51 older adults for the SID-Photo study, and n = 49 young and n = 54 older adults for the SID-Video study. We computed a 2 × 2 design (study x age) permutation *F*-test.

RT in SID-Photo and SID-Video

To evaluate the effect of photos vs videos as feedback on RT, we processed each participant's RT data as described above and calculated condition averages for each participant. Then, we z-transformed the data sets from each study to account for baseline differences in RT between studies (see the results of the simple RT task), which implied that we could not evaluate the main effect of feedback type (study) on raw RTs but only interpret the relative differences between anticipating incentivized (i.e., positive and negative) and neutral feedback between static vs dynamic feedback. We conducted an outlier analysis using the Tukey method (Tukey, 1977) and eliminated one outlier from the group of young adults in the SID-Photo study and two from the group of young adults in the SID-Video study resulting in n = 51 young and n = 52 older adults for the SID-Photo study, and n = 47 young and n = 55 older adults for the SID-Video study.

We analyzed RT in a 2 × 2 × 3 mixed design (between factors study and age; within-factor condition with three levels: neutral, positive, negative) permutation *F*-test. Pair-wise comparisons between condition levels were computed using two-sided permutation paired *t*-tests (positive vs neutral, negative vs neutral, and positive vs negative) with an adjusted alpha-level controlling for multiple comparisons using Bonferroni correction (α= 0.05/ 3 = 0.0167). Because the expected interaction of the factors study and condition was not significant, we conducted a 2 × 2 × 3 mixed Bayesian ANOVA in jamovi (Version 1.6.23; The jamovi project, 2020) using the default settings, to verify the results of the permuted mixed F-test and evaluate the evidence against the interaction (calculated as age + condition BF_{10}/age + condition + age * condition BF_{10}).

Explicit cue valence ratings

To analyze the scores from the explicit rating task in the SID-Video study, we computed the average of the four ratings in each condition (neutral, positive, negative) for each subject. Four older participants were removed from the analysis due to data loss resulting from technical problems. The data set contained no outliers as confirmed by an outlier analysis using the Tukey method (Tukey, 1977) leaving n = 49 young and n = 51 older adults for the analysis.

The explicit rating scores were analyzed using a 2 × 3 mixed design (between factor age; within-factor condition with three levels: neutral, positive, negative) permutation *F*-test. The significant main effect of condition was followed up by pair-wise comparisons using permutation paired *t*-tests (positive vs neutral, negative vs neutral, and positive vs negative; two-sided; α= 0.05/ 3 = 0.0167). To explore the significant interaction, we compared the average ratings in each condition between the young and older adults using three two-sample permutation t-tests with adjusted alpha-levels controlling for multiple comparisons using Bonferroni correction (two-sided; α= 0.05/3 = 0.0167). Since none of these tests were significant and would leave the interaction inconclusive, we conducted three exploratory post-hoc two-sample permutation *t*-test comparing the condition differences (positive minus neutral, negative minus neutral, and positive minus negative) between young and older adults with adjusted alpha-levels controlling for multiple comparisons using Bonferroni correction (two-sided; α= 0.05/3 = 0.0167).

Implicit cue valence–SC-IAT

Based on the SC-IAT and a suggestion by Karpinski and Steinman (2006), we calculated the so-called D-score, which designates an association of the cue with positive or negative valence. To this end, we first removed responses below 350 ms as well as above 1500 ms and replaced the RTs of incorrect responses by the block mean plus an error penalty of 400 ms. Then, we computed the average RTs for the positive congruent, positive incongruent, negative congruent, and negative incongruent blocks for each participant. To compute the individual D-scores for the positive cues, we subtracted the average RT of the positive congruent block from the average RT of the positive incongruent block. The resulting value was divided by the standard deviation of all RTs of correct responses in the positive congruent and positive incongruent block. For the negative cue, the D-scores were computed by subtracting the average RT of the negative incongruent block from the RT of the negative congruent block. The resulting value was divided by the standard deviation of all RTs of correct responses in the negative congruent and negative incongruent block. Positive D-scores designate associating the cue with positive valence while negative D-scores designate associating the cue with negative valence.

Two older participants were not included in the analysis due to data loss resulting from technical problems. Error rates were below 20% in all participants. One young and one older adult were removed from data analyses due to extremely slow responses (>20% slower than 1500 ms). The data set contained no outliers as confirmed by an outlier analysis using the Tukey method (Tukey, 1977) leaving n = 48 young and n = 52 older adults for the analysis.

D-scores were analyzed using a 2 × 2 mixed design (between factor age; within-factor condition with two levels: positive, negative) permutation *F*-test. We further performed one-sample permutation *t*-tests on the D-scores for the positive and negative cue across both age groups with adjusted alpha-levels controlling for multiple comparisons using Bonferroni correction (two-sided; α= 0.05/ 2 = 0.025).

Emotional valence ratings of feedback videos

To evaluate the perceived emotional valence of feedback videos, we averaged the two ratings per video and then across all videos of one condition for each participant. We conducted an outlier analysis using the Tukey method (Tukey, 1977) and removed data from one outlier in the young adults and one in the older adults leaving n = 48 young and n = 54 older adults for the analysis. We analyzed the emotional valence ratings using a 2 × 3 mixed design permutation F-test (between factor age; within-factor condition with three levels: neutral, positive, negative). The significant main effect of condition was followed up by three pair-wise comparisons using permutation paired t-tests (positive vs neutral, negative vs neutral, and positive vs negative; two-sided) with adjusted alpha-levels controlling for multiple comparisons using Bonferroni correction (α= 0.05/3 = 0.0167). The significant interaction was explored by comparing the average ratings in each condition between young and older adults using three two-sample permutation t-tests with adjusted alpha-levels controlling for multiple comparisons using Bonferroni correction (two-sided; α= 0.05/3 = 0.0167).

Credibility ratings of feedback videos

The credibility ratings of feedback videos were first averaged per video and then across all videos of one condition for each participant. All 49 young and 55 older adults were included in the analysis since the data set contained no outliers as confirmed by an outlier analysis using the Tukey method (Tukey, 1977). We analyzed the credibility ratings with a 2 × 3 mixed design (between factor age; within-factor condition with three levels: neutral, positive, negative) permutation *F*-test and followed up on the significant interaction by comparing the average ratings in each condition between young and older adults using three two-sample permutation *t*-tests with adjusted alpha-levels controlling for multiple comparisons using Bonferroni correction (two-sided; α= 0.05/3 = 0.0167).

Partial correlations of explicit and implicit cue valence with feedback valence ratings

To assess the link between cue valence and feedback video valence independent of age, we performed partial correlations between cue valence and feedback video valence in each condition using spearman correlation coefficients in jamovi (Version 1.6.23; The jamovi project, 2020). First, we correlated explicit cue valence and feedback video valence and adjusted the alpha-levels to control for multiple comparisons using Bonferroni correction (two-sided; adjusted α= 0.05/3 = 0.0167). Second, we correlated implicit cue valence, measured by the D-scores in the SC-IAT, and feedback video valence and again used Bonferroni correction to control for multiple comparisons (two-sided; adjusted α= 0.05/ 3 = 0.0167). Since some subjects did not provide all necessary ratings, only 48 young and 51 older adults were included in both analyses.

5.4 Results

5.4.1 Simple RT task

In the simple RT task, participants had to respond to a target as fast as possible. RTs were used to adjust the SID task to the individual response speed and analyzed to inspect possible baseline differences between the SID-Photo and SID-Video study. The average RT in the SID-Photo study was 379 ms (SD = 40 ms) for young adults and 427 ms (SD = 74 ms) for older adults. In the SID-Video study, the average RT was 259 ms (SD = 33 ms) for young adults and 312 ms (SD = 50 ms) for older adults. The 2 × 2 design (study x age) permutation *F*-test on RT in the simple RT task showed a significant main effect of study ($F_{(1,202)}$ = 257.9, *p* = 0.0001, CI 95% = [−0.0001 0.0005], η^2_p = 0.5608; Fig. 16a) and a significant main effect of age (*F*(1,202) = 47.9, *p* = 0.0001, CI95% = [-0.0001 0.0005], η^2_p = 0.1919; Fig. 16b), but no significant interaction ($F_{(1,202)}$ = 0.1, *p* = 0.6663, CI 95% = [0.6532, 0.6793], η^2_p = 0.0009).

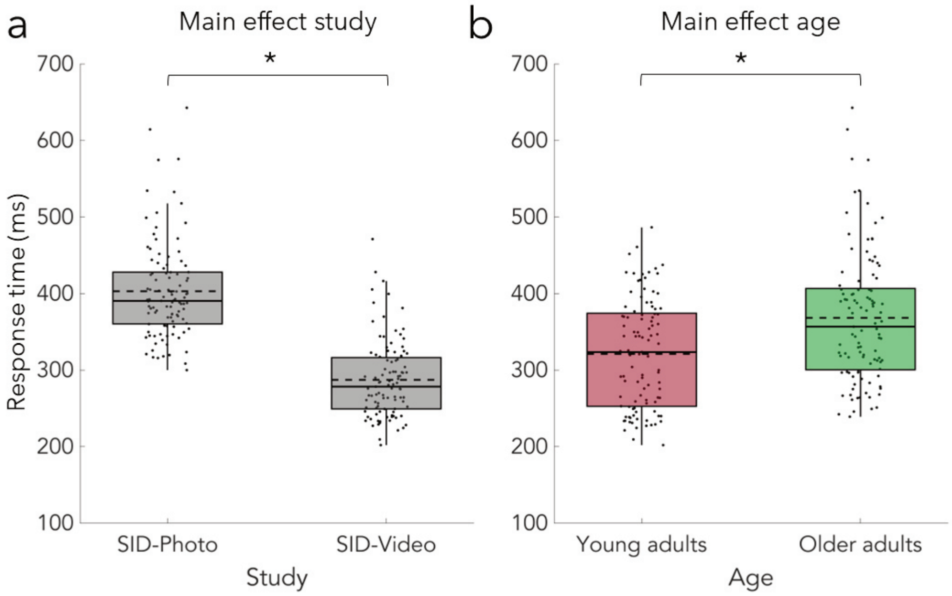

Figure 16. Results of the simple RT task in the SID-Photo and SID-Video study. **a** RT was significantly slower in the SID-Photo study than in the SID-Video study (main effect of study) and **b** young adults responded significantly faster than older adults (main effect of age). Statistical comparisons were made using a 2 × 2 design (study x age) permutation *F*-test. Data is presented in boxplots overlaid with data points. Boxes span from the lower to the upper quantile and whiskers of the boxplots depict data points that are the furthest from the center while still being inside the range of 1.5 times the interquartile range from the lower or upper quartile. Solid lines indicate the median, dashed lines indicate the mean. Asterisks mark significant differences ($p < 0.001$).

5.4.2 RT in SID-Photo and SID-Video

In the SID task, participants had to respond to a target as fast as possible with faster RTs being interpreted as increased motivation. The target was preceded by a cue signaling the condition (neutral, positive, negative) and potential feedback to be received (see Fig. 15a). In the positive condition, positive feedback was received for fast responses; in the negative condition, negative feedback was received for slow responses; and, in the neutral condition the feedback was always neutral. The SID-Photo task used images of volunteers showing neutral, positive, or negative mimics and gestures; and the SID-Video task used videos of volunteers showing neutral, positive, and negative mimics, gestures, and giving verbal feedback. RT was z-transformed to account for baseline differences in RT between studies.

In both tasks, z-transformed RT was faster for young (SID-Photo: Neutral: M =−0.36, SD = 0.72; Positive; M =−0.54, SD = 0.60; Negative: M =−0.50, SD = 0.64; SID-Video: Neutral: M =−0.27, SD = 0.65; Positive: M =−0.48, SD = 0.56; Negative: M =−0.48, SD = 0.59) than for older (SID-Photo: Neutral: M = 0.50, SD = 0.96; Positive; M = 0.36, SD = 1.01; Negative: M = 0.34, SD = 0.90; SID-Video: Neutral: M = 0.40, SD = 1.08; Positive: M = 0.19, SD = 0.96; Negative: M = 0.26, SD = 1.04) adults. The 2 × 2 × 3 mixed design permutation *F*-test showed significant main effects of age (*p* = 0.0001, Fig. 17a) and condition (*p* = 0.0001; Fig. 17b) but no significant main effect of study and no significant interactions. Post-hoc permutation paired *t*-tests revealed a significant difference between the positive vs and negative vs neutral (*p* = 0.0001) but not positive vs negative condition (Fig. 17b). See Table 5 for all statistical details. In line with these results, the 2 × 2 × 3 mixed Bayesian ANOVA provided extreme evidence for the main effects model with the factors age and all other models. Moreover, the analysis provided strong evidence against the interaction of age and condition (age + condition BF_{10}/age + condition + age * condition $BF_{10} = 2.44 \times 10^{13}/1.01 \times 10^{12} = 24.15$). This means that the data is 24.15 times more likely under the two main effects model than under the model that includes their interaction. Table 6 provides an overview of all Bayes factors for the full model comparison.

Table 5.

Results of the social incentive delay (SID) task.

2x2x3 F-test	df	*F*	*P*	CI95%	η2p
Main effect study	1, 201	0.05	0.8134	[0.8026 0.8242]	0.0002
Main effect age	1, 201	51.15	0.0001	[-0.0001 0.0005]	0.2029
Main effect condition	2, 402	14.62	0.0001	[-0.0001 0.0005]	0.0678
Interaction study * age	1, 201	0.60	0.4243	[0.4106 0.4380]	0.0030
Interaction study * condition	2, 402	0.04	0.8182	[0.8075 0.8289]	0.0010
Interaction age * condition	2, 402	0.04	0.9578	[0.9522 0.9634]	0.0002
Interaction study * age * condition	2, 402	0.40	0.6609	[0.6477 0.6740]	0.0020
Post hoc tests for main effect condition	df	*t*	*P* *	CI95%	*d*
Positive vs neutral	204	-4.63	0.0001	[-0.0001 0.0005]	-0.32
Negative vs neutral	204	-3.85	0.0001	[-0.0001 0.0005]	-0.26
Positive vs negative	204	-0.89	0.3589	[0.3456 0.3722]	-0.06

* Adjusted alpha $\alpha = 0.05/3 = 0.0167$

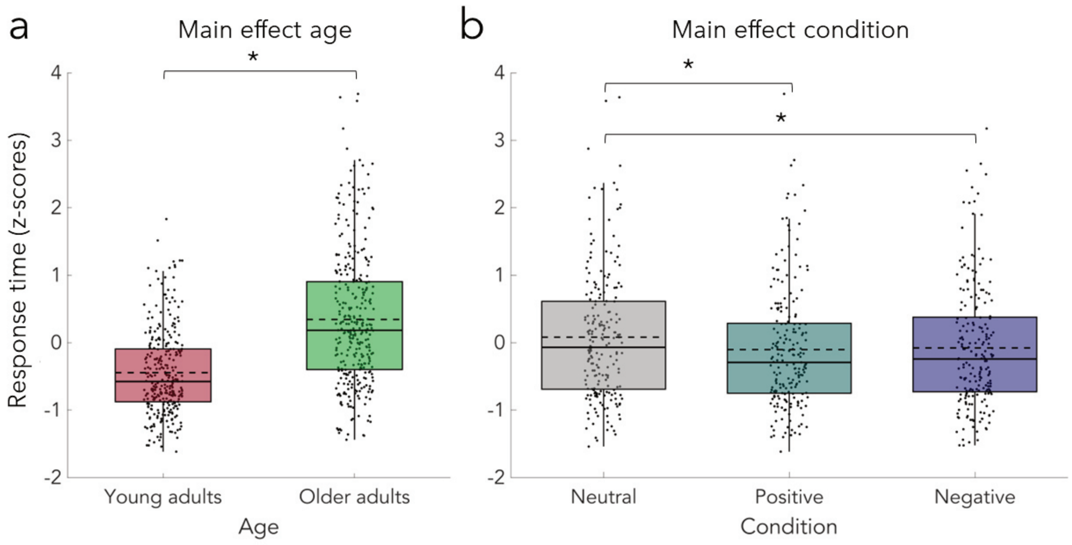

Figure 17. Results of the SID-Photo and SID-Video tasks. **a** Significant main effect of age. RTs are z-transformed. **b** Significant main effect of condition and significant differences between positive vs neutral and negative vs neutral but not positive vs negative condition. Statistical comparisons were made using a 2 × 2 × 3 mixed design (between factors study and age; within-factor condition) permutation *F*-test and two-sided permutation paired *t*-tests (with Bonferroni correction). Data are presented in boxplots overlaid with data points. Boxes span from the lower to the upper quantile and whiskers of the boxplots depict data points that are the furthest from the center while still being inside the range of 1.5 times the interquartile range from the lower or upper quartile. Solid lines indicate the median, dashed lines indicate the mean.

Table 6.

Full model comparison for the Bayesian 2x2x3 mixed ANOVA.

Model	BF_{10}
Null Model	1.0000
Condition	38217.93
Age	6.45×10^{8}
Condition + Age	2.44×10^{13}
Condition + Age + Condition*Age	1.01×10^{12}
Study	0.31
Condition + Study	12771.44
Age + Study	1.81×10^{8}
Condition + Age + Study	7.03×10^{12}
Condition + Age + Condition*Age + Study	2.84×10^{11}
Condition + Study + Condition*Study	573.35
Condition + Age + Study + Condition*Study	2.94×10^{11}
Condition + Age + Condition*Age + Study + Condition*Study	1.44×10^{10}
Age + Study + Age*Study	9.87×10^{7}
Condition + Age + Study + Age*Study	3.51×10^{12}
Condition + Age + Condition*Age + Study + Age*Study	1.17×10^{11}
Condition + Age + Study + Condition*Study + Age*Study	1.73×10^{11}
Condition + Age + Condition*Age + Study + Condition*Study + Age*Study	7.44×10^{9}
Condition + Age + Condition*Age + Study + Condition*Study + Age*Study + Condition*Age*Study	4.20×10^{8}

All Bayes Factors reflect the comparison to the null model. BF = Bayes Factor

5.4.3 Explicit cue valence ratings

The explicit cue valence rating was part of the SID-Video study (Fig. 15b). Here, we measured subjective emotional cue valence by using a rating scale ranging from unpleasant to pleasant (coded as −10 and 10, respectively). To keep a similar structure for both SID tasks, we added extra blocks at the end of the SID-Video task including trials in which the cue was followed by the rating instead of the target.

On average, the valence of the neutral cue was rated 0.00 (SD = 3.38) by young and 1.21 (SD = 3.80) by older adults, while the valence of the positive cue was rated 4.03 (SD = 2.98) by young and 3.21 (SD = 3.60) by older adults, and the valence of the negative cue was rated −0.56 (SD = 3.06) by young and 0.83 (SD = 3.72) by older adults. The 2 × 3 mixed design permutation *F*-test (age × condition) showed a significant main effect of condition ($p = 0.0001$; Fig. 18a) and a significant interaction of the two factors ($p = 0.0082$; Fig. 18b), but no significant main effect of age. Post-hoc permutation paired *t*-tests for the main effect of condition (Fig. 18a) showed significant differences between positive vs neutral ($p = 0.0001$) and positive vs negative ($p = 0.0001$), but not negative vs neutral ($p = 0.1428$). The posthoc two-sample permutation *t*-tests comparing the average ratings in each condition between young and older adults showed no significant effects. Therefore, we performed three additional exploratory post-hoc two-sample permutation *t*-test (Fig. 18b), which revealed that the differences between positive and neutral ($p = 0.0106$) as well as positive and negative ($p = 0.0150$) but not negative and neutral cue ratings are significantly larger in the young compared to the older adults. See Table 7 for the statistical details.

5.4.4 Implicit cue valence – SC-IAT

The Single Category Implicit Association Test (SC-IAT) (Karpinski and Steinman, 2006) was used to assess implicit cue valence (Fig. 15c). It is based on the notion that processing highly associated categories leads to faster RTs (Greenwald et al., 1998) despite being unaware of them. The strength of the association is assumed to be reflected in a D-score: positive D-scores indicate a positive valence association with the cue, while negative D-scores indicate a negative valence association. On average, the D-score for the positive cue was 0.14 (SD = 0.33) in young and 0.16 (SD = 0.34) in older adults while the D-score for the negative cue was 0.04 (SD = 0.37) in young and −0.06 (SD = 0.40) in older adults. The 2 × 2 mixed design permutation *F*-test (age x condition) on D-scores from the SC-IAT showed a significant main effect of condition ($p = 0.0042$; Fig. 19) but no significant main effect of age and no significant interaction. The one-sample permutation *t*-tests on the D-scores for the positive and negative cue across both age groups showed that the D-score for the positive cue was significantly different from zero ($p = 0.0003$) while the D-score for the negative cue was not (Fig. 19). See Table 7 for the detailed statistics.

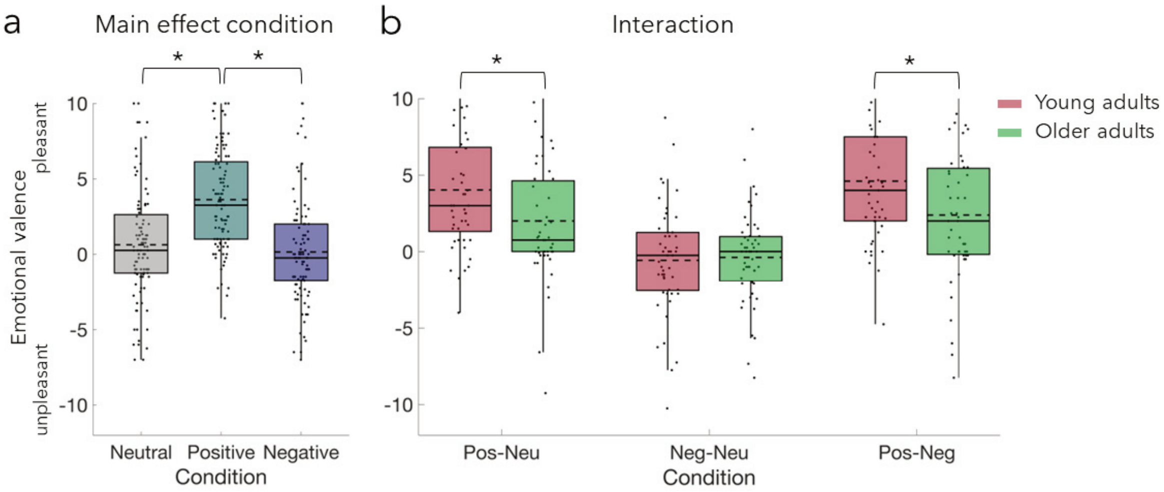

Figure 18. Results of the explicit cue valence rating. **a** Significant main effect of condition and significant differences between positive vs neutral and positive vs negative but not negative vs neutral condition. **b** Differences between conditions in emotional valence ratings for young and older adults. The rating differences between positive and neutral cue as well as positive and negative cue were significantly smaller in the older adults. Statistical comparisons were made using a 2 × 3 mixed design (between factor age; within-factor condition) permutation *F*-test and two-sided two-sample permutation *t*-tests (with Bonferroni correction). Data is presented in boxplots overlaid with data points. Boxes span from the lower to the upper quantile and whiskers of the boxplots depict data points that are the furthest from the center while still being inside the range of 1.5 times the interquartile range from the lower or upper quartile. Solid lines indicate the median, dashed lines indicate the mean. Asterisks mark significant differences ($p < 0.0167$).

5.4.5 Emotional valence ratings of feedback videos

The emotional valence of the video feedback stimuli was rated on a scale from negative to positive (coded as -10 and 10, respectively) to assess age-related differences in socio-emotional processing. Although the video stimuli were validated in a pre-study (see methods for details), we also used the data to ensure significant differences in valance ratings and agreement with the intended emotional valence.

Table 7.

Results of the explicit cue valence ratings and Single-Category Implicit Association Test (SC-IAT) on implicit cue valence.

Explicit cue valence

2x3 *F*-test	df	*F*	*P*	CI95%	η2p
Main effect age	1, 98	1.32	0.2553	[0.2433 0.2674]	0.0133
Main effect condition	2, 169	46.58	0.0001	[-0.0001 0.0005]	0.3222
Interaction age * condition	2, 196	4.89	0.0082	[0.0057 0.0107]	0.0476

Post hoc tests for main effect condition	df	*t*	*P* *	CI95%	*d*
Positive vs neutral	99	7.14	0.0001	[-0.0001 0.0005]	0.71
Negative vs neutral	99	-1.47	0.1428	[0.1331 0.1525]	-0.14
Positive vs negative	99	7.79	0.0001	[-0.0001 0.0005]	0.77

Post hoc tests for interaction	df	*t*	*P* *	CI95%	*d*
Young vs older: Neutral	98	-1.68	0.1006	[0.0922 0.1089]	-0.33
Young vs Older: Positive	98	1.22	0.2200	[0.2085 0.2314]	0.24
Young vs Older: Negative	98	-2.04	0.0440	[0.0383 0.0497]	-0.40

Exploratory post hoc tests	df	*t*	*P* *	CI95%	*d*
Young vs older: Positive – neutral	99	2.47	0.0106	[0.0078 0.0134]	0.49
Young vs older: Negative – neutral	99	-0.29	0.7818	[0.7704 0.7933]	-0.05
Young vs older: Positive – negative	99	2.55	0.0150	[0.0116 0.0184]	0.51

Implicit cue valence

2x2 *F*-test	df	*F*	*P*	CI95%	η2p
Main effect age	1, 98	0.78	0.3951	[0.3816 0.4087]	0.0079
Main effect condition	1, 98	9.27	0.0042	[0.0024 0.0060]	0.0864
Interaction age * condition	1, 98	1.44	0.2358	[0.2240 0.2475]	0.0145

One-sample tests	df	*t*	*P* **		*d*
Positive	99	4.47	0.0003		0.45
Negative	99	-0.36	0.7121		-0.03

* Adjusted alpha $\alpha = 0.05/3 = 0.0167$

** Adjusted alpha $\alpha = 0.05/2 = 0.025$

On average, the valence of neutral feedback videos was rated −0.43 (SD = 1.47) by young and 0.17 (SD = 2.21) by older adults, while valence of positive feedback videos was rated 6.54 (SD = 2.32) by young and 5.78 (SD = 2.80) by older adults; valence of negative feedback videos was rated −6.41 (SD = 2.75) by young and −3.69 (SD = 4.11) by older adults. The 2 × 3 mixed design permutation *F*-test (age x condition) on the emotional valence ratings of feedback videos showed a significant main effect of age ($p = 0.0003$; Fig. 20a), a significant main effect of condition ($p = 0.0001$; Fig. 20b), and a significant interaction ($p = 0.0003$; Fig. 20c). The post-hoc permutation paired *t*-tests (Fig. 20b) showed significant differences between the positive vs neutral ($p = 0.0001$) and negative vs neutral ($p = 0.0001$), and positive vs negative ($p = 0.0001$) condition. The post-hoc two-sample permutation *t*-tests for the interaction comparing the average ratings in each condition between the young and older adults showed a significant difference in the ratings of the negative feedback videos ($p = 0.0003$, Fig. 20c), but no differences between the ratings of young and older adults in the neutral and positive condition. See Table 8 for the complete statistics.

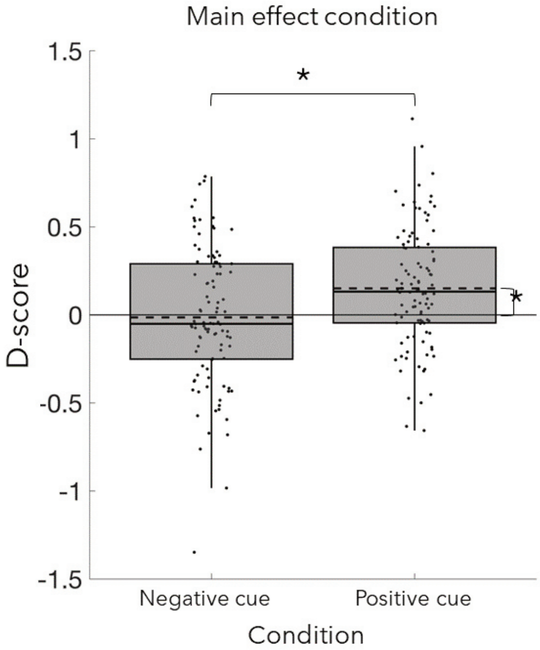

Figure 19. Results of the single category implicit association test. D-scores for the positive and negative cues averaged across young and older adults. The D-score designates an association of the cue with positive or negative valence. D-scores for the positive cue were significantly higher than for the negative cue (main effect of condition). Only the D-score for the positive cue was significantly different from zero. Statistical comparisons were made using a 2 × 2 mixed design (between factor age; within-factor condition) permutation *F*-test and two-sided one-sample permutation *t*-tests (with Bonferroni correction). Data is presented in boxplots overlaid with data points. Boxes span from the lower to the upper quantile and whiskers of the boxplots depict data points that are the furthest from the center while still being inside the range of 1.5 times the interquartile range from the lower or upper quartile. Solid lines indicate the median, dashed lines indicate the mean. Asterisks mark significant differences ($p < 0.005$).

5.4.6 Credibility ratings of feedback videos

Participants were instructed to report the credibility of the feedback and emotion in the video clips on a scale from unbelievable to believable (coded as −10 and 10, respectively). Although the video stimuli were validated in a pre-study (see methods for details), we also used the data to check for systematic differences that might influence the interpretation of other results. On average, the credibility of neutral feedback videos was rated 4.02 (SD = 2.73) by young and 2.43 (SD = 2.88) by older adults, while credibility of positive feedback videos was rated 1.94 (SD = 3.53) by young and 4.94 (SD = 3.31) by older adults; credibility of negative feedback videos was rated 2.59 (SD = 3.91) by young and 3.73 (SD = 3.79) by older adults. The 2 × 3 mixed design permutation *F*-test (age x condition, Fig. 21) on the credibility ratings of feedback videos showed a significant interaction (p = 0.0001), but no significant main effect of age and no significant main effect of condition. The post-hoc two-sample *t*-tests for the interaction, comparing the average ratings in each condition between the young and older adults, showed significant differences in the neutral (p = 0.0050; Fig. 21), and positive (p = 0.0001; Fig. 21), but not negative condition. See Table 8 for the detailed statistics.

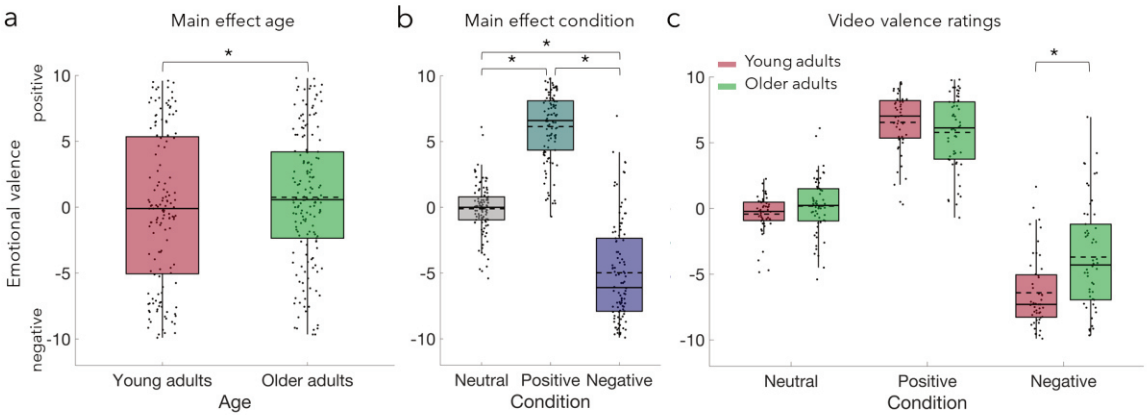

Figure 20. Results of the explicit emotional valence rating for the feedback videos. The analysis also showed **a** a significant main effect of age and **b** a significant main effect of condition. Ratings of neutral, positive, and negative feedback videos were significantly different from each other. The condition averages corresponded with the indented valence. **c** The analysis showed a significant interaction which resulted from the significantly less negative ratings of negative feedback videos by the older adults. Statistical comparisons were made using a 2 × 3 mixed design permutation *F*-test (between factor age; within-factor condition), two-sided permutation paired *t*-tests, and two-sided two-sample permutation *t*-tests (with Bonferroni correction). Data are presented in boxplots overlaid with data points. Boxes span from the lower to the upper quantile and whiskers of the boxplots depict data points that are the furthest from the center while still being inside the range of 1.5 times the interquartile range from the lower or upper quartile. Solid lines indicate the median, dashed lines indicate the mean. Asterisks mark significant differences ($p < 0.001$).

Table 8.

Results of the emotional valence and credibility ratings for feedback videos.

Emotional valence					
2x3 *F*-test	df	*F*	*P*	CI95%	η2p
Main effect age	1, 100	11.11	0.0003	[-0.0001 0.0009]	0.1000
Main effect condition	2, 200	359.42	0.0001	[-0.0001 0.0005]	0.7823
Interaction age * condition	2, 200	8.71	0.0003	[-0.0001 0.0009]	0.0802
Post hoc tests for main effect condition	df	*t*	*P* *	CI95%	*d*
Positive vs neutral	101	18.26	0.0001	[-0.0001 0.0005]	1.80
Negative vs neutral	101	-14.49	0.0001	[-0.0001 0.0005]	1.43
Positive vs negative	101	19.16	0.0001	[-0.0001 0.0005]	1.89
Post hoc tests for interaction	df	*t*	*P* *	CI95%	*d*
Young vs older: Neutral	100	-1.61	0.1102	[0.1015 0.1189]	-0.32
Young vs Older: Positive	100	1.48	0.1384	[0.1288 0.1479]	0.29
Young vs Older: Negative	100	-3.86	0.0003	[-0.0001 0.0009]	-0.76
Credibility					
2x3 *F*-test	df	*F*	*P*	CI95%	η2p
Main effect age	1, 102	2.52	0.1140	[0.1050 0.1226]	0.0242
Main effect condition	2, 204	0.35	0.6911	[0.6783 0.7039]	0.0035
Interaction age * condition	2, 204	22.23	0.0001	[-0.0001 0.0005]	0.1790
Post hoc tests for interaction	df	*t*	*P* *	CI95%	*d*
Young vs older: Neutral	102	2.87	0.0050	[0.0030 0.0070]	0.56
Young vs older: Positive	102	-4.46	0.0001	[-0.0001 0.0005]	-0.87
Young vs older: Negative	102	-1.49	0.1316	[0.1222 0.1409]	-0.29

* Adjusted alpha $\alpha = 0.05/3 = 0.0167$

5.4.7 Partial correlations of explicit and implicit cue valence with feedback valence ratings

To further investigate evaluative learning, we assessed the link between cue valence and feedback video valence by using partial correlations controlling for age. Explicit cue valence correlated with feedback video valence in the positive condition ($r_s = 0.4389$, $p < 0.0001$; Fig. 22b) but not in the neutral ($r_s = 0.0596$, $p = 0.5597$; Fig. 22a) or negative ($r_s = 0.0856$, $p = 0.4018$; Fig. 22c) condition. Implicit cue valence did not correlate with feedback video valence in any condition (positive: $r_s = -0.1302$, $p = 0.2012$; Fig. 22d; negative: $r_s = 0.1144$, $p = 0.2619$; Fig. 22e).

5.5 Discussion

We investigated the effects of more realistic social feedback on motivation, evaluative learning, and socio-emotional processing in young (18–35 years) and older (50–84 years) adults. Overall, RT was accelerated by the possibility to obtain positive and avoid negative social feedback regardless of age, which confirms previous work. More realistic dynamic video feedback did not further accelerate RT but valence ratings of video feedback stimuli showed age-related differences that are compatible with a typical age-related positivity bias in socio-emotional processing. Regarding evaluative learning, explicit and implicit measures of emotional cue valence revealed that reward cues were associated with positive, and punishment cues with neutral emotional valence. Explicit cue valence correlated with feedback video valence in the positive condition independent of age, indicating a specific transfer of emotional valance. As such, our results suggest that dynamic and static social feedback act as motivators across the life span. Further, older and younger adults alike show evaluative learning for predictors of positive social feedback, but the socio-emotional processing of dynamic social stimuli is modulated by age.

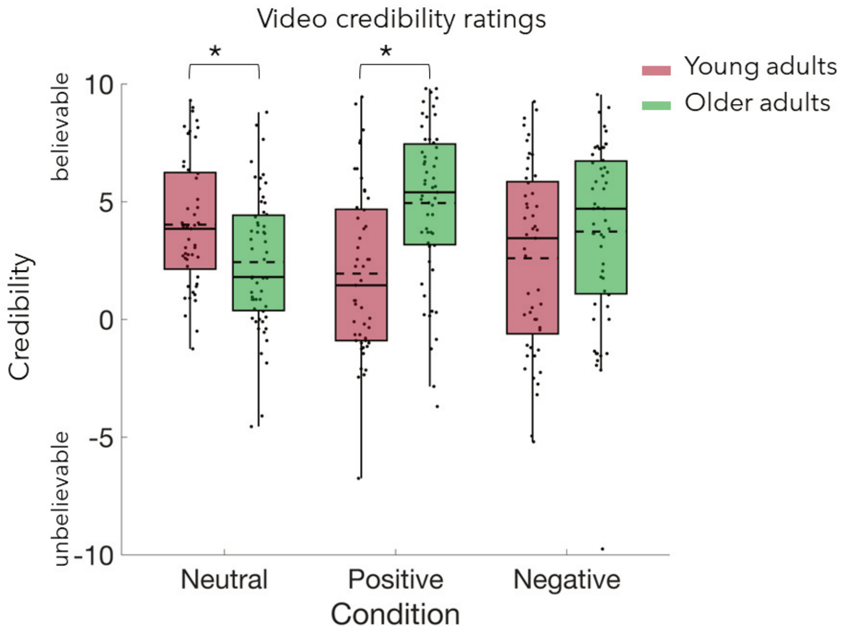

Figure 21. Results of the credibility rating for the feedback videos. On average, the credibility of the feedback videos was positive. Ratings by young and older adults differed significantly in the neutral and positive condition. Statistical comparisons were made using a 2 × 3 mixed design permutation *F*-test (between factor age; within-factor condition) and two-sided two-sample permutation *t*-tests (with Bonferroni correction). Data are presented in boxplots overlaid with data points. Boxes span from the lower to the upper quantile and whiskers of the boxplots depict data points that are the furthest from the center while still being inside the range of 1.5 times the interquartile range from the lower or upper quartile. Solid lines indicate the median, dashed lines indicate the mean. Asterisks mark significant differences ($p < 0.01$).

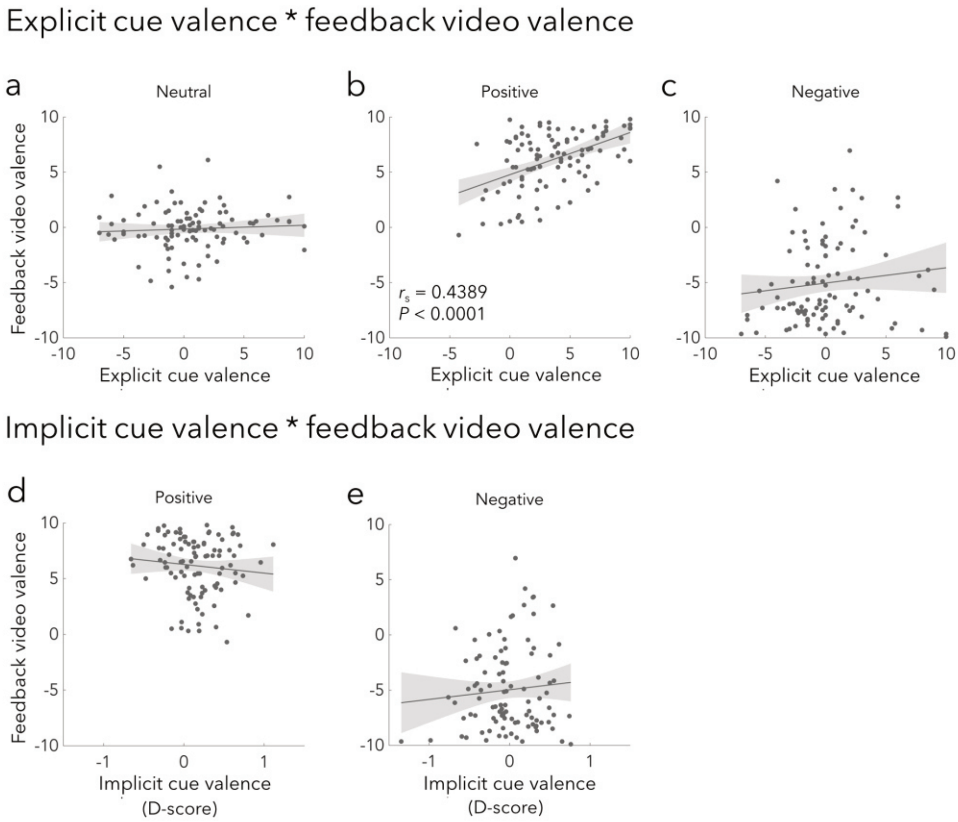

Figure 22. Results of the partial correlations between cue valence and feedback valence. **a–c** Partial correlations between explicit cue valence and feedback video valence in the neutral, positive, and negative condition. Cue valence and feedback video valence were significantly correlated in the positive condition. **d, e** Partial correlations between implicit cue valence and feedback video valence in the positive and negative condition. Statistical analyses were made condition using Spearman correlation coefficients (two-sided, with Bonferroni correction). Plots show the individual data points together with the fitted generalized linear model (GLM) and 95% confidence bounds (shaded area).

Human behavior, including learning and motivation, is profoundly modulated by social reinforcers. Compatible with such a view and the existing literature (Kohls et al., 2013; Rademacher et al., 2014), we find that RTs are faster when anticipating positive and negative compared to neutral social feedback in both young and older adults (Fig. 17). At the neural level, a behavioral advantage by social and monetary reinforcers has often been linked to the mesolimbic system, including the dopaminergic midbrain, VS and other interconnected brain regions, such as the prefrontal cortex (Haber and Knutson, 2010; Martins et al., 2021). Importantly, the mesolimbic system degenerates during healthy aging (Bäckman et al., 2006) leading to impaired learning and memory (Howard and Howard, 2013; Samanez-Larkin et al., 2014). However, the absence of age-related differences in RT acceleration, as observed here, is in line with the notion that social affiliation constitutes a fundamental human motive across the life span (Carstensen, 1998), and they could also be accounted for by the simple nature of our task. Indeed, age-related impairments are often reported in more difficult learning tasks (Mata et al., 2011) and they are probably based on reduced prediction error signaling in frontostriatal circuits (Samanez-Larkin et al., 2014). Moreover, the restoration of the prediction error via L-DOPA administration (Chowdhury et al., 2013a) and providing additional information about future values (Samanez-Larkin et al., 2011) improved learning in older adults. Our results are consistent with these observations and indicate that possible age-related declines of the mesolimbic system do not necessarily affect RT in the SID task. In a broader context, our observations further underline that older adults are capable of behavioral adaptation and learning under specific circumstances.

The finding that RTs accelerated for static photo and dynamic video feedback alike (Fig. 17) was unexpected given that dynamic social information should be more immersive and therefore promote behavioral invigoration (Rademacher et al., 2014; Rymarczyk et al., 2016). Instead, our results suggest that behavioral invigoration (as indicated by RT acceleration) is normalized to the distribution of available options within a context. This view is compatible with the "value normalization framework", which was originally proposed for neural responses to rewards in choice tasks (Rangel and Clithero, 2012). However, it may also be applicable to other settings (Sallet et al., 2007), and therefore useful to explain the behavioral effects in our study. Precisely, the presentation of static photo and dynamic video feedback in two separate tasks (instead of a trial-by-trial variation) may have led to normalized rank values of positive and negative social feedback relative to neutral feedback within each experimental context. As a result, RTs were equally accelerated to obtain positive and avoid negative social feedback regardless of static or dynamic feedback. A similar rationale has been proposed in the context of "adaptive scaling" of reward predictions errors, as shown in monkeys (Tobler et al., 2005) and the human mesolimbic system (Bunzeck et al., 2010). Together, anticipating positive and negative social feedback accelerated RTs in young and older adults which indicates increased motivation, but there was no additional benefit of using dynamic video feedback. This result may be explained by context dependent value normalization and may translate to other measures of physical effort. Nonetheless, more research is needed to test this hypothesis and the effects of increasingly naturalistic social stimuli (Fan et al., 2021) on motivation and cognition.

Our older adults had less pronounced ratings of negative social feedback videos (Fig. 20), which is compatible with the literature on the age-related positivity effect typically shown for static pictures such as faces (Iidaka et al., 2002; Mather and Carstensen, 2003; Czerwon et al., 2011). While this has often been interpreted as prioritization of emotional goals in older adults (Carstensen, 1998), we can extend the literature by demonstrating the positivity effect in a set of more ecologically valid affective social video stimuli. From a more mechanistical point of view, the positivity effect in older adults may be an expression of cognitive change strategies, specifically reappraisal (Gross, 1998), used for emotion regulation. These strategies can help to achieve emotional goals (Kryla-Lighthall and Mather, 2016) depending on specific contexts. In our study, the reappraisal of social stimuli in older adults did not reduce the motivation to avoid negative feedback but seems to be limited to the exposition to negative emotional content. This may be, again, explained by value normalization or adaptive scaling, or the primacy of early emotion regulation in younger and older adults (Livingstone and Isaacowitz, 2021), such as the avoidance of negative information (Gross, 1998). Furthermore, according to the strength and vulnerability integration model, older adults have difficulties in recovering from sustained arousal (Charles, 2010) leading to the avoidance of negative situations. Together, while young and older adults differ in their socio-emotional processing when being confronted with negative affective social information, they are similarly motivated to avoid negative social information when possible.

We found evidence for evaluative learning of cue valence in young and older adults. Specifically, our data indicate the transfer of positive emotional valence from dynamic social feedback to the initially neutral cues (Figs. 18 and 19). Moreover, explicit valence ratings of positive cues correlated with valence ratings of positive feedback videos (Fig. 22). In general terms, these results are compatible with the notion of evaluative learning and valence transfer (De Houwer, 2007; Hütter and Rothermund, 2020) and they demonstrate that older adults are still able to learn emotional associations from positive dynamic social feedback for predictive cues, while age-related problems in implicit learning may occur in a task-dependent manner, for example in probabilistic sequential learning settings (Howard and Howard, 2013). In contrast, ratings and D-scores for the negative cues were not significantly different from neutral (Figs. 18 and 19) and no correlation was found between negative cues and negative feedback videos (Fig. 22). While this indicates a specific effect for positive cues and feedback, it may be explained by the different numbers in neutral, positive, and negative feedbacks. In fact, positive cues preceded positive feedback in 83% of the trials but negative cues preceded negative feedback only in 17% of the trials. While this imbalance is a limitation and higher rates of negative feedback could have induced evaluative learning for the negative cues, we intended to not frustrate or demotivate our participants.

The assessment of cue valence was characterized by age effects in the explicit (Fig. 18) but not in the implicit test (Fig. 19). Specifically, for explicit ratings of cue valence, the differences of positive vs neutral and positive vs negative were smaller in older compared to younger adults. On the one hand, this could imply weaker explicit emotional memory in older adults along with general deficits in explicit memory (Fleischman et al., 2004). On the other hand, these results could be interpreted in a dual-process framework of cognition (Evans and Stanovich, 2013). From this perspective, the explicit cue and video ratings are influenced by higher order cognitive processes, e.g., emotion regulation strategies, while the results of implicit measures reflect automatic responses. This interpretation is further supported by a significant correlation of explicit but not implicit cue ratings with feedback video ratings in the positive condition.

The actors in the feedback videos were 24 and 27 years old and may have been perceived differently by the two age groups. This is also known as intergroup biases (Molenberghs and Louis, 2018), which could directly or indirectly affect learning, socio-emotional processing, and motivation. In fact, faces of the own age group are better remembered than faces of other age groups (Ebner and Johnson, 2009; Rhodes and Anastasi, 2012) and higher amounts of contact to the own group reduces emotion recognition in the other age group (Ebner and Johnson, 2009). However, both, young and older participants, are better at recognizing emotions from young than older faces (Ebner and Johnson, 2009) probably due to stronger expressivity in younger faces (Fölster et al., 2014). Moreover, emotions induced by receiving positive social feedback (Ellemers et al., 2004) or viewing emotional faces (van der Schalk et al., 2011) are not modulated by the source (ingroup vs outgroup). In addition, attitudes towards specific age groups could influence how the feedback is perceived, for example depending on the competence attributed to the person giving feedback. However, while younger adults (21–35 years) favored the ingroup by devaluating the competence of middle-aged (36–54 years) and older (>55 years) adults, older adults showed no bias in favor of their own age group (Kite et al., 2005). Regarding motivation, individuals are more willing to exert efforts to enhance the impression that other ingroup members have compared to the outgroup (Ellemers et al., 2004). Together, older adults typically show no own age bias in emotion recognition or competence attribution, and emotional responses to feedback are typically not modulated by ingroup vs outgroup settings. However, intergroup biases in the motivation to gain social approval from the ingroup compared to the outgroup could have an influence although this was not explicitly shown for different age groups.

Another aspect that should be noted is that photo and video feedback stimuli differed not only with respect to dynamics but also durations (750 ms and 2400 ms, respectively). From a conceptual point of view, photo and video duration should have been matched, e.g., by a longer presentation of the photos. However, from a motivational point of view, prolonged static image presentation could induce boredom, which is an unpleasant emotional state leading to less task engagement and motivation.

Finally, we would like to discuss possible limitations of our study design, i.e., between vs within subjects. The exposure to multiple kinds of incentives within subjects has psychological consequences and the valuation of static and dynamic social incentives may depend on the availability of the other (Charness et al., 2012). To this end, it is unclear whether a within-subjects design would have produced the same or different results, and our study is informative for future studies and possible learning tools, which most likely would implement one but not both types of social feedback. From a practical point of view, having both conditions (static and dynamic feedback) with similar trial numbers as we have in our current version, a possible experiment would be twice as long. This could have a negative effect on motivation and behavior and, therefore, the validity of the results. One disadvantage of using a between-subject design are context effects. Specifically, the SID-Video study was performed during the COVID-19 pandemic while the SID-Photo study was conducted one year before. Due to social distancing and contact restrictions, the social interaction with the experimenters might have increased the subjects' motivation, leading to greater effort and, therefore, to overall faster RTs than in the SID-Photo study. Thus, differences in RTs between studies could be coincidental, and the effects of realistic social feedback on motivation may have been masked by the aforementioned effects.

To conclude, anticipating positive and negative social feedback is an essential part in the learning process that invigorates behavior in young and older adults, but there was no additional benefit of dynamic over static social stimuli. Our data also indicate a transfer of emotional valence from social video feedback to initially neutral cues in both young and older subjects, which differed between groups only in the explicit task. Together with a positivity effect in older adults, this is compatible with theories on dual-processing as well as cognitive control strategies for emotion regulation and it indicates specific developmental changes in evaluative learning during healthy aging. As such, our work gives insights into the effects of age on motivation, learning, and socioemotional information processing.

6 General discussion

- Summary of results
- Anticipating positive and negative social incentives recruits the human substantia nigra
- Interaction between the mesolimbic system and the basal forebrain during social incentive anticipation
- A more general perspective on “Cortical and Subcortical Social Information processing” – the CASSI model
- The effects of social feedback anticipation on motivation and learning
- Limitations and future directions
- Conclusion

The aim of the present thesis was to investigate the neuropsychological mechanisms of social incentive processing, focusing on subcortical functions underlying the anticipation of positive and negative social feedback and its effects on motivated behavior in young and older adults. Precisely, the conducted studies aimed to investigate a) valence (positive or negative) processing in the human SN and b) the interaction between the mesolimbic system and the BF during social feedback anticipation, c) the influence of aging on motivation, learning, and socio-emotional processing, and d) the influence of different social feedback modalities (i.e. static vs. dynamic) on motivation and learning.

In the following, the key findings of the three studies will first be summarized. Next, the neural and behavioral results are discussed with respect to the current state of research and their novel contributions to our understanding of the neuropsychological mechanisms underlying social incentive processing. The results will be integrated across the studies to address the overarching research questions. Furthermore, a general model of the neurocognitive processing of social incentives is proposed. The discussion closes with an examination of the limitations of the current studies and suggestions for future research directions, followed by the final conclusion.

6.1 Summary of results

Study I (Sobczak et al., 2021) investigated the effects of social incentives on behavioral and neural processing. We conducted the SID task in young (n=51) and older (n=52) healthy controls, non-operated PD patients ON and OFF medication (n=24), and PD patients OFF medication with intraoperative iEEG recordings in the SN (n=12). On the behavioral level, anticipating positive and negative social feedback was associated with faster RT in all healthy controls and non-operated PD patients. This effect was not modulated by age or medical treatment. The effect could not be detected in intraoperative PD patients, probably due to the small sample size. On the neural level, intraoperative SN recordings showed that spectral power in alpha-beta (9-20 Hz) oscillations was increased during the anticipation of both positive and negative social feedback.

Study II (Sobczak et al., 2023) examined the regional processing and interregional functional relations of the lateral, ventral, and medial SN, NAcc, NBM, and MS/DB during social reward and punishment anticipation. 36 healthy young adults performed the SID task while undergoing high-resolution fMRI. On the behavioral level, we replicated faster RTs for positive and negative compared to neutral feedback anticipation. On the neural level, we found evidence for functional connectivity that related to the valence of the anticipated feedback. We specifically identified connectivity of the lSN–NBM for neutral feedback anticipation, vSN–NBM for positive feedback anticipation, and lSN-MS/DB, lSN-NAcc and mSN-NAcc for negative feedback anticipation. Furthermore, we observed valence-unrelated functional connectivity of the mSN-NBM, NAcc-NBM, NAcc-MS/DB for all three conditions possibly involved in more general anticipatory processing.

Study III (Sobczak and Bunzeck, 2023) tested the effects of social feedback on motivation, evaluative learning, and socio-emotional processing in healthy young and older adults. First, we investigated the effects of static vs dynamic social feedback on motivation, by reusing the behavioral data of the SID task with photo feedback in healthy young (n=51) and older (n=52) controls from study I and comparing it to a new set of data of young (n=49) and older (n=55) adults using the SID task with prerecorded feedback videos. The RT effect was replicated and again showed no modulation by age, except overall RT slowing, and no additional effects of video feedback. Second, we tested the influence of aging on socio-emotional processing and evaluative learning by measuring the emotional valence of the feedback stimuli and associated predictive cues. Older adults reported less negative affect for social punishment video stimuli, suggesting age differences in socio-emotional processing. Furthermore, the results indicated evaluative learning for cues associated with positive social feedback but not neutral or negative cues.

6.2 Anticipating positive and negative social incentives recruits the human substantia nigra

Regarding research question a), studies I and II shed light on the role of the SN in processing positive and negative social feedback anticipation. IEEG recordings showed that the anticipation of both social reward and punishment recruits the SN, but there was no evidence for discriminative signaling in neural oscillations (study I, experiment 1; Sobczak et al., 2021). In addition, the fMRI results indicated that both events trigger increased activity in the SN, but there is a valence-related functional topography, i.e. a reward-associated ventral part, and a punishment-associated lateral part (study II; Sobczak et al., 2023). Together, these results emphasize the role of the SN in signaling both the anticipation of positive and negative social feedback.

These findings are consistent with initial human fMRI studies showing that the SN/VTA signals the anticipation of positive and negative outcomes, i.e. monetary reward (Wittmann et al., 2005; Adcock et al., 2006) and electric shocks (Bauch et al., 2014). The lack of discriminative iEEG responses (study I, experiment 1; Sobczak et al., 2021) may simply indicate that our data mainly reflect the responses from one of the two DA neuron populations described by Matsumoto and Hikosaka (2009). Specifically our data may predominantly represent the population responding with excitation to both positive and negative cues, which was also reported to be larger than the other (Matsumoto and Hikosaka, 2009).

Moreover, it is crucial to highlight that the results of study I significantly contribute to the literature by providing direct electrophysiological evidence in humans for anticipatory SN activity. As such, they complement the observation by Zaghloul et al. (2009) showing responses to unexpected monetary rewards in iEEG recordings from the human SN. These two findings are compatible with the typical activity pattern of dopaminergic midbrain neurons responding to unexpected rewards and to reward-predicting stimuli (Schultz et al., 1997) which have been established in animal models (as explained in 1.4.3 The neural mechanisms of reward and punishment processing). Thus, these results in humans provide essential pieces of evidence for the validity of findings from animal studies (Zaghloul et al., 2009).

Observing which brain regions respond to certain events is essential to gain insight into their function but it is equally important to understand how information is propagated throughout the brain. One means of neural communication is through oscillations which connect distributed neural populations and brain regions to transfer information (Buzsaki and Draguhn, 2004; Fries, 2005). Our results suggest that alpha-beta oscillations are a possible mechanism of anticipating rewards and punishments. This is in line with scalp EEG findings showing a link between beta oscillations and monetary reward anticipation (Bunzeck et al., 2011), monetary reward delivery (Cohen et al., 2007; Marco-Pallares et al., 2008; Marco-Pallarés et al., 2015), and VS activity (Mas-Herrero et al., 2015). Furthermore, it extends the literature by showing that alpha-beta oscillations also play a role in social punishment anticipation. Together, this suggests a prominent role of beta oscillations in incentive processing which may also serve communication between the SN/VTA and other brain regions involved in these processes, such as the VS and PFC (Marco-Pallarés et al., 2015; Lansink et al., 2016).

In fact, high-resolution fMRI in study II revealed valence-related patterns of functional connectivity involving SN subregions and other mesolimbic and BF structures. Specifically, the findings show firstly that functional connectivity between the vSN and the NBM is involved in the anticipation of positive events, i.e. social reward. Secondly, the anticipation of negative events, i.e. social punishment, involves functional connectivity of the lSN–MS/DB, lSN–NAcc, and mSN–NAcc. In addition, the MVPA suggested that the mSN and vSN differentiate between positive and neutral predictors. These observations are partly in line with previous findings by Matsumoto and Hikosaka (2009) and Guitart-Masip et al. (2011). Our results align more closely with the findings of one other high-resolution fMRI study in humans (Pauli et al., 2015) using pleasant and unpleasant liquids that showed expected value responses in the ventromedial SN and dorsolateral SN to cues predicting appetitive and aversive outcomes, respectively. While both types of events elicit increased activity, the location of the activity determined its function, i.e. the processing of positive or negative valence during anticipation. Moreover, the expected value signals in the brain correlated positively with affective ratings of the appetitive and negatively with ratings of the aversive predictors suggesting that the neural responses relate to affective processing (Pauli et al., 2015). Along these lines, the role of the vSN in reward and the lSN in punishment anticipation is further supported by our findings. Together, our findings provide additional evidence for a functional topography within the SN/VTA related to the processing of positive and negative information and extend the literature by showing that it potentially translates to social stimuli.

Regarding the role of the SN/VTA in social information processing, our findings are in line with the literature suggesting that this brain region is involved in several social contexts, e.g. when viewing social cues after social isolation (Tomova et al., 2020) and pictures of a loved one (Fisher et al., 2010; Acevedo et al., 2012), during social learning in humans (Smith-Collins et al., 2013; Diaconescu et al., 2017), and sociability in mice (Wang et al., 2021).

Despite these insights, certain limitations should be acknowledged. The results are not entirely consistent with the findings by Zhang et al. (2017) and Guitart-Masip et al. (2011). Both studies suggest that valence is encoded within the mSN. However, in study II, the decoding models of the MVPA that would have indicated valence signaling (neutral vs. positive vs. negative and positive vs. negative) failed to provide direct evidence of valence coding. Methodological differences, such as the task (SID task vs. a gambling task and a combination of a conditioning paradigm with go/ no-go trials), the reward type (social vs. monetary), and the focus on different phases of reward processing (anticipation vs. outcome), may explain discrepancies (study II; Sobczak et al., 2023).

Furthermore, the valence-related connectivity patterns are reflected in correlations that were significant in one condition but were not necessarily significantly different from the other conditions, challenging a simple categorization into salience or valence coding. Nevertheless, these findings may indicate that functional connectivity between mesolimbic and BF subregions is relevant for the anticipation of social feedback (study

II; Sobczak et al., 2023). Additionally, the fMRI findings do not necessarily relate to dopaminergic activity and clarification of this aspect would require psychopharmacological intervention studies. Regarding study I, it remains an open question whether the iEEG results can be generalized to healthy humans. Direct proof of the comparability of the results is not practical, because such invasive iEEG recordings can only be performed in specific clinical cases, e.g. PD patients undergoing brain surgery, but not healthy individuals. However, it can be argued that we recorded the signal of the remaining intact dopaminergic neurons and therefore, in theory, the signal should not differ between HOA and PD (Zaghloul et al., 2009). Future iEEG studies could be analyzed using spike sorting (Yebra and Rutishauser, 2022) or machine learning (Federau et al., 2021) to establish a closer link with direct physiological recordings in animals.

Together, the common ground of the research in the field is that the SN exhibits a functional topography, but the exact delineations are debated. Our fMRI results are most consistent with the findings of Pauli et al. (2015), indicating a functional segregation into two subregions, a reward-associated ventral part, and a punishment-associated lateral part, and emphasize the role of the SN/VTA in social information processing.

6.3 Interaction between the mesolimbic system and the basal forebrain during social incentive anticipation

Regarding research question b), study II provides further insight into the interaction between subcortical brain regions, i.e. the NAcc, SN/VTA, MS/DB, and NBM, during the anticipation of positive and negative social feedback. More specifically, we found valence-related and valence-unrelated functional connectivity patterns involving these regions. The anticipation of positive feedback involved functional coupling of the vSN–NBM while negative feedback anticipation involved functional connectivity of the lSN–MS/DB, lSN–NAcc, and mSN–NAcc. Anticipating neutral feedback was associated with connectivity of the lSN–NBM. These findings largely converge with the notion of a functional segregation of the SN as described above and extend this idea by proposing two divergent functional pathways between subregions of the BF and SN, i.e. a lSN-MS/DB pathway involved in negative motivational valence and a vSN-NBM pathway involved in positive motivational valence.

In this sense, our results indicate a substantial contribution of the BF to motivational processing, especially incentive anticipation. This is in line with other studies demonstrating involvement of the BF in the anticipation and outcome processing (see

1.4.3 The neural mechanisms of reward and punishment processing) of several non-social and social stimuli (food reward, pleasant and unpleasant liquids, air-puffs, electrical shocks, social reward, social punishment; Wilson and Rolls, 1990; Hangya et al., 2015; Monosov et al., 2015; Guo et al., 2019; Bortolini et al., 2021; Martins et al., 2021; Robert et al., 2021). Importantly, our findings agree with the results of a meta-analysis of the SID task showing responses to social punishment cues in the septal nuclei in humans (Martins et al., 2021).

Moreover, specific projections of the BF have been associated with the mediation of approach and avoidance behavior in mice. For instance, while activation of glutamatergic projections from the MS to the lateral habenula (lHb) elicited place avoidance associated with the delivery of aversive stimuli, it was reduced by the activation of GABAergic projections from the MS to the lHb (Zhang et al., 2018). Similarly, suppressing cholinergic projections from the BF to the medial PFC during the anticipation of negative outcomes impaired the learning of aversive associations with a negative cue in mice (Tu et al., 2022). Regarding social behavior, the inhibition of inhibitory BF projections targeting VTA GABA neurons led to a reduced DA release into the NAcc and less social interaction (Wang et al., 2021). Together, the BF and its subcortical and cortical connections are involved in the processing of motivational valence and the regulation of behavior, including the social domain.

On a larger scale, our findings support the role of the BF in motivational and cognitive aspects of social information processing. For instance, the septum is involved in experiencing and expressing emotions, including general emotional valence but also specific affiliative emotions, i.e. feelings of warmth and tenderness (Moll et al., 2012), and prosocial sentiments such as pride, guilt, pity, or embarrassment (Zahn et al., 2009; Moll et al., 2011). As explained in the introduction (see 1.1 Psychological concepts of motivation), the evaluation of stimuli as pleasant or unpleasant (i.e., valence) and associated emotions are a key component of motivational processing (Padilla-Coreano et al., 2022). In the social environment, valence helps to interpret social situations and execute appropriate actions. For example, emotional expressions, including mimic and gesture, are an essential part of human communication that can facilitate approach or avoidance behavior (Kohls et al., 2013). In addition to valence processing, the septum signals PEs in social contexts, as demonstrated in a social trustworthiness learning task (Diaconescu et al., 2017) and a prosocial learning task (Lockwood et al., 2016). Together, in line with previous studies our findings suggest that the function of the BF in social information processing could relate to valence processing and PE signaling. The processing of other types of social valence, such as social rank, social memory, and social isolation, have been associated with a neural circuit including the medial PFC, NAcc, basolateral amygdala, and hippocampus (Padilla-Coreano et al., 2022). However, the BF has been neglected in this and other human models so far.

Our results favor the integration of the BF in such models. Functional connectivity is a suitable means to understanding the overall organization of functional communication in the brain, going beyond isolated brain activation signatures (Shahhosseini and Miranda, 2022). Using functional connectivity analysis, study II shows that parts of the mesolimbic system and BF are coupled together, depending on the anticipated social valence. In line with our findings, other studies show associations of BF functional connectivity with social and non-social valence processing. For instance, coupling between cholinergic BF neurons and the auditory cortex increased during auditory fear conditioning (Guo et al., 2019), resting-state functional connectivity between the BF and amygdala correlated negatively with social anxiety traits (Zhu et al., 2023), and functional connectivity patterns of the NBM and septum with a wider social information processing network (including the VTA, NAcc, amygdala, insula, and orbitofrontal cortex) during positive and negative social interactions were differently affected by intranasal oxytocin (Rilling et al., 2018). Together, in addition to isolated brain activation signatures implicating the mesolimbic system and BF in motivational and social information processing, a growing body of human neuroimaging research suggests their mutual interaction in these processes.

Functional coupling unrelated to the anticipated emotional valence of social feedback involved the mSN–NBM, NAcc–NBM, and NAcc–MS/DB. Our finding is in line with the assumption of a neural circuit between the BF, PFC, and mesolimbic regions – including the NAcc, SN/VTA, and amygdala – that supports top-down attentional control (Demeter and Sarter, 2013). Although the correlative nature of our results does not allow a directional interpretation of information flow between these brain regions, these functional links involving the SN, NAcc, and BF, may implicate some kind of mechanism that guides attention towards relevant information. The cholinergic projections between the NBM and PFC are known for their role in sustained attention (Sarter et al., 2001, 2006). Due to the NBM's efferent cholinergic projections to the frontal cortex and afferent projections from the VS, its functional engagement may reflect a route from the mesolimbic system to frontal regions that provides information about relevant stimuli for higher cognitive processes (Haber and Knutson, 2010). Assuming that our results are related to attentional processing, this suggests a new aspect of the mesolimbic BF-PFC attentional circuitry, namely that a functional coupling of the NBM with a specific part of the SN/VTA, the mSN, is involved. Together, research suggests a neural network, connecting the BF, PFC, and mesolimbic areas, possibly influencing attention toward relevant (social) information.

While study II has yielded valuable insights, there are limitations that warrant discussion. Functional connectivity, as utilized in this study, is an undirected measure that identifies regions' coupling without implying causality. Therefore, directional relationships cannot be inferred. Future studies will need to use different methods to address this point and draw conclusions about the direction of communication (i.e. bottom-up or top-down) between brain regions, thereby refining models of neural anticipatory processes. Furthermore, as noted above, the valence-related connectivity patterns are based on significant correlations that were not necessarily significantly different between conditions. As such, they neither provide direct evidence of differences between conditions nor evidence of absence of such differences. While this limits the interpretation of our findings, they still may indicate that functional connectivity between mesolimbic and BF subregions is involved in the anticipation of social feedback.

Moreover, the focus of the study on social stimuli without comparison to non-social stimuli may limit the generalizability of the findings. Various investigations suggest a common neural currency of reward value across social and non-social reinforcers on a larger scale (Rademacher et al., 2010). More specifically, anticipatory processes may be more domain-general while domain-specific processing may be exhibited during outcome processing (Rademacher et al., 2010; Gu et al., 2019). However, these studies targeted brain regions, e.g., the SN/VTA, as a whole but not their compartments. Therefore, these observations do not exclude the possibility of differential processing in specialized subregions (Ruff and Fehr, 2014). Consequently, it remains unclear whether our findings are unique to the anticipation of social incentives or whether they can be generalized to other domains.

As explained in the introduction (see 1.4.3 The neural mechanisms of reward and punishment processing), the VS including the NAcc is a brain region that is known for its role in anticipation and outcome processing of reinforcers. However, study II showed less NAcc involvement than expected. As noted above, effects may be different depending on the level of investigation and it has been hypothesized that subregions within NAcc serve distinct functions (Haber and Knutson, 2010). Specifically, the core is thought to be implicated in processing salience, whereas the shell is associated with signaling valence (Bromberg-Martin et al., 2010). Future studies investigating these subregions, i.e. the core and shell, could help elucidate discrepancies and provide insight into the functional connectivity among subregions of the NAcc, SN/VTA, and BF (Chowdhury et al., 2013c).

On a final note, this study did not explore the impact of gender on the anticipation of social reward and punishment. However, previous research has shown gender-related differences in connectivity patterns and responses to social incentives. For example, women exhibit the engagement of a wider neural network during the SID task compared to men (Spreckelmeyer, 2009), and the effects of intranasal oxytocin on functional connectivity during positive and negative social interactions differ between genders (Rilling et al., 2018). Although our sample had a balanced gender ratio (21 female and 17 male participants), the statistical power to detect gender differences would be limited due to the small size of the subsamples, so this aspect remains unclear.

Summing up, our results are in line with previous research implicating the BF in motivational valence and social information processing. Furthermore, we extend the existing literature on the interaction between the mesolimbic system and the BF in motivation and social information processing. Study II shows that social reward and punishment anticipation involves functional coupling of these brain regions in humans and, more importantly, that valence-related functional connectivity patterns between specific subregions could make the difference in these processes. As such, it provides valuable insights into the role of the BF and its interaction with other relevant structures which have been neglected in human models of motivation and social information processing. The next section will elaborate on an extended model integrating the BF in a lager network underlying these functions.

6.4 A more general perspective on "Cortical And Subcortical Social Information processing" – the CASSI model

The content of this section is based on parts of a published article and has been adapted for this dissertation for consistency. The article has been published in *Current Opinion in Behavioral Sciences*:

Sobczak A, Bunzeck N. 2024. The basal forebrain serves social information processing. Current Opinion in Behavioral Sciences ***56****:101372. doi:10.1016/j.cobeha.2024.101372*

As alluded to above, the mesolimbic system and BF are pivotal in processing motivational and social information. While the previous sections have focused on specific mechanisms supported by these subcortical brain regions (e.g. social reward anticipation), this section aims to integrate recent findings into a more general model of cortical and subcortical social information processing (CASSI). The proposed model extends previous human models and aims to illustrate how cortical and subcortical social information processing can contribute to motivation and behavior.

While the SN/VTA, NAcc, amygdala, hippocampus, and PFC have been acknowledged as parts of a pathway for motivation and goal-directed behavior (Rajmohan and Mohandas, 2007; Haber and Knutson, 2010; Hippmann et al., 2021), and social valence processing (Padilla-Coreano et al., 2022) in previous models, parts of the BF have largely been neglected. Anatomically, the NAcc, SN/VTA, MS/DB, and NBM are interconnected (see 1.4.1 Relevant neuroanatomical concepts) and maintain various connections throughout the brain including cortical sensory areas and prefrontal regions (Cacciola et al., 2016; Zhang et al., 2017; Chaves-Coira et al., 2018), as well as limbic structures such as the amygdala and hippocampus (Mesulam et al., 1983; Haber and Knutson, 2010). This makes them ideal components of a complex and interconnected valuation system.

For instance, the BF receives projections from the VS and projects to the PFC. Functional engagement of the NBM may reflect an indirect route from the mesolimbic system to frontal regions providing relevant information for higher cognitive processes (Haber and Knutson, 2010). Furthermore, the cholinergic projections of the NBM and PFC are involved in sustained attention (Sarter et al., 2001, 2006). Along these lines, functional coupling between the NAcc and NBM during social feedback anticipation as shown in study II (irrespective of the valence of the feedback) in humans may also implicate a mechanism that guides attention towards relevant information.

Regarding the role of BF projections to the PFC in mediating social behavior, there is no conclusive evidence yet. However, two recent reviews have highlighted the role of the PFC in social valence processing (Padilla-Coreano et al., 2022) and aspects of social cognition, e.g. facial emotion recognition, theory-of-mind, and self-perception, together with the posterior cingulate cortex, precuneus, and amygdala (Hiser and Koenigs, 2018). Given the BF's association with social valence processing and various aspects of social cognition (see 4.5 Discussion), it seems plausible that the BF works in concert with the PFC to promote social behavior. However, this suggested link still requires empirical validation.

Taken together, we suggest that primary and association areas receive sensory information, which then enters the BF and SN/VTA, where it is further processed, e.g. via valence signaling, value computations, and prediction errors (Haber and Knutson, 2010;

Iglesias et al., 2013; Diaconescu et al., 2017; Monosov, 2020). Other components of the BF, such as the ventral pallidum (Zaborszky et al., 2012), and connections between the BF and basolateral amygdala, lHb, and lateral hypothalamus may also be involved (Root et al., 2015; Golden et al., 2016; Jimenez et al., 2018; Swanson et al., 2022; Rodriguez et al., 2023). These neural signals are then interpreted and translated into social motivation and behavior by higher cortical areas, especially the PFC, which is known for its involvement in executive control and goal directed behaviors (Arco and Mora, 2009). These can include biological and socio-emotional aspects. A schematic illustration of the potential flow of information between cortical and subcortical areas working in concert to promote social cognition, motivation, and behavior is shown in Figure 23. With the proposed model, we suggest that the contribution of the BF to motivational and cognitive aspects has been neglected in other models and should be given more attention in future research.

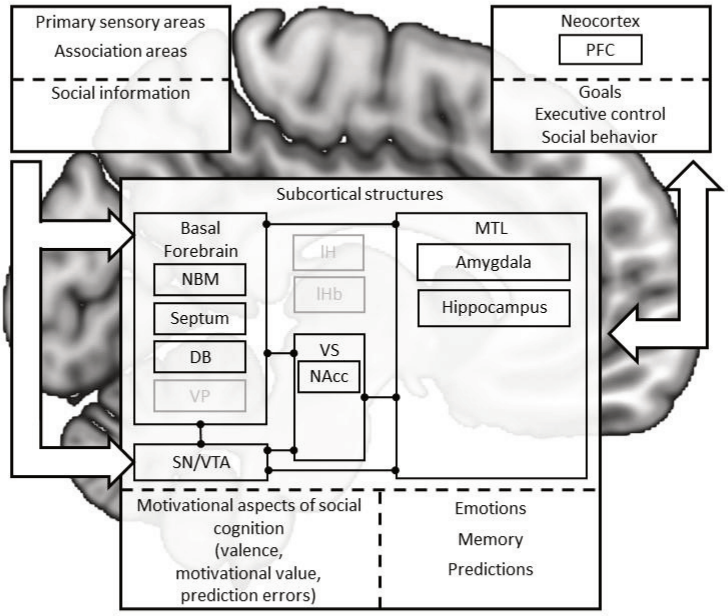

Figure 23. Hypothesized model of cortical and subcortical social information processing (CASSI). The model illustrates the interaction of brain regions and their function in the processing of social information. The arrows indicate a possible flow of information from sensory cortices to higher cortical areas via subcortical structures. Connections between subcortical brain regions are based on anatomical and functional links. The mental aspects and processes of social cognition associated with specific brain regions are outlined at the bottom of the respective boxes, separated by a dashed line. lHb = lateral habenula; lH lateral hypothalamus; VP = ventral pallidum; NBM = nucleus basalis of Meynert; DB = diagonal band; SN/VTA = substantia nigra / ventral tegmental area; VS = ventral striatum; MTL = medial temporal lobe; PFC = prefrontal cortex (adapted from Sobczak and Bunzeck, 2024).

6.5 The effects of social feedback anticipation on motivation and learning

In the following, the perspective is shifted from the neural to the behavioral level, addressing research questions c) and d). Earlier studies have demonstrated that social incentives modulate behavioral invigoration, including accelerated RTs to target stimuli (Kohls et al., 2013) and increased hand-grip force (Pessiglione et al., 2007) to obtain rewards or avoid punishment (see 1.5 Behavioral invigoration through incentives). In line with these findings, healthy young adults showed accelerated RTs associated with the anticipation of positive and negative social feedback in the SID task across the three studies. Furthermore, they all showed that the social feedback stimuli evoked emotions as intended. As such, they succeeded in showing a consistent behavioral effect providing a solid basis for the neuroimaging results.

Furthermore, in addition to the observed behavioral change following predictors of social feedback, the findings of study III indicate processes of evaluative learning in the SID task. The valence of the feedback stimuli was transferred to the predictive cues in the positive condition. This is in line with learning theories proposing that stimuli can gain an emotional valence through contingency with an event itself in addition to acquiring predictive value for the respective positive or negative events (see 1.3 Concepts of learning). While evaluative learning was only observed in the positive, but not in the negative condition, this may be explained by the different numbers in positive and negative feedback. Nonetheless, the RT effect was observed in both the positive and negative condition indicating behavioral modulation by social feedback anticipation. Together, the SID task yielded reliable behavioral effects on motivation and included validated social feedback stimuli that elicit emotional responses in young adults.

6.5.1 The impact of aging on motivation, learning, and socio-emotional processing

This thesis investigated age-related changes in social motivation, learning, and socio-emotional processing at the behavioral level. Regarding research question c), we initially expected a diminished RT effect among older adults, based on changes in neural systems that are associated with age (see 1.6.1 The mesolimbic system and basal forebrain and 1.6.3 Memory, learning, and incentive processing) such as reduced dopaminergic functioning (Hämmerer and Eppinger, 2012) and impaired anticipation signals in the NAcc and SN/VTA (Schott et al., 2007). However, studies 1 and 3 revealed faster RT in both young and older healthy individuals when anticipating positive and negative social feedback, indicating no age modulation.

As explained in 1.6.3 Memory, learning, and incentive processing, the literature on age differences has been inconsistent. Our findings align with studies showing an intact RT and increased vigor to obtain rewards in older adults effect (Rademacher et al., 2014; Hird et al., 2022). Discrepancies to other studies may be explained by the incentive type or task complexity. For instance, some studies find faster RT for monetary rewards in young but not older participants (Spaniol et al., 2015; Bowen et al., 2019). However, others replicate the RT effect in older adults for monetary and social rewards (Rademacher et al., 2014). While the preservation of the RT effect in older adults may appear contrary to the findings of neuroimaging studies, it suggests that age differences could hinge on task specificity, particularly in reward-learning tasks with uncertain cue-outcome contingencies (Chowdhury et al., 2013b; Samanez-Larkin et al., 2014; de Boer et al., 2017). Unlike tasks with probabilistic contingencies, our task provided explicit instructions and fixed stimulus-outcome associations throughout, aligning more with studies showing no age differences in RT in similar tasks despite differences in neural processing (Rademacher et al., 2014). The observation of preserved abilities in aging despite discrepancies in neural processing could indicate neural compensatory mechanisms like upregulation (i.e., enhanced activation of a brain region typically involved) or reorganization (i.e., additional activation of another brain region that is typically unrelated to the task) (Cabeza et al., 2018). These mechanisms may be counteracting age-related structural degenerations of the mesolimbic system to achieve comparable behavior. Together, our findings argue against a general decline of basic motivational processing in aging. Under certain conditions, age-related declines in the dopaminergic system may not adversely impact older adults' capacity for behavioral adaptation and learning.

Socio-emotional changes associated with age include for example the prioritization of emotional goals and the so-called positivity effect (see 1.6.2 Social motivation and emotion). Study I and study III present seemingly contradictory findings regarding the positivity effect in older adults. While study I found no significant differences in emotional valence ratings of social feedback stimuli across age groups, study III showed that older participants rated negative social feedback less negatively. The latter aligns with previous research findings, such as less negative ratings of negative and neutral faces by older adults (Czerwon et al., 2011) and the assumptions of the SST (Carstensen et al., 1999). A methodological difference between the two studies that may account for discrepancies is that valence rating was limited to four seconds in study I, whereas the time was not limited in study III. Since the positivity effect is a result of emotion regulation in older adults that requires attentional and cognitive control, it may depend on available resources for active regulation that were possibly limited by time pressure in study I (Ziaei and Fischer, 2016).

Interestingly, the positivity of stimulus ratings did not influence the RT effect. Older adults were equally motivated to avoid negative social feedback, possibly reflecting different underlying emotion regulation strategies (Livingstone and Isaacowitz, 2021). In the rating task without time pressure, where negative stimuli could not be avoided, older adults may have regulated their emotions through reappraisal, while they avoided exposure to negative stimuli in the SID task through good task performance.

According to the principles of evaluative learning (see 1.3 Concepts of learning), the valence of stimuli can change depending on the valence of associated stimuli, e.g. a reward. Along these lines, study III found that reward cues were associated with positive, and punishment cues with neutral emotional valence in explicit and implicit measures across both age groups. This is partly in line with one other study showing positive self-reported affect elicited by cues predicting monetary gain while cues predicting loss elicited negative affect in young and older adults (Samanez-Larkin et al., 2007). Contrary to our findings, negative cues elicited negative affect which was reduced in older adults suggesting a positivity effect. This discrepancy may be explained by less frequent negative feedback in our design. As the correlation between positive cue valence ratings and positive feedback valence ratings suggests, cue valence may be transferred from the outcome, but the effect may not emerge when feedback is presented less frequently. Moreover, our results show age differences in the emotional valence of positive cues in the explicit ratings, while there was no influence of age in the implicit test. This may be attributed to weaker explicit emotional memory in older adults along with general a decline in explicit memory but could also reflect different underlying cognitive processes. According to dual-processing theories (Evans and Stanovich, 2013), higher cognitive functions such as emotion regulation strategies impact explicit measures such as self-reports, while implicit measures mirror automatic reactions. This account is supported by the correlation between explicit cue ratings with feedback stimulus ratings. However, since the emotional valence of cues was only assessed in the SID task with video feedback, it is unclear how these results translate to photo stimuli. Together, young and older adults show effects of valence transfer from positive feedback videos to predictive cues, indicating evaluative learning.

Together, the anticipation of positive and negative feedback invigorated behavior in young and older adults, as indicated by the RT effect, confirming that social feedback is a strong motivator across the life span. Emotions associated with outcome processing, i.e. the actual feedback, showed a positivity effect in older adults which is in line with age-related socio-emotional changes and the SST (Carstensen, 1998, 2021). Finally, our data indicate that emotional valence of social video feedback transferred to initially neutral cues in both age groups, which differed between young and older subjects only in the explicit task, possibly due to specific developmental changes in evaluative learning or emotion regulation strategy use during healthy aging. As such, our study advances existing literature in five key areas. First, we provide evidence against a general decline of basic motivational processing with age. Second, we replicate the positivity effect in dynamic social stimuli. Third, we examine the emotional valence of cues predicting social reward and punishment, complementing previous work that focused on the anticipatory affect of cues predicting monetary gain and loss (Samanez-Larkin et al., 2007). Fourth, we supplement traditional self-report methods with implicit assessments, and lastly, we provide insights into the relationship between cue and outcome valence through correlation analyses.

6.5.2 The effects of social feedback anticipation in Parkinson’s Disease

Since the SN and DA are crucially involved in motivation and learning (see 1.4 Neural substrates of motivation, learning, and social information processing), including reward and punishment anticipation, the pathological degeneration of DA neurons, such as in PD (see 1.8 Changes of incentive processing in Parkinson's Disease), may affect motivational processing and related behaviors. As expected, study I found no RT effect elicited by anticipating social feedback in intraoperative PD patients after medication withdrawal (n= 11). However, the second PD patient group (n = 21) revealed an intact RT effect, as observed in healthy young and older controls, without any modulatory effect of medical treatment. Corresponding with bradykinesia, one of the cardinal symptoms of PD, the only effect of medication withdrawal was slower overall RT (Kalia and Lang, 2015). Additional analyses indicated that the absence of the RT effect in the iEEG-PD group may be explained by the small sample size. Other explanations may include impaired cognitive, emotional, or motivational processing due to the circumstances of the awake surgery and anesthesia, pathological processes, or a combination of these factors. Our findings indicate that patients with PD demonstrate the capacity to anticipate social rewards and punishments and adjust their behavior accordingly under specific circumstances.

This observation is noteworthy, considering the pathological degeneration of SN DA neurons and reductions in DA functioning (Fearnley and Lees, 1991; Kalia and Lang, 2015), impairments in predictive signaling within the midbrain and VS (Schott et al., 2007), and difficulties in probabilistic learning reported in PD (Knowlton et al., 1996). Our results, particularly in the OFF-medication condition, align with prior research indicating the retention of the RT effect using monetary rewards in unmedicated PD patients (Schott et al., 2007). Conversely, contrasting results from other studies suggest behavioral differences related to medication status, showing better avoidance learning after medication is withdrawn (OFF), but enhanced learning from positive outcomes while medicated (ON) (Frank, 2004). Notably, our study did not detect such discrepancies. Our findings support the notion that basal ganglia degeneration impairs probabilistic stimulus-response learning more than fixed cue-outcome associations in HOA and PD (Knowlton et al., 1996; Frank, 2004; Mattox et al., 2006; Shohamy et al., 2008; Samanez-Larkin et al., 2012, 2014). Additionally, the preserved anticipatory signals in the SN among intraoperative PD patients (study I), further emphasizes intact value anticipation in simple cue-outcome associations.

On a final note, the influence of disease-related changes of socioemotional processing and dopaminergic medication on performance in the SID task was unclear. For instance, PD is associated with facial hypomimia which could potentially influence emotional processing via reduced facial mimicry (Prenger et al., 2020). Especially the identification of negative emotions such as fear and sadness seems to be impaired in PD (Czernecki et al., 2021). In our study however, the ratings of social stimuli were similar to observations in healthy young and older adults. We found no effect of medication status on socio-emotional processing of social feedback stimuli and no positivity effect in PD patients. As such, our findings are consistent with one other study showing no difference in valence ratings for emotional stimuli between PD patients ON medication and healthy controls (Moonen et al., 2017). Comparable behavior may be facilitated by compensatory neural mechanisms, such as increased PFC activation (Moonen et al., 2017). It is also possible that positive emotions and valence as a broader categorization may remain unaffected. This suggests that emotional valence processing in the PD groups was not impaired and is unlikely to have adverse effects on our behavioral findings.

Together, our results are in line with others and support the notion that, despite the pathological degeneration of SN DA neurons and problems with learning, PD patients can anticipate social reward and punishment and adjust their behavior to obtain positive and avoid negative outcomes under certain conditions.

6.5.3 The impact of social feedback modalities on motivation

Regarding research question d), study III investigated the effects of different social feedback modalities on motivation showing that RT was accelerated by the possibility to obtain positive and avoid negative social feedback, which confirms previous work. Contrary to our expectations, the RT effect did not differ between feedback modalities, implicating that dynamic video feedback did not boost the effect compared to static photo feedback.

The ecological validity of findings is a recurring topic and of particular interest in social neuroscience. There are increasing efforts to use naturalistic stimuli and develop paradigms that resemble realistic scenarios, but most experimental work is still primarily based on simplistic feedback. While we hypothesized that dynamic social information promotes behavioral invigoration due to its increased immersive character and emotional intensity (Rademacher et al., 2014; Rymarczyk et al., 2016), the results may be explained by value normalization (Rangel and Clithero, 2012) and adaptive scaling (Tobler et al., 2005; Bunzeck et al., 2010). Both frameworks are rooted in cognitive neuroscience and were suggested to explain neural correlates of reward (Rangel and Clithero, 2012) and reward prediction error (Tobler et al., 2005; Bunzeck et al., 2010) respectively. Nonetheless, they may be applicable beyond their original background (Sallet et al., 2007). In our case, behavioral invigoration (i.e. the acceleration of RT) is normalized to the distribution of available options within a context. That is, when positive and negative social feedback are normalized relative to neutral feedback within each experiment, they have the same rank regardless of being presented in a static or dynamic fashion. Consequently, behavioral invigoration is equally adapted across settings to obtain positive and avoid negative feedback.

However, there are certain considerations limiting the interpretation of these results. First, we were unable to test baseline differences in RT between the SID-Photo and SID-Video task because the simple RT task already showed differences at baseline, which would have introduced a confounding factor. Second, to test the assumption of greater emotional intensity of videos compared to photos, a comparison of valence ratings or additional assessment of arousal would have been necessary. However, a comparison was not planned a priori, and study I and study III used different scales for valence assessment, preventing a post hoc comparison. Third, while employing a between-design was based on practical considerations, e.g. prolonged experiment duration and adverse effects on motivation, this design choice limits the interpretation of our findings. Specifically, the value of static and dynamic feedback may depend on the availability of the other (Charness et al., 2012), leaving it unclear whether a within-design would have yielded different results.

Together, study III contributes to the existing literature by employing more naturalistic stimuli in an established paradigm and successfully replicating a well-established effect. Anticipating positive and negative social feedback accelerated RTs indicating increased motivation. Notably, our findings did not reveal additional benefits of dynamic over static stimuli, leading to the conclusion that social feedback is a strong motivator regardless of its modality.

6.6 Limitations and future directions

The preceding chapters have already elaborated on potential limitations including the differences in feedback uncertainty between conditions (see 3.5 Discussion and 4.5 Discussion), intergroup biases, external validity of social stimuli and paradigms (5.5 Discussion), the common currency hypothesis (4.5 Discussion), gender differences (6.3 Interaction between the mesolimbic system and the basal forebrain during social incentive anticipation), regions of interest definition (4.5 Discussion), as well as neuroimaging resolution and causality (6.3 Interaction between the mesolimbic system and the basal forebrain during social incentive anticipation). However, one conceptual aspect that has not been addressed above relates to the design of the SID task and instrumental conditioning (1.3 Concepts of learning). It has been suggested that participants mostly anticipate punishment avoidance, rather than punishment itself (Martins et al., 2021). Consequently, punishment avoidance constitutes a negative reinforcer with a positive valence, and the punishment (avoidance) cue would be associated with positive emotional valence as well. The results of study III argue against this assumption by showing neutral but not positive valence for negative cues. Similarly, another study found negative anticipatory affect for monetary loss cues in the MID task (Samanez-Larkin et al., 2007). To interpret neuroimaging findings, it is important to know the valence of emotions induced by punishment-avoidance cues. However, due to the limited number of studies investigating cue-elicited affect, more evidence is needed. Together, certain features of the experimental paradigm can be improved. In general, the MID/SID task has the potential to provide a solid framework for reproducible science and allows for the manipulation of individual aspects that form a basis for testing specific effects, such as the implementation of live feedback. Future research should use novel and established behavioral paradigms that tap into more realistic and ecologically valid forms of social interactions (Schilbach et al., 2013; Fan et al., 2021).

Furthermore, understanding anatomical connections and functional interactions of the BF and the mesolimbic system in concert with other brain regions, such as the PFC, is essential to grasp the full picture on the underlying mechanisms of social motivation. Future research should therefore combine structural and functional measures of brain activity. This could include diffusion tensor imaging, markers of iron and myelin, gray matter volume, functional and effective connectivity in MRI, and EEG (Vaillancourt et al., 2012; Steiger et al., 2016; Andreou et al., 2017; Hippmann et al., 2021). Additionally, from a methodological point of view, it is important to note that the SN/VTA and BF are rather small structures, which calls for advanced imaging methods with high spatial and temporal resolution. Two other potential regions of interest in the cholinergic system are the pedunculopontine and laterodorsal tegmental nucleus in the brainstem (He et al., 2023), whose roles in human social motivation have largely been neglected (Dautan et al., 2016). Since fMRI cannot determine which neurotransmitters are involved, study protocols could integrate psychopharmacological interventions. Apart from issues on dopaminergic and cholinergic neuromodulation, future research might focus on other neurotransmitters, such as GABA and glutamate as well as understanding their interactions. Furthermore, these approaches may provide a way to disentangle the extent to which social and nonsocial stimuli rely on the same or specialized brain circuits and thereby help to investigate whether these stimuli are processed via a common coding system (Ruff and Fehr, 2014).

Considering the developmental aspects of social motivation, future research could focus on the neural mechanisms underlying preserved and altered aspects of motivational, social, and emotional functioning in healthy older adults. Regarding motivational processing, it has been shown that reward-related invigoration of RT is linked with structural integrity of the SN/VTA (Steiger and Bunzeck, 2017) and that elderly show increased activity within brain regions recruited by young adults during the same task (Cabeza et al., 2018). Future research could extend our knowledge of how preserved behavioral functioning and structural characteristics relate to compensatory processes such as upregulation and reorganization (Cabeza et al., 2018). Regarding the neural mechanisms underlying age-related changes in socio-emotional processing, research has primarily focused on the PFC, amygdala, insula, and mesolimbic dopaminergic system (Mather, 2016), while the role of the BF has been neglected. Further explorations of a link between age-related BF degeneration and socio-emotional changes could provide novel insights into human social behavior across the lifespan (Shen et al., 2022).

This might include a dissociation of trajectories associated with healthy and pathological aging, especially in AD and PD (Bunzeck et al., 2024).

In sum, future research requires a focus on the interplay of cortical and subcortical structures, advanced methods, and a lifespan approach.

6.7 Conclusion

Our findings provide novel insights into the neural processing of appetitive and aversive social information within the SN/VTA and the interplay between the mesolimbic system and the BF. The human SN signals the anticipation of positive and negative social information via alpha-beta oscillations and consists of functional subregions, including a reward-associated ventral part and a punishment-associated lateral part. Moreover, mesolimbic and BF subregions show valence-unrelated and valence-related connectivity patterns during the anticipation of social feedback. Complementing the focus on subcortical processing in the empirical studies, the CASSI model highlights the integration of information between cortical and subcortical areas that work together to promote social cognition, motivation, and behavior.

Furthermore, this work improves our understanding of motivation, learning, and socioemotional processing in aging. Anticipating social feedback invigorates behavior in healthy young and older adults as well as patients with PD. Using dynamic social stimuli had no benefit over static stimuli, suggesting that social feedback is a strong motivator regardless of its modality and age. We demonstrated that predictive cues are associated with emotional valence which is probably transferred from the feedback to predictive cues, indicating evaluative learning. Finally, we found age differences in socioemotional processing demonstrated by a positivity effect in the evaluation of negative social feedback videos.

As such, this dissertation and its studies contributed to elucidating some of the mechanisms underlying social motivation, and its development across the lifespan. Future studies should explore cortical-subcortical brain interactions, including neglected areas such as the BF in humans, and use advanced methods integrating structural, functional, and psychopharmacological approaches. Social neuroscience should continue to move towards studying ecologically valid forms of social interactions to understand social motivational processing mechanisms comprehensively. Ultimately, further research could help to differentiate between the processes of healthy and pathological ageing and to better understand and treat neurological and psychiatric disorders that are associated with dysregulations within this system.

List of tables

List of figures

References

Acevedo BP, Aron A, Fisher HE, Lucy L. Brown (2012) Neural correlates of marital satisfaction and well-being: Reward, empathy, and affect. Clinical Neuropsychiatry: Journal of Treatment Evaluation:20–31.

Adcock RA, Thangavel A, Whitfield-Gabrieli S, Knutson B, Gabrieli JDE (2006) Reward-motivated learning: mesolimbic activation precedes memory formation. Neuron 50:507–517.

Agostinelli LJ, Geerling JC, Scammell TE (2019) Basal forebrain subcortical projections. Brain Struct Funct 224:1097–1117.

Aharon I, Etcoff N, Ariely D, Chabris CF, O'Connor E, Breiter HC (2001) Beautiful Faces Have Variable Reward Value: fMRI and Behavioral Evidence.

Alderfer CP (1969) An empirical test of a new theory of human needs. Organizational Behavior and Human Performance 4:142–175.

Almeida IL de L, Rego JF, Teixeira ACG, Moreira MR (2022) Social isolation and its impact on child and adolescent development: a systematic review. Rev paul pediatr 40:e2020385.

Amaro E, Barker GJ (2006) Study design in fMRI: Basic principles. Brain and Cognition 60:220–232.

Andreou C, Frielinghaus H, Rauh J, Mußmann M, Vauth S, Braun P, Leicht G, Mulert C (2017) Theta and high-beta networks for feedback processing: a simultaneous EEG–fMRI study in healthy male subjects. Translational Psychiatry 7:e1016–e1016.

Antonucci TC, Fiori KL, Birditt K, Jackey LMH (2010) Convoys of Social Relations: Integrating Life-Span and Life-Course Perspectives. In: The Handbook of Life-Span Development (Lerner RM, Lamb ME, Freund AM, eds), pp hlsd002012. Hoboken, NJ, USA: John Wiley & Sons, Inc.

Aosaki T, Tsubokawa H, Ishida A, Watanabe K, Graybiel A, Kimura M (1994) Responses of tonically active neurons in the primate's striatum undergo systematic changes during behavioral sensorimotor conditioning. J Neurosci 14:3969–3984.

Apicella P (2007) Leading tonically active neurons of the striatum from reward detection to context recognition. Trends in Neurosciences 30:299–306.

Apicella P, Legallet E, Trouche E (1997) Responses of tonically discharging neurons in the monkey striatum to primary rewards delivered during different behavioral states: Exp Brain Res 116:456–466.

Arco AD, Mora F (2009) Neurotransmitters and prefrontal cortex–limbic system interactions: implications for plasticity and psychiatric disorders. J Neural Transm 116:941–952.

Aron AR, Shohamy D, Clark J, Myers C, Gluck MA, Poldrack RA (2004) Human Midbrain Sensitivity to Cognitive Feedback and Uncertainty During Classification Learning. Journal of Neurophysiology 92:1144–1152.

Aschenbrenner S, Tucha O, Lange KW (2000) Regensburger Wortflüssigkeits-Test. Göttingen: Hogrefe.

Ashburner J (2007) A fast diffeomorphic image registration algorithm. NeuroImage 38:95–113.

Atri A, Sherman S, Norman KA, Kirchhoff BA, Nicolas MM, Greicius MD, Cramer SC, Breiter HC, Hasselmo ME, Stern CE (2004) Blockade of Central Cholinergic Receptors Impairs New Learning and Increases Proactive Interference in a Word Paired-Associate Memory Task. Behavioral Neuroscience 118:223–236.

Avena NM, Rada PV (2012) Cholinergic modulation of food and drug satiety and withdrawal. Physiology & Behavior 106:332–336.

Bäckman L, Ginovart N, Dixon RA, Wahlin T-BR, Wahlin Å, Halldin C, Farde L (2000) Age-Related Cognitive Deficits Mediated by Changes in the Striatal Dopamine System. AJP 157:635–637.

Bäckman L, Nyberg L, Lindenberger U, Li S-C, Farde L (2006) The correlative triad among aging, dopamine, and cognition: Current status and future prospects. Neuroscience & Biobehavioral Reviews 30:791–807.

Balleine BW, Dickinson A (1998) Goal-directed instrumental action: contingency and incentive learning and their cortical substrates. Neuropharmacology 37:407–419.

Barch DM et al. (2013) Function in the human connectome: Task-fMRI and individual differences in behavior. NeuroImage 80:169–189.

Barker DJ, Root DH, Zhang S, Morales M (2016) Multiplexed neurochemical signaling by neurons of the ventral tegmental area. Journal of Chemical Neuroanatomy 73:33–42.

Barman A, Richter S, Soch J, Deibele A, Richter A, Assmann A, Wüstenberg T, Walter H, Seidenbecher CI, Schott BH (2015) Gender-specific modulation of neural mechanisms underlying social reward processing by Autism Quotient. Social Cognitive and Affective Neuroscience 10:1537–1547.

Bauch EM, Rausch VH, Bunzeck N (2014) Pain anticipation recruits the mesolimbic system and differentially modulates subsequent recognition memory: Pain Anticipation Recruits the Mesolimbic System. Human Brain Mapping 35:4594–4606.

Baumeister RF, Leary MR (1995) The need to belong: Desire for interpersonal attachments as a fundamental human motivation. Psychological Bulletin 117:497–529.

Becerra L, Breiter HC, Wise R, Gonzalez RG, Borsook D (2001) Reward Circuitry Activation by Noxious Thermal Stimuli. Neuron 32:927–946.

Beer JS, Ochsner KN (2006) Social cognition: A multi level analysis. Brain Research 1079:98–105.

Behrens TEJ, Hunt LT, Woolrich MW, Rushworth MFS (2008) Associative learning of social value. Nature 456:245–249.

Beier KT, Steinberg EE, DeLoach KE, Xie S, Miyamichi K, Schwarz L, Gao XJ, Kremer EJ, Malenka RC, Luo L (2015) Circuit Architecture of VTA Dopamine Neurons Revealed by Systematic Input-Output Mapping. Cell 162:622–634.

Benke T, Karner E, Delazer M (2013) FAB-D: German version of the Frontal Assessment Battery. Journal of Neurology 260:2066–2072.

Berke JD (2018) What does dopamine mean? Nature Neuroscience 21:787–793.

Berridge KC (2018) Evolving Concepts of Emotion and Motivation. Front Psychol 9:1647.

Berry SD, Thompson RF (1979) Medial Septal Lesions Retard Classical Conditioning of the Nictitating Membrane Response in Rabbits. Science 205:209–211.

Bertrand D, Wallace TL (2020) A Review of the Cholinergic System and Therapeutic Approaches to Treat Brain Disorders. In: Behavioral Pharmacology of the Cholinergic System (Shoaib M, Wallace TL, eds), pp 1–28 Current Topics in Behavioral Neurosciences. Cham: Springer International Publishing.

Bettinardi RG (2017) computeCohen_d(x1, x2, varargin) - File Exchange - MATLAB Central. Available at: https://de.mathworks.com/matlabcentral/fileexchange/62957-computecohen_d-x1-x2-varargin.

Bhanji JP, Delgado MR (2014) The social brain and reward: social information processing in the human striatum: Social brain and reward. Wiley Interdisciplinary Reviews: Cognitive Science 5:61–73.

Bjork JM, Smith AR, Chen G, Hommer DW (2010) Adolescents, Adults and Rewards: Comparing Motivational Neurocircuitry Recruitment Using fMRI Lauwereyns J, ed. PLoS ONE 5:e11440.

Björklund A, Dunnett SB (2007) Dopamine neuron systems in the brain: an update. Trends in Neurosciences 30:194–202.

Blandini F, Nappi G, Tassorelli C, Martignoni E (2000) Functional changes of the basal ganglia circuitry in Parkinson’s disease. Progress in Neurobiology 62:63–88.

Bortolini T, Melo B, Basilio R, Fischer R, Zahn R, de Oliveira-Souza R, Knutson B, Moll J (2021) Striatal and septo-hypothalamic responses to anticipation and outcome of affiliative rewards. Neuroimage 243:118474.

Borup J, West RE, Graham CR (2012) Improving online social presence through asynchronous video. The Internet and Higher Education 15:195–203.

Bowen HJ, Grady CL, Spaniol J (2019) Age differences in the neural response to negative feedback. Aging, Neuropsychology, and Cognition 26:463–485.

Bradley MM, Lang PJ (1994) Measuring emotion: The self-assessment manikin and the semantic differential. Journal of Behavior Therapy and Experimental Psychiatry 25:49–59.

Brainard DH (1997) The Psychophysics Toolbox. Spatial Vis 10:433–436.

Brassen S, Gamer M, Peters J, Gluth S, Buchel C (2012) Don't Look Back in Anger! Responsiveness to Missed Chances in Successful and Nonsuccessful Aging. Science 336:612–614.

Brett M, Anton J-L, Valabregue R, Poline J-B (2002) Region of interest analysis using an SPM toolbox [abstract]. In, pp 13. Sendai, Japan.

Bromberg-Martin ES, Matsumoto M, Hikosaka O (2010) Dopamine in Motivational Control: Rewarding, Aversive, and Alerting. Neuron 68:815–834.

Bunzeck N, Dayan P, Dolan RJ, Duzel E (2010) A common mechanism for adaptive scaling of reward and novelty. Hum Brain Mapp 31:1380–1394.

Bunzeck N, Guitart-Masip M, Dolan RJ, Duzel E (2011) Contextual Novelty Modulates the Neural Dynamics of Reward Anticipation. Journal of Neuroscience 31:12816–12822.

Bunzeck N, Guitart-Masip M, Dolan RJ, Duzel E (2014) Pharmacological Dissociation of Novelty Responses in the Human Brain. Cerebral Cortex 24:1351–1360.

Bunzeck N, Schütze H, Stallforth S, Kaufmann J, Düzel S, Heinze H-J, Düzel E (2007) Mesolimbic Novelty Processing in Older Adults. Cerebral Cortex 17:2940–2948.

Bunzeck N, Steiger TK, Krämer UM, Luedtke K, Marshall L, Obleser J, Tune S (2024) Trajectories and contributing factors of neural compensation in healthy and pathological aging. Neuroscience & Biobehavioral Reviews 156:105489.

Burciu RG, Vaillancourt DE (2018) Imaging of Motor Cortex Physiology in Parkinson's Disease. Mov Disord 33:1688–1699.

Buzsáki G, Anastassiou CA, Koch C (2012) The origin of extracellular fields and currents — EEG, ECoG, LFP and spikes. Nat Rev Neurosci 13:407–420.

Buzsaki G, Draguhn A (2004) Neuronal Oscillations in Cortical Networks. Science 304:1926–1929.

Cabeza R, Albert M, Belleville S, Craik FIM, Duarte A, Grady CL, Lindenberger U, Nyberg L, Park DC, Reuter-Lorenz PA, Rugg MD, Steffener J, Rajah MN (2018) Maintenance, reserve and compensation: the cognitive neuroscience of healthy ageing. Nature Reviews Neuroscience 19:701–710.

Cacciola A, Milardi D, Anastasi GP, Basile GA, Ciolli P, Irrera M, Cutroneo G, Bruschetta D, Rizzo G, Mondello S, Bramanti P, Quartarone A (2016) A Direct Cortico-Nigral Pathway as Revealed by Constrained Spherical Deconvolution Tractography in Humans. Front Hum Neurosci 10:374.

Cai Y, Ford CP (2018) Dopamine Cells Differentially Regulate Striatal Cholinergic Transmission across Regions through Corelease of Dopamine and Glutamate. Cell Reports 25:3148-3157.e3.

Camara E (2008) Functional connectivity of reward processing in the brain. Front Hum Neurosci 2.

Caplette L (2017) Simple RM/Mixed ANOVA for any design - File Exchange - MATLAB Central. Available at:

https://de.mathworks.com/matlabcentral/fileexchange/64980-simple-rm-mixed-anova-for-any-design.

Carstensen LL (1998) A Life-Span Approach to Social Motivation. In: Motivation and Self-Regulation across the Life Span, 1st ed. (Heckhausen J, Dweck CS, eds), pp 341–364. Cambridge University Press.

Carstensen LL (2021) Socioemotional Selectivity Theory: The Role of Perceived Endings in Human Motivation. The Gerontologist 61.

Carstensen LL, Isaacowitz DM, Charles ST (1999) A Theory of Socioemotional Selectivity. American Psychologist:17.

Carstensen LL, Turan B, Scheibe S, Ram N, Ersner-Hershfield H, Samanez-Larkin GR, Brooks KP, Nesselroade JR (2011) Emotional experience improves with age: Evidence based on over 10 years of experience sampling. Psychology and Aging 26:21–33.

Carter RM (2009) Activation in the VTA and nucleus accumbens increases in anticipation of both gains and losses. Front Behav Neurosci 3.

Cauda F, Cavanna AE, D'agata F, Sacco K, Duca S, Geminiani GC (2011) Functional Connectivity and Coactivation of the Nucleus Accumbens: A Combined Functional Connectivity and Structure-Based Meta-analysis. Journal of Cognitive Neuroscience 23:2864–2877.

Charles ST (2010) Strength and vulnerability integration: A model of emotional well-being across adulthood. Psychological Bulletin 136:1068–1091.

Charles ST, Mather M, Carstensen LL (2003) Aging and emotional memory: The forgettable nature of negative images for older adults. Journal of Experimental Psychology: General 132:310–324.

Charness G, Gneezy U, Kuhn MA (2012) Experimental methods: Between-subject and within-subject design. Journal of Economic Behavior & Organization 81:1–8.

Chaves-Coira I, Martín-Cortecero J, Nuñez A, Rodrigo-Angulo ML (2018) Basal Forebrain Nuclei Display Distinct Projecting Pathways and Functional Circuits to Sensory Primary and Prefrontal Cortices in the Rat. Front Neuroanat 12:69.

Chevallier C, Kohls G, Troiani V, Brodkin ES, Schultz RT (2012) The social motivation theory of autism. Trends in Cognitive Sciences 16:231–239.

Choi U-S, Kim S-Y, Sim HJ, Lee S-Y, Park S-Y, Jeong J-S, Seol KI, Yoon H-W, Jhung K, Park J-I, Cheon K-A (2015) Abnormal brain activity in social reward learning in children with autism spectrum disorder: an fMRI study. Yonsei Med J 56:705–711.

Chowdhury R, Guitart-Masip M, Lambert C, Dayan P, Huys Q, Düzel E, Dolan RJ (2013a) Dopamine restores reward prediction errors in old age. Nature Neuroscience 16:648–653.

Chowdhury R, Guitart-Masip M, Lambert C, Dolan RJ, Düzel E (2013b) Structural integrity of the substantia nigra and subthalamic nucleus predicts flexibility of instrumental learning in older-age individuals. Neurobiology of Aging 34:2261–2270.

Chowdhury R, Lambert C, Dolan RJ, Düzel E (2013c) Parcellation of the human substantia nigra based on anatomical connectivity to the striatum. NeuroImage 81:191–198.

Chung A, Rimal RN (2016) Social norms: A review. RCR 4:1–28.

Cohen JY, Haesler S, Vong L, Lowell BB, Uchida N (2012) Neuron-type-specific signals for reward and punishment in the ventral tegmental area. Nature 482:85–88.

Cohen MX, Elger CE, Ranganath C (2007) Reward expectation modulates feedback-related negativity and EEG spectra. NeuroImage 35:968–978.

Cook DA, Artino AR (2016) Motivation to learn: an overview of contemporary theories. Med Educ 50:997–1014.

Corbin N, Todd N, Friston KJ, Callaghan MF (2018) Accurate modeling of temporal correlations in rapidly sampled fMRI time series. Hum Brain Mapp 39:3884–3897.

Creed MC, Ntamati NR, Tan KR (2014) VTA GABA neurons modulate specific learning behaviors through the control of dopamine and cholinergic systems. Front Behav Neurosci 8.

Cremers HR, Veer IM, Spinhoven P, Rombouts SARB, Roelofs K (2015) Neural sensitivity to social reward and punishment anticipation in social anxiety disorder. Front Behav Neurosci 8.

Crouse RB, Kim K, Batchelor HM, Girardi EM, Kamaletdinova R, Chan J, Rajebhosale P, Pittenger ST, Role LW, Talmage DA, Jing M, Li Y, Gao X-B, Mineur YS, Picciotto MR (2020) Acetylcholine is released in the basolateral amygdala in response to predictors of reward and enhances the learning of cue-reward contingency. eLife 9:e57335.

Cummins DD (2000) How the Social Environment Shaped the Evolution of Mind. Synthese 122:3–28.

Czernecki V, Benchetrit E, Houot M, Pineau F, Mangone G, Corvol J-C, Vidailhet M, Levy R (2021) Social cognitive impairment in early Parkinson's disease: A novel "mild impairment"? Parkinsonism & Related Disorders 85:117–121.

Czerwon B, Lüttke S, Werheid K (2011) Age Differences in Valence Judgments of Emotional Faces: The Influence of Personality Traits and Current Mood. Experimental Aging Research 37:503–515.

Daniel R, Pollmann S (2010) Comparing the Neural Basis of Monetary Reward and Cognitive Feedback during Information-Integration Category Learning. Journal of Neuroscience 30:47–55.

D'Ardenne K, McClure SM, Nystrom LE, Cohen JD (2008) BOLD Responses Reflecting Dopaminergic Signals in the Human Ventral Tegmental Area. Science 319:1264–1267.

Dautan D, Souza AS, Huerta-Ocampo I, Valencia M, Assous M, Witten IB, Deisseroth K, Tepper JM, Bolam JP, Gerdjikov TV, Mena-Segovia J (2016) Segregated cholinergic transmission modulates dopamine neurons integrated in distinct functional circuits. Nat Neurosci 19:1025–1033.

de Boer L, Axelsson J, Riklund K, Nyberg L, Dayan P, Bäckman L, Guitart-Masip M (2017) Attenuation of dopamine-modulated prefrontal value signals underlies probabilistic reward learning deficits in old age. eLife 6:1–25.

de Hemptinne C, Ryapolova-Webb ES, Air EL, Garcia PA, Miller KJ, Ojemann JG, Ostrem JL, Galifianakis NB, Starr PA (2013) Exaggerated phase-amplitude coupling in the primary motor cortex in Parkinson disease. Proceedings of the National Academy of Sciences 110:4780–4785.

De Houwer J (2006) Using the Implicit Association Test does not rule out an impact of conscious propositional knowledge on evaluative conditioning. Learning and Motivation 37:176–187.

De Houwer J (2007) A Conceptual and Theoretical Analysis of Evaluative Conditioning. Span J Psychol 10:230–241.

De Jaegher H, Di Paolo E, Gallagher S (2010) Can social interaction constitute social cognition? Trends in Cognitive Sciences 14:441–447.

de Quervain DJ-F, Fischbacher U, Treyer V, Schellhammer M, Schnyder U, Buck A, Fehr E (2004) The Neural Basis of Altruistic Punishment. Science 305:1254–1258.

Deichmann R, Nöth U, Merola A, Weiskopf N (2022) The Basics of Functional Magnetic Resonance Imaging. In: EEG - fMRI (Mulert C, Lemieux L, eds), pp 49–77. Cham: Springer International Publishing.

Delaveau P, Salgado-Pineda P, Wicker B, Micallef-Roll J, Blin O (2005) Effect of Levodopa on Healthy Volunteers' Facial Emotion Perception: An fMRI Study. Clinical Neuropharmacology 28:255–261.

Delaveau P, Salgado-Pineda P, Witjas T, Micallef-Roll J, Fakra E, Azulay J-P, Blin O (2009) Dopaminergic Modulation of Amygdala Activity During Emotion Recognition in Patients With Parkinson Disease. Journal of Clinical Psychopharmacology 29:548–554.

Delgado MR, Locke HM, Stenger VA, Fiez JA (2003) Dorsal striatum responses to reward and punishment: Effects of valence and magnitude manipulations. Cognitive, Affective, & Behavioral Neuroscience 3:27–38.

Delgado MR, Nystrom LE, Fissell C, Noll DC, Fiez JA (2000) Tracking the Hemodynamic Responses to Reward and Punishment in the Striatum. Journal of Neurophysiology 84:3072–3077.

Delmonte S, Balsters JH, McGrath J, Fitzgerald J, Brennan S, Fagan AJ, Gallagher L (2012) Social and monetary reward processing in autism spectrum disorders. Mol Autism 3:7.

Demeter E, Sarter M (2013) Leveraging the cortical cholinergic system to enhance attention. Neuropharmacology 64:294–304.

Diaconescu AO, Mathys C, Weber LAE, Kasper L, Mauer J, Stephan KE (2017) Hierarchical prediction errors in midbrain and septum during social learning. Social Cognitive and Affective Neuroscience 12:618–634.

Doñamayor N, Marco-Pallarés J, Heldmann M, Schoenfeld MA, Münte TF (2011) Temporal dynamics of reward processing revealed by magnetoencephalography. Human Brain Mapping 32:2228–2240.

Dreher J-C, Meyer-Lindenberg A, Kohn P, Berman KF (2008) Age-related changes in midbrain dopaminergic regulation of the human reward system. Proceedings of the National Academy of Sciences 105:15106–15111.

Dugré JR, Dumais A, Bitar N, Potvin S (2018) Loss anticipation and outcome during the Monetary Incentive Delay Task : a neuroimaging systematic review and meta-analysis. PeerJ 6:e4749.

Duprez J, Houvenaghel J-F, Dondaine T, Péron J, Haegelen C, Drapier S, Modolo J, Jannin P, Vérin M, Sauleau P (2019) Subthalamic nucleus local field potentials recordings reveal subtle effects of promised reward during conflict resolution in Parkinson’s disease. NeuroImage 197:232–242.

Düzel E, Bunzeck N, Guitart-Masip M, Wittmann B, Schott BH, Tobler PN (2009) Functional imaging of the human dopaminergic midbrain. Trends in Neurosciences 32:321–328.

Düzel S, Münte TF, Lindenberger U, Bunzeck N, Schütze H, Heinze H-J, Düzel E (2010) Basal forebrain integrity and cognitive memory profile in healthy aging. Brain Research 1308:124–136.

Ebner NC, Johnson MK (2009) Young and older emotional faces: Are there age group differences in expression identification and memory? Emotion 9:329–339.

Eckart C, Bunzeck N (2013) Dopamine modulates processing speed in the human mesolimbic system. NeuroImage 66:293–300.

Edelstein WA, Glover GH, Hardy CJ, Redington RW (1986) The intrinsic signal-to-noise ratio in NMR imaging. Magn Reson Med 3:604–618.

Eickhoff SB, Stephan KE, Mohlberg H, Grefkes C, Fink GR, Amunts K, Zilles K (2005) A new SPM toolbox for combining probabilistic cytoarchitectonic maps and functional imaging data. NeuroImage 25:1325–1335.

Ellemers N, Doosje B, Spears R (2004) Sources of respect: the effects of being liked by ingroups and outgroups. Eur J Soc Psychol 34:155–172.

Eppinger B, Heekeren HR, Li S-C (2015) Age-related prefrontal impairments implicate deficient prediction of future reward in older adults. Neurobiology of Aging 36:2380–2390.

Eppinger B, Schuck NW, Nystrom LE, Cohen JD (2013) Reduced Striatal Responses to Reward Prediction Errors in Older Compared with Younger Adults. Journal of Neuroscience 33:9905–9912.

Erixon-Lindroth N, Farde L, Robins Wahlin T-B, Sovago J, Halldin C, Bäckman L (2005) The role of the striatal dopamine transporter in cognitive aging. Psychiatry Research: Neuroimaging 138:1–12.

Evans IEM, Llewellyn DJ, Matthews FE, Woods RT, Brayne C, Clare L (2019) Living alone and cognitive function in later life. Archives of Gerontology and Geriatrics 81:222–233.

Evans JStBT, Stanovich KE (2013) Dual-Process Theories of Higher Cognition: Advancing the Debate. Perspect Psychol Sci 8:223–241.

Everitt BJ, Robbins TW (1997) CENTRAL CHOLINERGIC SYSTEMS AND COGNITION. Annu Rev Psychol 48:649–684.

Ezrin-Waters C, Resch L (1986) The Nucleus Basalis of Meynert. Can j neurol sci 13:8–14.

Fairhurst M, Wiech K, Dunckley P, Tracey I (2007) Anticipatory brainstem activity predicts neural processing of pain in humans: Pain 128:101–110.

Fallon JH, Moore RY (1978) Catecholamine innervation of the basal forebrain IV. Topography of the dopamine projection to the basal forebrain and neostriatum. J Comp Neurol 180:545–579.

Fan S, Dal Monte O, Chang SWC (2021) Levels of naturalism in social neuroscience research. iScience 24:102702.

Fearnley JM, Lees AJ (1991) Ageing and Parkinson's Disease: Substantia nigra regional selectivity. Brain 114:2283–2301.

Federau C, Scalzo F, Lee-Messer CW, Zaharchuk G (2021) Editorial: Machine Learning in Neuroimaging. Front Neurol 12:778765.

Filbey FM, Dunlop J, Myers US (2013) Neural Effects of Positive and Negative Incentives during Marijuana Withdrawal García AV, ed. PLoS ONE 8:e61470.

Fiorillo CD, Tobler PN, Schultz W (2003) Discrete coding of reward probability and uncertainty by dopamine neurons. Science 299:1898–1902.

Fisher HE, Brown LL, Aron A, Strong G, Mashek D (2010) Reward, Addiction, and Emotion Regulation Systems Associated With Rejection in Love. Journal of Neurophysiology 104:51–60.

Fleischman DA, Wilson RS, Gabrieli JDE, Bienias JL, Bennett DA (2004) A Longitudinal Study of Implicit and Explicit Memory in Old Persons. Psychology and Aging 19:617–625.

Fölster M, Hess U, Werheid K (2014) Facial age affects emotional expression decoding. Front Psychol 5.

Frank MJ (2004) By Carrot or by Stick: Cognitive Reinforcement Learning in Parkinsonism. Science 306:1940–1943.

Fredrickson BL, Carstensen LL (1990) Choosing social partners: How old age and anticipated endings make people more selective. Psychology and Aging 5:335–347.

Freed WJ (2022) Motivation and Desire: A New Way to Think About Why We do Everything and its Basis in Neuroscience. Cham: Springer International Publishing.

Freeman SM, Palumbo MC, Lawrence RH, Smith AL, Goodman MM, Bales KL (2018) Effect of age and autism spectrum disorder on oxytocin receptor density in the human basal forebrain and midbrain. Transl Psychiatry 8:257.

Frehner SS, Dooley KT, Palumbo MC, Smith AL, Goodman MM, Bales KL, Freeman SM (2022) Effect of sex and autism spectrum disorder on oxytocin receptor binding and mRNA expression in the dopaminergic pars compacta of the human substantia nigra. Phil Trans R Soc B 377:20210118.

Freitas S, Simões MR, Alves L, Santana I (2013) Montreal Cognitive Assessment: Validation Study for Mild Cognitive Impairment and Alzheimer Disease. Alzheimer Disease & Associated Disorders 27:37–43.

Fried I, Rutishauser U, Cerf M, Kreiman G eds. (2014) Single neuron studies of the human brain: probing cognition. Cambridge, Massachusetts: The MIT Press.

Fries P (2005) A mechanism for cognitive dynamics: neuronal communication through neuronal coherence. Trends in Cognitive Sciences 9:474–480.

Friston KJ ed. (2007) Statistical parametric mapping: the analysis of funtional brain images, 1st ed. Amsterdam ; Boston: Elsevier/Academic Press.

Fritz HJ, Ray N, Dyrba M, Sorg C, Teipel S, Grothe MJ (2019) The corticotopic organization of the human basal forebrain as revealed by regionally selective functional connectivity profiles. Hum Brain Mapp 40:868–878.

Gasiorowska A, Wydrych M, Drapich P, Zadrozny M, Steczkowska M, Niewiadomski W, Niewiadomska G (2021) The Biology and Pathobiology of Glutamatergic, Cholinergic, and Dopaminergic Signaling in the Aging Brain. Front Aging Neurosci 13:654931.

Gaykema RP, Zaborszky L (1996) Direct catecholaminergic-cholinergic interactions in the basal forebrain. II. Substantia nigra-ventral tegmental area projections to cholinergic neurons. J Comp Neurol 374:555–577.

Gazzaniga MS, Ivry RB, Mangun GR (2002) Cognitive neuroscience: the biology of the mind, 2nd ed. New York: Norton.

Ghosal S, Sandi C, van der Kooij MA (2019) Neuropharmacology of the mesolimbic system and associated circuits on social hierarchies. Neuropharmacology 159:107498.

Glover GH (2011) Overview of Functional Magnetic Resonance Imaging. Neurosurgery Clinics of North America 22:133–139.

Godefroy O, Roussel M, Despretz P, Quaglino V, Boucart M (2010) Age-Related Slowing: Perceptuomotor, Decision, or Attention Decline? Experimental Aging Research 36:169–189.

Goerlich KS, Votinov M, Lammertz SE, Winkler L, Spreckelmeyer KN, Habel U, Gründer G, Gossen A (2017) Effects of alexithymia and empathy on the neural processing of social and monetary rewards. Brain Struct Funct 222:2235–2250.

Goetz CG et al. (2008) Movement Disorder Society-sponsored revision of the Unified Parkinson's Disease Rating Scale (MDS-UPDRS): Scale presentation and clinimetric testing results. Movement Disorders 23:2129–2170.

Golden SA et al. (2016) Basal forebrain projections to the lateral habenula modulate aggression reward. Nature 534:688–692.

González C, Miranda MI, Gutiérrez H, Ormsby C, Bermúdez-Rattoni F (2000) Differential participation of the NBM in the acquisition and retrieval of conditioned taste aversion and Morris water maze. Behavioural Brain Research 116:89–98.

Göttlich M, Beyer F, Krämer UM (2015) BASCO: a toolbox for task-related functional connectivity. Front Syst Neurosci 9.

Gottsdanker R (1982) Age and Simple Reaction Time. Journal of Gerontology 37:342–348.

Graybiel AM, Aosaki T, Flaherty AW, Kimura M (1994) The Basal Ganglia and Adaptive Motor Control. Science 265:1826–1831.

Greenwald G, McGhee DE, Schwartz JLK (1998) Measuring Individual Differences in Implicit Cognition: The Implicit Association Test. Journal of personality and social psychology 74:1464–1480.

Greiner B (2015) Subject pool recruitment procedures: organizing experiments with ORSEE. J Econ Sci Assoc 1:114–125.

Griguoli M, Pimpinella D (2022) Medial septum: relevance for social memory. Front Neural Circuits 16:965172.

Gritti I, Henny P, Galloni F, Mainville L, Mariotti M, Jones BE (2006) Stereological estimates of the basal forebrain cell population in the rat, including neurons containing choline acetyltransferase, glutamic acid decarboxylase or phosphate-activated glutaminase and colocalizing vesicular glutamate transporters. Neuroscience 143:1051–1064.

Gritti I, Mainville L, Jones BE (1993) Codistribution of GABA- with acetylcholine-synthesizing neurons in the basal forebrain of the rat. J Comp Neurol 329:438–457.

Gross JJ (1998) The Emerging Field of Emotion Regulation: An Integrative Review. Review of General Psychology 2:271–299.

Grothe M, Heinsen H, Teipel SJ (2012) Atrophy of the Cholinergic Basal Forebrain Over the Adult Age Range and in Early Stages of Alzheimer's Disease. Biological Psychiatry 71:805–813.

Gu R, Huang W, Camilleri J, Xu P, Wei P, Eickhoff SB, Feng C (2019) Love is analogous to money in human brain: Coordinate-based and functional connectivity meta-analyses of social and monetary reward anticipation. Neuroscience & Biobehavioral Reviews 100:108–128.

Guitart-Masip M, Bunzeck N, Stephan KE, Dolan RJ, Duzel E (2010) Contextual Novelty Changes Reward Representations in the Striatum. Journal of Neuroscience 30:1721–1726.

Guitart-Masip M, Fuentemilla L, Bach DR, Huys QJM, Dayan P, Dolan RJ, Duzel E (2011) Action Dominates Valence in Anticipatory Representations in the Human Striatum and Dopaminergic Midbrain. Journal of Neuroscience 31:7867–7875.

Gunnar MR (2017) Social Buffering of Stress in Development: A Career Perspective. Perspect Psychol Sci 12:355–373.

Guo W, Robert B, Polley DB (2019) The Cholinergic Basal Forebrain Links Auditory Stimuli with Delayed Reinforcement to Support Learning. Neuron 103:1164-1177.e6.

Haber SN (2014) The place of dopamine in the cortico-basal ganglia circuit. Neuroscience 282:248–257.

Haber SN (2016) Corticostriatal circuitry. Dialogues in Clinical Neuroscience 18.

Haber SN, Knutson B (2010) The Reward Circuit: Linking Primate Anatomy and Human Imaging. Neuropsychopharmacology 35:4–26.

Hämmerer D, Eppinger B (2012) Dopaminergic and prefrontal contributions to reward-based learning and outcome monitoring during child development and aging. Developmental Psychology 48:862–874.

Hangya B, Ranade SP, Lorenc M, Kepecs A (2015) Central Cholinergic Neurons Are Rapidly Recruited by Reinforcement Feedback. Cell 162:1155–1168.

Härting C, Wechsler D (2000) Wechsler-Gedächtnistest - revidierte Fassung WMS-R. Bern: Huber.

Hasselmo ME (2006) The role of acetylcholine in learning and memory. Current Opinion in Neurobiology 16:710–715.

Hautzinger M, Keller F, Kühner C (2009) Beck-Depression-Inventar. Göttingen: Hogrefe.

He G, Li Y, Deng H, Zuo H (2023) Advances in the study of cholinergic circuits in the central nervous system. Ann Clin Transl Neurol 10:2179–2191.

Hebart MN, Görgen K, Haynes J-D (2015) The Decoding Toolbox (TDT): a versatile software package for multivariate analyses of functional imaging data. Front Neuroinform 8.

Hedden T, Gabrieli JDE (2004) Insights into the ageing mind: a view from cognitive neuroscience. Nat Rev Neurosci 5:87–96.

Heimer L, de Olmos JS, Alheid GF, Pearson J, Sakamoto N, Shinoda K, Marksteiner J, Switzer RC (1999) The human basal forebrain. Part II. In: Handbook of Chemical Neuroanatomy, pp 57–226. Elsevier.

Helmstaedter C, Lendt M, Lux S (2001) Verbaler Lern- und Merkfähigkeitstest. Göttingen: Beltz Test.

Hennigan K, D'Ardenne K, McClure SM (2015) Distinct Midbrain and Habenula Pathways Are Involved in Processing Aversive Events in Humans. Journal of Neuroscience 35:198–208.

Henninger F, Shevchenko Y, Mertens UK, Kieslich PJ, Hilbig BE (2019) lab.js: A free, open, online study builder. PsyArXiv. Available at: https://osf.io/fqr49.

Hermans D, Vansteenwegen D, Crombez G, Baeyens F, Eelen P (2002) Expectancy-learning and evaluative learning in human classical conditioning: affective priming as an indirect and unobtrusive measure of conditioned stimulus valence. Behaviour Research and Therapy 40:217–234.

Hersen M, Sledge WH eds. (2002) Encyclopedia of psychotherapy. Amsterdam ; Boston: Academic Press.

Herweg NA, Sommer T, Bunzeck N (2018) Retrieval Demands Adaptively Change Striatal Old/New Signals and Boost Subsequent Long-Term Memory. J Neurosci 38:745–754.

Hétu S, Luo Y, D'Ardenne K, Lohrenz T, Montague PR (2017) Human substantia nigra and ventral tegmental area involvement in computing social error signals during the ultimatum game. Social Cognitive and Affective Neuroscience 12:1972–1982.

Hikosaka O, Sesack SR, Lecourtier L, Shepard PD (2008) Habenula: Crossroad between the Basal Ganglia and the Limbic System. Journal of Neuroscience 28:11825–11829.

Hippmann B, Tzvi E, Göttlich M, Weiblen R, Münte TF, Jessen S (2021) Effective connectivity underlying reward-based executive control. Hum Brain Mapp:hbm.25564.

Hird EJ, Beierholm U, De Boer L, Axelsson J, Backman L, Guitart-Masip M (2022) Dopamine and reward-related vigor in younger and older adults. Neurobiology of Aging 118:34–43.

Hirschmann J, Özkurt TE, Butz M, Homburger M, Elben S, Hartmann CJ, Vesper J, Wojtecki L, Schnitzler A (2013) Differential modulation of STN-cortical and cortico-muscular coherence by movement and levodopa in Parkinson's disease. NeuroImage 68:203–213.

Hiser J, Koenigs M (2018) The Multifaceted Role of the Ventromedial Prefrontal Cortex in Emotion, Decision Making, Social Cognition, and Psychopathology. Biol Psychiatry 83:638–647.

Holt-Lunstad J, Smith TB (2012) Social Relationships and Mortality: Social Relationships and Mortality. Social and Personality Psychology Compass 6:41–53.

Hoofs V, Prével A, Krebs RM (2020) Expecting the good: Symbolic valence signals provoke action biases and undermine goal-directed behavior. Acta Psychologica 206:103063.

Horvitz JC (2000) Mesolimbocortical and nigrostriatal dopamine responses to salient non-reward events. Neuroscience 96:651–656.

Houwer J de, Hughes S (2020) The psychology of learning: an introduction from a functional-cognitive perspective. Cambridge, Massachusetts: The MIT Press.

Howard JH, Howard DV (2013) Aging mind and brain: is implicit learning spared in healthy aging? Front Psychol 4:1–4.

Huang Y, Sun B, Debarros J, Zhang C, Zhan S, Li D, Zhang C, Wang T, Huang P, Lai Y, Brown P, Cao C, Tan H (2021) Increased theta/alpha synchrony in the habenula-prefrontal network with negative emotional stimuli in human patients. eLife 10:e65444.

Hütter M, Rothermund K (2020) Automatic processes in evaluative learning. Cognition and Emotion 34:1–20.

Iglesias S, Mathys C, Brodersen KH, Kasper L, Piccirelli M, den Ouden HEM, Stephan KE (2013) Hierarchical Prediction Errors in Midbrain and Basal Forebrain during Sensory Learning. Neuron 80:519–530.

Iidaka T, Okada T, Murata T, Omori M, Kosaka H, Sadato N, Yonekura Y (2002) Age-related differences in the medial temporal lobe responses to emotional faces as revealed by fMRI. Hippocampus 12:352–362.

Jaeger D, Jung R eds. (2015) Encyclopedia of Computational Neuroscience. New York, NY: Springer New York.

Jankovic J (2008) Parkinson’s disease: clinical features and diagnosis. Journal of Neurology, Neurosurgery & Psychiatry 79:368–376.

Jenkinson M, Beckmann CF, Behrens TEJ, Woolrich MW, Smith SM (2012) FSL. NeuroImage 62:782–790.

Jensen J, McIntosh AR, Crawley AP, Mikulis DJ, Remington G, Kapur S (2003) Direct Activation of the Ventral Striatum in Anticipation of Aversive Stimuli. Neuron 40:1251–1257.

Jimenez JC, Su K, Goldberg AR, Luna VM, Biane JS, Ordek G, Zhou P, Ong SK, Wright MA, Zweifel L, Paninski L, Hen R, Kheirbek MA (2018) Anxiety Cells in a Hippocampal-Hypothalamic Circuit. Neuron 97:670-683.e6.

Joshua M, Adler A, Mitelman R, Vaadia E, Bergman H (2008) Midbrain Dopaminergic Neurons and Striatal Cholinergic Interneurons Encode the Difference between Reward and Aversive Events at Different Epochs of Probabilistic Classical Conditioning Trials. Journal of Neuroscience 28:11673–11684.

Kaasinen V, Vilkman H, Hietala J, Någren K, Helenius H, Olsson H, Farde L, Rinne J (2000) Age-related dopamine D2/D3 receptor loss in extrastriatal regions of the human brain. Neurobiol Aging 21:683–688.

Kalbe E, Kessler J, Emmans D, Ebersbach G, Calabrese P (2005) PANDA: ökonomische Erfassung kognitiver und affektiver Beeinträchtigungen bei dementen Parkinson-Patienten. Aktuelle Neurologie 32.

Kalia LV, Lang AE (2015) Parkinson’s disease. The Lancet 386:896–912.

Karpinski A, Steinman RB (2006) The Single Category Implicit Association Test as a measure of implicit social cognition. Journal of Personality and Social Psychology 91:16–32.

Kinard JL, Mosner MG, Greene RK, Addicott M, Bizzell J, Petty C, Cernasov P, Walsh E, Eisenlohr-Moul T, Carter RM, McLamb M, Hopper A, Sukhu R, Dichter GS (2020)

Neural Mechanisms of Social and Nonsocial Reward Prediction Errors in Adolescents with Autism Spectrum Disorder. Autism Research 13:715–728.

Kirsch P, Schienle A, Stark R, Sammer G, Blecker C, Walter B, Ott U, Burkart J, Vaitl D (2003) Anticipation of reward in a nonaversive differential conditioning paradigm and the brain reward system: NeuroImage 20:1086–1095.

Kite ME, Stockdale GD, Whitley BE, Johnson BT (2005) Attitudes Toward Younger and Older Adults: An Updated Meta-Analytic Review. J Social Issues 61:241–266.

Knight M, Seymour TL, Gaunt JT, Baker C, Nesmith K, Mather M (2007) Aging and goal-directed emotional attention: Distraction reverses emotional biases. Emotion 7:705–714.

Knowlton BJ, Mangels JA, Squire LR (1996) A Neostriatal Habit Learning System in Humans. Science 273:1399–1402.

Knutson B, Adams CM, Fong GW, Hommer D (2001a) Anticipation of Increasing Monetary Reward Selectively Recruits Nucleus Accumbens. The Journal of Neuroscience 21:RC159–RC159.

Knutson B, Fong GW, Adams CM, Varner JL, Hommer D (2001b) Dissociation of reward anticipation and outcome with event-related fMRI. Neuroreport 12:3683–3687.

Knutson B, Greer SM (2008) Anticipatory affect: neural correlates and consequences for choice. Philosophical Transactions of the Royal Society B: Biological Sciences 363:3771–3786.

Knutson B, Westdorp A, Kaiser E, Hommer D (2000) FMRI Visualization of Brain Activity during a Monetary Incentive Delay Task. NeuroImage 12:20–27.

Kohls G, Perino MT, Taylor JM, Madva EN, Cayless SJ, Troiani V, Price E, Faja S, Herrington JD, Schultz RT (2013) The nucleus accumbens is involved in both the pursuit of social reward and the avoidance of social punishment. Neuropsychologia 51:2062–2069.

Krebs RM, Heipertz D, Schuetze H, Duzel E (2011) Novelty increases the mesolimbic functional connectivity of the substantia nigra/ventral tegmental area (SN/VTA) during reward anticipation: Evidence from high-resolution fMRI. NeuroImage 58:647–655.

Kryla-Lighthall N, Mather M (2016) The Role of Cognitive Control in Older Adults' Emotional Well-Being. In: Handbook of theories of aging, Third edition. (Bengtson VL, Settersten RA, Kennedy BK, Morrow-Howell N, Smith J, eds). New York: Springer Publishing Company, LLC.

Künig G, Leenders KL, Martin-Sölch C, Missimer J, Magyar S, Schultz W (2000) Reduced reward processing in the brains of Parkinsonian patients. Neuroreport 11:3681–3687.

Lachaux JP, Rudrauf D, Kahane P (2003) Intracranial EEG and human brain mapping. Journal of Physiology-Paris 97:613–628.

Lange K, Kühn S, Filevich E (2015) "Just Another Tool for Online Studies" (JATOS): An Easy Solution for Setup and Management of Web Servers Supporting Online Studies Margulies D, ed. PLOS ONE 10:e0130834.

Lansink CS, Meijer GT, Lankelma JV, Vinck MA, Jackson JC, Pennartz CMA (2016) Reward Expectancy Strengthens CA1 Theta and Beta Band Synchronization and Hippocampal-Ventral Striatal Coupling. Journal of Neuroscience 36:10598–10610.

Leek MR (2001) Adaptive procedures in psychophysical research. Perception & Psychophysics 63:1279–1292.

Li S-C, Lindenberger U, Bäckman L (2010) Dopaminergic modulation of cognition across the life span. Neuroscience & Biobehavioral Reviews 34:625–630.

Lisman J, Grace AA, Duzel E (2011) A neoHebbian framework for episodic memory; role of dopamine-dependent late LTP. Trends in Neurosciences 34:536–547.

Livingstone KM, Isaacowitz DM (2021) Age and emotion regulation in daily life: Frequency, strategies, tactics, and effectiveness. Emotion 21:39–51.

Ljungberg T, Apicella P, Schultz W (1992) Responses of monkey dopamine neurons during learning of behavioral reactions. Journal of Neurophysiology 67:145–163.

Lockwood PL, Apps MAJ, Valton V, Viding E, Roiser JP (2016) Neurocomputational mechanisms of prosocial learning and links to empathy. Proc Natl Acad Sci USA 113:9763–9768.

Logothetis NK (2003) The Underpinnings of the BOLD Functional Magnetic Resonance Imaging Signal. J Neurosci 23:3963–3971.

Luck SJ (2014) An introduction to the event-related potential technique, Second edition. Cambridge, Massachusetts: The MIT Press.

Luo SX, Huang EJ (2016) Dopaminergic Neurons and Brain Reward Pathways. The American Journal of Pathology 186:478–488.

Lutz K, Widmer M (2014) What can the monetary incentive delay task tell us about the neural processing of reward and punishment? Neuroscience and Neuroeconomics:33.

Maguire MJ, Abel AD (2013) What changes in neural oscillations can reveal about developmental cognitive neuroscience: Language development as a case in point. Developmental Cognitive Neuroscience 6:125–136.

Marco-Pallares J, Cucurell D, Cunillera T, García R, Andrés-Pueyo A, Münte TF, Rodríguez-Fornells A (2008) Human oscillatory activity associated to reward processing in a gambling task. Neuropsychologia 46:241–248.

Marco-Pallarés J, Münte TF, Rodríguez-Fornells A (2015) The role of high-frequency oscillatory activity in reward processing and learning. Neuroscience & Biobehavioral Reviews 49:1–7.

Maris E, Oostenveld R (2007) Nonparametric statistical testing of EEG- and MEG-data. J Neurosci Methods 164:177–190.

Martins D, Rademacher L, Gabay AS, Taylor R, Richey JA, Smith DV, Goerlich KS, Nawijn L, Cremers HR, Wilson R, Bhattacharyya S, Paloyelis Y (2021) Mapping social reward and punishment processing in the human brain: A voxel-based meta-analysis of neuroimaging findings using the social incentive delay task. Neuroscience & Biobehavioral Reviews 122:1–17.

Mas-Herrero E, Ripollés P, HajiHosseini A, Rodríguez-Fornells A, Marco-Pallarés J (2015) Beta oscillations and reward processing: Coupling oscillatory activity and hemodynamic responses. NeuroImage 119:13–19.

Maslow AH (1943) A Theory of Motivation. Psychological Review 50:370–396.

Maslow AH, Frager R (1987) Motivation and personality, 3rd ed. New York: Harper and Row.

Mata R, Josef AK, Samanez-Larkin GR, Hertwig R (2011) Age differences in risky choice: a meta-analysis: Mata et al. Annals of the New York Academy of Sciences 1235:18–29.

Mather M (2016) The Affective Neuroscience of Aging. Annual Review of Psychology 67:213–238.

Mather M, Canli T, English T, Whitfield S, Wais P, Ochsner K, John DEG, Carstensen LL (2004) Amygdala Responses to Emotionally Valenced Stimuli in Older and Younger Adults. Psychol Sci 15:259–263.

Mather M, Carstensen LL (2003) Aging and Attentional Biases for Emotional Faces. Psychological Science 14:409–415.

Mather M, Knight M (2005) Goal-directed memory: The role of cognitive control in older adults' emotional memory. Psychology and Aging 20:554–570.

Matsumoto M, Hikosaka O (2009) Two types of dopamine neuron distinctly convey positive and negative motivational signals. Nature 459:837–841.

Mattis S (1988) Dementia Rating Scale. Florida: Psychological Assessment Resources.

Mattox ST, Valle-Inclán F, Hackley SA (2006) Psychophysiological evidence for impaired reward anticipation in Parkinson's disease. Clinical Neurophysiology 117:2144–2153.

Mesulam M, Shaw P, Mash D, Weintraub S (2004) Cholinergic nucleus basalis tauopathy emerges early in the aging-MCI-AD continuum. Ann Neurol 55:815–828.

Mesulam M-M, Mufson EJ, Wainer BH, Levey AI (1983) Central cholinergic pathways in the rat: An overview based on an alternative nomenclature (Ch1–Ch6). Neuroscience 10:1185–1201.

Mewhort DJK, Kelly M, Johns BT (2009) Randomization tests and the unequal-N/unequal-variance problem. Behavior Research Methods 41:664–667.

Mir P, Trender-Gerhard I, Edwards MJ, Schneider SA, Bhatia KP, Jahanshahi M (2011) Motivation and movement: the effect of monetary incentive on performance speed. Experimental Brain Research 209:551–559.

Mirenowicz J, Schultz W (1996) Preferential activation of midbrain dopamine neurons by appetitive rather than aversive stimuli. Nature 379:449–451.

Molenberghs P, Louis WR (2018) Insights From fMRI Studies Into Ingroup Bias. Front Psychol 9:1868.

Moll J, Bado P, De Oliveira-Souza R, Bramati IE, Lima DO, Paiva FF, Sato JR, Tovar-Moll F, Zahn R (2012) A Neural Signature of Affiliative Emotion in the Human Septohypothalamic Area. J Neurosci 32:12499–12505.

Moll J, Zahn R, De Oliveira-Souza R, Bramati IE, Krueger F, Tura B, Cavanagh AL, Grafman J (2011) Impairment of prosocial sentiments is associated with frontopolar and septal damage in frontotemporal dementia. NeuroImage 54:1735–1742.

Monosov IE (2020) How Outcome Uncertainty Mediates Attention, Learning, and Decision-Making. Trends in Neurosciences 43:795–809.

Monosov IE, Leopold DA, Hikosaka O (2015) Neurons in the Primate Medial Basal Forebrain Signal Combined Information about Reward Uncertainty, Value, and Punishment Anticipation. Journal of Neuroscience 35:7443–7459.

Moonen AJH, Weiss PH, Wiesing M, Weidner R, Fink GR, Reijnders JSAM, Weber WM, Leentjens AFG (2017) An fMRI study into emotional processing in Parkinson's disease: Does increased medial prefrontal activation compensate for striatal dysfunction? Siegel A, ed. PLoS ONE 12:e0177085.

Morris G, Arkadir D, Nevet A, Vaadia E, Bergman H (2004) Coincident but Distinct Messages of Midbrain Dopamine and Striatal Tonically Active Neurons. Neuron 43:133–143.

Murphy K, Bodurka J, Bandettini PA (2007) How long to scan? The relationship between fMRI temporal signal to noise ratio and necessary scan duration. NeuroImage 34:565–574.

Murray HA, Harvard University eds. (1938) Explorations in personality. New York: Oxford University Press.

Nair-Roberts RG, Chatelain-Badie SD, Benson E, White-Cooper H, Bolam JP, Ungless MA (2008) Stereological estimates of dopaminergic, GABAergic and glutamatergic neurons in the ventral tegmental area, substantia nigra and retrorubral field in the rat. Neuroscience 152:1024–1031.

Nasreddine ZS, Phillips NA, Bédirian V, Charbonneau S, Whitehead V, Collin I, Cummings JL, Chertkow H (2005) The Montreal Cognitive Assessment, MoCA: A Brief Screening Tool For Mild Cognitive Impairment. Journal of the American Geriatrics Society 53:695–699.

O'Doherty JP, Deichmann R, Critchley HD, Dolan RJ (2002) Neural Responses during Anticipation of a Primary Taste Reward. Neuron 33:815–826.

Okada K, Nishizawa K, Kobayashi T, Sakata S, Hashimoto K, Kobayashi K (2021) Different cholinergic cell groups in the basal forebrain regulate social interaction and social recognition memory. Sci Rep 11:13589.

Oldham S, Murawski C, Fornito A, Youssef G, Yücel M, Lorenzetti V (2018) The anticipation and outcome phases of reward and loss processing: A neuroimaging meta-analysis of the monetary incentive delay task. Human Brain Mapping 39:3398–3418.

Oostenveld R, Fries P, Maris E, Schoffelen J-M (2011) FieldTrip: Open Source Software for Advanced Analysis of MEG, EEG, and Invasive Electrophysiological Data. Computational Intelligence and Neuroscience 2011:1–9.

Ota M, Yasuno F, Ito H, Seki C, Nozaki S, Asada T, Suhara T (2006) Age-related decline of dopamine synthesis in the living human brain measured by positron emission tomography with l-[β-11C]DOPA. Life Sciences 79:730–736.

Padilla-Coreano N, Tye KM, Zelikowsky M (2022) Dynamic influences on the neural encoding of social valence. Nat Rev Neurosci.

Panek PE, Barrett GV, Sterns HL, Alexander RA (1978) Age differences in perceptual style, selective attention, and perceptual-motor reaction time. Experimental Aging Research 4:377–387.

Park HRP, Kostandyan M, Boehler CN, Krebs RM (2018) Smiling faces and cash bonuses: Exploring common affective coding across positive and negative emotional and motivational stimuli using fMRI. Cogn Affect Behav Neurosci 18:550–563.

Pasquereau B, Tremblay L, Turner RS (2019) Local Field Potentials Reflect Dopaminergic and Non-Dopaminergic Activities within the Primate Midbrain. Neuroscience 399:167–183.

Pauli WM, Larsen T, Collette S, Tyszka JM, Seymour B, O'Doherty JP (2015) Distinct Contributions of Ventromedial and Dorsolateral Subregions of the Human Substantia Nigra to Appetitive and Aversive Learning. Journal of Neuroscience 35:14220–14233.

Pelli DG (1997) The VideoToolbox software for visual psychophysics: transforming numbers into movies. Spat Vis 10:437–442.

Pessiglione M, Schmidt L, Draganski B, Kalisch R, Lau H, Dolan RJ, Frith CD (2007) How the Brain Translates Money into Force: A Neuroimaging Study of Subliminal Motivation. Science 316:904–906.

Petty RE, Briñol P (2012) The Elaboration Likelihood Model. In: Handbook of Theories of Social Psychology: Volume 1, pp 224–245. 1 Oliver's Yard, 55 City Road, London EC1Y 1SP United Kingdom: SAGE Publications Ltd.

Poldrack RA (2007) Region of interest analysis for fMRI. Soc Cogn Affect Neurosci 2:67–70.

Prenger MTM, Madray R, Van Hedger K, Anello M, MacDonald PA (2020) Social Symptoms of Parkinson's Disease Stocchi F, ed. Parkinson's Disease 2020:1–10.

Rademacher L, Krach S, Kohls G, Irmak A, Gründer G, Spreckelmeyer KN (2010) Dissociation of neural networks for anticipation and consumption of monetary and social rewards. NeuroImage 49:3276–3285.

Rademacher L, Salama A, Gründer G, Spreckelmeyer KN (2014) Differential patterns of nucleus accumbens activation during anticipation of monetary and social reward in young and older adults. Social Cognitive and Affective Neuroscience 9:825–831.

Rajmohan V, Mohandas E (2007) The limbic system. Indian J Psychiatry 49:132–139.

Rangel A, Clithero JA (2012) Value normalization in decision making: theory and evidence. Current Opinion in Neurobiology 22:970–981.

Rapanelli M, Wang W, Hurley E, Feltri ML, Pittenger C, Frick LR, Yan Z (2023) Cholinergic neurons in the basal forebrain are involved in behavioral abnormalities associated with Cul3 deficiency: Role of prefrontal cortex projections in cognitive deficits. Transl Psychiatry 13:22.

Ravel S, Legallet E, Apicella P (2003) Responses of Tonically Active Neurons in the Monkey Striatum Discriminate between Motivationally Opposing Stimuli. J Neurosci 23:8489–8497.

Redgrave P, Prescott TJ, Gurney K (1999) Is the short-latency dopamine response too short to signal reward error? Trends in Neurosciences 22:146–151.

Reitan RM, Wolfson D (1985) The Halstead–Reitan Neuropsycholgical Test Battery: Therapy and clinical interpretation. Tucson, AZ: Neuropsychological Press.

Rhodes MG, Anastasi JS (2012) The own-age bias in face recognition: A meta-analytic and theoretical review. Psychological Bulletin 138:146–174.

Richey J, Ghane M, Valdespino A, Coffman MC, Strege MV, White SW, Ollendick TH (2017) Spatiotemporal dissociation of brain activity underlying threat and reward in social anxiety disorder. Social Cognitive and Affective Neuroscience 12:81–94.

Richey JA, Rittenberg A, Hughes L, Damiano CR, Sabatino A, Miller S, Hanna E, Bodfish JW, Dichter GS (2014) Common and distinct neural features of social and non-social reward processing in autism and social anxiety disorder. Soc Cogn Affect Neurosci 9:367–377.

Richoz A-R, Lao J, Pascalis O, Caldara R (2018) Tracking the recognition of static and dynamic facial expressions of emotion across the life span. Journal of Vision 18:5.

Richter A, Reinhard F, Kraemer B, Gruber O (2020) A high-resolution fMRI approach to characterize functionally distinct neural pathways within dopaminergic midbrain and nucleus accumbens during reward and salience processing. European Neuropsychopharmacology 36:137–150.

Rieckmann A, Bäckman L (2009) Implicit Learning in Aging: Extant Patterns and New Directions. Neuropsychology Review 19:490–503.

Rilling JK, Chen X, Chen X, Haroon E (2018) Intranasal oxytocin modulates neural functional connectivity during human social interaction. American J Primatol 80:e22740.

Rinne JO, Hietala J, Ruotsalainen U, Säkö E, Laihinen A, Någren K, Lehikoinen P, Oikonen V, Syvälahti E (1993) Decrease in Human Striatal Dopamine D $_2$ Receptor Density with Age: A PET Study with [^{11} C]Raclopride. J Cereb Blood Flow Metab 13:310–314.

Riva D, Bulgheroni S, Aquino D, Di Salle F, Savoiardo M, Erbetta A (2011) Basal Forebrain Involvement in Low-Functioning Autistic Children: A Voxel-Based Morphometry Study. AJNR Am J Neuroradiol 32:1430–1435.

Robbins TW, Everitt BJ (1996) Neurobehavioural mechanisms of reward and motivation. Current Opinion in Neurobiology 6:228–236.

Robert B, Kimchi EY, Watanabe Y, Chakoma T, Jing M, Li Y, Polley DB (2021) A functional topography within the cholinergic basal forebrain for encoding sensory cues and behavioral reinforcement outcomes. eLife 10:e69514.

Rodriguez LA, Kim S-H, Page SC, Nguyen CV, Pattie EA, Hallock HL, Valerino J, Maynard KR, Jaffe AE, Martinowich K (2023) The basolateral amygdala to lateral septum circuit is critical for regulating social novelty in mice. Neuropsychopharmacol 48:529–539.

Rogers BP, Morgan VL, Newton AT, Gore JC (2007) Assessing functional connectivity in the human brain by fMRI. Magnetic Resonance Imaging 25:1347–1357.

Root DH, Melendez RI, Zaborszky L, Napier TC (2015) The ventral pallidum: Subregion-specific functional anatomy and roles in motivated behaviors. Progress in Neurobiology 130:29–70.

Ruff CC, Fehr E (2014) The neurobiology of rewards and values in social decision making. Nat Rev Neurosci 15:549–562.

Ruxton GD, Neuhäuser M (2013) Improving the reporting of P-values generated by randomization methods. Methods in Ecology and Evolution 4:1033–1036.

Ryan RM, Deci EL (2000) Self-determination theory and the facilitation of intrinsic motivation, social development, and well-being. American Psychologist 55:68–78.

Rymarczyk K, Żurawski Ł, Jankowiak-Siuda K, Szatkowska I (2016) Do Dynamic Compared to Static Facial Expressions of Happiness and Anger Reveal Enhanced Facial Mimicry? Bard KA, ed. PLoS ONE 11:e0158534.

Salgado S, Kaplitt MG (2015) The Nucleus Accumbens: A Comprehensive Review. Stereotact Funct Neurosurg 93:75–93.

Sallet J, Quilodran R, Rothe M, Vezoli J, Joseph J-P, Procyk E (2007) Expectations, gains, and losses in the anterior cingulate cortex. Cognitive, Affective, & Behavioral Neuroscience 7:327–336.

Samanez-Larkin GR, Gibbs SEB, Khanna K, Nielsen L, Carstensen LL, Knutson B (2007) Anticipation of monetary gain but not loss in healthy older adults. Nature Neuroscience 10:787–791.

Samanez-Larkin GR, Kuhnen CM, Yoo DJ, Knutson B (2010) Variability in Nucleus Accumbens Activity Mediates Age-Related Suboptimal Financial Risk Taking. Journal of Neuroscience 30:1426–1434.

Samanez-Larkin GR, Levens SM, Perry LM, Dougherty RF, Knutson B (2012) Frontostriatal White Matter Integrity Mediates Adult Age Differences in Probabilistic Reward Learning. Journal of Neuroscience 32:5333–5337.

Samanez-Larkin GR, Wagner AD, Knutson B (2011) Expected value information improves financial risk taking across the adult life span. Social Cognitive and Affective Neuroscience 6:207–217.

Samanez-Larkin GR, Worthy DA, Mata R, McClure SM, Knutson B (2014) Adult age differences in frontostriatal representation of prediction error but not reward outcome. Cognitive, Affective, & Behavioral Neuroscience 14:672–682.

Sarter M, Gehring WJ, Kozak R (2006) More attention must be paid: The neurobiology of attentional effort. Brain Research Reviews 51:145–160.

Sarter M, Givens B, Bruno JP (2001) The cognitive neuroscience of sustained attention: where top-down meets bottom-up. Brain Research Reviews 35:146–160.

Sato W, Yoshikawa S (2007) Enhanced Experience of Emotional Arousal in Response to Dynamic Facial Expressions. J Nonverbal Behav 31:119–135.

Schilbach L, Timmermans B, Reddy V, Costall A, Bente G, Schlicht T, Vogeley K (2013) Toward a second-person neuroscience. Behav Brain Sci 36:393–414.

Schliebs R, Arendt T (2011) The cholinergic system in aging and neuronal degeneration. Behavioural Brain Research 221:555–563.

Schott BH, Minuzzi L, Krebs RM, Elmenhorst D, Lang M, Winz OH, Seidenbecher CI, Coenen HH, Heinze H-J, Zilles K, Duzel E, Bauer A (2008) Mesolimbic Functional Magnetic Resonance Imaging Activations during Reward Anticipation Correlate with Reward-Related Ventral Striatal Dopamine Release. Journal of Neuroscience 28:14311–14319.

Schott BH, Niehaus L, Wittmann BC, Schutze H, Seidenbecher CI, Heinze H-J, Duzel E (2007) Ageing and early-stage Parkinson’s disease affect separable neural mechanisms of mesolimbic reward processing. Brain 130:2412–2424.

Schultz W (2007) Behavioral dopamine signals. Trends in Neurosciences 30:203–210.

Schultz W (2015) Neuronal Reward and Decision Signals: From Theories to Data. Physiological Reviews 95:853–951.

Schultz W, Apicella P, Ljungberg T (1993) Responses of monkey dopamine neurons to reward and conditioned stimuli during successive steps of learning a delayed response task. The Journal of Neuroscience 13:900–913.

Schultz W, Dayan P, Montague PR (1997) A Neural Substrate of Prediction and Reward. Science 275:1593–1599.

Shahhosseini Y, Miranda MF (2022) Functional Connectivity Methods and Their Applications in fMRI Data. Entropy 24:390.

Shen C, Rolls ET, Cheng W, Kang J, Dong G, Xie C, Zhao X-M, Sahakian BJ, Feng J (2022) Associations of Social Isolation and Loneliness With Later Dementia. Neurology 99:e164–e175.

Shohamy D, Myers CE, Kalanithi J, Gluck MA (2008) Basal ganglia and dopamine contributions to probabilistic category learning. Neuroscience & Biobehavioral Reviews 32:219–236.

Simpson EH, Balsam PD (2015) The Behavioral Neuroscience of Motivation: An Overview of Concepts, Measures, and Translational Applications. In: Behavioral Neuroscience of Motivation (Simpson EH, Balsam PD, eds), pp 1–12 Current Topics in Behavioral Neurosciences. Cham: Springer International Publishing.

Singer T, Seymour B, O'Doherty JP, Stephan KE, Dolan RJ, Frith CD (2006) Empathic neural responses are modulated by the perceived fairness of others. Nature 439:466–469.

Smith-Collins APR, Fiorentini C, Kessler E, Boyd H, Roberts F, Skuse DH (2013) Specific neural correlates of successful learning and adaptation during social exchanges. Social Cognitive and Affective Neuroscience 8:887–896.

Snow BJ, Tooyama I, McGeer EG, Yamada T, Calne DB, Takahashi H, Kimura H (1993) Human positron emission tomographic [18F]Fluorodopa studies correlate with dopamine cell counts and levels. Ann Neurol 34:324–330.

Sobczak A, Bunzeck N (2023) Effects of positive and negative social feedback on motivation, evaluative learning, and socio-emotional processing. npj Sci Learn 8:28.

Sobczak A, Repplinger S, Bauch EM, Brueggemann N, Lohse C, Hinrichs H, Buentjen L, Voges J, Zaehle T, Bunzeck N (2021) Anticipating social incentives recruits alpha-beta oscillations in the human substantia nigra and invigorates behavior across the life span. NeuroImage:118696.

Sobczak A, Yousuf M, Bunzeck N (2023) Anticipating social feedback involves basal forebrain and mesolimbic functional connectivity. NeuroImage 274:120131.

Spaniol J, Bowen HJ, Wegier P, Grady C (2015) Neural responses to monetary incentives in younger and older adults. Brain Research 1612:70–82.

Spreckelmeyer KN, Krach S, Kohls G, Rademacher L, Irmak A, Konrad K, Kircher T, Gründer G (2009) Anticipation of monetary and social reward differently activates mesolimbic brain structures in men and women. Social Cognitive and Affective Neuroscience 4:158–165.

Sprengelmeyer R, Young AW, Mahn K, Schroeder U, Woitalla D, Büttner T, Kuhn W, Przuntek H (2003) Facial expression recognition in people with medicated and unmedicated Parkinson's disease. Neuropsychologia 41:1047–1057.

Steiger TK, Bunzeck N (2017) Reward Dependent Invigoration Relates to Theta Oscillations and Is Predicted by Dopaminergic Midbrain Integrity in Healthy Elderly. Frontiers in Aging Neuroscience 9.

Steiger TK, Weiskopf N, Bunzeck N (2016) Iron Level and Myelin Content in the Ventral Striatum Predict Memory Performance in the Aging Brain. Journal of Neuroscience 36:3552–3558.

Stelly CE, Haug GC, Fonzi KM, Garcia MA, Tritley SC, Magnon AP, Ramos MAP, Wanat MJ (2019) Pattern of dopamine signaling during aversive events predicts active avoidance learning. Proceedings of the National Academy of Sciences:201904249.

Suhara T, Fukuda H, Inoue O, Itoh T, Suzuki K, Yamasaki T, Tateno Y (1991) Age-related changes in human D1 dopamine receptors measured by positron emission tomography. Psychopharmacology 103:41–45.

Swanson JL, Ortiz-Guzman J, Srivastava S, Chin P-S, Dooling SW, Hanson Moss E, Kochukov MY, Hunt PJ, Patel JM, Pekarek BT, Tong Q, Arenkiel BR (2022) Activation of basal forebrain-to-lateral habenula circuitry drives reflexive aversion and suppresses feeding behavior. Sci Rep 12:22044.

Thayer S (1980) The effect of expression sequence and expressor identity on judgments of the intensity of facial expression. J Nonverbal Behav 5:71–79.

The jamovi project (2020) jamovi (Version 1.6.23) [Computer Software]. Available at: https://www.jamovi.org.

The MathWorks, Inc. (2018) MATLAB 2018b. Available at: https://www.mathworks.com.

Thomas RA, West RE, Borup J (2017) An analysis of instructor social presence in online text and asynchronous video feedback comments. The Internet and Higher Education 33:61–73.

Threlfell S, Lalic T, Platt NJ, Jennings KA, Deisseroth K, Cragg SJ (2012) Striatal Dopamine Release Is Triggered by Synchronized Activity in Cholinergic Interneurons. Neuron 75:58–64.

Tobler PN, Fiorillo CD, Schultz W (2005) Adaptive Coding of Reward Value by Dopamine Neurons. Science 307:1642–1645.

Toller G, Adhimoolam B, Grunwald T, Huppertz H-J, Kurthen M, Rankin KP, Jokeit H (2015) Right mesial temporal lobe epilepsy impairs empathy-related brain responses to dynamic fearful faces. J Neurol 262:729–741.

Tomova L, Wang KL, Thompson T, Matthews GA, Takahashi A, Tye KM, Saxe R (2020) Acute social isolation evokes midbrain craving responses similar to hunger. Nat Neurosci 23:1597–1605.

Tritsch NX, Sabatini BL (2012) Dopaminergic Modulation of Synaptic Transmission in Cortex and Striatum. Neuron 76:33–50.

Tu G, Halawa A, Yu X, Gillman S, Takehara-Nishiuchi K (2022) Outcome-Locked Cholinergic Signaling Suppresses Prefrontal Encoding of Stimulus Associations. J Neurosci 42:4202–4214.

Tukey JW (1977) Exploratory Data Analysis. Reading, Massachusetts: Addison-Wesley Publishing Company.

Ungless MA (2004) Uniform Inhibition of Dopamine Neurons in the Ventral Tegmental Area by Aversive Stimuli. Science 303:2040–2042.

Vaillancourt DE, Spraker MB, Prodoehl J, Zhou XJ, Little DM (2012) Effects of aging on the ventral and dorsal substantia nigra using diffusion tensor imaging. Neurobiology of Aging 33:35–42.

van den Berg P, Kemperman A, de Kleijn B, Borgers A (2016) Ageing and loneliness: The role of mobility and the built environment. Travel Behaviour and Society 5:48–55.

van der Schalk J, Fischer A, Doosje B, Wigboldus D, Hawk S, Rotteveel M, Hess U (2011) Convergent and divergent responses to emotional displays of ingroup and outgroup. Emotion 11:286–298.

Verneau M, van der Kamp J, Savelsbergh GJP, de Looze MP (2014) Age and Time Effects on Implicit and Explicit Learning. Experimental Aging Research 40:477–511.

Vila J (2021) Social Support and Longevity: Meta-Analysis-Based Evidence and Psychobiological Mechanisms. Front Psychol 12:717164.

Vinckier F, Pessiglione M, Forgeot d'Arc B (2021) Absence of covert face valuation in Autism. Transl Psychiatry 11:463.

Võ MLH, Conrad M, Kuchinke L, Urton K, Hofmann MJ, Jacobs AM (2009) The Berlin Affective Word List Reloaded (BAWL-R). Behavior Research Methods 41:534–538.

Volkow ND, Ding Y-S, Fowler JS, Wang G-J, Logan J, Gatley SJ, Hitzemann R (1996a) Dopamine Transporters Decrease with Age. Journal of Nuclear Medicine 37:554–558.

Volkow ND, Fowler JS, Gatley SJ, Logan J, Wang G-J, Ding Y-S, Dewey S (1996b) PET Evaluation of the Dopamine System of the Human Brain. :15.

Wake SJ, Izuma K (2017) A common neural code for social and monetary rewards in the human striatum. Social Cognitive and Affective Neuroscience 12:1558–1564.

Wang DV, Tsien JZ (2011) Convergent Processing of Both Positive and Negative Motivational Signals by the VTA Dopamine Neuronal Populations Tanimoto H, ed. PLoS ONE 6:e17047.

Wang J, Li J, Yang Q, Xie Y-K, Wen Y-L, Xu Z-Z, Li Y, Xu T, Wu Z-Y, Duan S, Xu H (2021) Basal forebrain mediates prosocial behavior via disinhibition of midbrain dopamine neurons. Proceedings of the National Academy of Sciences 118:e2019295118.

Wang Y, Chan GLY, Holden JE, Dobko T, Mak E, Schulzer M, Huser JM, Snow BJ, Ruth TJ, Calne DB, Stoessl AJ (1998) Age-dependent decline of dopamine D1 receptors in human brain: A PET study. Synapse 30:56–61.

Ward EV, Berry CJ, Shanks DR, Moller PL, Czsiser E (2020) Aging Predicts Decline in Explicit and Implicit Memory: A Life-Span Study. Psychol Sci 31:1071–1083.

Weishaupt D, Köchli VD, Marincek B, Froehlich JM (2009) Wie funktioniert MRI? eine Einführung in Physik und Funktionsweise der Magnetresonanzbildgebung ; mit 9 Tabellen, 6. Aufl. Heidelberg: Springer.

Williams EH, Bilbao-Broch L, Downing PE, Cross ES (2020) Examining the value of body gestures in social reward contexts. NeuroImage 222:117276.

Williams EH, Cross ES (2018) Decreased reward value of biological motion among individuals with autistic traits. Cognition 171:1–9.

Wilson F, Rolls E (1990) Learning and memory is reflected in the responses of reinforcement- related neurons in the primate basal forebrain. J Neurosci 10:1254–1267.

Wittmann BC, Schott BH, Guderian S, Frey JU, Heinze H-J, Düzel E (2005) Reward-related FMRI activation of dopaminergic midbrain is associated with enhanced hippocampus-dependent long-term memory formation. Neuron 45:459–467.

Wolf D, Grothe M, Fischer FU, Heinsen H, Kilimann I, Teipel S, Fellgiebel A (2014) Association of basal forebrain volumes and cognition in normal aging. Neuropsychologia 53:54–63.

Wolfe HE, Livingstone KM, Isaacowitz DM (2022) More Positive or Less Negative? Emotional Goals and Emotion Regulation Tactics in Adulthood and Old Age Luong G, ed. The Journals of Gerontology: Series B 77:1603–1614.

Wrase J, Kahnt T, Schlagenhauf F, Beck A, Cohen MX, Knutson B, Heinz A (2007) Different neural systems adjust motor behavior in response to reward and punishment. NeuroImage 36:1253–1262.

Wu T, Hallett M (2013) The cerebellum in Parkinson's disease. Brain 136:696–709.

Yan C, Wang Y, Su L, Xu T, Yin D, Fan M, Deng C, Wang Z, Lui SSY, Cheung EFC, Chan RCK (2016) Differential mesolimbic and prefrontal alterations during reward anticipation and consummation in positive and negative schizotypy. Psychiatry Research: Neuroimaging 254:127–136.

Yebra M, Rutishauser U (2022) How can we process microelectrode data to isolate single neurons in humans? PsyArXiv. Available at: https://osf.io/fersu.

Yu AJ, Dayan P (2005) Uncertainty, Neuromodulation, and Attention. Neuron 46:681–692.

Zaborszky L, Hoemke L, Mohlberg H, Schleicher A, Amunts K, Zilles K (2008) Stereotaxic probabilistic maps of the magnocellular cell groups in human basal forebrain. NeuroImage 42:1127–1141.

Zaborszky L, van den Pol A, Gyengesi E (2012) The Basal Forebrain Cholinergic Projection System in Mice. In: The Mouse Nervous System, pp 684–718. Elsevier.

Zaghloul KA, Blanco JA, Weidemann CT, McGill K, Jaggi JL, Baltuch GH, Kahana MJ (2009) Human Substantia Nigra Neurons Encode Unexpected Financial Rewards. Science 323:1496–1499.

Zahn R, De Oliveira-Souza R, Moll J (2020) Moral Motivation and the Basal Forebrain. Neuroscience & Biobehavioral Reviews 108:207–217.

Zahn R, Moll J, Paiva M, Garrido G, Krueger F, Huey ED, Grafman J (2009) The Neural Basis of Human Social Values: Evidence from Functional MRI. Cerebral Cortex 19:276–283.

Zajonc RB (1968) Attitudinal effects of mere exposure. Journal of Personality and Social Psychology 9:1–27.

Zaki J, Ochsner K (2009) The Need for a Cognitive Neuroscience of Naturalistic Social Cognition. Annals of the New York Academy of Sciences 1167:16–30.

Zhang G-W, Shen L, Zhong W, Xiong Y, Zhang LI, Tao HW (2018) Transforming Sensory Cues into Aversive Emotion via Septal-Habenular Pathway. Neuron 99:1016-1028.e5.

Zhang K, Chen CD, Monosov IE (2019) Novelty, Salience, and Surprise Timing Are Signaled by Neurons in the Basal Forebrain. Current Biology 29:134-142.e3.

Zhang Y, Larcher KM-H, Misic B, Dagher A (2017) Anatomical and functional organization of the human substantia nigra and its connections. Elife 6.

Zhu X, Zhou H, Geng F, Wang J, Xu H, Hu Y (2023) Functional Connectivity Between Basal Forebrain and Superficial Amygdala Negatively Correlates with Social Fearfulness. Neuroscience 510:72–81.

Ziaei M, Fischer H (2016) Emotion and Aging. In: Neuroimaging Personality, Social Cognition, and Character, pp 259–278. Elsevier.

Zimmermann P, Fimm B (2002) A test battery for attentional performance. Applied Neuropsychology of Attention.

Zink CF, Tong Y, Chen Q, Bassett DS, Stein JL, Meyer-Lindenberg A (2008) Know Your Place: Neural Processing of Social Hierarchy in Humans. Neuron 58:273–283.

Appendix

A Supplementary material study I

Anticipating social incentives recruits alpha-beta oscillations in the human substantia nigra and invigorates behavior across the life span

Alexandra Sobczak[a], Stefan Repplinger[b], Eva M. Bauch[a], Norbert Brueggemann[c,d,e], Christina Lohse[c,], Hermann Hinrichs[b], Lars Buentjen[b], Juergen Voges[b], Tino Zaehle[b,f] & Nico Bunzeck[a, e]

[a] Department of Psychology, University of Lübeck, Ratzeburger Allee 160, 23562 Lübeck, Germany

[b] Departments of Neurology and Stereotactic Neurosurgery, Otto-von-Guericke University, Leipziger Straße 44, 39120 Magdeburg, Germany

[c] Department of Neurology, University Medical Center Schleswig-Holstein, Ratzeburger Allee 160, 23562 Lübeck, Germany

[d] Institute of Neurogenetics, University of Lübeck, Ratzeburger Allee 160, 23562 Lübeck, Germany

[e] Center of Brain, Behavior and Metabolism, University of Lübeck, Ratzeburger Allee 160, 23562 Lübeck, Germany

[f] Center for Behavioral Brain Sciences (CBBS), 39106, Magdeburg

Supplementary table A S1.

Neuropsychological test results for iEEG-PD-OFF patients. Percentile ranks (PR)[1] are provided for TAP, TMT, RWT, VLMT, and WMS-R.

Patient No.	TAP Alertness[2] Go/NoGo[3]	TMT (A,B, B/A)	RWT[4]	VLMT[5]	WMS-R[6]	(M)DRS (total)	BDI-II[7]
1	50, 38, 86	42-46, 18-21, 18	36, 32, 76, 36	20, <5, <5, 15-20, <5	<20, <12, 7, 45	143	3
2	4, 10, 14	58, 42, 34	6, 30, 8, 10	20, 40-45, 15, 30-35, 20	34, 52, 50, 2	142	15
4	42, 16, 46	5, 14, n.a.	73, 46, 72, 86	30, <5, 20-25, 15-20, >75	76, 53, 8, 67	142	8
6	34, 38, 62	66-69, 58, 51	16, 5, 36, 95	85, 85-90, 85-95, 85-95, 40-45	34, 13, 5, 11	143	7
7	n.a.	23, 10, 8	51, 46, 57, 4	20, <5, <5, 5-10, 10	15, 53, 28, 67	141	11
9	34, 38, 62	41, 79, 16	42, 67, 98, 86	55-60, 40-45, 30-40, 25, 10	76, 53, 57, 27	141	11
10	34, 54, 27	90, 62, 5	41, 29, 53, 69	55-60, 40-45, 45-50, 45-50, 50-75	13, 2, 71, 55	142	5
11	16, 31, 8	24, 14, 34	n.a, n.a.38, n.a.	30, 75-80, 20-25, 30-35, 50-75	53, 13, 8, 10	140	10
12	50,69, 46	69,96,82	47, 26, 98, 84	50-60, 50-70, 5-10, 30-35, 20	67,38,27,45	144	16
13	2, 2, 12	2-3, n.a., n.a.	61, 40, 90, 83	<5, <5, <5, <5, <5	15, 13, 28, 67	138	11
15	73, 73, 79	58-62, 12-14, <1	69, 80, 74, 45	40, 75-80, <5, 15-20, <5	67,12, 27, 10	141	3

Note: Rec. site, recording site; LH, left hemisphere; RH, right hemisphere; UPDRS, Unified Parkinson Rating Scale; TMT, Trail Making Test; RWT, Regensburger Wortflüssigkeit-Test; VLMT, Verbal Learning and Memory Test; WM, working memory; FAB, Frontal Assessment Battery; (M)DRS, Mattis Dementia Rating Scale; BDI-II, Beck Depression Inventory

[1] PR > 95 far above average; 84-95 above average; 16-84 average; 15-5 below average; <5 far below average; n.a. = data not available

[2] median RT with warning tone, median RT without warning tone

[3] median RT

[4] simple lexical (words starting with K), lexical intra-dimensional switch (words starting with G/R), simple semantic (category animals), semantic intra-dimensional switch (kind of sport/fruit)

[5] DG 1-5, interference, DG 6, DG 7, W – F

[6] digit span forward, digit span backward, Corsi block-tapping test forward, Corsi block-tapping test backward

[7] BDI-II score: 0-8 no depression; 9-13 minimal depression; 14-19 slight depression; 20-28 moderate depression,; 29-63 severe depression

Supplementary analysis A S2. Analysis of RT in HOA vs PD2-OFF vs iEEG-PD-OFF

We compared RTs of HOA, PD2-OFF, and iEEG-PD-OFF patients using a permutation F-test in a 3x3 mixed (between-subject factor group; within-subject factor condition) design with subsampling (HOA *n* = 11, PD2-OFF *n* = 11, iEEG-PD-OFF *n* = 11) in MATLAB. The analysis revealed a significance ratio of 0.59 for the main effect of group, meaning that 59% of the permutation tests showed significant results. The significance ratio for the main effect of condition was 0.01, meaning that 1% of the permutation tests showed a significant result. The significance ratio for the interaction were 0, meaning that 0% of the permutation tests showed a significant result. However, pair-wise permutation t-tests showed no significant differences between groups (HOA vs PD2-OFF significance ratio = 0; HOA vs iEEG-PD-OFF significance ratio = 0 ; PD2-OFF vs iEEG-PD-OFF significance ratio = 0). Permutation paired t-tests were used for pair-wise comparisons of factor levels with an adjusted alpha-level of 0.016 (0.05 / 3) using Bonferroni correction.

Together, the main effect of group could not be resolved. However, the main conclusion remains: There were no significant differences in RT between conditions, and, importantly, no significant interaction between the factors group and condition, when limiting the analysis to *n* = 11 HOA, *n* = 11 PD2-OFF patients, and *n* = 11 iEEG-PD-OFF patients. This suggests that the sample size of the iEEG-PD-OFF group was simply too small in order to detect an equally sized RT effect if it were present.

Supplementary analysis A S3. RT in PD2-OFF vs iEEG-PD-OFF

We conducted a permutation F-test in a 2x3 mixed (between-subject factor group; within-subject factor condition) design on RT in the PD2-OFF and iEEG-PD-OFF patients. There was no significant main effect of group ($p = 0.80$), no significant main effect of condition ($p = 0.14$), and no significant interaction ($p = 0.49$). Together with the significant main effect of condition in the 2x3 (within-subject factor medication status; within-subject factor condition) permutation F-test on RT in PD2-ON and PD2-OFF patients (see methods and results) the interpretation is unclear. Therefore, we conducted an additional Bayesian ANOVA. There was no clear evidence for or against the main effect of group (BF_{01}=1.77), weak evidence against the main effect of condition (BF_{01}=3.24), moderate evidence against the combined main effects model (BF_{01}=5.80), and strong evidence against the combined model with both main effects and the interaction (BF_{01}=24.07). This means that the data is 4.15 times less likely in a model that included the interaction term vs a model that only includes the two main effects.

We conclude that an interaction between the factors group and condition is unlikely. However, the effect of condition does not survive the joint analysis of PD2-OFF and iEEG-PD-OFF. One possible explanation could be that the PD2-ON group biased the analysis of the PD2 sample and lacked power to detect an interaction between PD2-OFF and PD2-ON. This does not necessarily imply the absence of the effect OFF medication. It is also possible that the effect is smaller OFF medication but too small to be detected with the present sample size.

Supplementary analysis A S4. Average cluster power of early vs late trials

We performed an analysis of early vs late trials on the iEEG data. Specifically, we compared the average cluster power of the first vs second half of all trials in one condition using permuted paired t-tests. Two outliers were excluded ($n = 10$, see definition of outliers in the methods section). Early vs late trials did not differ significantly in average cluster power (Neutral 1st vs 2nd half: $p = 0.362$; positive 1st vs 2nd half $p = 0.737$; Negative 1st vs 2nd half $p = 0.069$; supplementary figure 1). The alpha level was adjusted to 0.016 (0.05 / 3) using Bonferroni correction.

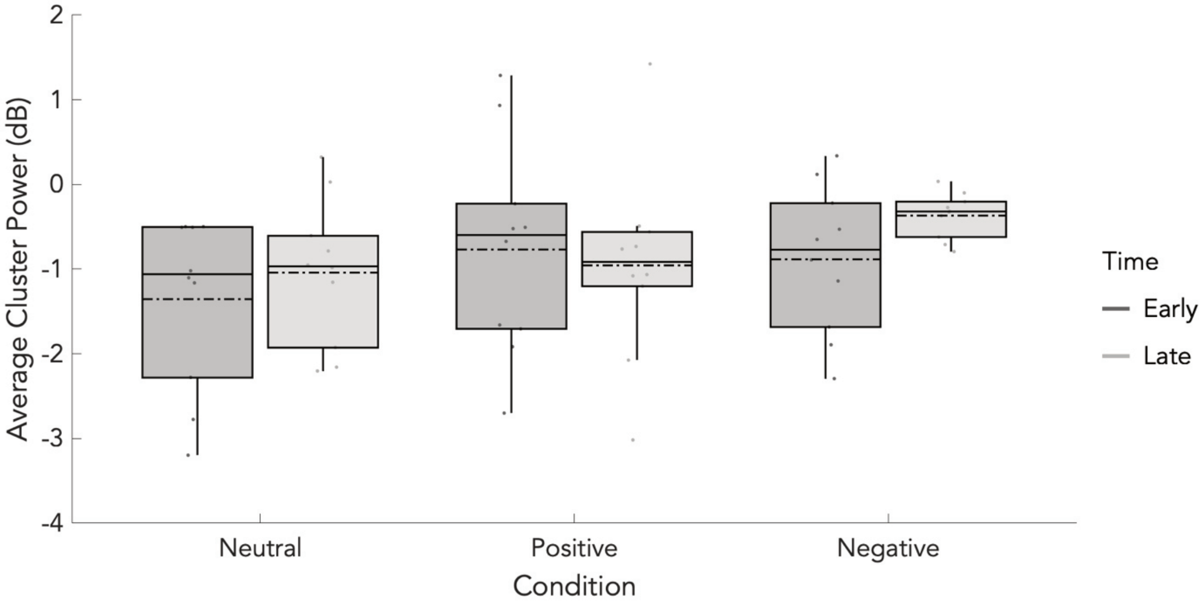

Supplementary figure A S5. Average cluster power for early vs late trials per condition. Early trials were defined as the first half of all trials of one condition and late trials were defined as the second half of all trials in one condition. Two outliers were excluded (n = 10, see definition of outliers in the methods section). There were no significant differences in average cluster power between early and late trials (neutral early vs late: p = 0.362; positive early vs late p = 0.737; negative early vs late p = 0.069). The alpha level was adjusted to 0.016 (0.05 / 3) using Bonferroni correction. Solid horizontal lines mark the median and dashed horizontal lines mark the mean. Whiskers are drawn to the distance of 1.5 times the inter-quartile range or to the lowest and largest data point that falls into this distance. Data points that fall out of this distance are also displayed.

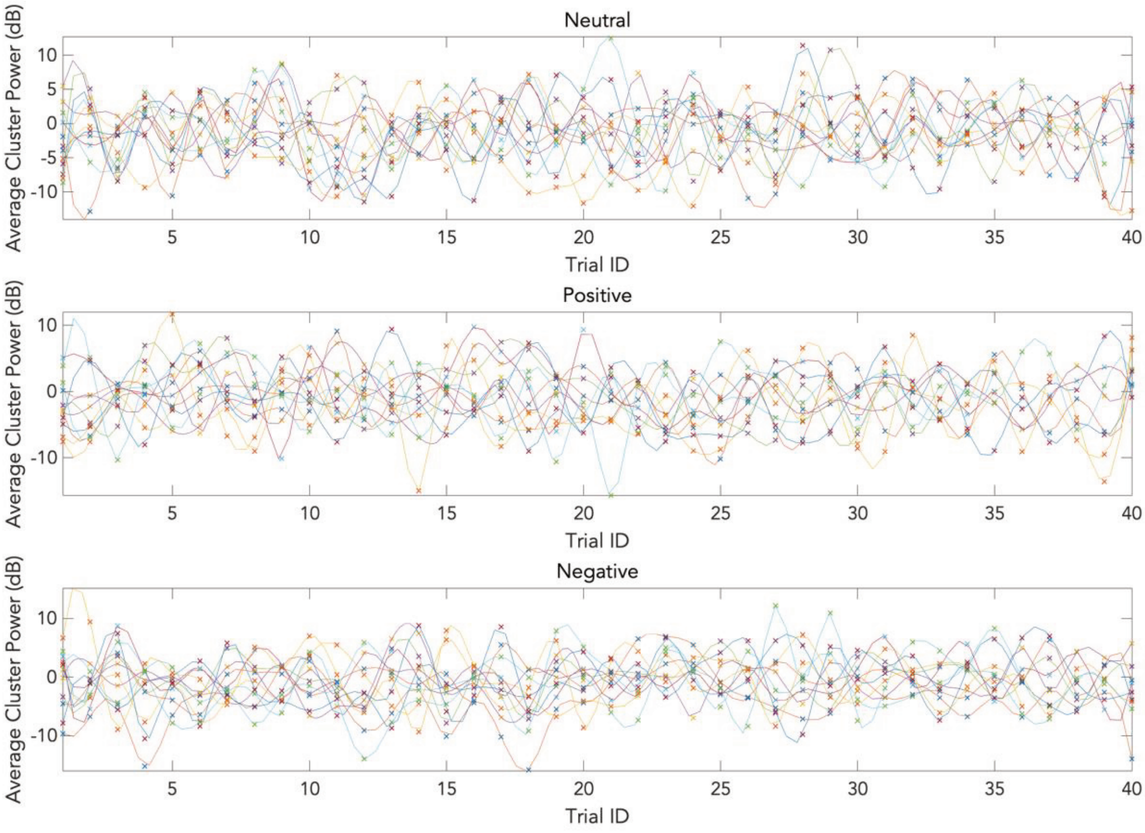

Supplementary figure A S6. Average cluster power as a function of trial ID per condition. Colored lines depict the different subjects.

B Supplementary material study II

Anticipating social feedback involves basal forebrain and mesolimbic functional connectivity

Supplementary material

Alexandra Sobczak[1], Musfa Yousuf [1], Nico Bunzeck[1, 2]

[1] Department of Psychology, University of Lübeck, Ratzeburger Allee 160, 23562 Lübeck, Germany

[2] Center of Brain, Behavior and Metabolism, University of Lübeck, Ratzeburger Allee 160, 23562 Lübeck, Germany

Corresponding authors: alexandra.sobczak@gmx.de, nico.bunzeck@uni-luebeck.de

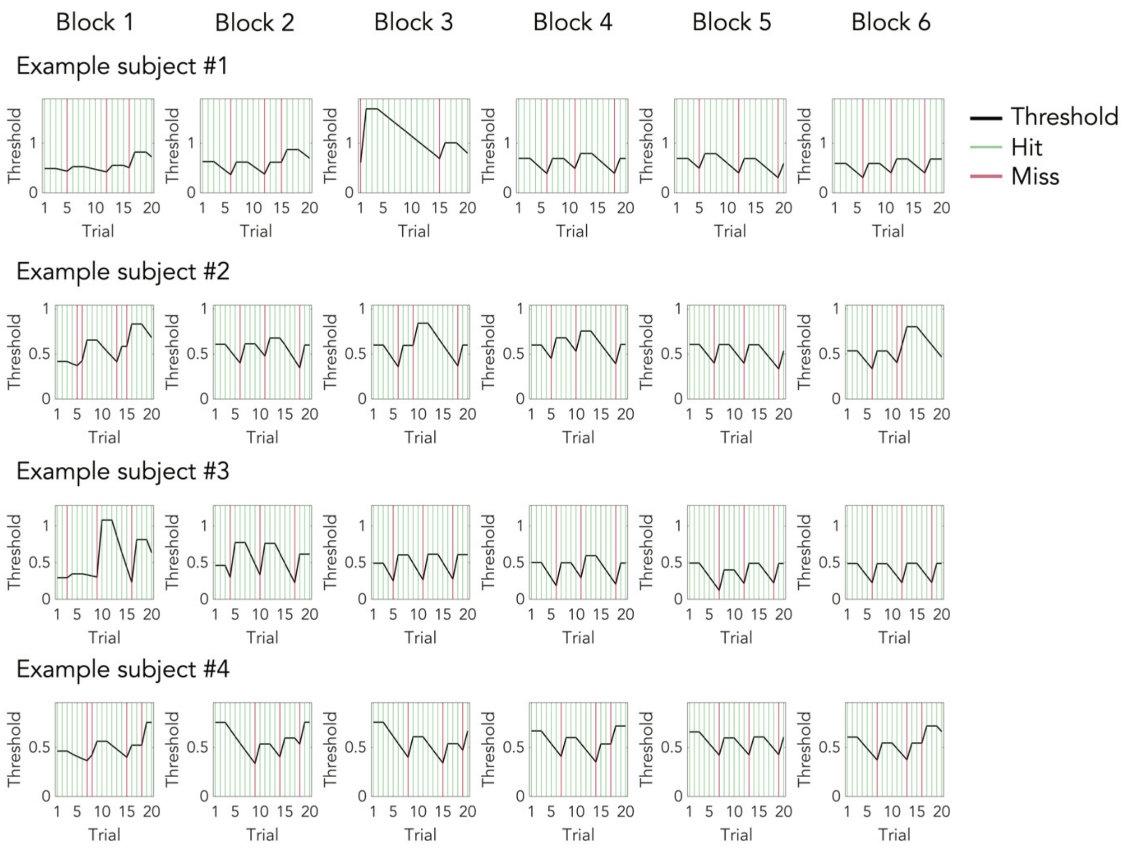

Supplementary figure B S1. Adaptive calculation of the response time threshold plotted for four example subjects. Plots show the adaptive calculation of the response time threshold (black line) in the social incentive delay task using the staircase method. Hits are depicted by green vertical lines and misses are depicted by red vertical lines.

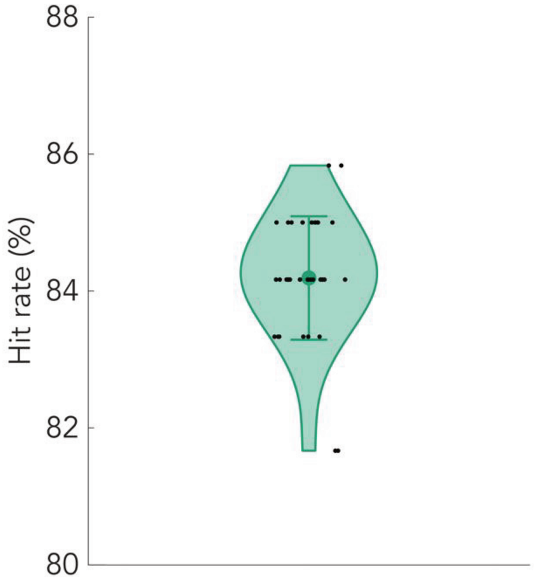

Supplementary figure B S2. Hit rates. Hit rate data for the social incentive delay task. Average hit rate was 84%. Error bars indicate the standard deviation (SD = 0.9%).

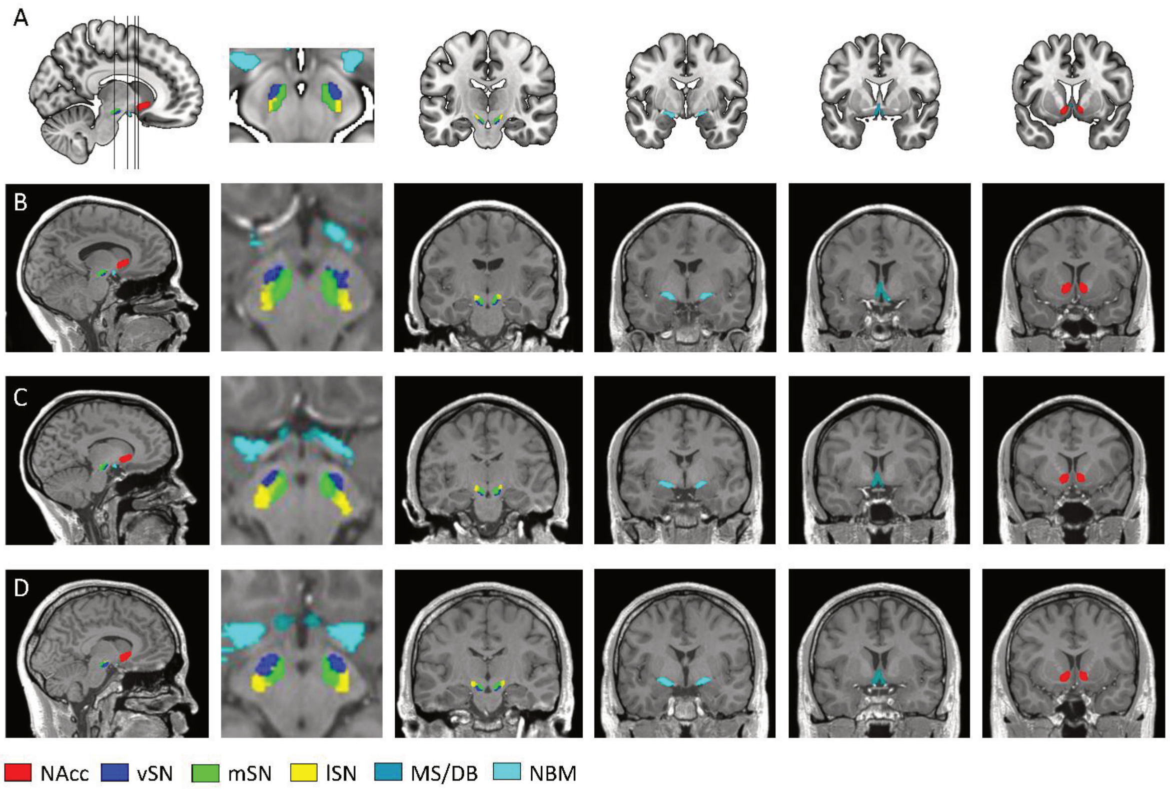

Supplementary figure B S3. Regions of interest (ROIs). **A** ROIs overlayed on an MNI T1 template. Saggital view indicates locations of coronal slices. Axial closeup shows the subregions of the substantia nigra. **B-D** Transformed masks for the regions of Interest (ROIs) in native space for three example subjects overlayed on individual T1 images. NAcc: nucleus accumbens; vSN: ventral substantia nigra; mSN: medial substantia nigra; lSN: lateral substantia nigra; MS/DB: medial septum/diagonal band; NBM: Nucleus basalis of Meynert.

Supplementary table B S4. Multivariate pattern analysis

Results of the bootstrap one-sample t-tests on extracted accuracy minus chance values of the multivariate pattern analysis.

Decoding model	Region of interest					
	NAcc	vSN	mSN	lSN	MS/DB	NBM
Neu/Pos/Neg	AMC = 0.08 $t_{(35)} = 0.09$ $P = 0.4541$ $d = 0.005$	AMC = 0.22 $t_{(35)} = 0.33$ $P = 0.3589$ $d = 0.06$	AMC = 0.66 $t_{(35)} = 1.05$ $P = 0.1347$ $d = 0.18$	AMC = 0.36 $t_{(35)} = 0.50$ $P = 0.3127$ $d = 0.08$	AMC = 1.21 $t_{(35)} = 1.08$ $P = 0.1419$ d = 0.17	AMC = 0.55 $t_{(35)} = 0.66$ $P = 0.2383$ $d = 0.11$
Pos/Neu	AMC = 0.19 $t_{(35)} = 0.14$ $P = 0.4331$ $d = 0.01$	AMC = 2.34 $t_{(35)} = 2.66$ $P = 0.0042$* $d = 0.45$	AMC = 2.66 $t_{(35)} = 2.95$ $P = 0.0014$* $d = 0.53$	AMC = 1.34 $t_{(35)} = 1.22$ $P = 0.1113$ $d = 0.20$	AMC = -0.07 $t_{(35)} = -0.07$ $P = 0.5248$ $d = -0.01$	AMC = 1.07 $t_{(35)} = 0.72$ $P = 0.2215$ $d = 0.10$
Neg/Neu	AMC = 0.31 $t_{(35)} = 0.30$ $P = 0.3735$ $d = 0.03$	AMC = -0.20 $t_{(35)} = -0.22$ $P = 0.5854$ $d = -0.03$	AMC = 0.52 $t_{(35)} = 0.53$ $P = 0.2909$ $d = 0.09$	AMC = -0.22 $t_{(35)} = -0.25$ $P = 0.6170$ $d = 0.04$	AMC = 1.92 $t_{(35)} = 1.08$ $P = 0.1343$ $d = 0.18$	AMC = -0.07 $t_{(35)} = -0.07$ $P = 0.5248$ $d = -0.01$
Pos/Neg	AMC = 0.56 $t_{(35)} = 0.37$ $P = 0.3541$ $d = 0.06$	AMC = -0.69 $t_{(35)} = -0.71$ $P = 0.7718$ $d = -0.10$	AMC = 0.05 $t_{(35)} = 0.05$ $P = 0.4817$ $d = 0.02$	AMC = 0.53 $t_{(35)} = 0.58$ $P = 0.2747$ $d = 0.10$	AMC = 0.55 $t_{(35)} = 0.66$ $P = 0.2383$ $d = 0.11$	AMC = 0.33 $t_{(35)} = 0.35$ $P = 0.3555$ $d = 0.06$

Two-tailed tests. Bonferroni-corrected alpha-levels ($\alpha = 0.05/4 = 0.0125$). Asterisks indicate $p < \alpha$. Neu: Neutral; Pos: Positive; Neg: Negative; AMC: accuracy minus chance; *d*: Cohen's d. NAcc: Nucleus accumbens; vSN: ventral substantia nigra; mSN: medial substandia nigra; lSN: lateral substantia nigra; MS/DB: medial septum/ diagonal band; NBM: Nucleus basalis of Meynert.

Supplementary table B S5. Functional connectivity analysis

Results of the bootstrap one-sample t-tests on extracted Fisher's z-values of the functional connectivity analysis.

	NAcc	vSN	mSN	lSN
		Neutral		
NAcc	-	z = 0.02 $t_{(35)}$ = 0.97 *P* = 0.3189 *d* = 0.16	z = 0.03 $t_{(35)}$ = 1.32 *P* = 0.1737 *d* = 0.22	z = 0.07 $t_{(35)}$ = 2.33 *P* = 0.0197 *d* = 0.40
MS/DB	z = 0.11 $t_{(35)}$ = 3.28 *P* = 0.0025* *d* = 0.56	z = -0.00 $t_{(35)}$ = -0.03 *P* = 0.9744 *d* = -0.02	z = 0.01 $t_{(35)}$ = 0.38 *P* = 0.7036 *d* = 0.06	z = 0.01 $t_{(35)}$ = 0.33 *P* = 0.7336 *d* = 0.06
NBM	z = 0.14 $t_{(35)}$ = 3.97 *P* = 0.0001* *d* = 0.67	z = 0.04 $t_{(35)}$ = 1.63 *P* = 0.0921 *d* = 0.27	z = 0.08 $t_{(35)}$ = 2.97 *P* = 0.0023* *d* = 0.50	z = 0.06 $t_{(35)}$ = 2.36 *P* = 0.0157* *d* = 0.40
		Positive		
NAcc	-	z = 0.03 $t_{(35)}$ = 1.30 *P* = 0.1879 *d* = 0.22	z = 0.05 $t_{(35)}$ = 1.72 *P* = 0.0823 *d* = 0.29	z = 0.02 $t_{(35)}$ = 0.53 *P* = 0.5760 *d* = 0.07
MS/DB	z = 0.12 $t_{(35)}$ = 3.66 *P* = 0.0003* *d* = 0.62	z = 0.03 $t_{(35)}$ = 1.08 *P* = 0.2637 *d* = 0.18	z = 0.01 $t_{(35)}$ = 0.37 *P* = 0.7038 *d* = 0.07	z = -0.02 $t_{(35)}$ = -0.58 *P* = 0.5488 *d* = -0.09
NBM	z = 0.15 $t_{(35)}$ = 4.05 *P* = 0.0001* *d* = 0.69	z = 0.09 $t_{(35)}$ = 3.01 *P* = 0.0033* *d* = 0.50	z = 0.13 $t_{(35)}$ = 3.88 *P* = 0.0003* *d* = 0.66	z = 0.04 $t_{(35)}$ = 1.68 *P* = 0.0893 *d* = 0.29
		Negative		
NAcc	-	z = 0.07 $t_{(35)}$ = 2.18 *P* = 0.0281 *d* = 0.37	z = 0.10 $t_{(35)}$ = 3.26 *P* = 0.0021* *d* = 0.57	z = 0.11 $t_{(35)}$ = 3.22 *P* = 0.0009* *d* = 0.55
MS/DB	z = 0.17 $t_{(35)}$ = 3.93 *P* = 0.0001* *d* = 0.67	z = 0.04 $t_{(35)}$ = 1.11 *P* = 0.2555 *d* = 0.18	z = 0.04 $t_{(35)}$ = 0.97 *P* = 0.3103 *d* =0.15	z = 0.11 $t_{(35)}$ = 3.39 *P* = 0.0017* *d* = 0.58
NBM	z = 0.16 $t_{(35)}$ = 4.30 *P* = 0.0001* *d* = 0.73	z = 0.07 $t_{(35)}$ = 2.46 *P* = 0.0173 *d* = 0.42	z = 0.10 $t_{(35)}$ = 3.58 *P* = 0.0011* *d* = 0.61	z = 0.05 $t_{(35)}$ = 1.55 *P* = 0.1187 *d* = 0.27

Adjusted $\alpha = 0.0167$. Asterisks indicate $p < \alpha$. NAcc: Nucleus accumbens; vSN: ventral substantia nigra; mSN: medial substandia nigra; lSN: lateral substantia nigra; MS/DB: medial septum/ diagonal band; NBM: Nucleus basalis of Meynert

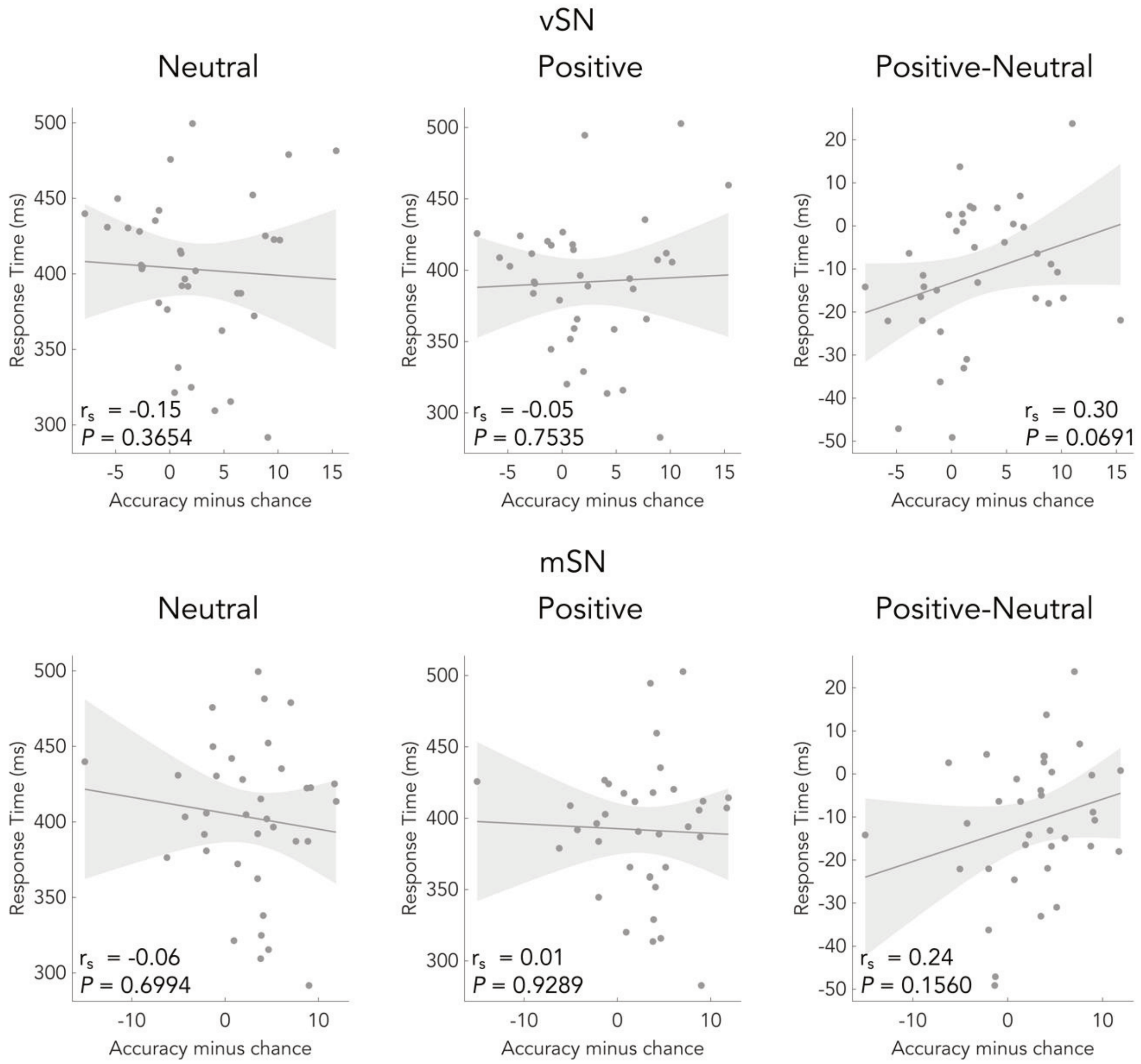

Supplementary figure B S6. Correlations between the accuracy minus chance values from the multivariate pattern analysis and response time. Spearman correlations. Adjusted α = 0.05/6 = 0.0083. vSN: ventral substantia nigra; mSN: medial substantia nigra.

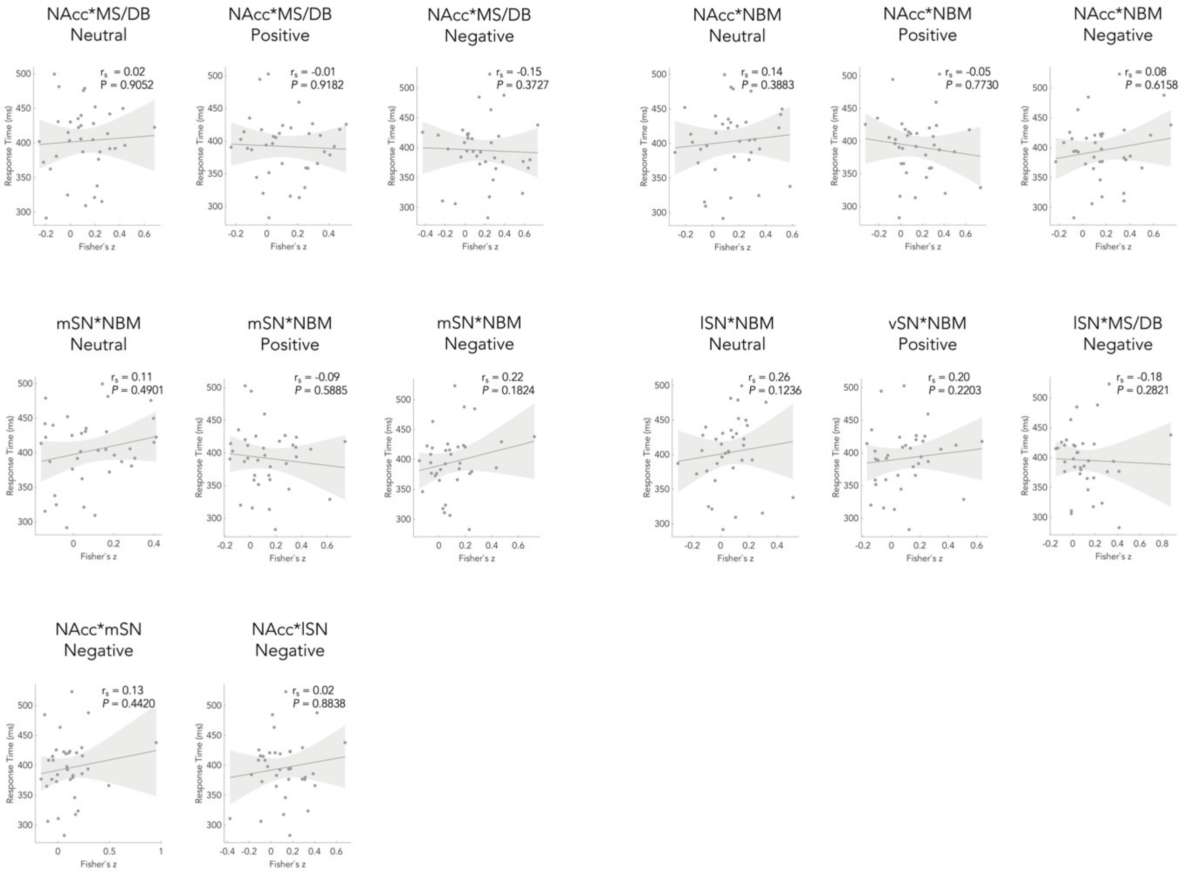

Supplementary figure B S7. Correlations between z-values from the functional connectivity analysis and response time. Spearman correlations. Adjusted α = 0.05/14 = 0.0035. NAcc: Nucleus accumbens; vSN: ventral substantia nigra; mSN: medial substandia nigra; lSN: lateral substantia nigra; MS/DB: medial septum/ diagonal band; NBM: Nucleus basalis of Meynert.

C Review Article

The Basal Forebrain Serves Social Information Processing

Alexandra Sobczak, Nico Bunzeck

Published in Current Opinion in Behavioral Sciences (2024). 56:101372. doi: 10.1016/j.cobeha.2024.101372

Abstract

Empirical evidence suggests a critical, but little-understood, contribution of the basal forebrain (BF) to motivational aspects of social cognition. Therefore, we review the current literature on reward and punishment processing in the BF, including social information, in both animals and more recently human imaging studies. This also includes interactions with other subcortical structures, especially the ventral striatum and substantia nigra/ventral tegmental area, which are part of the mesolimbic system. Importantly, the BF typically degenerates during healthy aging and shows abnormalities in autistic spectrum disorders, which may help to further understand its role in social information processing. Finally, we suggest a model of cortical and subcortical social information processing bringing together BF contributions in concert with the dopaminergic midbrain, medial temporal lobe, and prefrontal cortex to promote social cognition.

Introduction

The basal forebrain (BF) is involved in attentional control, learning, and memory, and, as shown in more recent studies, motivational processing (Atri et al., 2004; Hasselmo, 2006; Zhang et al., 2019; Sobczak et al., 2023). To further clarify the latter aspect, this review aims to characterize the BF's role in social cognition with a focus on motivational aspects that shape social behaviors. Social motivation refers to the desire for social connectedness and focuses on emotional and motivational influences guiding social behavior (Chevallier et al., 2012), while social cognition refers to the perception and understanding of social information (Beer and Ochsner, 2006). The two concepts are interrelated in the sense that aspects of social cognition can shape motivational responses, and motivational states can influence how social information is being processed. For instance, viewing social cues evokes neural signatures of craving during states of acute social isolation. This implies an increased value of social interaction, that is, motivational aspects, and changes in the perception of social information, that is, social cognition (Tomova et al., 2020). Moreover, the evaluation of stimuli as pleasant or unpleasant (i.e. valence) is an essential neurocognitive function and a key component of motivational processing (Padilla-Coreano et al., 2022). In the social domain, valence helps to interpret social situations and execute appropriate actions. For example, emotional expressions, including mimic and gesture, are an essential part of human communication that can facilitate approach or avoidance behavior (Sobczak and Bunzeck, 2023). A recent review suggested a neural circuit implicated in social valence processing, for example, social rank, social memory, and social isolation, including the medial prefrontal cortex (mPFC), nucleus accumbens (NAcc), basolateral amygdala, and hippocampus based on findings in primates and rodents (Padilla-Coreano et al., 2022). Here, we argue that this circuit needs to be extended by the BF given its role in motivation and social cognition as evident in animals and humans.

In the following, we will first provide basic information about social motivation, social cognition, and BF anatomy. Then we will link conceptual understandings of social cognition with BF information processing from both animal work and human imaging studies, which indicate a role of the BF in a variety of behaviors, ranging from basic needs to more complex aspects, such as social acknowledgment and connectedness (Baumeister and Leary, 1995). We discuss important anatomical connections to the prefrontal cortex (PFC), medial temporal lobe (MTL), and dopaminergic system alongside research on aging and autistic spectrum disorder (ASD) to gain novel insights into the underlying mechanisms of cortical and subcortical social information processing (CASSI).

Social motivation

While social motivation promotes social interactions and social connectedness, it is also clear that successful social relationships are beneficial from an evolutionary perspective (e.g. food-sharing, protection, and care) (Baumeister and Leary, 1995). Furthermore, positive social relationships can reduce stress (Gunnar, 2017) and contribute to better health (Vila, 2021). Conversely, social deprivation, such as weak relationships and isolation, is associated with increased risk of mortality (Holt-Lunstad and Smith, 2012), reduced mental health (Almeida et al., 2022), and poor cognitive function in old age (Evans et al., 2019).

Social motivation is reflected in many behaviors involving social orienting (preferences for social stimuli), seeking and liking (finding social interactions rewarding), and social maintaining (e.g. prosocial behaviors, efforts to build and keep social bonds, and avoiding loneliness) (Baumeister and Leary, 1995; Chevallier et al., 2012; Freed, 2022). Social interactions are intrinsically rewarding (Chevallier et al., 2012) but also external social feedback, even simple facial expressions, such as smiles or frowns, can serve as rewards or punishments and modulate behavior (Martins et al., 2021). Along these lines, susceptibility to feedback from others likely supports the learning of skills or behaviors that are advantageous for the individual and community (Freed, 2022). Social preference, prosocial behaviors, social reward and punishment, and social learning involve the BF as we will explain below.

Social cognition

Social cognition includes three domains: i) perception of the self, ii) perception of others, and iii) social knowledge (Beer and Ochsner, 2006). Self-perception (i) includes recognizing own mental states and personal feelings, thereby providing insights into a situation or relationship. It may be used as reference to others or to make inferences about emotions, intentions, and mental states (Beer and Ochsner, 2006). The perception of others (ii) includes face processing, emotion recognition, empathy, and theory-of-mind. Social knowledge (iii) involves procedural and declarative knowledge, for example, social norms, social scripts, moral, trustworthiness, prosocial behavior, and memorizing social structures, hierarchies, or individuals. These three dimensions can all be linked to the BF as we will review and conclude below.

Neuroanatomy of the basal forebrain and interconnection with other systems

The BF is a collection of several structures, including the septum, diagonal band nuclei (DB), substantia innominata (SI), nucleus basalis of Meynert (NBM), and the ventral pallidum (VP) (Zaborszky et al., 2012). The SI is a heterogeneous region and overlaps with the NBM, VP, and extended amygdala (Agostinelli et al., 2019). Across these regions, the BF contains different populations of neurons, such as cholinergic, glutamatergic, and GABAergic ones. The BF is the major source of cortical, hippocampal, and amygdala cholinergic innervation (Mesulam et al., 1983), but most subcortical projections of the BF are glutamatergic and GABAergic, cholinergic projections are sparse (Agostinelli et al., 2019).

While a detailed description of all projections is beyond the scope of this review, there are several important projections from and to the BF, which likely play a role in social cognition and motivation. The medial septal nucleus (MS) and the vertical DB mainly project to the hippocampus, while the NBM mainly projects to the neocortex and amygdala (Mesulam et al., 1983; Ezrin-Waters and Resch, 1986; Zaborszky et al., 2008). Importantly, the BF shares anatomical connections with the mesolimbic system, which is also involved in learning and motivation (Bromberg-Martin et al., 2010; Lisman et al., 2011; Eckart and Bunzeck, 2013; Bunzeck et al., 2014; Herweg et al., 2018). For example, the ventral striatum (VS) projects to the NBM (Haber and Knutson, 2010), the SI projects to the substantia nigra/ ventral tegmental area (SN/VTA) (Agostinelli et al., 2019), and the VP shares reciprocal connections with the SN/VTA and VS (Haber and Knutson, 2010). The SN/VTA shares reciprocal connections with the VS (Haber and Knutson, 2010) and provides input to the SI, DB (Gaykema and Zaborszky, 1996), and septum (Beier et al., 2015). Moreover, connections between the BF and basolateral amygdala, lateral habenula (lHb), and lateral hypothalamus may also be involved (Root et al., 2015; Golden et al., 2016; Jimenez et al., 2018; Swanson et al., 2022; Rodriguez et al., 2023).

Empirical evidence for a role of the basal forebrain in motivation and social cognition

The BF signals valence across a variety of stimuli, including food (Bortolini et al., 2021), liquids, air-puffs, and electrical shocks in animals (Wilson and Rolls, 1990; Hangya et al., 2015; Monosov et al., 2015; Robert et al., 2021) but also social incentives in humans (Bortolini et al., 2021; Sobczak et al., 2023). Specifically, cholinergic neurons in the NBM and DB in mice respond to reward delivery (Hangya et al., 2015), and neurons in the SI and MS/DB in primates respond to reward-predicting stimuli (Wilson and Rolls, 1990; Monosov et al., 2015). In humans, affiliative rewards increased activity in the septo-hypothalamic area (Bortolini et al., 2021) and predictors of positive social feedback increased functional coupling between the NBM and interconnected ventral SN (Sobczak et al., 2023). The anticipation and delivery of punishments, on the other hand, elicit responses in the SI and MS/DB as shown in monkeys and mice (Wilson and Rolls, 1990; Monosov et al., 2015; Robert et al., 2021). In this regard, cholinergic neurons in the NBM and DB appear to be particularly sensitive to the delivery of punishments (Hangya et al., 2015).

Aversive learning involves several BF projections, including cholinergic, GABAergic and glutamatergic neurons. For instance, glutamatergic projections from the MS to the lHb support aversive learning while aversion is antagonized by GABAergic projections from the MS to the lHb in mice (Zhang et al., 2018). The suppression of cholinergic projections from the BF to the mPFC during the anticipation of a negative outcome impairs the learning of aversive associations with a negative cue in mice (Tu et al., 2022). In humans, anticipating social punishment (avoidance) was associated with increased BOLD activity in septal nuclei (Martins et al., 2021) and increased functional connectivity between the MS/DB and lateral SN (Sobczak et al., 2023). Another study found that functional connectivity patterns of the NBM and septum with a wider social information processing network (including the VTA, NAcc, amygdala, insula, and orbitofrontal cortex) depend on the valence of social interactions (Rilling et al., 2018). Similar to dopamine (DA) neurons in the midbrain, cholinergic BF neurons initially respond to outcome and shift to predictive cues in contingency learning tasks for both appetitive (Crouse et al., 2020) and aversive stimuli (Guo et al., 2019).

Importantly, there is empirical evidence that the BF is involved in social cognition, which links to the three dimensions mentioned above (processing of the self, others, and social knowledge) and further includes aspects of social learning and social valence processing. For example, resting-state functional connectivity between the BF and amygdala negatively correlates with (subclinical) social anxiety traits (Zhu et al., 2023). With regard to cooperation and socially adequate behavior, learning the trustworthiness of individuals and their corresponding behavioral adaptation (Diaconescu et al., 2017), along with acquiring the ability to engage in a prosocial manner (Lockwood et al., 2016), recruits the septal nuclei. In prosocial learning, septal activity and learning speed are influenced by trait empathy (Lockwood et al., 2016). The septum is also associated with moral motivation (Zahn et al., 2020) and prosocial sentiments such as pride, guilt, pity, or embarrassment, which are critical components of moral conscience (Zahn et al., 2009; Moll et al., 2011). The septo-hypothalamic area in the BF is implicated in the experience and expression of emotions, including not only general emotional valence but also specific affiliative emotions, that is, feelings of warmth and tenderness (Moll et al., 2012). Moreover, the MS and NBM are involved in social recognition memory in rodents (Okada et al., 2021; Griguoli and Pimpinella, 2022), which is another important aspect of social cognition.

The involvement of the BF in social behavior is further highlighted in individuals with ASD, who not only have problems with social relations, communication, and adaptive behavior, but also show gray matter reductions and altered oxytocin binding in the BF compared with healthy controls (Riva et al., 2011; Freeman et al., 2018). In addition, research in mice has shown differences in social information processing that may relate to ASD-like abnormalities, namely reduced social preference following MS/DB damage (Okada et al., 2021) and after impairment of cholinergic BF neurons (Rapanelli et al., 2023). Social problems may also be explained by impaired valuation (Vinckier et al., 2021), including reduced social value processing in the mesolimbic system Delmonte et al., 2012; Frehner et al., 2022) and PFC (Choi et al., 2015), and atypical neural mechanisms of social reward prediction errors (Kinard et al., 2020) in individuals with ASD. Especially, the interaction between the mesolimbic system and BF may play a role since the inhibition of inhibitory BF projections targeting VTA GABA (gamma-aminobutyric acid) neurons led to a reduced DA release into the NAcc and less social behavior (Wang et al., 2021) in mice.

Taken together, the evidence reviewed above suggests two main points: first, social information, such as trustworthiness, prosocial behavior, and prosocial emotions, signals inherent value comparable to primary reinforcers such as pleasant liquids, air-puffs, or electrical shocks. Second, the BF and its projections are involved in the processing of complex social information related to the three domains of social cognition. For example, it is involved in the experience and expression of emotions (i.e. self-perception), empathy, and social anxiety (i.e. perception of others), as well as moral motivation, trustworthiness, prosocial behavior, and social memory (i.e. social knowledge). However, a specific assignment of the three domains to specific BF regions remains unwarranted based on current empirical studies and, therefore, needs to be addressed in future research.

Age-related changes

Age-related changes of the BF involve only a moderate cell loss (Schliebs and Arendt, 2011) and gray matter decreases (Grothe et al., 2012), but its functioning appears to be affected by dendritic, synaptic, and axonal degeneration, as well as the accumulation of neurofibrillary tangles (Mesulam et al., 2004; Schliebs and Arendt, 2011). At the same time, healthy aging is associated with changes in cognitive abilities but also motivational and socio-emotional processing (Carstensen, 2021). Healthy older adults show more positive emotions and emotional stability (Carstensen et al., 2011), together with increased value of positive social interaction (Rademacher et al., 2014), which indicates a possible structure–function relationship of the BF with motivational value processing of socio-emotional information during healthy aging. In the cognitive domain, there is a relationship between BF structural integrity and verbal learning (Mesulam et al., 2004; Düzel et al., 2010), as well as general intelligence (Wolf et al., 2014). But the neural mechanisms underlying age-related changes in socio-emotional processing have primarily focused on the PFC, amygdala, insula, and mesolimbic dopaminergic system (Mather, 2016), while the role of the BF has been neglected.

A more general perspective on the 'Cortical and Subcortical Social Information processing' model

How can subcortical social information processing within the BF contribute to motivation and behavior? As outlined above, subcortical brain regions signal motivational value and complex social information. In fact, the BF shares widespread anatomical connections, including sensory areas (Chaves-Coira et al., 2018), the mesolimbic system (Gaykema and Zaborszky, 1996; Haber and Knutson, 2010; Beier et al., 2015), and PFC (Ezrin-Waters and Resch, 1986; Chaves-Coira et al., 2018), making it a pivotal component in a complex and interconnected valuation system. Owing to its afferent projections from the VS and its efferent projections to the PFC, a functional engagement of the NBM may reflect an indirect route from the mesolimbic system to frontal regions providing relevant information for higher cognitive processes (Haber and Knutson, 2010). Furthermore, the cholinergic projections of the NBM and PFC are involved in sustained attention (Sarter et al., 2001, 2006). Along these lines, functional coupling between the NAcc and NBM during social feedback anticipation (irrespective of the valence of the feedback) in humans (Sobczak et al., 2023) may also implicate a mechanism that guides attention toward relevant information.

Regarding the role of BF projections to the PFC in mediating social behavior, there is no conclusive evidence yet. However, two recent reviews have highlighted the role of the PFC in social valence processing (Padilla-Coreano et al., 2022) and aspects of social cognition, for example, facial emotion recognition, theory-of-mind, and self-perception, together with the posterior cingulate cortex, precuneus, and amygdala (Hiser and Koenigs, 2018). Given the BF's association with social valence processing and various aspects of social cognition, it seems plausible that the BF works in concert with the PFC to promote social behavior. However, this suggested link still requires empirical validation.

Taken together, we suggest that primary and association areas receive sensory information, which then enters the BF and SN/VTA, where it is further processed, for example, via value computations and prediction errors (Haber and Knutson, 2010; Iglesias et al., 2013; Diaconescu et al., 2017; Monosov, 2020). These neural signals are then interpreted and translated into social motivation and behavior by higher cortical areas, especially the PFC, which is known for its involvement in executive control and goal-directed behaviors (Arco and Mora, 2009). These can include biological and socio-emotional aspects of oneself, others, and social knowledge. A schematic illustration of the potential flow of information between cortical and subcortical areas working in concert to promote social cognition, motivation, and behavior is shown in Figure C S1. With the proposed model, we suggest that the contribution of the BF to motivational and cognitive aspects has been neglected in other models and should be given more attention in future research.

Open questions and future research

Further understanding anatomical connections and functional interactions of the BF and mesolimbic system in concert with the PFC is essential to grasp the full picture on the underlying mechanisms of social motivation. Apart from issues on dopaminergic and cholinergic neuromodulation, future research might focus on other neurotransmitters, such as GABA and glutamate. In addition, the cholinergic system includes specific brainstem nuclei, namely the pedunculopontine and laterodorsal tegmental nucleus (Bertrand and Wallace, 2020), whose roles in human social motivation have largely been neglected (Dautan et al., 2016). It also remains unclear whether social and nonsocial stimuli are processed via a common coding system indicating the need to disentangle the extent to which these stimuli rely on the same or specialized brain regions (Ruff and Fehr, 2014). Along these lines, social behavior in animals often relies on other sensory modalities, including olfaction (including pheromones), which might involve overlapping and distinct brain circuits. Therefore, comparing animal and human models appears to be important. From a developmental perspective, further explorations of a link between age-related BF degeneration and socio-emotional changes can provide novel insights into human behavior across the lifespan (Shen et al., 2022). This might include a dissociation of trajectories associated with healthy and pathological aging, especially in Alzheimer's and Parkinson's disease (Bunzeck et al., 2024).

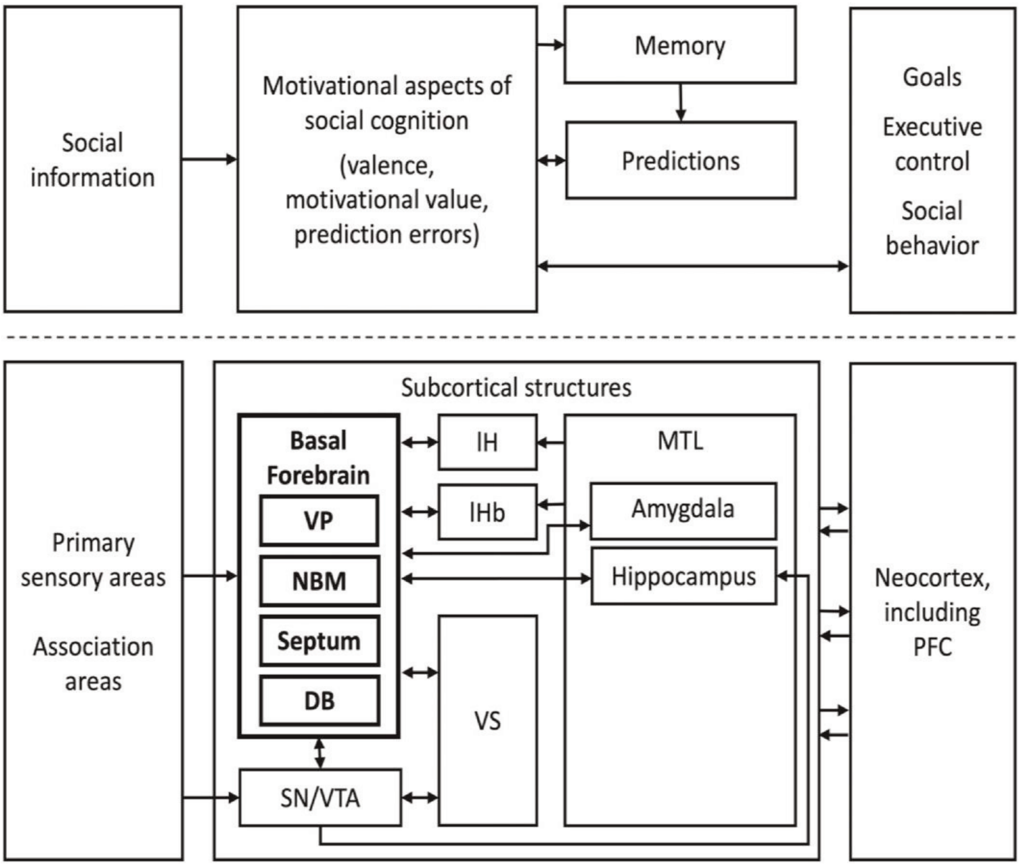

Supplementary figure C S1. Hypothesized model of CASSI. The upper panel illustrates the mental aspects and processes in social cognition, motivation, and behavior. The lower panel shows associated cortical and subcortical brain regions and a possible flow of information (depicted as arrows) involved in social information processing. Information from primary sensory and association areas enters the BF but also SN/VTA, where it is further processed, for example, via value computations and prediction errors. These neural signals are being interpreted and translated into social cognition, motivation, and behavior by higher cortical areas, especially the PFC, promoting executive control and goal-oriented behavior. The arrows indicate information flow, but they do not necessarily correspond to specific anatomical connections hypothalamus. lH; lateral hypothalamus, VP; ventral pallidum, NBM; nucleus basalis of Meynert, DB; diagonal band, SN/VTA; substantia nigra / ventral tegmental area, VS; ventral striatum, MTL; medial temporal lobe, PFC; prefrontal cortex.

Finally, from a methodological point of view, it is important to note that the BF is a rather small structure, which calls for advanced imaging methods with high spatial and temporal resolution. This should be combined with pharmacological strategies together with established and novel behavioral paradigms that tap into more realistic and ecologically valid forms of social interactions. In sum, future research requires more studies in humans, a focus on the interplay of cortical and subcortical structures, advanced methods, and a lifespan approach.

Conclusion

The BF plays a significant role in motivational aspects of cognition. In our model, called CASSI, we suggest that this is being achieved by an interplay of the BF with interconnected brain regions, especially the PFC, SN/ VTA, MTL, and VS. While the BF and SN/VTA compute value and prediction errors, the PFC interprets and translates these neural signals into social cognition, motivation, and behavior. Future research, especially in humans, is required to further validate or challenge our view by using advanced imaging methods in combination with psychopharmacology and novel experimental approaches across the lifespan.

D Acknowledgements

I am incredibly grateful for the past few years, which have been a time of learning and have allowed me to satisfy my curiosity. Although there have been challenging phases, the happy memories I have made along the way are countless and invaluable.

I would like to express my sincere gratitude to my supervisor Prof. Dr. Nico Bunzeck for the opportunity to conduct my PhD studies. Thank you for your constructive feedback on my work and your confidence in my academic abilities along this journey. Furthermore, I would like to thank Prof. Dr. Ulrike Krämer for her willingness to assess my thesis.

Special thanks go to the members of the Life Span group: To Davina, Tineke, and Alexandrina for guiding me through the early stages of my PhD, and to Marthe, Anne R., and Mushfa for the great company in the second half. Thank you all for the productive discussions, academic and emotional support, and your camaraderie that enriched my research experience. My gratitude also extends to Christa, Tanja, and Anne H. for their contributions and support in the jungle of administration and study coordination.

I want to thank Norbert Brüggemann and Christina Lohse for their collaboration and support in the PD patient study. I also thank the Hiwis, students, and interns, for helping me with conduction of my studies.

Thanks to my good friends near and far: Sophie, Theresa, Fabienne, Davina, Sara, Jörn, Carolin, Sandra, and Verena. Thank you all for celebrating my accomplishments with me, and for your advice and kind words during the stressful times that have been a source of strength throughout this journey. Very special thanks go to Sophie and Fabienne for their thoughtful comments on this thesis.

Special thanks go to my family: My mum and dad, Manuela and Rainer Sobczak, thank you for your unconditional love and for always supporting my academic interests. The countless opportunities you have made possible enabled me to pursue my PhD and I would not be where I am today without you. To my siblings Isabelle and Christian, my uncles, aunts, and grandparents for their faith in me and continuous encouragement. Special thanks to my grandma Edith for being a constant source of inspiration.

My deepest gratitude goes to my fiancé Fabian Ott, for his patience, support, attentive listening, and unwavering commitment to our work-life balance. You are my ultimate companion and confidant, enriching every aspect of my life.

E Curriculum vitae

Alexandra Sobczak

Research experience

12/2022 – 03/2024 04/2018 – 09/2022	**Research associate**, Institute of Psychology, University of Lübeck
08/2017 – 10/2017 02/2017 10/2016 – 12/2016	**Student research assistant**, Department of Psychology, Carl von Ossietzky University Oldenburg
03/2017 – 05/2017	**Student research internship**, Institute of Psychology, University of Lübeck
10/2016 – 02/2017	**Student research project**, Department of Psychology, Carl von Ossietzky University Oldenburg

Education

Since 04/2018	**PhD student** Institute of Psychology, University of Lübeck Thesis: *The effects of social feedback and underlying neuropsychological mechanisms*
10/2015 – 03/2018	**Master of Science** Neurocognitive Psychology, Carl von Ossietzky University Oldenburg Thesis: *An MEG study on effects of sublexical prior knowledge on degraded speech processing*
02/2014 – 08/2014	**Semester abroad** (B.Sc. Psychology), University of Queensland, Brisbane, Australia
09/2011 – 02/2015	**Bachelor of Science** Work and Organizational Psychology, Rhine-Waal University, Kamp-Lintfort Thesis: *Mental mechanisms and neurocognitive characteristics of mindfulness in stress management*

Articles in peer-reviewed journals

Sobczak A, Bunzeck N (2024) The basal forebrain serves social information processing. Current Opinion in Behavioral Sciences 56:101372.

Sobczak A, Bunzeck N (2023) Effects of positive and negative social feedback on motivation, evaluative learning, and socio-emotional processing. npj Sci Learn 8:28.

Sobczak A, Yousuf M, Bunzeck N (2023) Anticipating social feedback involves basal forebrain and mesolimbic functional connectivity. NeuroImage 274:120131.

Geritz J, Welzel J, Hansen C, Maetzler C, Hobert MA, Elshehabi M, **Sobczak A**, Kudelka J, Stiel C, Hieke J, Alpes A, Bunzeck N, Maetzler W (2022) Does Executive Function Influence Walking in Acutely Hospitalized Patients With Advanced Parkinson's Disease: A Quantitative Analysis. Front Neurol 13:852725.

Peters JO, Steiger TK, **Sobczak A**, Bunzeck N (2022) Set Size of Information in Long-Term Memory Similarly Modulates Retrieval Dynamics in Young and Older Adults. Front Psychol 13:817929.

Steiger TK, **Sobczak A**, Reineke R, Bunzeck N (2022) Novelty processing associated with neural beta oscillations improves recognition memory in young and older adults. Annals NY Academy of Science:nyas.14750.

Sobczak A, Repplinger S, Bauch EM, Brueggemann N, Lohse C, Hinrichs H, Buentjen L, Voges J, Zaehle T, Bunzeck N (2021) Anticipating social incentives recruits alpha-beta oscillations in the human substantia nigra and invigorates behavior across the life span. NeuroImage:118696.

Conference contributions

Sobczak A, Steiger TK, Sommer P, Bunzeck N. 2024. Curiosity and surprise differentially affect long term memory across the adult life span. Poster, Psychologie und Gehrin, Hamburg.

Sobczak A, Bunzeck N. 2022. Anticipating positive social feedback recruits the ventral and medial human substantial nigra: evidence from high-resolution fMRI. Poster, International Conference of Cognitive Neuroscience, Helsinki, Finland.

Sobczak A, Bunzeck N. 2022. Novelty anticipation recruits the medial temporal lobe, beta oscillations and drives recognition memory across the lifespan. Talk, International Conference of Cognitive Neuroscience, Helsinki, Finland.

Sobczak A, Bunzeck N. 2021. Functional connectivity of the nucleus accumbens with posterior cingulate and retrosplenial cortex is associated with anticipation of positive and negative social feedback. Poster, CBBM Symposium, Lübeck.

Sobczak A, Bauch EM, Heimrath K, Brueggemann N, Lohse C, Hinrichs H, Schmitt FC, Voges J, Heinze HJ, Zaehle T, Bunzeck N. 2020. Alpha-beta oscillations in the human substantia nigra signal the anticipation of appetitive and aversive social feedback: evidence from intracranial recordings. Talk, Neuromatch Conference 3.0, Online.

Sobczak, A, Bauch EM, Heimrath K, Hinrichs H, Schmitt FC, Voges J, Heinze HJ, Zaehle T, Bunzeck N. 2019. Alpha-beta oscillations in the human substantia nigra signal the anticipation of appetitive and aversive social reward feedback: evidence from intracranial recordings. Poster, Aging and Cognition, Zürich, Switzerland.

Sobczak A, Bauch EM, Heimrath K, Hinrichs H, Schmitt FC, Voges J, Heinze HJ, Zaehle T, Bunzeck N. 2019. Alpha-beta oscillations in the human substantia nigra signal the anticipation of appetitive and aversive social reward feedback: evidence from intracranial recordings. Poster, CBBM Symposium, Lübeck.

Scholarships and awards

Poster Award, CBBM Symposium, Lübeck, 2021

EUCAS Presidential Poster Award, 5th International Aging and Cognition Conference, Zürich, Schweiz, 2019

Landesstipendium Niedersachsen, 2016, 2017

PROMOS Stipendium, 2014

Eidesstattliche Erklärung

Ich versichere an Eides statt, die vorliegende Arbeit selbstständig und nur unter Benutzung der angegebenen Quellen und Hilfsmittel angefertigt zu haben.

Lübeck, 18.6.2024
Ort, Datum

A. Sobczak
Unterschrift